Study of the non-proteinogenic δ-amino acid ACCA, its biological investigation and application

by

Lara Pes, BSc, MSc

The thesis is submitted to University College Dublin in fulfilment of the requirements for the degree of Doctor of Philosophy

Based on research carried out in the
Centre for Synthesis and Chemical Biology
UCD School of Chemistry & Chemical Biology

Head of School: Professor Patrick J. Guiry
Under the supervision and direction of
Doctor Francesca Paradisi, PhD
Doctor Gethin McBean, PhD

National University of Ireland
University College Dublin
August 2013

CSCB
Centre for Synthesis & Chemical Biology

IRISH RESEARCH COUNCIL
COMHAIRLE TAIGHDE na hÉIREANN

Table of contents

Declaration

I declare that the work contained in this thesis has not been submitted before, in whole or in part, to this or any university for any degree and is, except where otherwise stated, the original work of the author.

_____

Lara Pes

August 2013

Abbreviations

(+)-HIP-B	(+)-3-hydroxy-4,5,6,6a-tetrahydro-3a*H*-pyrrolo[3,4-*d*]-isoxazole-6-carboxylic acid
Å	Angstrom
ACC	Aminocyclobutane-1,3-dicarboxylate
ACCA	*cis*-3-(aminomethyl)cyclobutane carboxylic acid
AMBA	Aminomethyl benzoic acid
AMPA	α-amino-3-hydroxy-5-methyl-4-isoxazole propionic acid
ANOVA	Analysis of variance
ATP	Adenosine triphosphate
Bn	Benzyl
Boc	*tert*-butoxycarbonyl
BSA	Bovine serum albumin
CAN	Cerium (IV) ammonium nitrate
CNS	Central nervous system
COMU	(1-Cyano-2-ethoxy-2-oxoethylidenaminooxy) dimethyl-amino-morpholino-carbenium hexafluoro-phosphate
δ	Chemical shift in ppm downfield of TMS
D	Debeys
DEPBT	3-(Diethoxy-phosphoryloxy)-3H-benzo[d][1,2,3] triazin-4-one
DFT	Density functional theory
DIC	*N,N'*-Diisopropylcarbodiimide
DMF	Dimethylformamide
DMEM	Dulbecco's modified eagle medium

DMSO	Dimethyl sulphoxide
DP	(2*S*,4*R*)-2-amino-4-(3-((2,2-diphenylethyl)amino)-3-oxopropyl)pentanedioic acid
DSC	Bis-(succinimidyl) carbonate
EAAT	Excitatory amino acid transporter
EDCI	1-Ethyl-3-(3-dimethylaminopropyl)carbodiimide
EDTA	Ethylenediaminetetraacetic acid
ES	Electronspray
Et_2O	Diethyl ether
EtOAc	Ethyl acetate
EtOH	Ethanol
Fmoc	Fluorenylmethiloxy carbonyl
FT	Fourier transform
GABA	γ-aminobutyric acid
Gln	Glutamine
Glu	Glutamic acid
Gly	Glycine
GPI-1046	(*S*)-3-(pyridin-3-yl)propyl-1-(3,3-dimethyl-2-oxopentanoyl) pyrrolidine-2-carboxylate
GSH	Glutathione
HATU	(7-Azabenzotriazol-1-yl)-*N*,*N*,*N*′,*N*′-tetramethyluronium hexafluorophosphate
HBTU	*O*-Benzotriazole-*N,N,N',N'*-tetramethyl-uronium-hexafluoro-phosphate
HDAC	Inhibitor of histone deacetylase
HEPES	2-[4-(2-hydroxyethyl)piperazin-1-yl]ethanesulphonic acid

HOAt	1-Hydroxy-7-azabenzotriazole
HPLC	High performance liquid chromatography
HRMS	High Resolution Mass Spectrometry
IKM159	(4a*S*,5a*R*,6*R*,8a*S*,8b*S*)-5a-(carboxymethyl)-8-oxo-2,4a,5a,6,7,8,8a,8b-octahydro-1*H*-pyrrolo [3',4':4,5]furo[3,2-*b*]pyridine-6 carboxylic acid
$^{i}Pr_2EtN$	*N,N'*-Diisopropylethylamine
KA	Kainic acid
KHB	Krebs-HEPES buffer
L-CBG	L-2-(2-carboxycyclobutyl)glycine
L-DOPA	L-3,4-dihydroxyphenylalanine
μ	Magnetic moment
MHz	Mega hertz
mp	Melting point
MS-153	(*R*)-(5-methyl-4,5-dihydro-1*H*-pyrazol-1-yl)(pyridin-3-yl)methanone
MW	Molecular weight
m/z	Mass-to-charge ratio
NMDA	*N*-methyl-D-aspartate
NMR	Nuclear Magnetic Resonance
NOESY	Nuclear Overhauser effect spectroscopy
Oxd	Oxazolidin-2-one
Phe	Phenylalanine
PMB	Para-methoxy-benzyl

ppm	Parts per million
Pr	Propyl
PrOH	Propanol
PTC	Phase transfer catalysis
PyBOP	benzotriazol-1-yl-oxytripyrrolidinophosphonium hexafluorophosphate
r.t.	Room temperature
SEM	Standard error of the mean
^{t}BuOH	*tert*-butanol
TEA	Triethylamine
TFA	Trifluoroacetic acid
TFB-TBOA	(2*S*,3*S*)-3-[3-[4-(trifluoromethyl)benzoylamino] benzyloxy]aspartate
THF	Tetrahydrofuran
TLC	Thin layer chromatography
UCPH	2-amino-4,7-diaryl-5-oxo-tetrahydro-4*H*-chromene-3-carbonitriles
Val	Valine
WAY-213613	(*S*)-2-amino-4-((4-(2-bromo-4,5-difluorophenoxy)phenyl)amino)-4-oxobutanoic acid
X_c^-	Cystine-glutamate exchanger

Abstract

The aim of this project is the investigation of the novel non-proteinogenic δ-amino acid *cis*-3-(aminomethyl)cyclobutane carboxylic acid (ACCA) and its possible applications.

ACCA was obtained after a 7 steps synthesis, from commercially available starting materials. The important characteristics of ACCA are the locked *cis* conformation of the amino and carboxylic acid groups and the presence of the cyclobutane moiety that render it a constrained molecule and therefore particularly interesting as building block for organic synthesis and peptidomimetics drug design. For these reasons ACCA can be considered a very versatile and useful molecule, with applications in different research fields, some of which are described herein.

A small library of dipeptides was also synthesised coupling ACCA with proteinogenic amino acids.

Considering ACCA resemblance with the neurotransmitter glutamic acid, the neural activity of the δ-amino acid, its ester and dipeptides have been investigated on rat C6 glioma cells through glutamate uptake experiments, showing an interesting increase in glutamate uptake.

Herein the incorporation of ACCA in a macrocycle tetrapeptide mimic, with potential as ligand for metal ions is also reported.

Chapter 1

Introduction

1.1-Serendipity in chemistry

Serendipity is by definition the "faculty of making fortunate discoveries by accident".[1]

A surprising number of important chemical discoveries come from fortuitous events. Penicillin is the classical example, but there are many other cases for instance in the field of polymers and dyes. A curious example in this regard is Perkin's discovery of the first synthetic dye, mauveine (Fig. 1.1).[2]

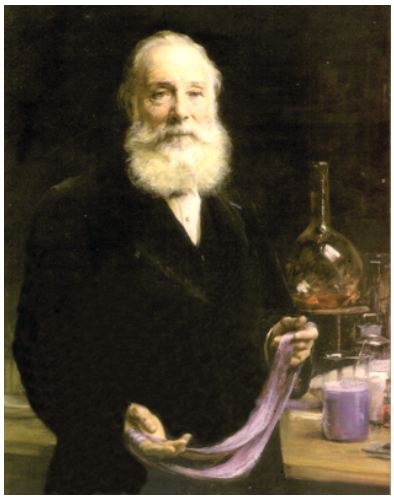

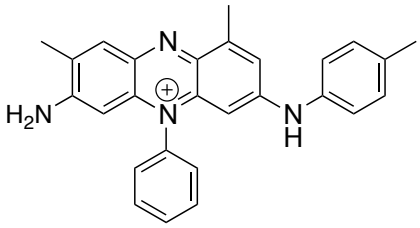

Fig. 1.1 portrait of William Perkin with a sample of clothe dyed with mauveine and mauveine chemical structure

William Henry Perkin entered the Royal College of Chemistry in London at the age of 15 and soon became staff assistant in Hoffman's group. In 1856, during the Easter vacation, he was working in the rudimental laboratory in his room on quinine synthesis starting from naphthalene. The project was challenging considering that the structure of quinine was not known yet. In one of his attempts, he reacted allyl iodide on toluidine and oxidised the product with potassium dichromate obtaining a red/brown precipitate.

Not satisfied by the result he changed the base toluidine for aniline sulphate. When he added the potassium dichromate he generated a black precipitate. Trying to recover the desired product, he extracted the back mixture with methanol and the organic solvent turned to a purple colour, similar to mauve.

Attracted by the interesting hue, Perkin decided to test the product as a dye, apparently using a piece of silk taken from his sister's wardrobe. What he found was that the dye, later named mauveine, was resistant to water and light. After optimising the synthetic procedure, he sold the dye to a Scottish company. Here he learned that purple was a valued colour, but was expensive to extract from natural sources (generally colours were obtained from vegetables, minerals and animals) and was not particularly resistant. Thus, at the age of 18, William Henry Perkin decided to patent the discovery, starting the business and research on synthetic dyes.

As it often happens in research, also in our case a serendipitous discovery gave birth to this thesis project, developed around the novel non-proteinogenic amino acid *cis*-3-(aminomethyl)cyclobutan carboxylic acid ACCA (Fig. 1.2).

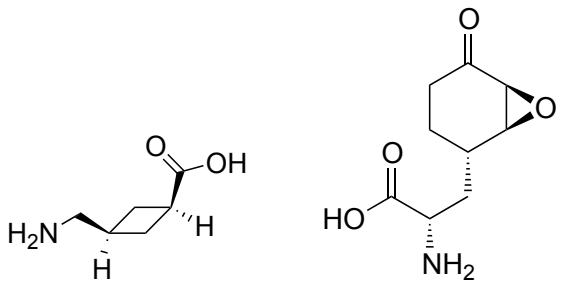

ACCA anticapsin

Fig 1.2 ACCA and anticapsin chemical structure

While working on the synthesis of an analogue of the natural antimicrobial amino acid anticapsin (Fig. 1.2), an unwanted side reaction generated the interesting precursor of ACCA. The origin of ACCA and the development of this thesis project will be treated in more details in chapter 2.

1.2-Peptidomimetics

A large majority of molecules present in living organisms and in Nature are proteins or peptides. Examples are neurotransmitters, neuromodulators, hormones, antibiotics, enzymes, some alkaloids, and some toxins or venoms. A striking number of them, with diverse biological activity, have been isolated from natural sources and characterised in the last fifty years.

Biological activities occur through the interactions of substrates with enzymes and receptors. Synthetic analogues can mimic natural compounds and therefore have the ability to interfere with the natural biological processes. For this reason, peptides that act as agonists or antagonists of natural molecules (peptidomimetics) can have medicinal properties and are of great interest in research.[3,4]

One of the big issues in the use of natural molecules for medicinal purposes is their poor bioavailability. They are easily recognised by endo- and exopeptidases and then degraded.[4] Also their typical flexibility represents a problem since it means poor specificity. In fact, in solution, peptides can adopt many different conformations, and the one required to bind to the receptor may not be the most stable one. Another drawback is given by their hydrophilicity, which makes them unable to pass through lipophilic cellular membranes (e.g. blood brain barrier) to exert their therapeutic action intracellularly. This delivery problem is often detected when scientific experiments pass from *in vitro* to *in vivo* trials.

Research in peptidomimetics obtained through small modifications or *de novo* synthesis, aims to develop new bioactive compounds with enhanced pharmacological properties.[3,4]

Conformationally constrained molecules play an important role in this field. Conformational constriction minimises the problem of protein flexibility and increases the binding affinity between the drug and the receptor.[5]

There are many techniques to give rigidity to peptides or to increase their proteolytic stability, such as introducing small modification to the structure or inserting non-natural amino acids in the peptide chain (Fig. 1.3). Examples are substitutions (generally alkylation or dialkylation) to the α-carbon or to the

nitrogen, insertion of D-amino acids, β-amino acids or cyclic molecules (proline analogues are widely used, like imidazole and tetrazole) or again amino acids with sterically hindered side chains.

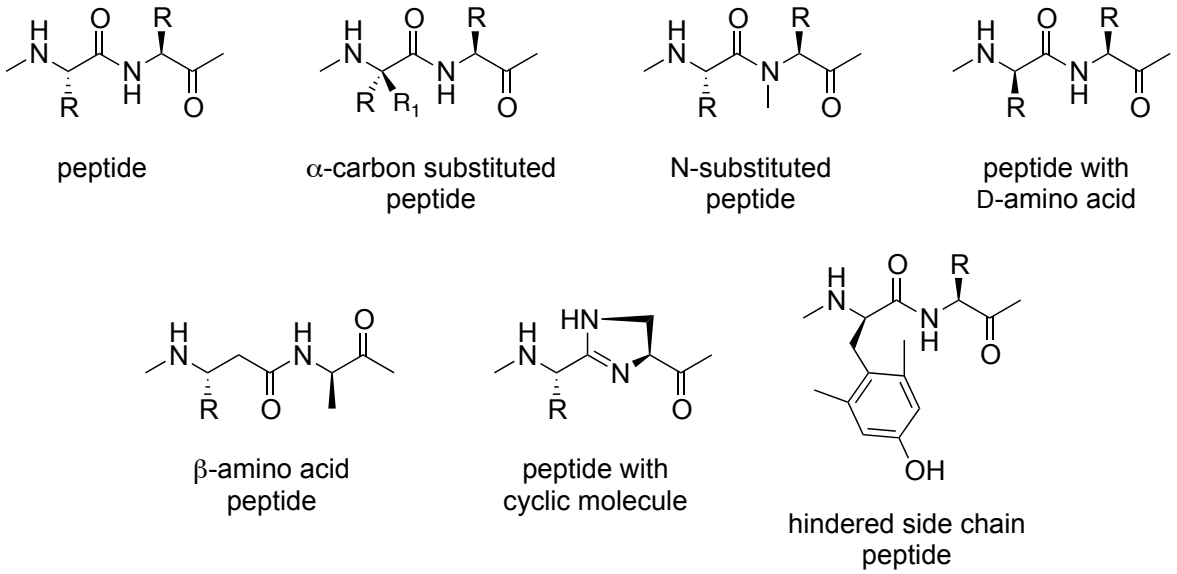

Fig. 1.3 strategies for modification of natural peptides

Modification can also be made on the peptide backbone (Fig. 1.4). The amide bond can be replaced with an appropriate isosteric group, such as CS-NH (thiopeptide), CH_2-NH (reducing the amide to amine, electronic properties change quite drastically) or CO-CH_2 (carbapeptide). The NH could be replaced with O to form an ester (depsipeptide) or the α-C can be substituted with NH (azapeptide) or with C=C (vinylogous peptide).[3,4]

Another approach for backbone modification is the use of retro-inverso isomers, where L-amino acids are replaced by D-amino acids, but with an opposite direction. One problem in this case is the inversion of the charges at the original N- and C-termini, which need to be maintained. In order to do so, moieties properly charged can be added at the extremities.[4]

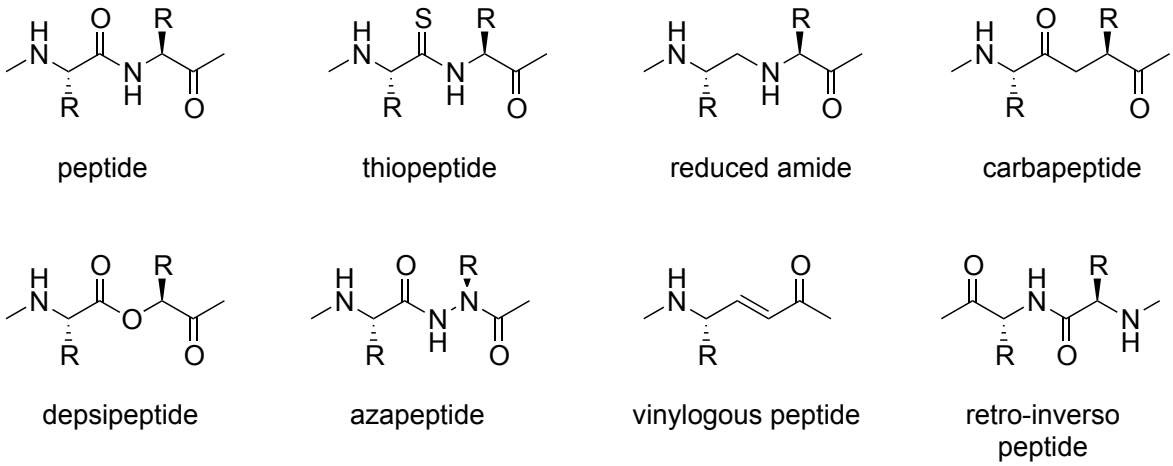

Fig. 1.4 peptides with modification on the backbone

An interesting example is represented by oligopyrrolinones. Oligopyrrolidones are part of the vinylogous peptide family since they possess a C=C double bond between the NH and the CO, where these double bonds are part of the cyclic structure pyrrolinone (Fig. 1.5). This constrained peptide is able to generate β-strand conformations. Compared to equine angiotensinogen, which shows a parallel β-sheet structure in its crystalline form, the olygopyrrolinone motif has an almost identical secondary structure: same dihedral angles ϕ, ψ, ω, same orientation of the side chains, hydrogen bond donor and acceptors in the right positions.[6]

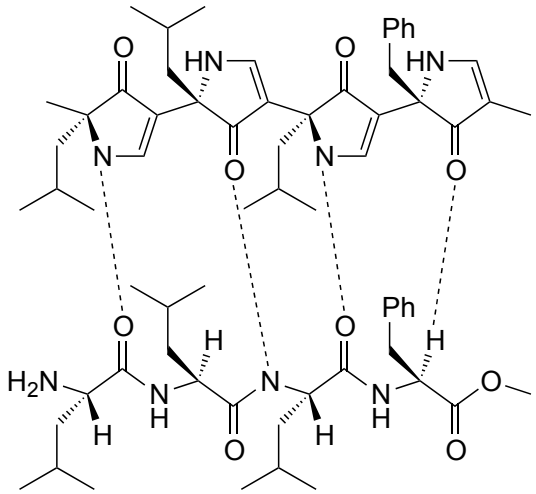

Fig. 1.5 example of oligopyrrolinone compared to the β-sheet structure of equine angiotensinogen

A peptidomimetic category not mentioned previously is the peptoids group. Peptoids are peptide-like compounds where the NH and the CH_2 in the amino acids swap positions, so that the side chain R is no longer connected to the carbon, but to the nitrogen (Fig. 1.6). The residues are connected together in an inverse manner compared to natural amino acids, resembling retro-inverso peptidomimetics. The absence of NH groups reduces the possibilities of H-bonds and gives to peptoids more flexibility. Furthermore, these compounds are resistant to proteolytic enzymes, but keep the same activity of corresponding natural peptides, therefore are more promising as orally active drugs.[3]

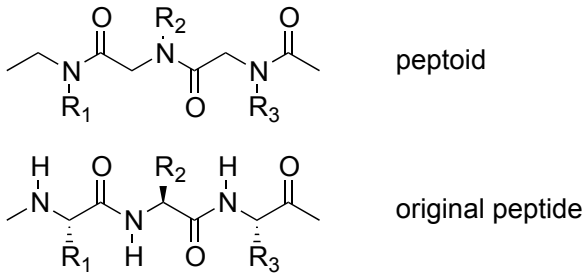

Fig. 1.6 comparison between peptoid and peptide generic structures

The interest in this class of peptidomimetics is recently increasing. Peptoids are generated through a straightforward synthetic process, are metabolically stable,

can cross cell membranes and find applications in different fields as therapeutic and diagnostic agents, molecular transporters, nanomaterials and many others. In the last year for instance fluorescent pH sensor peptoids have been studied (Fig. 1.7).[7]

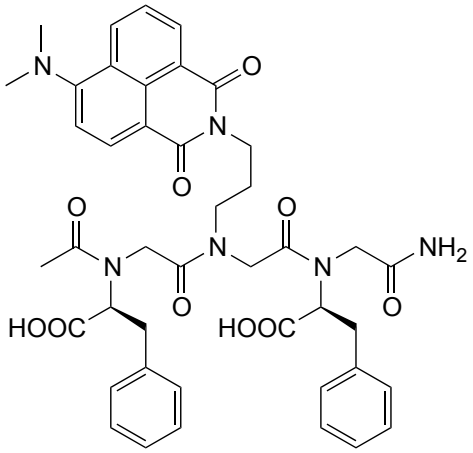

Fig. 1.7 fluorescent pH sensors peptoid

A widely used trick to achieve constrained peptides is the imitation of β-turns. A β-turn is a peptidic structural motif formed by four amino acids in a row (*i* to *i*+3), which produce a change in direction, without forming α-helices or β-sheets and the distance between the first and last α-carbon is less than 7 Å (hydrogen bond between the first and last amino acid of the turn). Although β-turns are the most common, smaller and bigger turns also exist (π-, α-, γ- and δ-turns with respectively 6, 5, 3, and 2 amino acids).[8]

Other important motives, often reproduced in peptidomimetics are Ω-loops, large conformationally stabilized curves (6-16 residues).

To form these curved structures, proline and proline derivatives (Fig. 1.8) are often employed. These constrained structures can influence heavily the peptide secondary structure since it prefers the *cis* conformation and therefore forces the ϕ angle to around -65°, impeding α-helix generation, but favouring turns. Not only Pro is used for these purposes, but also derivatives (Fig. 1.8).[9]

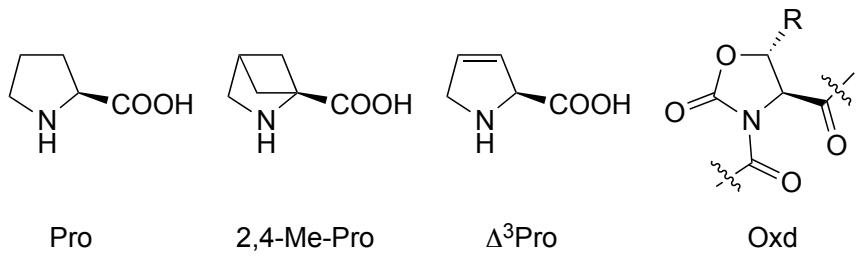

Fig. 1.8 Pro and derivatives used for turn formation

In Gentilucci's group, the insertion of oxazolidin-2-one (Oxd) into peptides has been studied (Scheme 1.1), starting from arylsulphonyl peptides in the presence of bis(succinimidyl) carbonate (DSC) and diisopropyl-ethyl amine ($^{i}Pr_2EtN$) and the influence of various factors (solvent, base, carbonate and sulphonyl group) has also been investigated.[9]

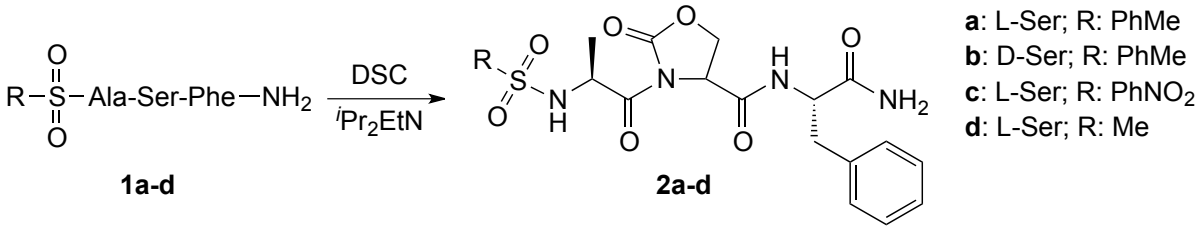

Scheme 1.1 Oxd formation reaction

The presence of Oxd induces β-turns in the peptide structure (Fig. 1.9).[10]

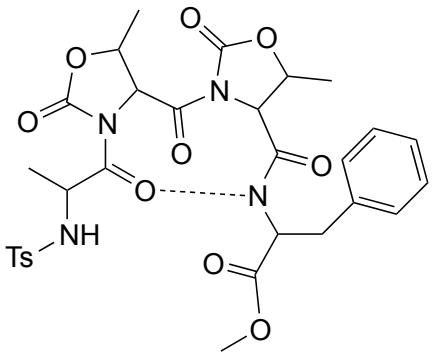

Fig. 1.9 example of peptide containing Oxd forming a β-turn[10]

Cyclisation of the entire molecule can also be used to mimic turns and loops and give rigidity to the overall structure.

1.2.1-Cyclobutane in peptidomimetics

One of the techniques previously mentioned adopted in peptidomimetics is the inclusion of cyclic moieties into peptides. An interesting cycle that can be exploited for this purpose is cyclobutane.

The reactivity of such structure can be placed between the very reactive cyclopropane and the very stable cyclopentane.

For instance, bromine and sulphuric acid react rapidly with cyclopropane, giving 1,3-dibromopropane and 1-propylsulphuric acid, but they do not interact with cyclobutane. Cyclobutanes can react instead with transition metal species provoking the cleavage of the C−C bond. With bigger cycloalkanes this reaction is no longer possible.[11]

The cyclobutane unit is a recurrent restricted element in natural compounds found in bacteria, fungi, plants and other organisms and can be observed also in primary and secondary metabolites. More than 200 cyclobutane-containing alkaloids and other synthetic compounds show interesting biological properties, like antibacterial and anticancer activity.[12,13]

Eder and colleagues isolated nakamuric acid, its corresponding methyl ester and the metabolites sceptrin and debromosceptrin (Fig. 1.10) from the Indopacific sponge *Agelas nakamurai*. All these structures showed antibacterial activity against several Gram-positive and Gram-negative bacteria.[13,14]

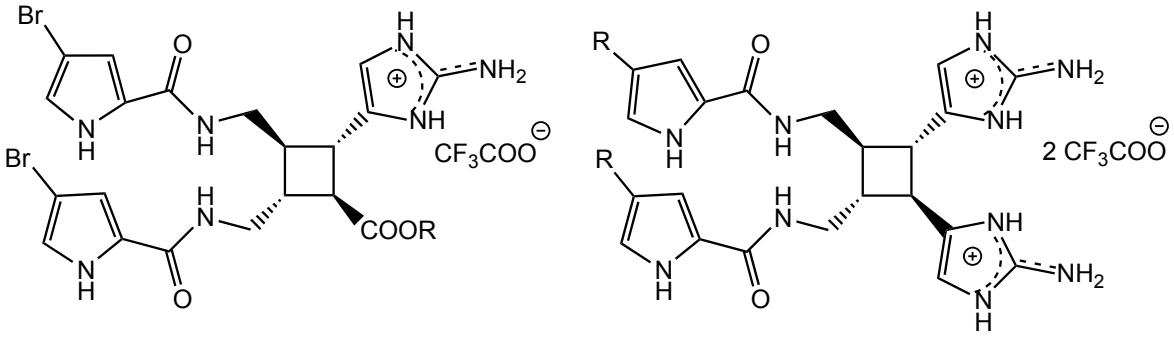

nakumeric acid sceptrin

Fig. 1.10 nakumeric acid (for R = H) and nakumeric acid metyl ester (R = CH_3); sceptrin (for R = Br) and debromosceptrin (for R = H) chemical structures

Other examples of cyclobutane moieties found in nature are shown in Fig. 1.11. These structures are isolated from the seeds of the legume *Atelia herbert smithii*, found in the Santa Rosa National Park in Costa Rica and possess anti-feedant properties.[15,16]

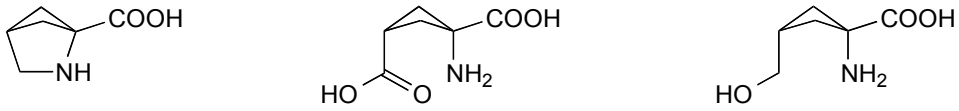

2,4- methanoproline 2,4-methanoglutamic acid 1-amino-3-(hydroxymethyl) cyclobutane carboxylic acid

Fig. 1.11 2,4- methanoproline, 2,4-methanoglutamic acid and its hydroxy amino acid chemical structures

Many plant species in the family of lycopodiaceae contain bioactive alkaloids, some of which incorporate cyclobutane.[17,18,19]

The compound in Fig. 1.12 and other similar alkaloids, containing the four membered ring, are isolated from Cocoa leaves.[20]

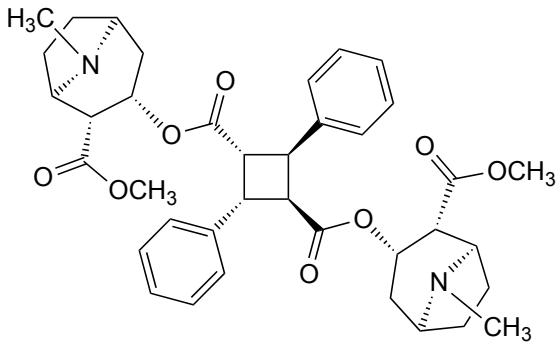

α-truxilline

Fig. 1.12 α-truxilline chemical structure

Many more examples are described in the work of Dembitsky.[12]

The use of this strained motif has widely spread in the field of organic synthesis only in the last 40 years, even if it has been known for more than a century. Often the four-membered cycle is inserted in the structure to exploit its tension and torsional effect, important characteristics in peptidomimetics.

Reactions that can take place on the cyclobutane are ring opening, ring enlargement (to five- or six-membered cycles) and ring contraction (to cyclopropanes). The synthetic techniques to generate these structures are cyclization of acyclic starting materials, ring expansion of cyclopropanes and the most common is photochemically induced [2+2] cycloaddition.[21,22]

Some examples of compounds of pharmaceutical interest, containing the four-membered ring, obtained through ring expansion (Scheme 1.2), ring contraction (Scheme 1.3) and [2+2] cycloaddition (Scheme 1.4), are reported below. The derivatives most recurrent in nature and in synthetic compounds are cyclobutanones and cyclobutenones.[23] Many other applications of cyclobutane derivatives in organic synthesis, are described in the reviews by Lee-Ruff and Mledenova and by Namyslo and Kaufmann.[22,24]

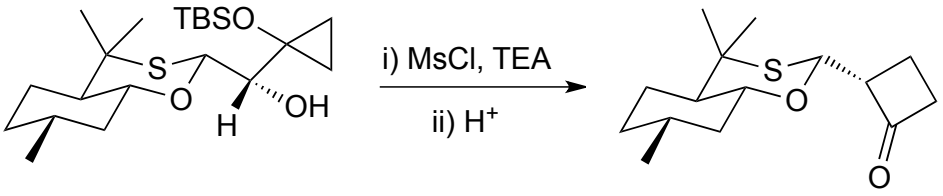

Scheme 1.2 oxathianylmethyl-substituted cyclopropane rearrangement to give cyclobutanone via mesylation[25]

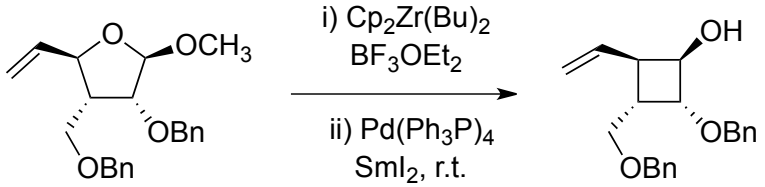

Scheme 1.3 ring restriction of substituted tetrahydrofuran to cyclobutane by zirconocene and subsequent boron trifluoride-ether complex reactions[26]

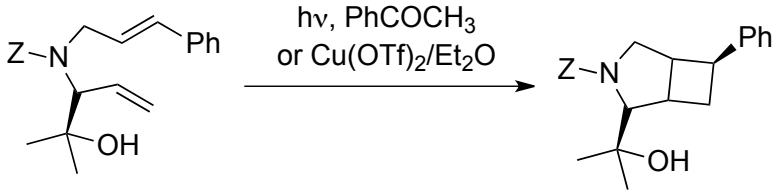

Scheme 1.4 [2+2] photoaddition reaction to generate 3-azabicyclo-[3.2.0]-heptane, important pharmacophore for psychotic diseases and intermediate for the synthesis of azepams[27]

The cyclobutane moiety can be found in nucleotides with antiviral and antineoplastic activity[28,29] and it has been employed to synthesise fatty acids, terpenes, steroids and amino acids.[23,24]

The latest, in particular, are widely studied in drug design and drug development because of their versatility and they can find applications in different fields.[30-33]

A number of papers have been published on amino acids containing a cyclobutane ring. Burgess and colleagues prepared the N-protected 1,3-cyclobutane amino acids (1*S*,3*R*)-3-((*tert*-butoxycarbonyl)amino)-2,2-dimethylcyclobutanecarboxylic acid and (1*S*,3*R*)-3-(((*tert*-

butoxycarbonyl)amino)methyl)-2,2-dimethyl-cyclobutane carboxylic acid starting from α-pinene (Fig 1.13).[34]

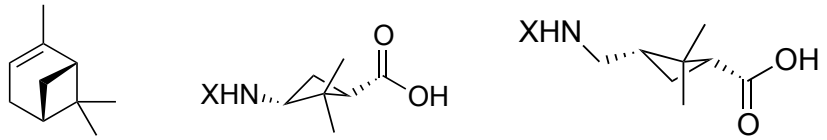

α-pinene 1,3-cyclobutane amino acids

Fig. 1.13 α-pinene, (1*S*,3*R*)-3-((*tert*-butoxycarbonyl)amino)-2,2-dimethylcyclobutanecarboxylic acid and (1*S*,3*R*)-3-(((*tert*-butoxycarbonyl)amino)methyl)-2,2-dimethylcyclobutanecarboxylic acid chemical structures (where X = Boc or Fmoc)

Andre *et al*. synthesized (+)-(1*R*,2*S*) and (-)-(1*S*,2*R*) stereoisomers of 2-(aminomethyl)cyclobutane-1-carboxylic acid as analogue of the GABA neurotransmitter. The key reaction was a photochemical [2+2] cycloaddition of ethylene and an unsaturated γ-lactam (Scheme 1.5).[35]

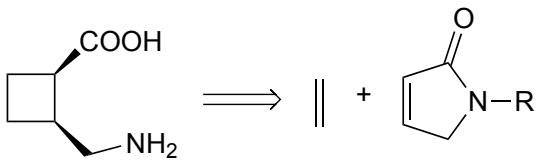

Scheme 1.5 retrosynthetic approach to 2-(aminomethyl)-cyclobutane-1-carboxylic acid[35]

Komarov and collaborators developed a library of spiro-[3.3]-heptane bicyclic glutamate analogues (Fig. 1.14).[36]

Fig. 1.14 spiro-[3.3]-heptane bicyclic glutamate analogues

This constrained cyclobutyl amino acids can also be incorporated in more complex structures like dipeptides, leading sometimes to unusual conformations and hydrogen-bonding interactions (Fig. 1.15).[37,38-40]

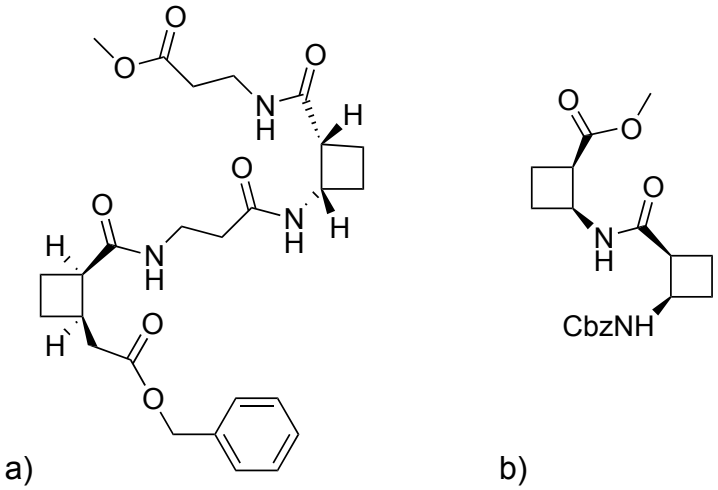

Fig. 1.15 a) tetrapeptide incorporating two units of (-)-2-aminocyclobutane-1-carboxylic acid alternate to two α-alanine residues, b) bis-(cyclobutane)-β-dipeptides chemical structure

This kind of amino acid has also been incorporated in peptides and peptide dendrimers (Fig. 1.16).[41-43,44]

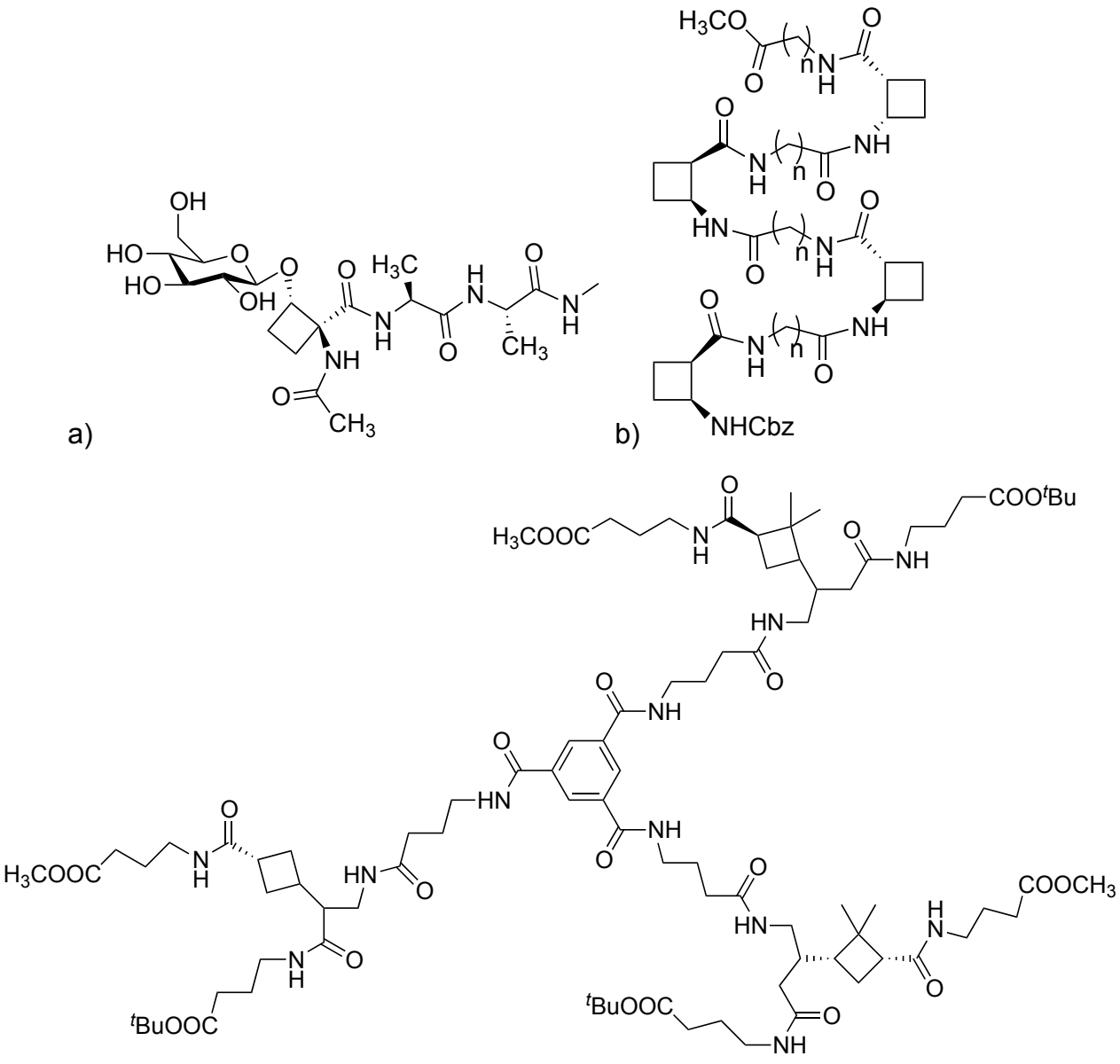

Fig. 1.16 a) glucopeptide[41], b) octamer[43] and c) peptide dendrimer[44] containing cyclobutane

The interesting aspect of the inclusion of cyclic structures in peptides is the diminishment of the conformational freedom, which can increase the affinity and the selectivity with the receptor, the bioavailability and the stability to enzymatic hydrolysis.[45]

1.2.2-Cyclic peptides in peptidomimetics

Among peptides, a big number of biologically active compounds have been found and for this reason there is a great interest in the synthesis of peptide-like molecules for therapeutic applications. Unfortunately, often problems such as metabolic stability, membranes permeability and poor specificity are encountered. The main issues are their high flexibility, the presence of charges at the peptide ends and the poor bioavailability due to degradation *via* peptidases. A possible solution can be found in cyclisation.[46,47]

Once in the cyclic form, peptides loose their conformational freedom and flexibility with significant advantages. The restricted conformation improves efficacy and selectivity towards the target. The absence of charged extremities renders them lipophilic and thus able to cross cell membranes, even though this is not valid for larger macrocycles. Furthermore cyclic peptides present better bioavailability due to their resistance to proteases and therefore they are biologically active for longer periods of time.[2,48]

Especially cyclopeptides with sizes between 500 and 2000 Da (just above small molecules) are good candidates for drug design.[49] In the case of small molecules, 500 Da is the upper limit for cell permeability and oral bioavailability (Lipinski's rule of 5), but cyclic molecules can behave differently showing good pharmacodynamic and pharmacokinetic properties even at higher molecular weights.[46]

An example is cyclosporine (MW = 1202 g/mol), an immunosuppressant cyclic peptide, orally available and selective towards the intracellular protein target.[50]

Peptide size is fundamental when it comes to selectivity. For instance macrocycles containing RGD peptides, small cyclic peptides formed by arginine (R), glycine (G) and aspartic acid (D), have big differences in selectivity. Cyclic compounds with high molecular weights (over 600 Da) can be effective with big and difficult targets *via* peptide-peptide interaction, while a small cycle wouldn't work.[51]

Macrocyclic compounds are formed by 12 or more atoms, they have a higher degree of complexity compared to linear peptides and diverse functional groups arranged to maintain a rigid structure. These characteristics give higher protein

target affinity and selectivity. Despite their pre-organisation, they are not entirely rigid compounds; there is a sort of equilibrium between pre-organisation and flexibility to adapt to the target binding site to better interact with it.[46,52]

The interest for cyclic peptides started in 1944, with the discovery of Gramicidin S (Fig. 1.17), isolated from the bacterium *bacillus brevis*,[53]. Its first application was during the Second World War to treat gunshot wounds and since then the research on cyclic peptides has grown exponentially.[51]

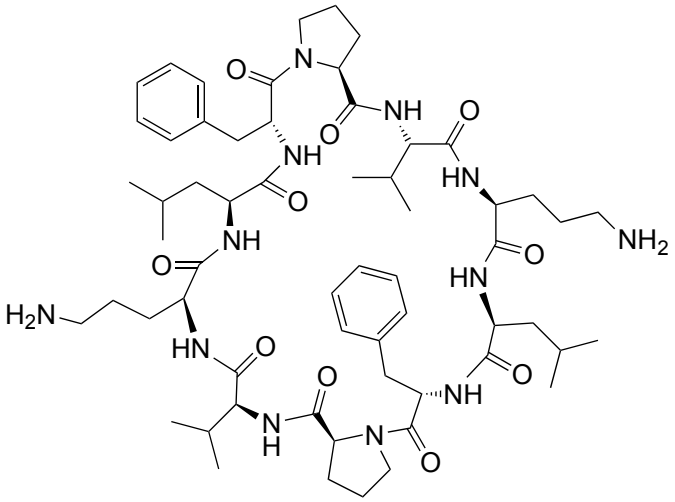

gramicidin S

Fig. 1.17 Gramicidin S chemical structure

Several natural cyclic peptides with interesting properties have been discovered. A number of cyclopeptides is found in marine organisms, like the class of compounds extracted from *Lissoclinum*, which contain heterocycles and show cytotoxic activities or ulicyclamide, lissoclinamide 7[54] and dolastatin 3, isolated from the sea hare *Dolabella auricularia*, with antineoplastic activity (Fig. 1.18).[55]

Some other examples of earthly origin are the insecticides family of destruxins[56] extracted from the fungus *oospora destructor*, the antibiotic family of polymixins found in gram positive bacteria such as *paenibacillus polymyxa*,[3] the phytotoxin tentoxin from the fungus *Alternaria alternata* and HC-toxin from the fungal plant pathogen *Cachliobolus carbonum* (Fig. 1.18) and many more could be mentioned.[51,57]

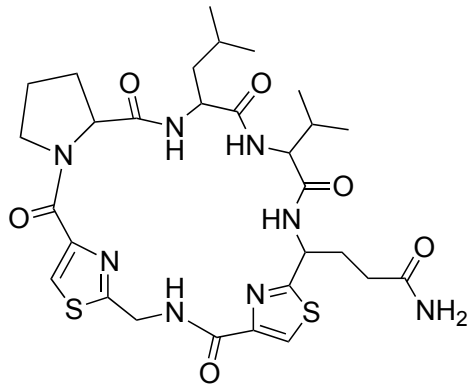

dolastatin 3

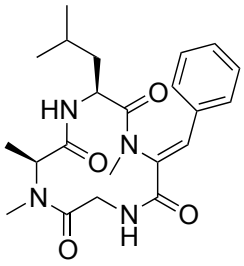

tentoxin

Fig. 1.18 examples of natural cyclic peptide: isolated from marine organisms (dolastatin 3), of earthly origin (tentoxin)

Some cyclopeptides are also fundamental in our body. For instance the hormone oxytocin (Fig. 1.19) is a neuromodulator, involved in sexual reproduction, maternal behaviours and social recognition, also called “love hormone”.[58,59]

Somatostatin (Fig. 1.19) is another very important cyclopeptidic hormone, which inhibits the secretion of compounds like the growth hormone and is involved in the treatment of hormone-related disorders.[60]

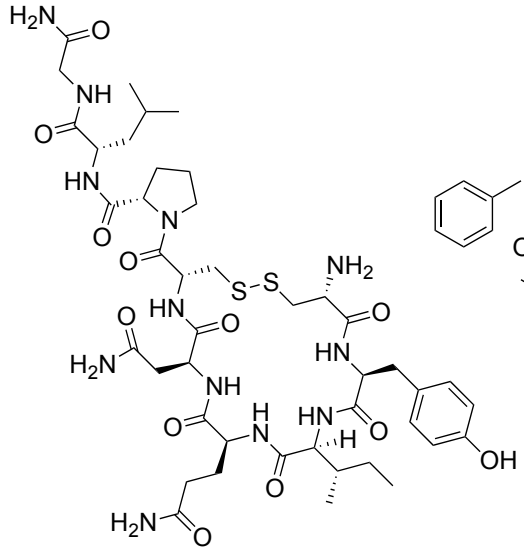

oxytocin

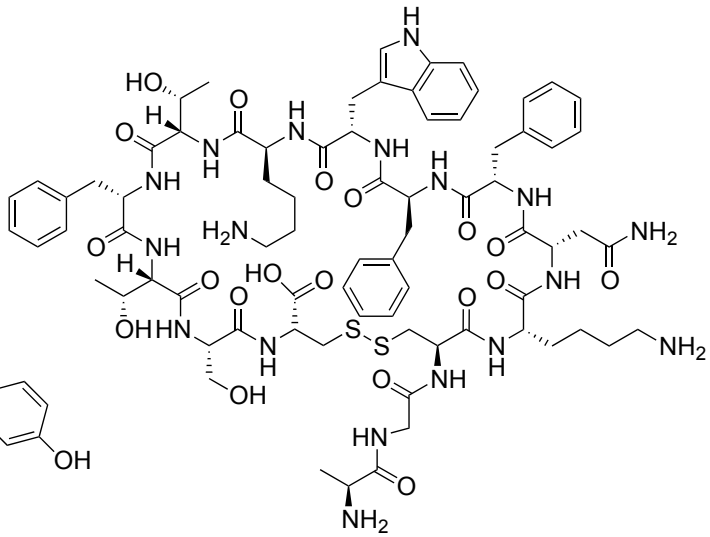

somatostatin

Fig. 1.19 examples of natural peptides in the human body

These natural molecules served as inspiration to generate new synthetic libraries of analogues and cyclic peptide-like compounds for biomedical purposes.

Unfortunately, when synthesising natural cyclic peptides analogues, the cyclisation step is difficult to achieve and often renders the overall synthesis challenging.[61]

A big contribution was made by Seebach in the field of biologically active natural cyclic tetrapeptides; for example he worked with β^3-peptides (namely peptides formed by α-unsubstituted-β-chiral-β-amino acids), cyclic molecules able to generate unnatural biopolymers able to adopt fascinating secondary structures like self-assembling transmembrane ion channels.[62-64] Such peptides assume flat conformations and interact together through extended hydrogen bonding between the backbones of two successive peptides generating tubular channel structures.

Cyclo[(-β^3-HTrp)$_4$-] and cyclo[(-β^3-HTrp-β-HLeu)$_2$-] were studied using liposome based proton transport assays and single channel conductance experiments by Ghadiri's group (Fig. 1.20) showing effective ion transport activity for K^+.[65]

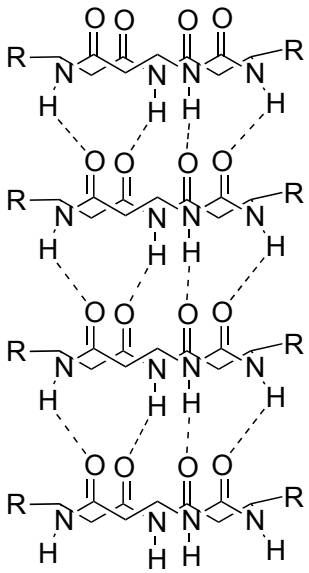

Fig. 1.20 example of self-assembling transmembrane ion channel

Other examples of synthetic cyclic peptides with diverse applications are octreotide, a somatostatin analogue and potent inhibitor of the growth hormone and tyroid-stimulating hormone,[66] and the pro-drug largazole and largazole thiol (Fig. 1.21).[67]

Peptides, and in particular cyclopeptides, are often studied in cancer research, as explained by Janin in his review.[68] In the article a large number of peptides are divided in five groups on the basis of their mechanism of action: compounds interacting with receptors, compounds interacting with nucleic acids, protein-protein interaction inhibitors, inhibitors of enzymes and proteins with mechanisms not known yet.

Examples of anticancer agents are apicidin analogues (Fig. 1.21), inhibitors of histone deacetylase (HDAC), falling within the category of enzyme inhibitors.[69,70]

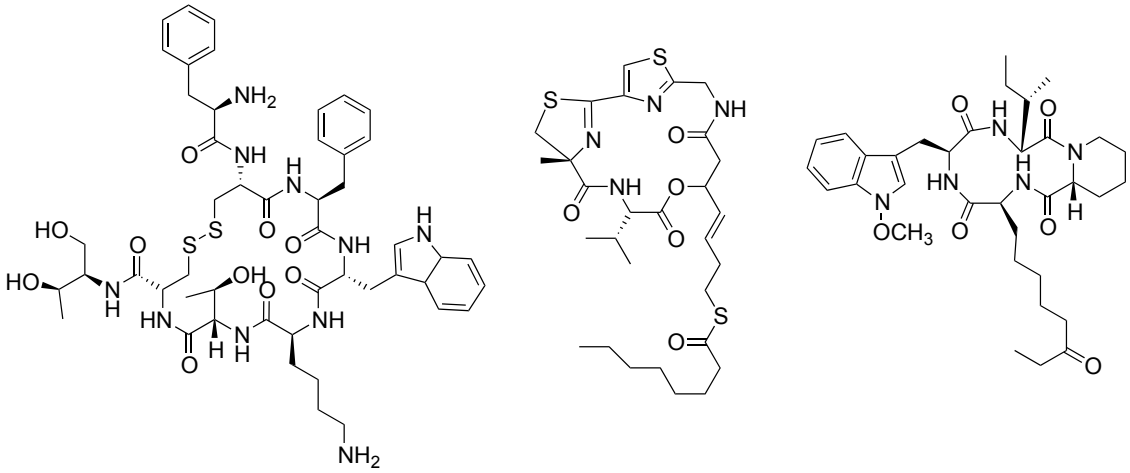

octreotide largazole apicidin

Fig. 1.21 examples of synthetic cyclic peptide drugs

Still in the area of medical application, Chia's group synthesised an analogue of cyclo-[Gly-Ser-Pro-Glu] (cyclo-[GSPE]), an antibacterial peptide from the marine bacteria strain *Ruegeria* using a solid support. This analogue is part of the category of the 12-membered head to tail cyclic tetrapeptides, rigid compounds present in nature and able to mimic reverse turns in solution. This characteristic gives them a role in molecular recognition for protein-receptor interactions.[71] From spectroscopic studies and calculations, they found three different

conformations, in a ratio 4:2:1, where the most abundant one is a reverse turn conformation with *cis-trans-cis-trans* pattern. This interesting behaviour was previously reported for this class of molecules when dissolved in hydrogen bond perturbing solvents such as water.[72]

Opioid cyclic peptides are often studied to find analogues with improved efficacy for pain relief.[47] Examples are analogues of endomorphins, mammalian endogenous opioid tetrapeptides found in the brain, with high affinity for the μ-opioid receptors. Few cyclic analogues were studied like ciclo[[cAmp]^{2}Endomorphin-2], where Pro^2 was substituted with *cis*-4-amino-L-Pro (cAmp) to allow the cyclisation[73] and ciclo[-Tyr-D-Pro-D-Trp-Phe-Gly-], which showed agonist properties (Fig. 1.22).[74,75]

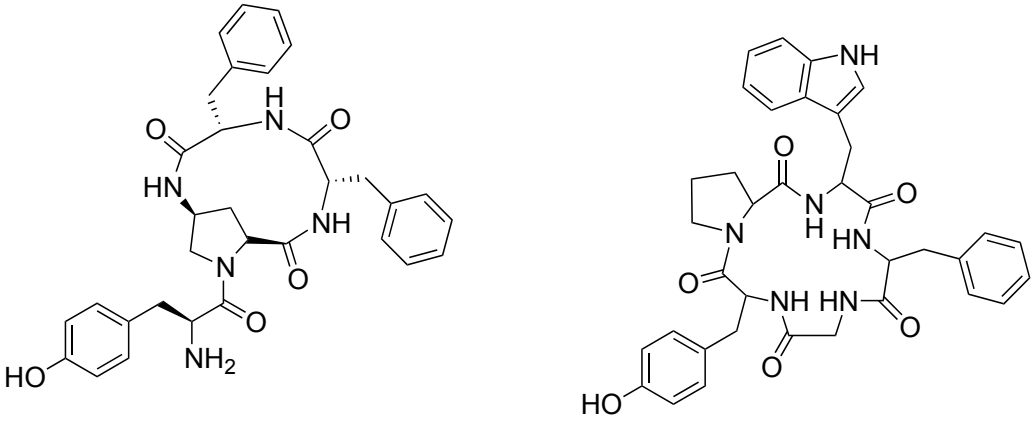

c[[cAmp]^{2}Endomorphin-2] c[-Tyr-D-Pro-D-Trp-Phe-Gly-]

Fig. 1.22 endomorphins analogues

For a completely different application, recently, Merck synthesised a RGD-like cyclic peptide formed by arginine, glycine, aspartate, D-phenylalanine and aminocyclohexan carboxylic acid. This compound is called “Ronacare® Cyclopeptide 5” and is the first cyclic and homodetic peptide (all the constituent amino acids are linked together covalently through peptide bonds) for cosmetic anti-age products. Its cyclic structure is ideal to better bind integrin receptors on the cell surface with high selectivity, mimicking natural processes for skin reparation. Integrins are cell adhesion molecules and regulate cell motility, growth and survival.[76,77]

Attractive applications for cyclopeptides are also found in the area of nanomaterial. In fact cyclic peptides can stack together through hydrogen bonding and serve as building block monomers for nanotubes,[78] with possible applications as drugs or as drug delivery agents.[79]

Cyclopeptides show interesting properties not only in their apo form, but also when coordinated to metal ions.

Cyclic peptide complexes have already been studied in the literature for various applications in different fields, such as diagnosis and therapies (scintigraphy and radiotherapy),[62] selective ligands,[80-82] and membrane ion transport.[83]

An interesting work in this regard was conducted by Ranganathan.[84] He built a number of non-natural cyclic peptides based on the model of valinomycin, a natural 36-membered cyclododecadepsipeptide, K^+ selective membrane ion carrier. Firstly he wanted to generate ball-like molecules, hydrophobic on the outside; he achieved this incorporating 2-5 small highly lipophilic molecules (e.g. adamantan) in alternation with amino acids (Fig. 1.23).

The results showed that the smallest macrocycle, with two adamantan molecules, is selective towards Na^+, while the one with three was more selective towards K^+ and the bigger ones were not very efficient in binding ions.

The next step was the synthesis of a different class of valinomycin analogues to mimic the depsipeptide structure (alternation of amides and esters) to increase flexibility and transport efficiency, using serine CH_2OH side chain to form the esters. Compounds in Fig. 1.16 and larger analogues with 3 adamantans resulted to be good transporters for Na^+, Mg^{2+} and Ca^{2+}.

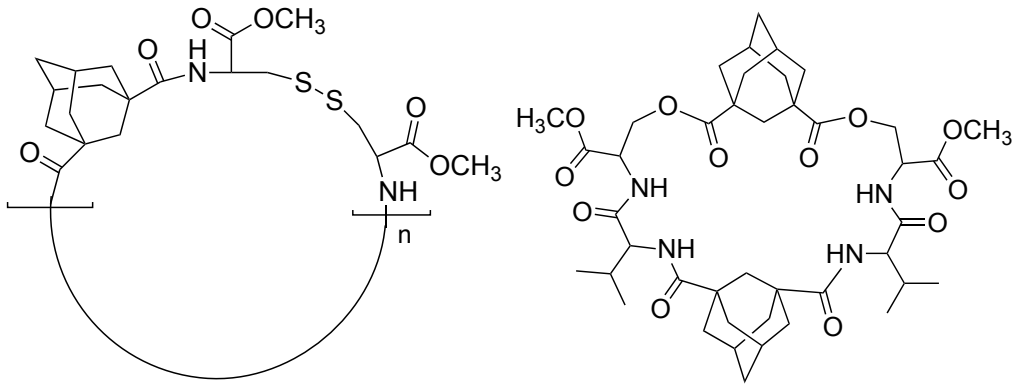

a) b)

Fig. 1.23 valinomycin analogues: a) amino acids alternated with lipophilic adamantan (n = 2-5) and b) serine-base cyclodepsipeptide

Other interesting results were obtained with aromatic cyclodepsipeptides (Fig. 1.24), exploiting cation π-interactions, as in the case of the hosts pyridinium and *N*-methyl acridinium ions.

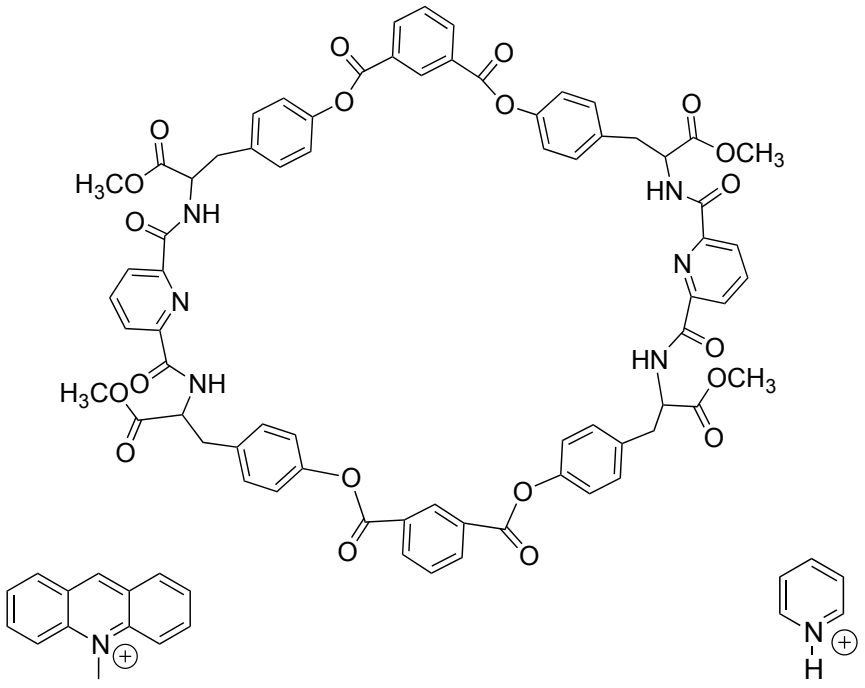

N-methyl acridinium pyridinium

Fig. 1.24 example of aromatic cyclodepsipeptides analogue of valinomycin and hosts

1.2.3-Synthetic approaches to cyclic peptides

Despite the great advantages and the wide range of applications of cyclic peptides, from drug discovery to nanomaterials, this class of molecules started to be thoroughly investigated only recently. This is especially due to the difficulties in their preparation, which sometimes is even impossible, using traditional techniques. Linear peptides, in order to cyclise, must adopt a conformation entropically unfavoured. Other factors that also influence the final cyclisation yield are ring size, peptide sequence and reaction conditions.[49] Especially for cycles of medium and small size, the geometry of the peptide at the energy ground state is not ideal to gain a closed conformation.

The cyclisation of peptides is typically achieved *via* amide bond formation connecting the C and N termini of a linear peptide in high dilutions, but this reaction does not work well for tetrapeptides and pentapeptides, due to the high energy barrier.[85] This problem is usually not present with larger peptides (more than seven amino acids), even though intermolecular reactivity issues can be still encountered.[51]

An example that clearly shows the difficulties with this class of compounds is the work of Schmidt and Langner, done in 1997. They attempted the synthesis of small natural peptides, four and five amino acids length, without any success, but obtaining instead dimerisation, trimerisation and epimerisation.[86]

There are four different possibilities of cyclisation for an open peptide: head to tail (connection between the C-terminus in one end of the open peptide and the N-terminus at the other end), head to side chain, side chain to tail and side chain to side chain (Fig. 1.25).

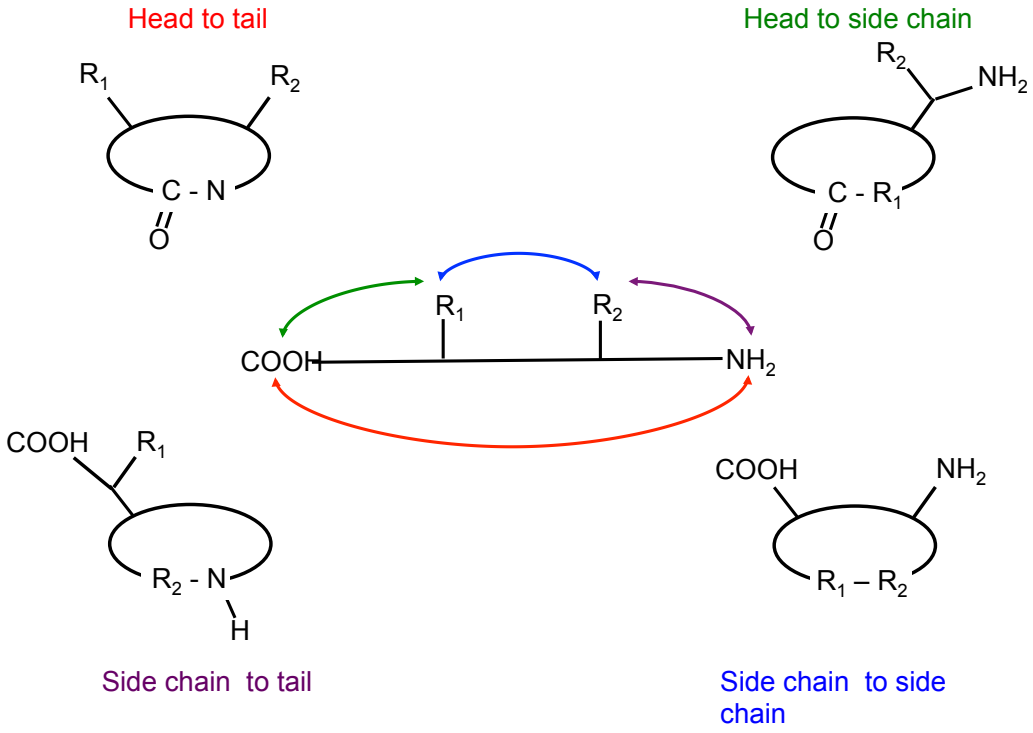

Fig. 1.25 the four ways in which peptides can cyclise

To build the cycle, a variety of coupling reagents have been used, from the classic carbodiimides, to triazole derivatives, to phosphate-based agents, to the more modern and more reactive uronium coupling reagent HATU, HBTU and COMU. The best results are generally obtained with HOAt-based reagents and especially HATU and the other new generation coupling reagents.[87,88]

A number of reactions can be selected for the final cyclisation of peptides, such as lactamisation,[89] lactonisation,[90] disulphide bridges[47,91] and condensation between glutamic or aspartic acid and lysine side chains.[92]

To avoid or, at least, minimise oligomerisation and polymerisation side reactions, macrocyclisations need to be carried out in high dilution conditions, usually at submillimolar concentration. To avoid inconvenient large volumes to work up and long reaction times that come with high dilution conditions, some tricks to create pseudo-dilution environment can be used, such as syringe-pumps[93] or anchoring the peptide to a solid support.[94,95] With this second methodology, the peptide has to be attached through a side chain, usually aspartic acid or glutamic acid carboxylate, and has to be cyclised in a head to tail fashion before cleaving it from the support[95]. Many examples of peptide

cyclisation on solid support have been reported, like Finn's cyclodimerisation using click chemistry.[96] Thakkar *et al*. studied on-resin cyclisation of medium and large size cycles (from cyclohexapeptides and above) using PyBOP as coupling reagent, which achieved quantitative yields for all the sequences, with negligible quantities of dimerisation.[49]

The most used type of peptide cyclisation is the head to tail method. The ring size could play an important role as well as the ring disconnection. In fact steric hindrance at the disconnection site can decrease the cyclisation yield, like in the case of *N*-alkyl, α,α-substituted or β-branched amino acids or when the two residues to couple have the same stereochemical configuration.[51]

Typically, in synthetic chemistry, the key to obtain the desired product is having the right balance between entropy and enthalpy. In particular for peptide cyclisation, the vicinity of the two reactive peptide edges increases the chance for the reaction to take place. For this reason, bringing the N- and C-termini near to each other, before the cyclisation step, lowers the activation energy barrier for the peptide closure. In order to render this pre-organised conformation possible, intramolecular interactions such as covalent bonds, H-bonding, electronic interactions need to be exploited.[87] The pre-organisation elements that take advantage from intramolecular interaction (mainly hydrogen bonds and transient β-sheet structures) are loops and reverse turns.[87,97] Unfortunately, these motives are not easily formed in short peptides since they do not have enough atoms in their chains and external help is needed.

Hydrogen-bonding plays a fundamental role in peptide secondary structure and conformation-directed macrocyclisation reactions.[98] The total synthesis of the antibiotic Ramoplanin A2 (Scheme 1.6) and the more recent synthesis of a library of analogues based on a 12 membered cyclic peptide using HATU, give good examples of their importance (Scheme 1.7). [87,99,100]

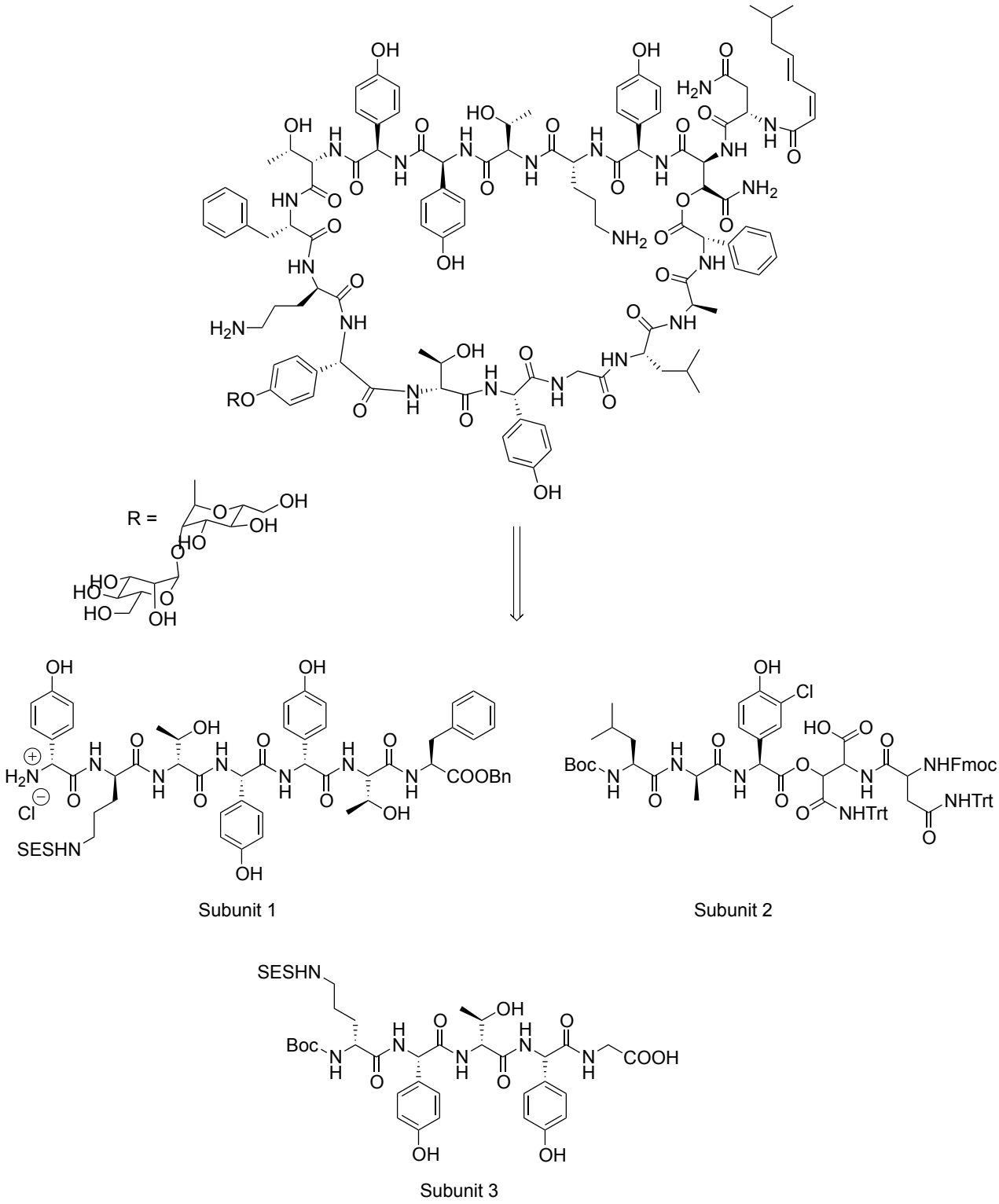

Scheme 1.6 retrosynthesis of the cyclic peptides ramoplanin A2

Ramoplanin A2 was built from three subunits assembled together. After their synthesis, subunit 1 and 2 were the most difficult to combine together. The carboxylate activation of the second subunit gave rather elimination of the acyloxy substituent, until the best option of DEPBT as coupling reagent was found. The reaction with the third subunit was performed using EDCI and HOAt after removal of the protecting groups. The final step of macrocyclisation was obtained using the same coupling reagent in good yields. The efficacy of the synthesis was probably due to the pre-organisation achieved through the careful insertion of β-sheets and a D-amine terminus, in addition to the hydrogen bond contribution.

In Chen's library (Scheme 1.7) the cyclisation step was possible also thanks to hydrogen bonds. These interactions played an important role in determining the different permeability properties of the analogues.[100]

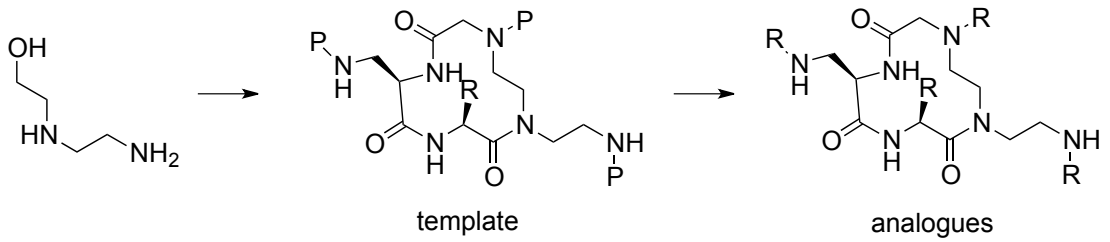

P = protecting group
R = functional group (benzyl, amide, sulphonamide, etc.)

Scheme 1.7 12 membered cyclic peptide template and analogues

As useful as hydrogen bonds, though less common, are π-interactions, which can play a pivotal role as in the case of cyclophane macrocycles synthesis.[101]

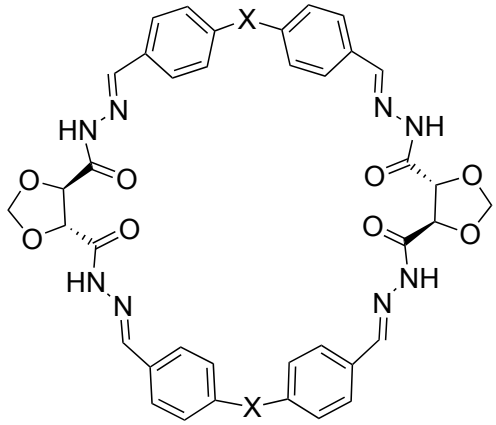

Fig. 1.26 cyclophane macrocycle synthesis exploiting π-interactions

As it can be noted in Fig. 1.26, the dicarbohydrazides prefer an anti-orientation. Computational calculations suggest the stabilisation by strong n → π* interactions and intramolecular H-bonds, which drive the reaction towards macrocyclisation rather than polymerisation. The macrocyclic product assumes, in solution, the favoured conformation through hydrogen bonding and π-π stacking.

There are different strategies to assist macrocyclisation through conformational pre-organisation, some could be defined “internal”, which involve covalent modifications and some other “external”, concerning molecular scaffolds.

An example of internal aid for loop formation is represented by the introduction of *cis*-amide bonds and D-amino acids in the peptide chain. Proline and Pro-mimetics are in fact often used for these purposes.[102,103]

An example of external element is represented by molecular imprinted cavities, reported by Tai and Lin (Fig. 1.27). Using high temperatures, linear peptides were induced to bind to the polymeric cavities and assume the less stable turned conformation before the cyclisation step.[104]

A polymeric template was employed, with cavities in which the linear peptide could bind to, through intermolecular interactions, assuming a forced loopy conformation to help cyclisation.

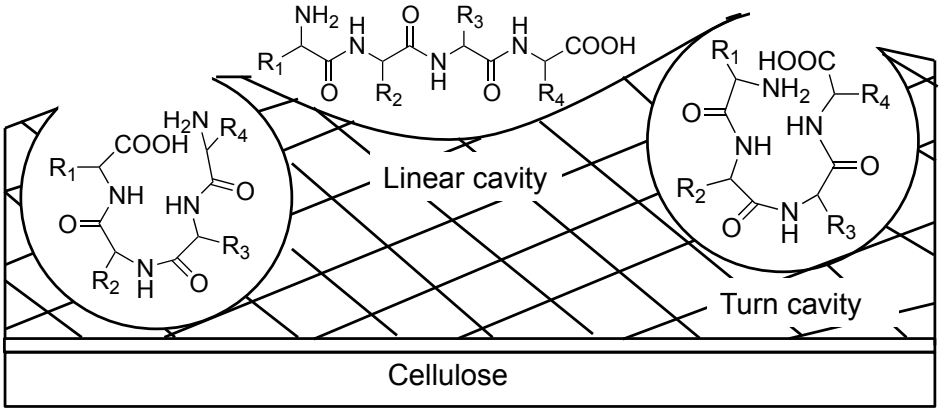

Fig. 1.27 peptide cyclisation driven by molecular imprinted cavities

Also templates such as cations, anions and uncharged organic molecules have often been used.[87] This technique takes inspiration from nature, where some cyclic peptides like gramicidin, valinomycin and anatamanide behaves as ionofores stably binding cations.[51]

Templates are able to organise the molecules in a way that favours the reaction, which would not happen or would not be efficient in its absence.[87]

One of the first works, where this method was adopted is explained by Beck *et al*. Two dipeptide esters were brought together through interaction with a metal ion (Ni^{2+}, Pd^{2+} and Cu^{2+}) aiding the nucleophilic attack of the amines to the esters in basic conditions and allowing the formation of the C_2-symmetric cyclic tetrapeptide. In order for this dimerisation to happen, the dipeptides need to coordinate to the metal centre in a trans manner (Scheme 1.8).[62,105]

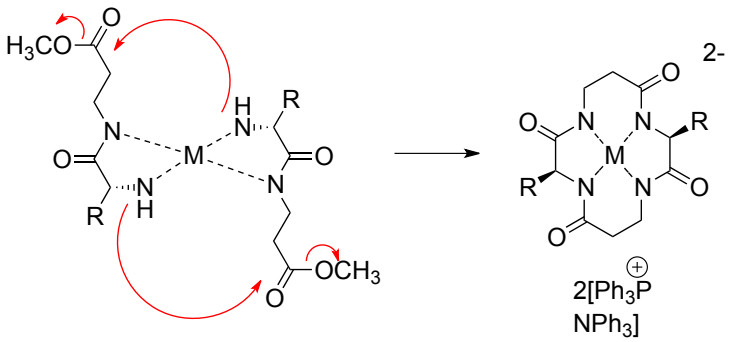

Scheme 1.8 macrocyclisation using templating metal ions: dipeptide dimerisation

Ye and co-workers showed instead that cyclisation of linear peptides can occur choosing a suitable metal, depending on the peptide size: Na^+ works better for pentapeptides, while the larger Cs^+ for heptapeptides.[106]

An entropically favoured method to obtain small macrocycles is the intramolecular ring contraction from a larger and easier to prepare cyclic peptide, usually as result of a *S*- to *N*-acyl rearrangement (Scheme 1.9).[87,107,108]

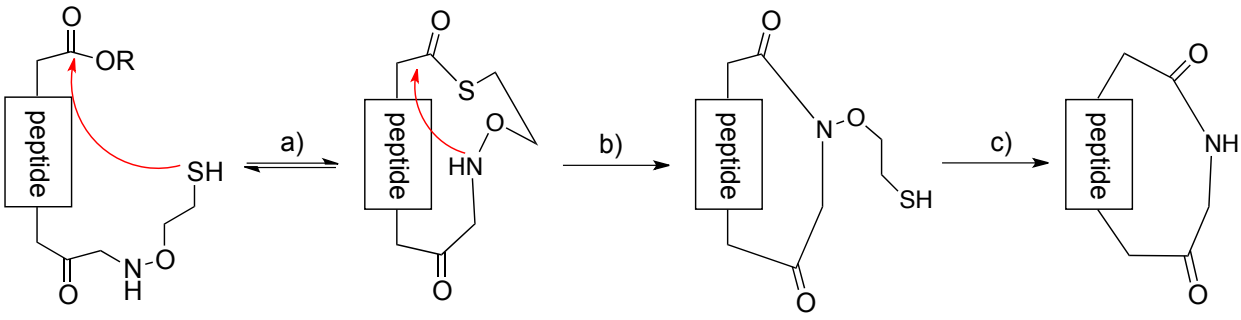

Scheme 1.9 *S*- to *N*-acyl rearrangement for peptide cyclisation; a) cyclisation at pH 7.5, b) *S*-*N* acyl rearrangement, c) Zn reduction

Despite the reversibility of this process, it is favoured over dimerisation or polymerisation since the macrothiolactone intermediate brings the N and C termini to be reacted close together in space, driving the acyl transfer.[3]

In Zhu's group they adopted the "substrate tailoring technique" using the formation of the heterocycle oxazole to drive the macrocyclisation reaction.[109] The favourable formation of the five membered ring oxazole lowers the entropic and enthalpic barrier allowing the macrocyclisation (Scheme 1.10).

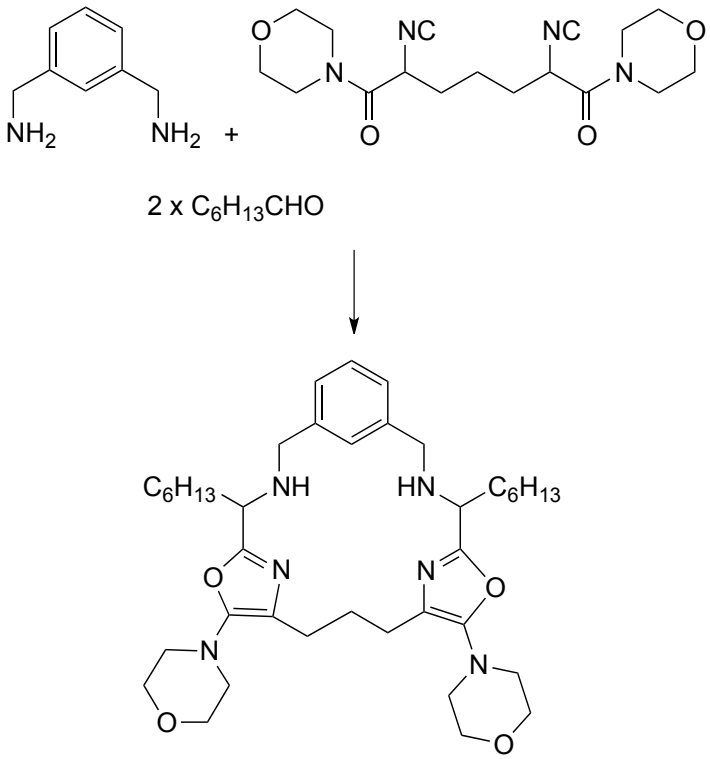

Scheme 1.10 substrate tailoring technique for macrocyclisation through formation of the heterocycle oxazole

Many other strategies have also been exploited for peptides and peptide-like cyclisation, with various levels of success,[51,87] among which the most interesting are activation of the carbonyl group with a thioester,[110,111] ring-closing metathesis,[112] electrostatically controlled[113] macrocyclisations[51] and others that have not been mentioned here.

1.3-Amino acid neurotransmitters and peptidomimetics

A field of research where peptidomimetics may be extensively employed is neurological disorders. In the brain, small molecules like amino acids have specific and very important functions, and at the same time can be involved in diseases. For this reason scientists are working to find mimetic compounds of these important molecules able to reproduce the same kind of activity with improved efficacy and selectivity.

A neurotransmitter is a chemical compound that transmits a signal between nerves, from the presynaptic neuron to the postsynaptic neuron, consequently to a nerve impulse.[114] This impulse, also called depolarisation or action potential, is due to the movement of ions through the voltage-gated ion channels and initiates the cascade of events that guarantees the signal transmission (Fig. 1.28).[115]

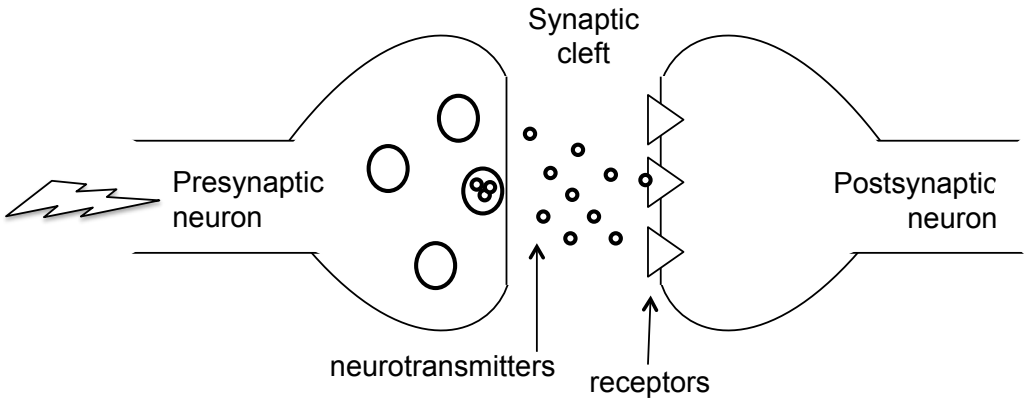

Fig. 1.28 schematic representation of a synapse

Neurotransmitters are found in synaptic vesicles in the axon terminal and they are released into the synaptic cleft and diffused after neuronal stimulation. Here they bind to specific receptors on the membrane of the postsynaptic site causing the propagation of the signal and consequently a biological effect.[116]
There are different classes of neurotransmitters such as monoamines (e.g. dopamine, norepinephrine, serotonin) and peptides (e.g. somatostatin, substance P, opioids), but among the most important we find amino acid

neurotransmitters.

Two main neurotransmitters in the mammalian central nervous system (CNS) are the amino acids L-Glutamic acid, which is responsible for excitatory synaptic transmission and γ-aminobutyric acid (GABA), responsible for inhibitory synaptic transmission. Other endogenous important amino acids are glycine and taurine, which are inhibitory neurotransmitters.[117,118] It is important to maintain a balanced chemical concentration of neurotransmitters to guarantee the neural activity in the brain; this principle in fact has widely been exploited in pharmacological modulation of behaviour, in therapies for emotional and affective problems, in cognitive and motor disturbances.[119] Neural activities that can be modulated interfering with this balance are arousal, attention, mood, learning, memory, motivation, sleep and dreaming.[120]

GABA is biosynthesised *via* enzymatic decarboxylation from glutamic acid and is involved in anxiety, insomnia, epilepsy, restlessness, aggressive behaviours and also in alcohol and drug addiction.[119]

For these reasons, many research groups are working on new GABA analogues which target GABA receptors with possible applications in the treatment of anxiety and depression, to name a few.

In this study, the synthesis of glutamic acid analogues is investigated because, unlike GABA, there are very few drugs in clinical trials despite its high involvement in brain functions and neurological diseases.

1.3.1-Glutamate

L-Glutamic acid (Glu) is one of the 20 proteinogenic amino acids and one of the main excitatory neurotransmitters in the mammalian CNS, involved in cognition, memory and learning.[121]

The majority of glutamate is contained in the cytosol of presynaptic vesicles in the brain nerve cells and only a minimal fraction is outside (4 μM), for a total of 5-10 mmol per Kg (wet weight).[122] The highest concentration is found inside nerve terminals.[123]

Compared to the cerebrospinal fluid, plasma has a high level of glutamate because the blood-brain barrier prevents direct transfer of glutamate to the brain.

Depolarisation of the presynaptic neuron stimulates glutamate exocytosis and activation of receptors. Receptor activation occurs when glutamate binds to their active site. This process is very quick thus, as soon as the neurotransmitter detaches from the receptor, it needs to be inactivated to avoid further stimulation, which would lead to dangerous hyperactivation of the receptor (excitotoxicity: glutamate toxic extracellular concentration > 10 μM). The concept of excitotoxicity if often associated with neurodegenerative diseases.

Nerve cells die because glutamate chronically activates its receptors, especially *N*-methyl-D-aspartate (NMDA) receptors, leading to a rise in intracellular calcium concentration with consequent mitochondrial damage and irreversible disruption of intracellular homeostasis.[124]

For this reason the glutamate concentration needs to be kept low, not only to avoid excitotoxicity, but also to allow a high signal-noise ratio for the signal transmission.

The main pathway for inactivation of glutamate is removal from the extracellular fluid *via* transporter proteins, present in neurones and glial cells (supportive and protective cells for neurons).

An alternative could be diffusion, but it works quickly only for very short distances (a few hundred nanometres) and for low extracellular glutamate concentration. Thus, glutamate uptake is the mechanism responsible for the

long-term maintenance of low extracellular glutamate levels and therefore responsible for protection of the neurones from excessive extracellular glutamate.

Like glutamate, glutamate transporters are also involved in neurological diseases; in fact transporter malfunctioning is closely correlated with brain dysfunction such as cerebral ischemia, hypoglycaemia, amyotrophic lateral sclerosis, Alzheimer's disease, traumatic brain injury, epilepsy and schizophrenia.

1.3.2-Glutamate receptor proteins

Glutamate receptor proteins are ion channels permeable to cations (conduction of Na^+ or both Na^+ and Ca^{2+}) and for this reason they are referred to as ionotropic glutamate receptors.[125,126]

Structures of natural glutamate analogues able to activate these receptors are shown in figure 1.29.

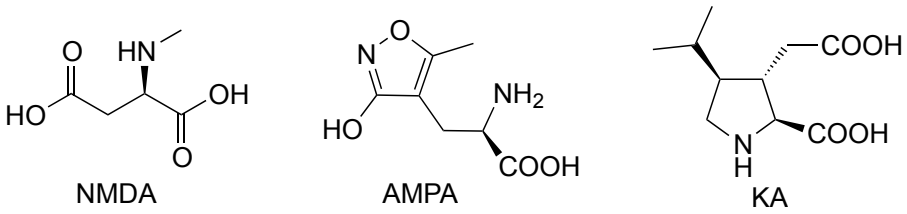

Fig. 1.29 glutamate receptors agonists: *N*-methyl-D-aspartate (NMDA), α-amino-3-hydroxy-5-methyl-4-isoxazole propionic acid (AMPA), kainic acid (KA)

Many research groups focus their attention on glutamate analogues able to inhibit or enhance the interactions with the receptors, hence the signal transmission. However, so far very few compounds were found to be effective and progressed into clinical trials. The molecules synthesised in this thesis will be tested for their interaction with glutamate transporter proteins rather than the receptors.

1.3.3-Glutamate transporter proteins

Glutamate transporter proteins are present in both neurons and glial cells, but the majority of the transport takes place into the latter, therefore, only transporters present in glial cells are of interest for this study.

In glial cells, Glu transporter proteins are found in the plasma membranes. There are two categories of plasma membrane glutamate transporters, high affinity (Na^+ dependent, K_m = 1-100 μM) and low affinity (Na^+ independent, K_m > 500 μM).[123]

High affinity glutamate transporters are driven by the gradients of Na^+ and K^+ (1 K^+ ion is exchanged for 3 Na^+ ions and 1 H^+) [127] and for this reason they are also called sodium dependent glutamate transporters or simply excitatory amino acid transporters (EAATs). They are divided in five groups, but only EAAT1 and EAAT2 are present in glial cells. Their mechanism of action is reported in Fig. 1.30.

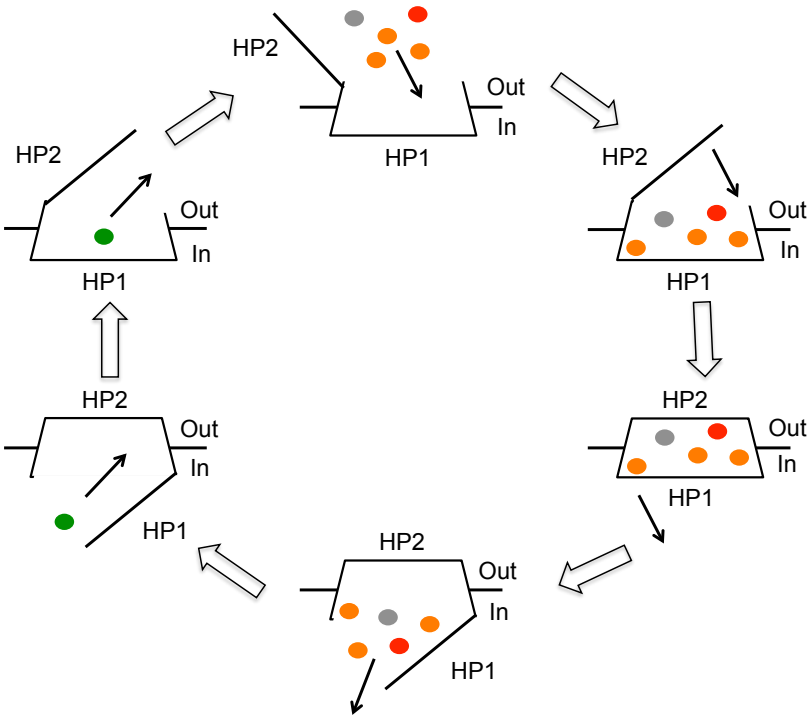

Fig. 1.30 mechanism of action of EAATs (Glu is red, Na^+ orange, H^+ grey, K^+ green). The first step consists of 1 Glu, 3 Na^+ and 1H^+ binding to the facing outward open transporter. After the binding, the gate hairpin 2 (HP2) closes the transporter and the inward facing gate haiprpin 1 (HP1) opens up letting Glu, Na^+ and H^+ into the cell. K^+ binds to the transporter generating a conformational change so to close HP1 and open HP2. The K^+ ion is finally released extracellularly and the transporter is ready to start the cycle again[128]

1.3.4-Glutamate metabolism

Glutamate is synthesised *de novo* from glucose and glutamine (Gln) in both glial cells and neurones.[129] In glial cells glutamate is recycled *via* the glutamine-glutamate cycle (Fig. 1.31): the uptaken glutamate is transformed in glutamine by the ATP-dependent enzyme glutamine synthetase. After being released into the extracellular fluid, glutamine goes into neurons where is re-converted into glutamate by the enzyme glutaminase.

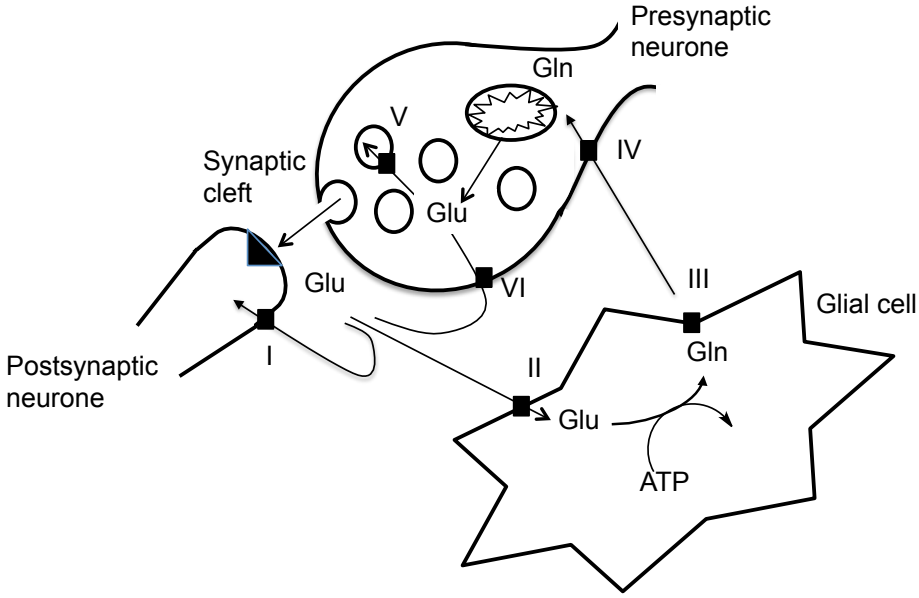

Fig 1.31 glutamine-glutamate cycle steps: Glu exocytosis from nerve terminal (ATP and Ca^{2+} dependent); Glu uptake by presynaptic (VI), postsynaptic (I) and extrasynaptic (glial cells) (II) glutamate transporters; conversion of Glu to glutamine in glial cells (glutamine synthetase; ATP-dependent process); glutamine release from glial cell *via* glutamine transporter (III); glutamine conversion to Glu in neurones (glutaminase); Glu loading into synaptic vesicles *via* vesicular glutamate transporter (V) [123]

Once inside the cell, glutamate can be reused for different purposes such as signal transmission and for metabolic processes (protein synthesis, energy metabolism, ammonia fixation). Furthermore, glutamate is involved in the synthesis of folic acid, GABA and glutathione.[123,130]

The latter, in particular, is a fundamental molecule for cell survival. Glutathione (L-γ-glutamyl-L-cysteinyl-glycine, GSH, Fig 1.32) is formed from the three amino acids glutamic acid, cysteine, glycine, and is an important antioxidant in living cells.

Glutamate is involved in the synthesis of GSH *via* the cystine-glutamate exchanger (X_c^-), a sodium independent, chloride dependent protein.[131,132] The main function of this low affinity protein, firstly described by Bannai in the 1980s, is to exchange stoichiometrically one molecule of intracellular glutamate for one molecule of extracellular cystine (oxidised form of cysteine: Cys-S-S-Cys, Fig. 1.32) through the cell membrane.[133,134]

Cysteine gets oxidised very easily to cystine and the oxidising conditions

present extracellularly favour the occurrence of this process, while the opposite happens inside the cell, where the main form is cysteine. Intracellular free cysteine is however kept low to avoid the risk of auto-oxidation, which would perturb the redox balance.[135]

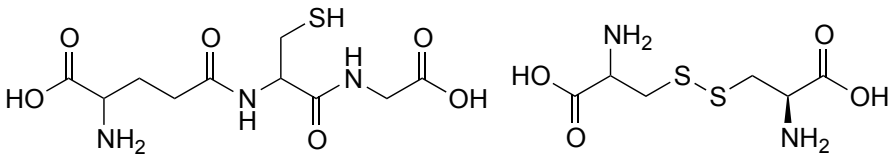

glutathione cystine

Fig. 1.32 cystine and glutathione chemical structures

Cystine is reduced to cysteine intracellularly and for this reason its concentration inside the cell is very low. On the contrary, the concentration of glutamate is higher inside the cell than outside. This trans-membrane gradient provides the driving force for the uptake of cystine and no electrochemical sodium gradient is needed (Fig. 1.33).[123,134,136,137]

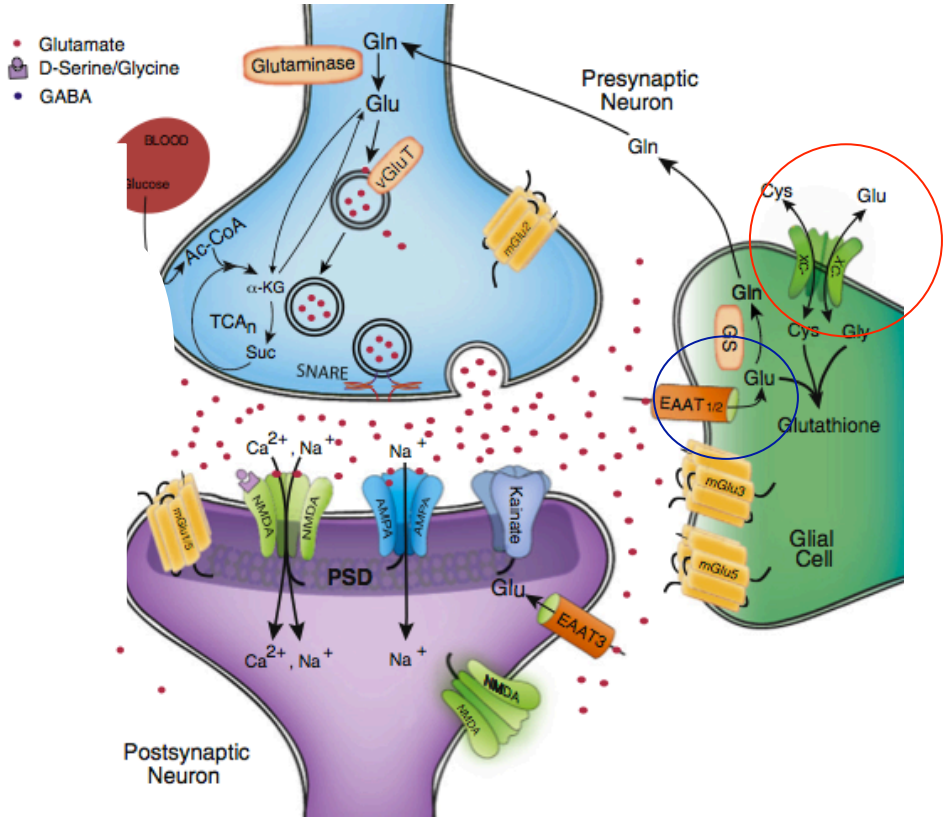

Fig. 1.33 glutamate and its metabolism in neurons and glial cells;[138] in the glial cell the high affinity glutamate transporter (orange protein circled in blue) and cystine glutamate exchanger (green protein circled in red) are highlighted*

Cystine is the primary source of cysteine, which is necessary for different functions, the most important being the biosynthesis of glutathione *via* the γ-glutamyl cycle.[139] Glial cells are responsible for cystine uptake through X_c^- antiporter and GSH synthesis. High affinity glutamate transporter proteins work in fact in cooperation with the cystine-glutamate exchanger, recycling the glutamate released extracellularly by the latter and avoiding excitotoxicity. A too high concentration of extracellular glutamate would result in inhibition of cystine-glutamate exchangers, due to competition of extracellular glutamate with cystine and therefore inhibition of glutathione synthesis. Low levels of glutathione can cause derangement of brain functions and eventually result in cell death.[140]

* Reprinted from The Journal of Pharmacology & Therapeutics, Vol. 132, Issue 3, C. Pittenger, M. H. Bloch, K. Williams, "Glutamate abnormalities in obsessive compulsive disorder: Neurobiology, pathophysiology, and treatment", pag. 318, copyright 2011, with permission from Elsevier

Since EAATs provide the intracellular glutamate used by the X_c^- for the exchange with cystine, inhibition of the Glu transporter has also an inhibitory effect on the exchanger.[131,141] Glutamate can be experimentally used as a substrate for X_c^- in place of cystine (avoiding the problem of reduction to cysteine) and cystine has been proven to be a low affinity substrate for the high affinity Glu transporters (however, this does not provide a pathway for cystine uptake due to the too low affinity compared to glutamate).[135]

1.3.5-Glutamate in diseases

1.3.5.1-Diseases involving EAATs

The involvement of glutamate and its receptors in nervous system disorders has been recognised for more than 40 years. Over the years an increasing number of studies have demonstrated the neurotoxicity of excitatory amino acids and only in the late 1980s glutamate receptor antagonists experiments started to show some activity, but no cure for neural diseases has yet been discovered.[122]

There are several mechanisms that can contribute to glutamate-mediated toxicity in neurons, for example over-activation of glutamate receptors. The overproduction can be caused by stress, acute neurological disorders as trauma and ischemia[142-144] and by chronic neurodegenerative diseases such as Parkinson's, Alzheimer's and Huntington's.[130,145-147]

Under brain pathological conditions or cellular injury, like stroke, trauma, multiple sclerosis and meningitis, there may be problems associated with the blood-brain barrier and the concentration of cerebrospinal glutamate can rise from 1 μM up to 20 μM.[14,129]

Another factor that could produce an increase in extracellular glutamate is sodium-dependent glutamate reverse transport. This behaviour can happen for instance in ischemia, where cellular ion gradients are compromised.[129] Also cysteine-glutamate exchangers release big quantities of glutamate due to up-regulation of the X^-_c exchanger in malignant glioma cells.[141]

It has been reported that old people have a lower expression of a specific EAAT and lower glutamate uptake and this decline seems to be more enhanced in the case of Alzheimer's disease.[122]

Amyotrophic lateral sclerosis is a common disease that provokes the loss of motor neurons in adults and progressively brings to paralysis and eventually death within 5 years. Although the precise mechanism is not known, it is believed that in this pathology, mitochondrial dysfunction leads to increased Ca^{2+} concentration and release of reactive oxygen species that inhibit glial EAATs, disrupting the glutamate clearance.[122,148]

Another motor dysfunction is Parkinson's disease, which is caused by degeneration of the nigrostriatal dopamine neurons. L-DOPA therapy is the classical treatment for Parkinson's disease, but newer therapies are aimed at the glutamate-mediated cell death; main approaches are blocking glutamate receptors or activation of glutamate transporters, like in the case of the drug riluzole (Fig. 1.34).[122,149]

Voutsinos-Porche's and other studies reported that seizures can occur as a consequence of down-regulation of glutamate transporters.[150] Some cures for epilepsy in fact up-regulate glutamate transporters. An example is the drug carbamazepine (Fig. 1.34).[151]

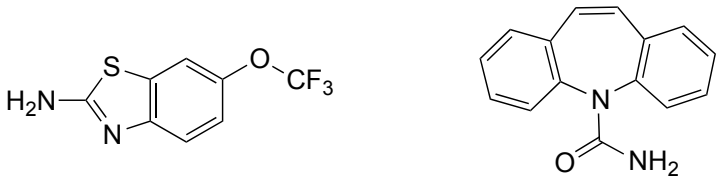

riluzole carbamazepine

Fig. 1.34 riluzole and carbamazepine chemical structure

Excitotoxicity may also be involved in alcoholism or alcohol withdrawal, hypoglycaemia and schizophrenia.[152-156]

To date, a wide range of glutamate analogues have been synthesised, studied and tested towards different glutamate receptors and transporters.

In some cases, basic modifications have been made on the glutamate backbone to improve the selectivity, for instance introducing substituents in the 4-position, such as simple methyl or larger structures as *N*-2,2-diphenylethyl-2-

aminocarboxyethyl group.[128]

The inclusion of cyclic structures is one of the most commonly employed ways to give rigidity to the molecule and consequently increase the selectivity towards the target of interest. Different ring sizes can be found in the literature (e.g. cyclopropane, cyclopentane), but here are reported some examples containing cyclobutane, which is the most interesting ring for this thesis purposes (Fig. 1.35).[123]

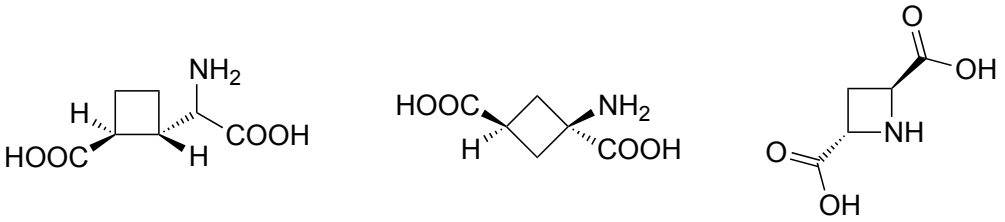

L-CBG ACC azetidine containing analogue

Fig. 1.35 glutamate analogues containing cyclic structures; where L-CBG = L-2-(2-carboxycyclobutyl) glycine, ACC = 1-aminocyclobutane-1,3-dicarboxylate

Examples are L-2-(2-carboxycyclobutyl) glycines (L-CBGs). The four stereoisomers L-CBG-I, L-CBG-II, L-CBG-III and L-CBG-IV were found to be active against EAATs.[157] Other examples of active cyclic glutamate analogues are 1-aminocyclobutane-1,3-dicarboxylate (ACC), which were synthesised by different groups.[158,34,37]

Interesting analogues containing azetidine 1,2- and 1,3-dicarboxylic acid were synthesised through Wittig olefination as a key step, followed by stereoselective rhodium catalysed hydrogenation.[159]

All the compounds mentioned so far have the common characteristic of being α-amino-dicarboxylic acids with the acid groups usually separated by 2-3 methylenes. It is generally believed that these features shouldn't be changed to allow interaction with the receptors and only some variations in the structure could be allowed at the distal carboxyl group, like derivatisation, replacement, inclusion of the α-amino group in the cyclic structure and modifications at the carbon skeleton.[123]

More recently, however, new types of glutamate analogues without the second carboxylic acid moiety have been investigated (Fig. 1.36).

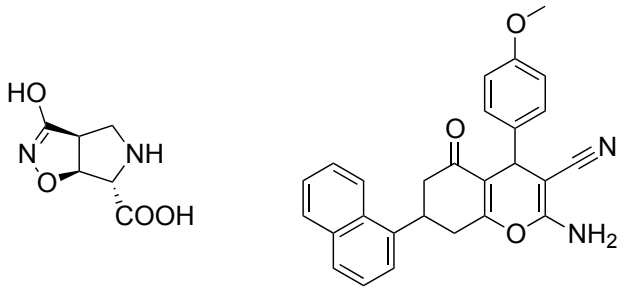

(+)-HIP-B UCPH-101

Fig. 1.36 glutamate analogues non-dicarboxylic acid; where (+)-HIP-B = (+)-3-hydroxy-4,5,6,6a-tetrahydro-3a*H*-pyrrolo[3,4-*d*]-isoxazole-6-carboxylic acid, UCPH-101 = 2-amino-4,7-diaryl-5-oxo-tetrahydro-4*H*-chromene-3-carbonitriles

In 2012 Callender *et al*. published the work on the new compound (+)-3-hydroxy-4,5,6,6a-tetrahydro-3a*H*-pyrrolo[3,4-*d*]-isoxazole-6-carboxylic acid ((+)-HIP-B), active as EAAT3 inhibitor.[160] Another example is 2-amino-4,7-diaryl-5-oxo-tetrahydro-4*H*-chromene-3-carbonitriles (UCPH-101), considered one of the best EAAT1 selective inhibitors discovered in the recent years.[128]

In contrast with the majority of the compounds seen so far, there is a different class of glutamate analogue, able to increase the protein transporter ability (Fig. 1.37).

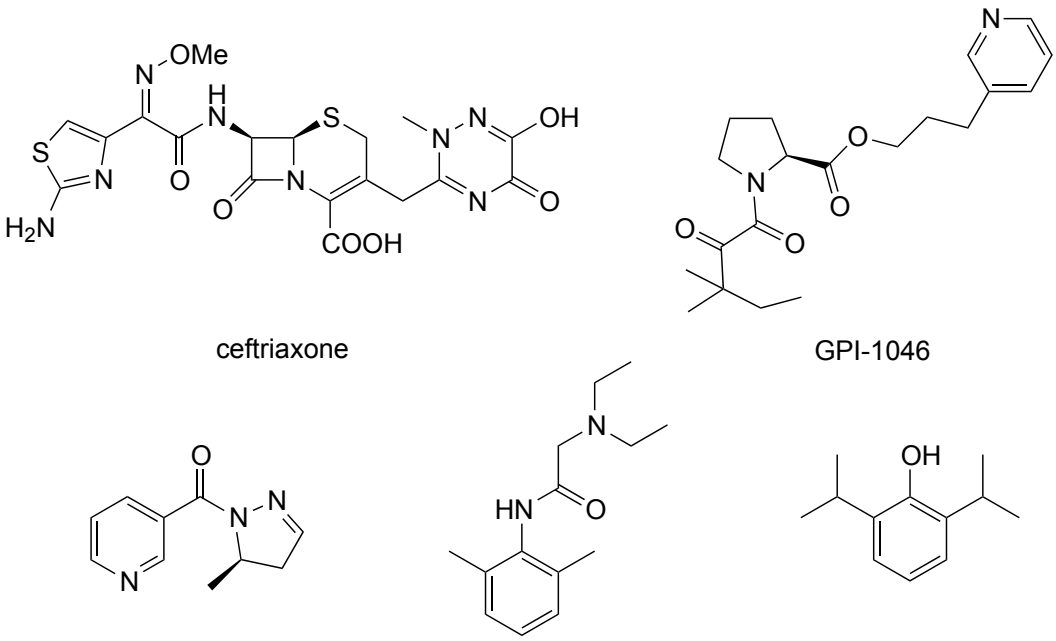

ceftriaxone GPI-1046

MS-153 lidocaine propofol

Fig. 1.37 some examples of glutamate analogues that enhance the activity of EAATs, where GPI-1046 = (*S*) -3-(pyridin-3-yl) propyl 1-(3,3-dimethyl-2-oxopentanoyl) pyrrolidine-2-carboxylate; MS-153 = (*R*) -(5-methyl-4,5-dihydro-1*H*-pyrazol-1-yl) (pyridin-3-yl) methanone[128]

Excitatory amino acid transporters are sensitive to changes in oxygen/energy level changes and they easily fail to work in abnormal brain conditions. Thus it is important to have drugs able to increase the uptake of excitotoxic glutamate in neurotoxic/neurodegenerative circumstances, making the damaged transporter work again.

Furthermore, in a limited number of cases, the origin of psychiatric disorders may be hypofunction of glutamatergic signaling. In fact, encouraging results on depression have been obtained after increasing synaptic Glu uptake.[128,161,162]

There are two different ways of enhancing the transporter activity: by increasing its expression (at a transcriptional, translational or posttranslational level) or by direct interaction at the level of the protein.

Only a small number of molecules are able to directly interact with the transporters. An example is the approved drug for amyotrophic lateral sclerosis, previously mentioned, riluzole (Fig 1.34), which unfortunately is not selective.

1.3.5.2-Diseases involving X_c^-

Recently, the cystine-glutamate exchanger dysfunction has been implicated in a number of diseases, above all in tumour growth, but has also been proposed as a source of glutamate dysregulation in brain disorders.[123,132] These proteins may also play a role in drug addiction, where a decrease in cystine-glutamate exchange has been registered with increased glutamergic transmission.[163]

The only way for tumours to expand in the brain is to kill other cells. In order to do so and be able to proliferate, glioma cells (a type of tumour developed in glial cells in which the cystine-glutamate exchanger is up-regulated) release excitotoxic glutamate through X_c^-.[131] This abnormal release of Glu in exchange for cystine, allows for extra production of GSH, which gives the tumour cells greater protection and resistance to reactive radicals and also to radiation, chemotherapy and other standard anti-cancer therapies. Effective strategies have not been found yet and are urgently needed.[135]

It has been shown by Sato *et al*. that tumour necrosis enhances the sodium independent cystine transporter in mouse peritoneal macrophages.[123,164] This continuous glutamate release causes a change in the glutamate gradient and therefore forces an inverse behaviour of the exchanger which recycles glutamate and takes it up instead of cystine resulting in decreased levels of glutathione production.[123,141]

X_c^- exchangers are good targets for cancer therapy, where it is possible to find selective drugs exploiting the differences in tumour cells with healthy cells. Analogues of glutamate and cystine have already been identified (e.g. L-homocysteate, L-quisqualate, L-α-aminoadipate, 4-carboxyphenylglycine).[135]

Inhibition of X_c^- would reduce cystine uptake and GSH production and furthermore, would reduce glutamate excitotoxicity, decreasing tumour growth and rendering tumour cells more susceptible to chemotherapy.[131,135] Inhibitors have to be non-substrate, otherwise glutamate would still be released extracellularly. However, this technique seems to impact more on extracellular Glu than intracellular GSH and therefore it would be more promising in the treatment of CNS malfunctions, than for tumour cure.[148]

An interesting example of a drug acting on the X_c^- is sulfasalazine (Fig. 1.38),

which acts on the glutamate antiporter decreasing GSH and tumour propagation.[163]

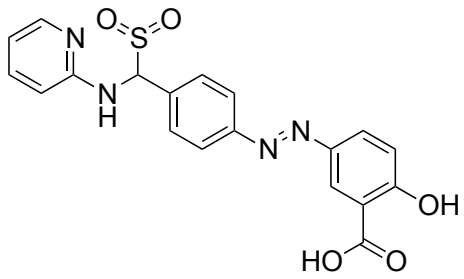

Fig. 1.38: sulfasalazine chemical structure

Despite the numerous efforts of researchers all over the world in finding effective glutamate analogues to target high affinity glutamate transporter and cystine/glutamate exchanger proteins, a specific cure to neurological disorders in which excitotoxicity is involved, has not been found so far. For this reason it is important to keep working in this field in order to find selective inhibitors/activators.

1.4-Bibliography

(1) Serendipity. In *Collins English Dictionary - Complete and Unabridged* © HarperCollins Publishers, 2003.

(2) Holme, I.: Sir William Henry Perkin: a review of his life, work and legacy. *Coloration Technology* **2006**, *122*, 235-251.

(3) Gante, J.: Peptidomimetics - tailored enzyme-inhibitors. *Angewandte Chemie. International edition in English* **1994**, *33*, 1699-1720.

(4) Giannis, A.; Kolter, T.: Peptidomimetics for Receptor Ligands-Discovery,Development, and Medical Perspectives. *Angewandte Chemie International Edition in English* **1993**, *32*, 1244-1267.

(5) Boger, D. L.; Labroli, M. A.; Marsilje, T. H.; Jin, Q.; Hedrick, M. P.; Baker, S. J.; Shim, J. H.; Benkovic, S. J.: Conformationally restricted analogues designed for selective inhibition of GAR Tfase versus thymidylate synthase or dihydrofolate reductase. *Bioorganic & Medicinal Chemistry* **2000**, *8*, 1075-1086.

(6) Smith, A. B.; Keenan, T. P.; Holcomb, R. C.; Sprengeler, P. A.; Guzman, M. C.; Wood, J. L.; Carroll, P. J.; Hirschmann, R.: Design, synthesis, and crystal structure of a pyrrolinone-based peptidomimetic possessing the conformation of a .beta.-strand: potential application to the design of novel inhibitors of proteolytic enzymes. *Journal of the American Chemical Society* **1992**, *114*, 10672-10674.

(7) Fuller, A. A.; Holmes, C. A.; Seidl, F. J.: A fluorescent peptoid pH-sensor. *Peptide Science* **2013**, *100*, 380-386.

(8) Chou, K.-C.: Prediction of Tight Turns and Their Types in Proteins. *Analytical Biochemistry* **2000**, *286*, 1-16.

(9) De Marco, R.; Tolomelli, A.; Campitiello, M.; Rubini, P.; Gentilucci, L.: Expedient synthesis of pseudo-Pro-containing peptides: towards constrained peptidomimetics and foldamers. *Organic & Biomolecular Chemistry* **2012**, *10*, 2307-2317.

(10) De Marco, R.; Greco, A.; Rupiani, S.; Tolomelli, A.; Tomasini, C.; Pieraccini, S.; Gentilucci, L.: In-peptide synthesis of di-oxazolidinone and dehydroamino acid-oxazolidinone motifs as [small beta]-turn inducers. *Organic & Biomolecular Chemistry* **2013**, *11*, 4316-4326.

(11) Wiberg, K. B.: *The chemistry of cyclobutanes, chapter 1*; John Wiley & Sons, Ltd, 2005.

(12) Dembitsky, V.: Bioactive cyclobutane-containing alkaloids. *Journal of Natural Medicines* **2008**, *62*, 1-33.

(13) Eder, C.; Proksch, P.; Wray, V.; van Soest, R. W. M.; Ferdinandus, E.; Pattisina, L. A.; Sudarsono: New Bromopyrrole Alkaloids from the Indopacific Sponge Agelas nakamurai. *Journal of Natural Products* **1999**, *62*, 1295-1297.

(14) O'Malley, D. P.; Li, K.; Maue, M.; Zografos, A. L.; Baran, P. S.: Total Synthesis of Dimeric Pyrrole,àíImidazole Alkaloids: Sceptrin, Ageliferin, Nagelamide E, Oxysceptrin, Nakamuric Acid, and the Axinellamine Carbon Skeleton [J. Am. Chem. Soc. 2007, 129, 4762,àí4775]. *Journal of the American Chemical Society* **2007**, *129*, 7702-7702.

(15) Hughes, P.; Clardy, J.: Total synthesis of cyclobutane amino acids from Atelia herbert smithii. *The Journal of Organic Chemistry* **1988**, *53*, 4793-4796.

(16) Bell, E. A.; Qureshi, M. Y.; Pryce, R. J.; Janzen, D. H.; Lemke, P.; Clardy, J.: 2,4-Methanoproline (2-carboxy-2,4-methanopyrrolidine) and 2,4-methanoglutamic acid (1-amino-1,3-dicarboxycyclobutane) in seeds of Ateleia herbert smithii Pittier (Leguminosae). *Journal of the American Chemical Society* **1980**, *102*, 1409-1412.

(17) Maki, Y.: Lycopodium alkaloids. *Gifu Yakka Daigaku Kiyo* **1961**, *11*, 1-8.

(18) Manske RHF, M. L.: The alkaloids of Lycopodium species. III. Lycopodium annotinum L. *Can J Res* **1943**, *21B*, 92–96.

(19) Ichikawa, M.; Takahashi, M.; Aoyagi, S.; Kibayashi, C.: Total Synthesis of (-)-Incarvilline, (+)-Incarvine C, and (-)-Incarvillateine. *Journal of the American Chemical Society* **2004**, *126*, 16553-16558.

(20) Moore JM; Casale JF; Klein RFX; Cooper DA; J, L.: Determination and in-depth chromatographic analyses of alkaoids in South American and greenhouse-cultivated coca leaves. *J Chromatogr* **1994**, *659*, 163–175.

(21) Boutureira, O.; Matheu, M. I.; Diaz, Y.; Castillon, S.: Advances in the enantioselective synthesis of carbocyclic nucleosides. *Chemical Society Reviews* **2013**, *42*, 5056-5072.

(22) Lee-Ruff, E.; Mladenova, G.: Enantiomerically Pure Cyclobutane Derivatives and Their Use in Organic Synthesis. *Chemical Reviews* **2003**, *103*, 1449-1484.

(23) Bellus, D. E., B: Cyclobutanones and cyclobutenones in nature and in synthesis. *Angew. Chem. Int. Ed. Engl.* **1988**, *27*, 797- 827.

(24) Namyslo, J. C.; Kaufmann, D. E.: The Application of Cyclobutane Derivatives in Organic Synthesis. *Chemical Reviews* **2003**, *103*, 1485-1538.

(25) Nemoto, H.; Ishibashi, H.; Mori, M.; Fujita, S.; Fukumoto, K.: Ring expansion of cyclopropylmethanols to cyclobutanes-an enantioselective total synthesis of (*R*)-(+)-dodecan-5-olide, and (*S*)-(+)- and (*R*)-(-)-5-[(Z)-dec-1-enyl]dihydrofuran-2(3H)-one. *Journal of the Chemical Society, Perkin Transactions 1* **1990**, *10*, 2835-2840.

(26) Ito, H.; Motoki, Y.; Taguchi, T.; Hanzawa, Y.: Zirconium-mediated, highly diastereoselective ring contraction of carbohydrate derivatives: synthesis of highly functionalized, enantiomerically pure carbocycles. *Journal of the American Chemical Society* **1993**, *115*, 8835-8836.

(27) Bach, T.; Kruger, C.; Harms, K.: The stereoselective synthesis of 2-substituted-3-azabicyclo[3.2.0]heptanes by intramolecular [2+2]-photocycloaddition reactions. *Synthesis* 2000, 305-320.

(28) Fernandez, F.; Lopez, C.; Hergueta, A. R.: Synthesis of a precursor of cyclobutane carbocyclic nucleosides from alpha-pinene. *Tetrahedron* **1995**, *51*, 10317-10322.

(29) Huryn, D. M.; Okabe, M.: AIDS-driven nucleoside chemistry. *Chemical Reviews* **1992**, *92*, 1745-1768.

(30) Miller, S. J.; Grubbs, R. H.: Synthesis of Conformationally Restricted Amino Acids and Peptides Employing Olefin Metathesis. *Journal of the American Chemical Society* **1995**, *117*, 5855-5856.

(31) Offermann, D. A.; McKendrick, J. E.; Sejberg, J. J. P.; Mo, B.; Holdom, M. D.; Helm, B. A.; Leatherbarrow, R. J.; Beavil, A. J.; Sutton, B. J.; Spivey, A. C.: Synthesis and Incorporation into Cyclic Peptides of Tolan Amino Acids and Their Hydrogenated Congeners: Construction of an Array of A-B-loop Mimetics of the Cε3 Domain of Human IgE. *The Journal of Organic Chemistry* **2012**, *77*, 3197-3214.

(32) Ramesh, V. V. E.; Roy, A.; Vijayadas, K. N.; Kendhale, A. M.; Prabhakaran, P.; Gonnade, R.; Puranik, V. G.; Sanjayan, G. J.: Conformationally rigid aromatic amino acids as potential building blocks for abiotic foldamers. *Organic & Biomolecular Chemistry* **2011**, *9*, 367-369.

(33) Ballano, G.; Zanuy, D.; Jimenez, A. I.; Cativiela, C.; Nussinov, R.; Aleman, C.: Structural Analysis of a beta-Helical Protein Motif Stabilized by Targeted Replacements with Conformationally Constrained Amino Acids. *The Journal of Physical Chemistry B* **2008**, *112*, 13101-13115.

(34) Burgess, K.; Li, S.; Rebenspies, J.: Chiral 1,3-cyclobutane amino acids: Syntheses and extended conformations. *Tetrahedron Letters* **1997**, *38*, 1681-1684.

(35) Andre, V.; Vidal, A.; Ollivier, J.; Robin, S.; Aitken, D. J.: Rapid access to cis-cyclobutane gamma-amino acids in enantiomerically pure form. *Tetrahedron Letters* **2011**, *52*, 1253-1255.

(36) Igor V. Komarov; Oleksandr O. Grygorenko; Dmytro S. Radchenko; Oleksiy S. Artamonov; Alexander N. Kostyuk; Tolmachev., A. A.: Libraries of conformationally restricted and rigid amino acids. *Chimica Oggi/Chemistry Today* **2006**, *24*, 22-23.

(37) Aguilera, J.; Moglioni, A. G.; Moltrasio, G. Y.; Ortuno, R. M.: Stereodivergent synthesis of the first bis(cyclobutane) gamma-dipeptides and mixed gamma-oligomers. *Tetrahedron: Asymmetry* **2008**, *19*, 302-308.

(38) Izquierdo, S.; Rua, F.; Sbai, A.; Parella, T.; Alvarez-Larena, A.; Branchadell, V.; Ortuno, R. M.: (+) - and (-) -2-Aminocyclobutane-1-carboxylic Acids and Their Incorporation into Highly Rigid beta-Peptides: Stereoselective Synthesis and a Structural Study. *The Journal of Organic Chemistry* **2005**, *70*, 7963-7971.

(39) Gorrea, E.; Nolis, P.; Torres, E.; Da Silva, E.; Amabilino, D. B.; Branchadell, V.; Ortuno, R. M.: Self-Assembly of Chiral trans-Cyclobutane-Containing β-Dipeptides into Ordered Aggregates. *Chemistry – A European Journal* **2011**, *17*, 4588-4597.

(40) Torres, E.; Gorrea, E.; Silva, E. D.; Nolis, P.; Branchadell, V.; Ortuno, R. M.: Prevalence of Eight-Membered Hydrogen-Bonded Rings in Some Bis(cyclobutane) beta-Dipeptides Including Residues with Trans Stereochemistry. *Organic Letters* **2009**, *11*, 2301-2304.

(41) Fernandez-Tejada, A.; Corzana, F.; Busto, J. H.; Avenoza, A.; Peregrina, J. M.: Stabilizing unusual conformations in small peptides and glucopeptides using a hydroxylated cyclobutane amino acid. *Organic & Biomolecular Chemistry* **2009**, *7*, 2885-2893.

(42) Gutierrez-Abad, R.; Carbajo, D.; Nolis, P.; Acosta-Silva, C.; Cobos, J.; Illa, O.; Royo, M.; Ortuño, R.: Synthesis and structural study of highly constrained hybrid cyclobutane-proline γ,γ-peptides. *Amino Acids* **2011**, *41*, 673-686.

(43) Celis, S.; Gorrea, E.; Nolis, P.; Illa, O.; Ortuno, R. M.: Designing hybrid foldamers: the effect on the peptide conformational bias of [small beta]- versus [small alpha]- and [gamma]-linear residues in alternation with (1R,2S) -2-aminocyclobutane-1-carboxylic acid. *Organic & Biomolecular Chemistry* **2012**, *10*, 861-868.

(44) Gutierrez-Abad, R.; Illa, O.; Ortuno, R. M.: Synthesis of Chiral Cyclobutane Containing C3-Symmetric Peptide Dendrimers. *Organic Letters* **2010**, *12*, 3148-3151.

(45) Humphrey, J. M.; Chamberlin, A. R.: Chemical Synthesis of Natural Product Peptides: Coupling Methods for the Incorporation of Noncoded Amino Acids into Peptides. *Chemical Reviews* **1997**, *97*, 2243-2266.

(46) Driggers, E. M.; Hale, S. P.; Lee, J.; Terrett, N. K.: The exploration of macrocycles for drug discovery - an underexploited structural class. *Nature Reviews Drug Discovery* **2008**, *7*, 608-624.

(47) Piekielna, J.; Perlikowska, R.; Gach, K.; Janecka, A.: Cyclization in Opioid Peptides. *Current Drug Targets* **2013**, *14*, 798-816.

(48) Hruby, V. J.: Conformational restrictions of biologically active peptides via amino acid side chain groups. *Life Sciences* **1982**, *31*, 189-199.

(49) Thakkar, A.; Thi Ba, T.; Pei, D.: Global Analysis of Peptide Cyclization Efficiency. *Acs Combinatorial Science* **2013**, *15*, 120-129.

(50) Kotz, J.: Bringing macrocycles full circle. *SciBX: Science-Business eXchange* **2012**, *5*.

(51) White, C. J.; Yudin, A. K.: Contemporary strategies for peptide macrocyclization. *Nature Chemistry* **2011**, *3*, 509-524.

(52) Wessjohann, L. A.; Ruijter, E.; Garcia-Rivera, D.; Brandt, W.: What can a chemist learn from nature's macrocycles? - A brief, conceptual view. *Molecular Diversity* **2005**, *9*, 171-186.

(53) Gause, G. F.; Brazhnikova, M. G.: Gramicidin S and its use in the Treatment of Infected Wounds. *Nature* **1944**, *154*, 703.

(54) Wipf, P.: Synthetic Studies of Biologically Active Marine Cyclopeptides. *Chemical Reviews* **1995**, *95*, 2115-2134.

(55) Pettit, G. R.; Kamano, Y.; Brown, P.; Gust, D.; Inoue, M.; Herald, C. L.: Structure of the cyclic peptide dolastatin 3 from dolabella-auricularia. *Journal of the American Chemical Society* **1982**, *104*, 905-907.

(56) Cavelier, F.; Verducci, J.; Andre, F.; Haraux, F.; Sigalat, C.; Traris, M.; Vey, A.: Natural cyclopeptides as leads for novel pesticides: Tentoxin and destruxin. *Pesticide Science* **1998**, *52*, 81-89.

(57) Walton, J. D.; Earle, E. D.; Stahelin, H.; Grieder, A.; Hirota, A.; Suzuki, A.: Reciprocal biological-activities of the cyclic tetrapeptides chlamydocin and HC-toxin. *Experientia* **1985**, *41*, 348-350.

(58) Cariboni, A.; Ruhrberg, C.: The Hormone of Love Attracts a Partner for Life. *Developmental Cell* **2011**, *21*, 602-604.

(59) Lee, H.-J.; Macbeth, A. H.; Pagani, J. H.; Scott Young 3rd, W.: Oxytocin: The great facilitator of life. *Progress in Neurobiology* **2009**, *88*, 127-151.

(60) Evers, B. M.; Parekh, D.; Townsend, C. M.; Thompson, J. C.: Somatostatin and analogs in the treatment of cancer - a review. *Annals of Surgery* **1991**, *213*, 190-198.

(61) Cavelierfrontin, F.; Pepe, G.; Verducci, J.; Siri, D.; Jacquier, R.: Prediction of the best linear precursor in the synthesis of cyclotetrapeptides by molecular mechanic calculations. *Journal of the American Chemical Society* **1992**, *114*, 8885-8890.

(62) Schapp, J.; Haas, K.; Sunkel, K.; Beck, W.: Cyclotetrapeptide complexes of nickel(II) and palladium(II) by template synthesis from dipeptide esters with functionalized side chains - Crystal structure of (*cyclo*-Gly-beta-Ala-Gly-beta-Ala-4H$^+$)Cu](PPN)$_2$. *European Journal of Inorganic Chemistry* **2003**, 3745-3751.

(63) Miller, S. A.; Griffiths, S. L.; Seebach, D.: C-alkylation of sarcosine residues in cyclic tetrapeptides via lithium enolates. *Helvetica Chimica Acta* **1993**, *76*, 563-595.

(64) Seebach, D.; Matthews, J. L.; Meden, A.; Wessels, T.; Baerlocher, C.; McCusker, L. B.: Cyclo-beta-peptides: Structure and tubular stacking of cyclic tetramers of 3-aminobutanoic acid as determined from powder diffraction data. *Helvetica Chimica Acta* **1997**, *80*, 173-182.

(65) Clark, T. D.; Buehler, L. K.; Ghadiri, M. R.: Self-Assembling Cyclic beta(3) -Peptide Nanotubes as Artificial Transmembrane Ion Channels. *Journal of the American Chemical Society* **1998**, *120*, 651-656.

(66) Battershill, P. E.; Clissold, S. P.: Octreotide - a review of its pharmacodynamic and pharmacokinetic properties, and therapeutic potential in conditions associated with excessive peptide secretion. *Drugs* **1989**, *38*, 658-702.

(67) Bowers, A.; West, N.; Taunton, J.; Schreiber, S. L.; Bradner, J. E.; Williams, R. M.: Total synthesis and biological mode of action of largazole: A potent Class I histone deacetylase inhibitor. *Journal of the American Chemical Society* **2008**, *130*, 11219-11222.

(68) Janin, Y. L.: Peptides with anticancer use or potential. *Amino Acids* **2003**, *25*, 1-40.

(69) Jung, M.: Inhibitors of histone deacetylase as new anticancer agents. *Current Medicinal Chemistry* **2001**, *8*, 1505-1511.

(70) Horne, W. S.; Olsen, C. A.; Beierle, J. M.; Montero, A.; Ghadiri, M. R.: Probing the Bioactive Conformation of an Archetypal Natural Product HDAC Inhibitor with Conformationally Homogeneous Triazole-Modified Cyclic Tetrapeptides. *Angewandte Chemie-International Edition* **2009**, *48*, 4718-4724.

(71) Lim, H. A.; Kang, C.; Chia, C. S. B.: Solid-Phase Synthesis and NMR Structural Studies of the Marine Antibacterial Cyclic Tetrapeptide: Cyclo GSPE. *International Journal of Peptide Research and Therapeutics* **2010**, *16*, 145-152.

(72) Che, Y.; Marshall, G. R.: Engineering cyclic tetrapeptides containing chimeric amino acids as preferred reverse-turn scaffolds. *Journal of Medicinal Chemistry* **2006**, *49*, 111-124.

(73) Mollica, A.; Pinnen, F.; Stefanucci, A.; Feliciani, F.; Campestre, C.; Mannina, L.; Sobolev, A. P.; Lucente, G.; Davis, P.; Lai, J.; Ma, S.-W.; Porreca, F.; Hruby, V. J.: The cis-4-Amino-L-proline Residue as a Scaffold for the Synthesis of Cyclic and Linear Endomorphin-2 Analogues. *Journal of Medicinal Chemistry* **2012**, *55*, 3027-3035.

(74) Cardillo, G.; Gentilucci, L.; Tolomelli, A.; Spinosa, R.; Calienni, M.; Qasem, A. R.; Spampinato, S.: Synthesis and Evaluation of the Affinity toward mu-Opioid Receptors of

Atypical, Lipophilic Ligands Based on the Sequence c[-Tyr-Pro-Trp-Phe-Gly-]. *Journal of Medicinal Chemistry* **2004**, *47*, 5198-5203.

(75) Bedini, A.; Baiula, M.; Gentilucci, L.; Tolomelli, A.; De Marco, R.; Spampinato, S.: Peripheral antinociceptive effects of the cyclic endomorphin-1 analog c[YpwFG] in a mouse visceral pain model. *Peptides* **2010**, *31*, 2135-2140.

(76) Merck: RonaCare® Cyclopeptide-5. Ringing in a unique, new peptide generation. 2010, taken from http://www.hcbio.com.tw/pdf/RonaCareCyclopeptide-5%20Level2.pdf.

(77) Merck: RonaCare® Cyclopeptide 5 2010, http://www.merck-performance-materials.com/en/cosmetics/ronacare/ronacare_cyclopeptide_5/ronacare_cyclopeptide_5.html, last update 3/12/12.

(78) Gao, X.; Matsui, H.: Peptide-Based Nanotubes and Their Applications in Bionanotechnology. *Advanced Materials* **2005**, *17*, 2037-2050.

(79) Tang, M.; Fan, J. F.; Liu, J.; He, L. J.; He, K.: Applications of Cyclic Peptide Nanotubes. *Progress in Chemistry* **2010**, *22*, 648-653.

(80) Kubik, S.: Large Increase in Cation Binding Affinity of Artificial Cyclopeptide Receptors by an Allosteric Effect. *Journal of the American Chemical Society* **1999**, *121*, 5846-5855.

(81) Garciaecheverria, C.; Albericio, F.; Giralt, E.; Pons, M.: Design, synthesis, and complexing properties of ((1) cys-(1') cys,(4) cys-(4') cys) -dithiobis(ac-L-(1) cys-L-pro-D-val-L-(4) cys-NH_2) - the 1st example of a new family of ion-binding peptides. *Journal of the American Chemical Society* **1993**, *115*, 11663-11670.

(82) Arena, G.; Impellizzeri, G.; Maccarrone, G.; Pappalardo, G.; Rizzarelli, E.: Co-ordination properties of cyclopeptides. Formation and stability of zinc(II) and copper(II) complexes of histidine-containing cyclopeptides, or imidazole. *Journal of the Chemical Society, Dalton Transactions* **1994**, *8*, 1227-1230.

(83) Ranganathan, D.: Designer Hybrid Cyclopeptides for Membrane Ion Transport and Tubular Structures‚Ä†. *Accounts of Chemical Research* **2001**, *34*, 919-930.

(84) Ranganathan, D.: Designer hybrid cyclopeptides for membrane ion transport and tubular structures. *Accounts of Chemical Research* **2001**, *34*, 919-930.

(85) Cavelier-Frontin, F.; Pepe, G.; Verducci, J.; Siri, D.; Jacquier, R.: Prediction of the best linear precursor in the synthesis of cyclotetrapeptides by molecular mechanic calculations. *Journal of the American Chemical Society* **1992**, *114*, 8885-8890.

(86) Schmidt, U.; Langner, J.: Cyclotetrapeptides and cyclopentapeptides: Occurrence and synthesis. *Journal of Peptide Research* **1997**, *49*, 67-73.

(87) Blankenstein, J.; Zhu, J. P.: Conformation-directed macrocyclization reactions. *European Journal of Organic Chemistry* **2005**, 1949-1964.

(88) Humphrey, J. M.; Chamberlin, A. R.: Chemical synthesis of natural product peptides: Coupling methods for the incorporation of noncoded amino acids into peptides. *Chemical Reviews* **1997**, *97*, 2243-2266.

(89) Montalbetti, C. A. G. N.; Falque, V.: Amide bond formation and peptide coupling. *Tetrahedron* **2005**, *61*, 10827-10852.

(90) Parenty, A.; Moreau, X.; Campagne, J. M.: Macrolactonizations in the total synthesis of natural products. *Chemical Reviews* **2006**, *106*, 911-939.

(91) Wu, C.; Leroux, J.-C.; Gauthier, M. A.: Twin disulfides for orthogonal disulfide pairing and the directed folding of multicyclic peptides. *Nature Chemistry* **2012**, *4*, 1045-1050.

(92) Lundquist, J. T.; Pelletier, J. C.: A new tri-orthogonal strategy for peptide cyclization. *Organic Letters* **2002**, *4*, 3219-3221.

(93) Malesevic, M.; Strijowski, U.; Baechle, D.; Sewald, N.: An improved method for the solution cyclization of peptides under pseudo-high dilution conditions. *Journal of Biotechnology* **2004**, *112*, 73-77.

(94) Kates, S. A.; Sole, N. A.; Johnson, C. R.; Hudson, D.; Barany, G.; Albericio, F.: A novel, convenient, 3-dimensional orthogonal strategy for solid-phase synthesis of cyclic-peptides. *Tetrahedron Letters* **1993**, *34*, 1549-1552.

(95) Alcaro, M. C.; Sabatino, G.; Uziel, J.; Chelli, M.; Ginanneschi, M.; Rovero, P.; Papini, A. M.: On-resin head-to-tail cyclization of cyclotetrapeptides: optimization of crucial parameters. *Journal of Peptide Science* **2004**, *10*, 218-228.

(96) Punna, S.; Kuzelka, J.; Wang, Q.; Finn, M. G.: Head-to-tail peptide cyclodimerization by copper-catalyzed azide-alkyne cycloaddition. *Angewandte Chemie-International Edition* **2005**, *44*, 2215-2220.

(97) Daidone, I.; Neuweiler, H.; Doose, S.; Sauer, M.; Smith, J. C.: Hydrogen-Bond Driven Loop-Closure Kinetics in Unfolded Polypeptide Chains. *Plos Computational Biology* **2010**, *6*.

(98) Felizmenio-Quimio, M. E.; Daly, N. L.; Craik, D. J.: Circular Proteins in Plants: Solution structure of a novel macrocyclic trypsin inhibitor frommomordica cochinchinensis. *Journal of Biological Chemistry* **2001**, *276*, 22875-22882.

(99) Jiang, W.; Wanner, J.; Lee, R. J.; Bounaud, P.-Y.; Boger, D. L.: Total Synthesis of the Ramoplanin A2 and Ramoplanose Aglycon. *Journal of the American Chemical Society* **2002**, *124*, 5288-5290.

(100) Chen, J.; Rong, F.; Shan, B.; Chen, Y.; Li, Y.; Yu, H.; Chen, L.; Kuang, T.; Li, S.; Chen, Y.; Du, J.; Ai, C.; Li, J.; Li, X.; Shi, C.; Jiang, Z.; Long, Y.; Gao, Q.; Wang, Z.; Xu, K.; Ran, X.; Yi, H.; Zhao, D.; Qiao, H.; Shen, J.; Liu, B.; Liu, C.; Wu, K.; Geng, X.; Tan, J.; McLeod, D.; Frost, H.; Bai, G.; Goetz, G.; Federico Iii, J.; Whitney-Pickett, C.; Troutman, M.; Noe, M. C.; Guimaraes, C.; Piotrowski, D. W.; Magee, T. V.: Synthesis of 12-membered macrocyclic templates and library analogs for PPI. *Tetrahedron Letters* **2013**, *54*, 3298-3301.

(101) Nour, H. F.; Hourani, N.; Kuhnert, N.: Synthesis of novel enantiomerically pure tetra-carbohydrazide cyclophane macrocycles. *Organic & Biomolecular Chemistry* **2012**, *10*, 4381-4389.

(102) Chamberlin, S. G.; Sargood, K. J.; Richter, A.; Mellor, J. M.; Anderson, D. W.; Richards, N. G. J.; Turner, D. L.; Sharma, R. P.; Alexander, P.; Davies, D. E.: Constrained Peptide Analogues of Transforming Growth Factor- Residues Cysteine 2132 Are Mitogenically Active: Use of proline mimetics to enhance biological potency. *Journal of Biological Chemistry* **1995**, *270*, 21062-21067.

(103) Fisk, J. D.; Powell, D. R.; Gellman, S. H.: Control of hairpin formation via proline configuration in parallel beta-sheet model systems. *Journal of the American Chemical Society* **2000**, *122*, 5443-5447.

(104) Tai, D.-F.; Lin, Y.-F.: Molecularly imprinted cavities template the macrocyclization of tetrapeptides. *Chemical Communications* **2008**, 5598-5600.

(105) Haas, K.; Ponikwar, W.; Noth, H.; Beck, W.: Facile synthesis of cyclic tetrapeptides from nonactivated peptide esters on metal centers. *Angewandte Chemie-International Edition* **1998**, *37*, 1086-1089.

(106) Ye, Y. H.; Gao, X. M.; Liu, M.; Tang, Y. C.; Tian, G. L.: Studies on the synthetic methodology of head to tail cyclization of linear peptides. *Letters in Peptide Science* **2003**, *10*, 571-579.

(107) Lecaillon, J.; Gilles, P.; Subra, G.; Martinez, J.; Amblard, M.: Synthesis of cyclic peptides via O-N-acyl migration. *Tetrahedron Letters* **2008**, *49*, 4674-4676.

(108) Meutermans, W. D. F.; Golding, S. W.; Bourne, G. T.; Miranda, L. P.; Dooley, M. J.; Alewood, P. F.; Smythe, M. L.: Synthesis of difficult cyclic peptides by inclusion of a novel photolabile auxiliary in a ring contraction strategy. *Journal of the American Chemical Society* **1999**, *121*, 9790-9796.

(109) Janvier, P.; Bois-Choussy, M.; Bienayme, H.; Zhu, J. P.: A one-pot four-component (ABC(2)) synthesis of macrocycles. *Angewandte Chemie-International Edition* **2003**, *42*, 811-814.

(110) Li, Y.; Yongye, A.; Giulianotti, M.; Martinez-Mayorga, K.; Yu, Y.; Houghten, R. A.: Synthesis of Cyclic Peptides through Direct Aminolysis of Peptide Thioesters Catalyzed by

Imidazole in Aqueous Organic Solutions. *Journal of Combinatorial Chemistry* **2009**, *11*, 1066-1072.

(111) Kleineweischede, R.; Hackenberger, C. P. R.: Chemoselective peptide cyclization by traceless Staudinger ligation. *Angewandte Chemie-International Edition* **2008**, *47*, 5984-5988.

(112) Miller, S. J.; Blackwell, H. E.; Grubbs, R. H.: Application of ring-closing metathesis to the synthesis of rigidified amino acids and peptides. *Journal of the American Chemical Society* **1996**, *118*, 9606-9614.

(113) Hili, R.; Rai, V.; Yudin, A. K.: Macrocyclization of Linear Peptides Enabled by Amphoteric Molecules. *Journal of the American Chemical Society* **2010**, *132*, 2889-+.

(114) Callender, R.; Gameiro, A.; Pinto, A.; De Micheli, C.; Grewer, C.: Mechanism of inhibition of the glutamate transporter EAAC1 by the conformationally constrained glutamate analogue (+)-HIP-B. *Biochemistry* **2012**, *51*, 5486-95.

(115) Kandel, E. R.; Schwartz, J. H.; Jessel, T. M.: *Principles of neural science*; 4th ed.; The McGraw Hill companies, Inc., 2000.

(116) Elias, L. J.; Saucier, D. M.: *Neuropsychology: Clinical and Experimental Foundations*; Allyn Bacon: Boston, 2006.

(117) Davis, K. L.; Charney, D.; Coyle, J. T.; Nemeroff, C.: *Neurophsycopharmacology: The fifth generation of progress; An official pubblication of the American College of Neuropsychopharmacology (chapter 12)* ; Lippincott Williams & Wilkins: Philadelphia, 2002.

(118) Lemke, T. L.; Williams, D. A.: *Foye's Principles of Medicinal Chemistry (p. 446)* ; 6th ed.; Lippincott Williams & Wilkins and Wolters Kluwer Business: Philadelphia, 2007.

(119) Uusi-Oukari, M.; Korpi, E. R.: Regulation of $GABA_A$ Receptor Subunit Expression by Pharmacological Agents. *Pharmacological Reviews* **2010**, *62*, 97-135.

(120) Perry, E.; Ashton, H.; Young, A.: *Neurochemistry of consciousness*; John Benjamins Publishing Company: Amsterdam, 2002.

(121) Alvarez, E. O.; Ruarte, M. B.: Glutamic acid and histamine-sensitive neurons in the ventral hippocampus and the basolateral amygdala of the rat: functional interaction on memory and learning processes. *Behavioural Brain Research* **2004**, *152*, 209-219.

(122) Sheldon, A. L.; Robinson, M. B.: The role of glutamate transporters in neurodegenerative diseases and potential opportunities for intervention. *Neurochemistry International* **2007**, *51*, 333-355.

(123) Danbolt, N.: Glutamate uptake. *Progress in Neurobiology* **2001**, *65*, 1-105.

(124) Namekata, K.; Harada, C.; Kohyama, K.; Matsumoto, Y.; Harada, T.: Interleukin-1 Stimulates Glutamate Uptake in Glial Cells by Accelerating Membrane Trafficking of Na+/K+-ATPase via Actin Depolymerization. *Molecular and Cellular Biology* **2008**, *28*, 3273-3280.

(125) Traynelis, S. F.; Wollmuth, L. P.; McBain, C. J.; Menniti, F. S.; Vance, K. M.; Ogden, K. K.; Hansen, K. B.; Yuan, H.; Myers, S. J.; Dingledine, R.: Glutamate receptor ion channels: structure, regulation, and function. *Pharmacological reviews* **2010**, *62*, 405-96.

(126) Brumfield, S.; Korakas, P.; Silverman, L. S.; Tulshian, D.; Matasi, J. J.; Qiang, L.; Bennett, C. E.; Burnett, D. A.; Greenlee, W. J.; Knutson, C. E.; Wu, W.-L.; Sasikumar, T. K.; Domalski, M.; Bertorelli, R.; Grilli, M.; Lozza, G.; Reggiani, A.; Li, C.: Synthesis and SAR development of novel mGluR1 antagonists for the treatment of chronic pain. *Bioorganic & Medicinal Chemistry Letters* **2012**, *22*, 7223-7226.

(127) Mim, C.; Balani, P.; Rauen, T.; Grewer, C.: The Glutamate Transporter Subtypes EAAT4 and EAATs 1-3 Transport Glutamate with Dramatically Different Kinetics and Voltage Dependence but Share a Common Uptake Mechanism. *The Journal of General Physiology* **2005**, *126*, 571-589.

(128) Bunch, L.; Erichsen, M. N.; Jensen, A. A.: Excitatory amino acid transporters as potential drug targets. *Expert Opinion on Therapeutic Targets* **2009**, *13*, 719-731.

(129) Nedergaard, M.; Takano, T.; Hansen, A. J.: Opinion: Beyond the role of glutamate as a neurotransmitter. *Nature Reviews Neuroscience* **2002**, *3*, 748-755.

(130) Lee, H.; Zhu, X. W.; O'Neill, M. J.; Webber, K.; Casadesus, G.; Marlatt, M.; Raina, A. K.; Perry, G.; Smith, M. A.: The role of metabotropic glutamate receptors in Alzheimer's disease. *Acta Neurobiol. Exp.* **2004**, *64*, 89-98.

(131) Sontheimer, H.: A role for glutamate in growth and invasion of primary brain tumors. *Journal of Neurochemistry* **2008**, *105*, 287-295.

(132) Pampliega, O.; Domercq, M.; Soria, F. N.; Villoslada, P.; Rodriguez-Antiguedad, A.; Matute, C.: Increased expression of cystine/glutamate antiporter in multiple sclerosis. *Journal of Neuroinflammation* **2011**, *8*.

(133) Bannai, S.: Exchange of cystine and glutamate across plasma membrane of human fibroblasts. *Journal of Biological Chemistry* **1986**, *261*, 2256-2263.

(134) McBean, G. J.: Cerebral cystine uptake: a tale of two transporters. *Trends in pharmacological sciences* **2002**, *23*, 299-302.

(135) Wiranowska, M.; Vrionis, F. D.: *Gliomas: Symptoms, Diagnosis and Treatment Options (chapter 18)* ; Nova Science Publishers Inc. ed.; Wiranowska M. and Vrionis F. D.: New York, 2013.

(136) Flynn, J.; McBean, G. J.: Kinetic and pharmacological analysis of L- S-35 cystine transport into rat brain synaptosomes. *Neurochemistry International* **2000**, *36*, 513-521.

(137) Mawatari, C.; Yasui, Y.; Sugitani, K.; Takadera, T.; Kato, S.: Reactive oxygen species involved in the glutamate toxicity of C6 glioma cells via X(C) over-bar antiporter system. *Neuroscience* **1996**, *73*, 201-208.

(138) Pittenger, C.; Bloch, M. H.; Williams, K.: Glutamate abnormalities in obsessive compulsive disorder: Neurobiology, pathophysiology, and treatment. *Pharmacology & Therapeutics* **2011**, *132*, 314-332.

(139) McBean, G.: The transsulfuration pathway: a source of cysteine for glutathione in astrocytes. *Amino Acids* **2012**, *42*, 199-205.

(140) Kato, S.; Negishi, K.; Mawatari, K.; Kuo, C. H.: A mechanism for glutamate toxicity in the C6 glioma cells involving inhibition of cystine uptake leading to glutathione depletion. *Neuroscience* **1992**, *48*, 903-914.

(141) Ye, Z.-C.; Rothstein, J. D.; Sontheimer, H.: Compromised Glutamate Transport in Human Glioma Cells: Reduction,ÄìMislocalization of Sodium-Dependent Glutamate Transporters and Enhanced Activity of Cystine,ÄìGlutamate Exchange. *The Journal of Neuroscience* **1999**, *19*, 10767-10777.

(142) Dirnagl, U.; Iadecola, C.; Moskowitz, M. A.: Pathobiology of ischaemic stroke: an integrated view. *Trends in Neurosciences* **1999**, *22*, 391-397.

(143) Choi, D.; Rothman, S.: The role of glutamate neurotoxicity in hypoxic-ischemic neuronal death. *Annual Review of Neuroscience* **1990**, *13*, 171-182.

(144) Meldrum, B. G., J: Excitatory amino acid neurotoxicity and neurodegenerative disease. *Trends in pharmacological sciences* **1990**, *11*, 379-387.

(145) Lynch, D. R.; Guttmann, R. P.: Excitotoxicity: Perspectives Based on *N*-Methyl-D-Aspartate Receptor Subtypes. *Journal of Pharmacology and Experimental Therapeutics* **2002**, *300*, 717-723.

(146) Olney, J. W.; Wozniak, D. F.; Farber, N. B.: Excitotoxic neurodegeneration in alzheimer disease: New hypothesis and new therapeutic strategies. *Archives of Neurology* **1997**, *54*, 1234-1240.

(147) Greenamyre, J. T.; Maragos, W. F.; Albin, R. L.; Penney, J. B.; Young, A. B.: Glutamate transmission and toxicity in Alzheimers-disease *Prog. Neuro-Psychopharmacol. Biol. Psychiatry* **1988**, *12*, 421-430.

(148) Jaiswal, M.; Zech, W.-D.; Goos, M.; Leutbecher, C.; Ferri, A.; Zippelius, A.; Carri, M.; Nau, R.; Keller, B.: Impairment of mitochondrial calcium handling in a mtSOD1 cell culture model of motoneuron disease. *BMC Neuroscience* **2009**, *10*.

(149) Carbone, M.; Duty, S.; Rattray, M.: Riluzole neuroprotection in a parkinson's disease model involves suppression of reactive astrocytosis but not GLT-1 regulation. *BMC Neuroscience* **2012**, *13*, 1-8.

(150) Voutsinos-Porche, B.; Koning, E.; Clement, Y.; Kaplan, H.; Ferrandon, A.; Motte, J.; Nehlig, A.: EAAC1 glutamate transporter expression in the rat lithium-pilocarpine model of temporal lobe epilepsy. *Journal of Cerebral Blood Flow & Metabolism* **2006**, *26*, 1419-1430.

(151) Lee, G.; Huang, Y.; Washington, J. M.; Briggs, N. W.; Zuo, Z.: Carbamazepine enhances the activity of glutamate transporter type 3 via phosphatidylinositol 3-kinase. *Epilepsy Research* **2005**, *66*, 145-153.

(152) Hughes, J. R.: Alcohol withdrawal seizures. *Epilepsy & Behavior* **2009**, *15*, 92-97.

(153) Camacho, A.; Massieu, L.: Role of Glutamate Transporters in the Clearance and Release of Glutamate during Ischemia and its Relation to Neuronal Death. *Archives of medical research* **2006**, *37*, 11-18.

(154) Dutta, R.; Trapp, B. D.: Mechanisms of neuronal dysfunction and degeneration in multiple sclerosis. *Progress in Neurobiology* **2011**, *93*, 1-12.

(155) Tamminga C. A.; Thaker G. K.; Buchanan R.: LImbic system abnormalities identified in schizophrenia using positron emission tomography with fluorodeoxyglucose and neocortical alterations with deficit syndrome. *Archives of General Psychiatry* **1992**, *49*, 522-530.

(156) Tsapakis, E. M.; Travis, M. J.: Glutamate and psychiatric disorders. *Advances in Psychiatric Treatment* **2002**, *8*, 189-197.

(157) Faure, S.; Jensen, A. A.; Maurat, V.; Gu, X.; Sagot, E.; Aitken, D. J.; Bolte, J.; Gefflaut, T.; Bunch, L.: Stereoselective Chemoenzymatic Synthesis of the Four Stereoisomers of l-2-(2-Carboxycyclobutyl) glycine and Pharmacological Characterization at Human Excitatory Amino Acid Transporter Subtypes 1, 2, and 3. *Journal of Medicinal Chemistry* **2006**, *49*, 6532-6538.

(158) Allan, R. D.; Hanrahan, J. R.; Hambley, T. W.; Johnston, G. A. R.; Mewett, K. N.; Mitrovic, A. D.: Synthesis and activity of a potent N-methyl-D-aspartic acid agonist, trans-1-aminocyclobutane-1,3-dicarboxylic acid, and related phosphonic and carboxylic acids. *Journal of Medicinal Chemistry* **1990**, *33*, 2905-2915.

(159) Burtoloso, A. C. B.; Correia, C. R. D.: Stereoselective synthesis of azetidine-derived glutamate and aspartate analogues from chiral azetidin-3-ones. *Tetrahedron* **2008**, *64*, 9928-9936.

(160) Callender, R.; Gameiro, A.; Pinto, A.; Micheli, C. D.; Grewer, C.: Mechanism of Inhibition of the Glutamate Transporter EAAC1 by the Conformationally Constrained Glutamate Analogue (+)-HIP-B. *Biochemistry* **2012**, *51*, 5486-5495.

(161) McCullumsmith, R. E.; Meador-Woodruff, J. H.: Striatal excitatory amino acid transporter transcript expression in schizophrenia, bipolar disorder, and major depressive disorder. *Neuropsychopharmacology* **2002**, *26*, 368-375.

(162) Choudary, P. V.; Molnar, M.; Evans, S. J.; Tomita, H.; Li, J. Z.; Vawter, M. P.; Myers, R. M.; Bunney, W. E.; Akil, H.; Watson, S. J.; Jones, E. G.: Altered cortical glutamatergic and GABAergic signal transmission with glial involvement in depression. *Proceedings of the National Academy of Sciences of the United States of America* **2005**, *102*, 15653-15658.

(163) Bridges, R. J.; Natale, N. R.; Patel, S. A.: System xc- cystine/glutamate antiporter: an update on molecular pharmacology and roles within the CNS. *British Journal of Pharmacology* **2012**, *165*, 20-34.

(164) Sato, H.; Fujiwara, K.; Sagara, J.; Bannai, S.: Induction of cystine transport activity in mouse peritoneal macrophages by bacterial lipopolysaccharide. *Biochem. J.* **1995**, *310*, 547-551.

Chapter 2

Synthesis of a novel constrained δ-amino acid and its dipeptides

2.1-Introduction

After ACCA precursor **7a** was obtained serendipitously (see paragraph 2.2.1), its interesting structure, containing the constrained cyclobutane core, inspired this project. The presence of NH_2 and COOH in the ACCA structure, allowed for its incorporation in peptidic structures to investigate the effect of the constriction on the secondary structure. We decided to start studying shorter structures like dipeptides to understand the efficiency of amide formation of ACCA, using peptides coupling procedures.

Since one of the techniques used in peptidomimetics is the inclusion of cyclic moieties into peptides, the presence of the cyclobutane ring in the ACCA structure led us to believe that this compound can easily find application as peptidomimetic.

2.2-Results and discussion

2.2.1-Synthesis of the novel non-proteinogenic δ-amino acid ACCA

The 7 steps synthesis of the non-proteinogenic δ-amino acid (ACCA, **9**) has been developed in a previous PhD project, starting from the commercially available methyl propiolate **1** and benzylamine **2a** and is here optimised (Scheme 2.1).

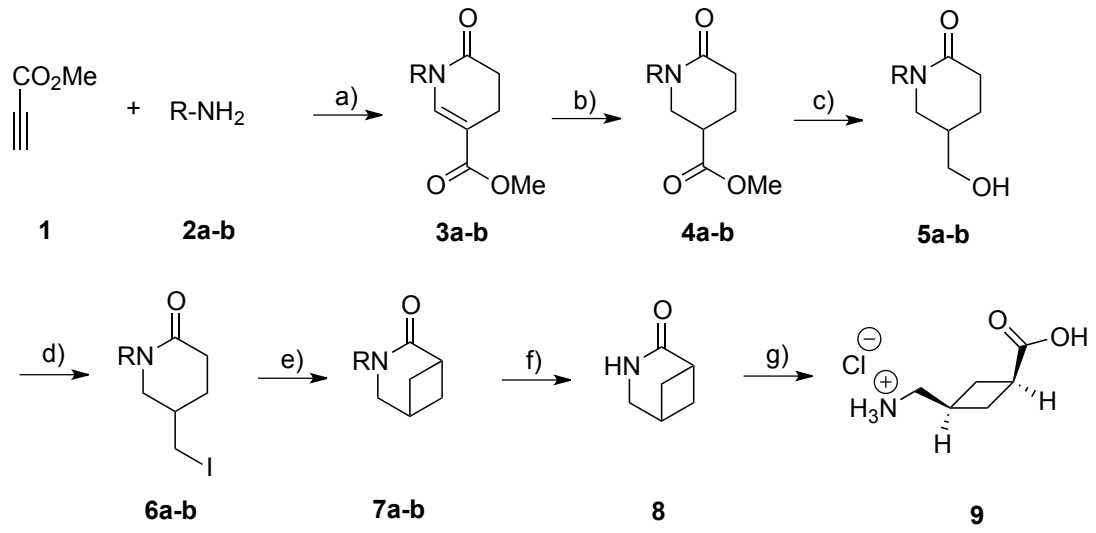

Ra = Bn
Rb = MPB

Scheme 2.1 Synthesis of conformationally constrained amino acid salt **9**. *Reagents and conditions:* a) (i) THF, -10 °C – rt, 1 h; (ii) Acryloyl chloride, rt, 12 h 43 %; b) H_2, Pd/C, $NaHCO_3$, EtOH, rt, 12 h, 95 % or HCO_2NH_4, Pd/C, EtOH, 68 °C, 1 h; c) $LiBH_4$, THF, 0 °C – rt, 12 h, 87 %; d) (i) CH_3SO_2Cl, TEA, CH_2Cl_2, -10 °C – rt, 16 h; (ii) NaI, acetone, reflux, 24 h, 79 %; or PPh_3, Imidazole, I_2, toluene, 3 h, 68 %; e) LHMDS, THF, -20 °C, 1 h, 86 %; f) NH_3 (l), Li (s), THF, ^{t}BuOH, -78 °C, 96 %; g) HCl 2 M, reflux, 12 h, 99 %

Dr. Elaine O'Reilly was working on the synthesis of the anticapsin analogue reported in Scheme 2.2 and her synthetic approach consisted in the coupling of compound **6a** with diketopiperazines[1] after deprotonation of the alpha-carbon using a strong base (LHMDS), but this coupling product was never achieved.

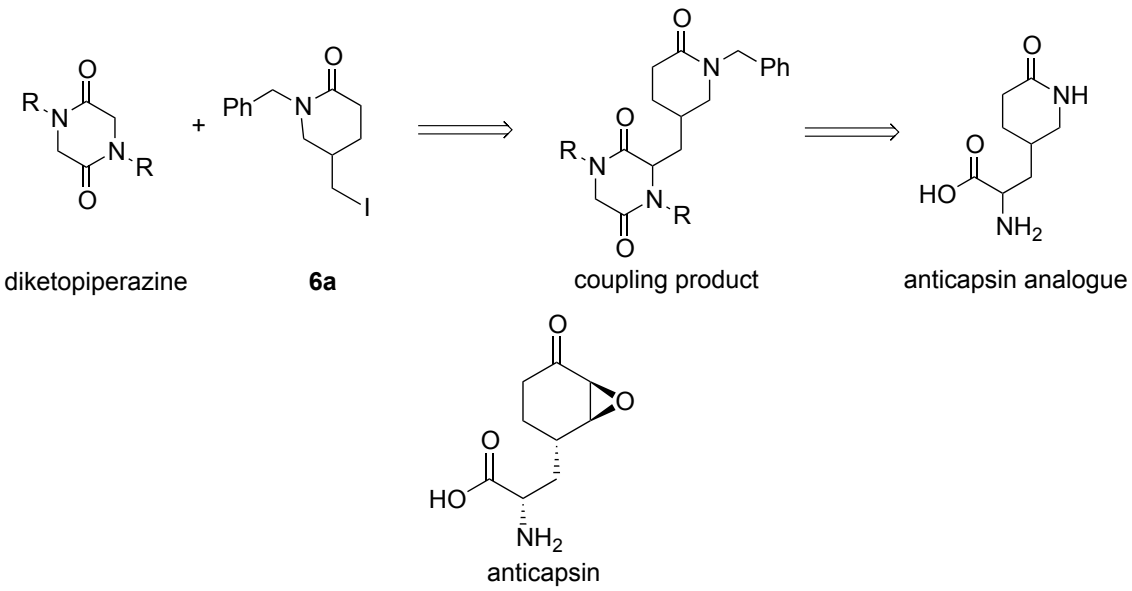

Scheme 2.2 retrosynthesis to the anticapsin analogue

To try and understand the reason why this reaction was failing, which previously worked very well with other iodide molecules,[2] compound **6a** was reacted alone with LHMDS, without the diketopiperazine, achieving in unexpectedly high yield compound **7a**. The presence of the intramolecular cyclobutane ring, just beside the hydrolysable amide moiety, seemed very attractive as precursor for a *cis*-locked amino acid, ACCA.

Our approach to the synthesis of ACCA **9** involves the construction of the nitrogen ring as described by Cook and colleagues.[3] Initially the formation of an enamine intermediate occurs *via* the conjugate addition of methyl propiolate **1** and benzylamine **2a** as mixture of the *cis/trans* isomers 45:55 and undergoes subsequently an aza-annulation reaction with acryloyl chloride, generating the ester **3a** in 43 % yield over two steps. A possible explanation for the low yield is that only one of the two stereoisomers undergoes the aza-anulation reaction. If the enamine intermediate is isolated and characterised with ^{1}H-NMR spectrum, it is possible to notice the presence of the two isomers (Fig. 2.1) with no need of purification. This first part of the reaction proceeds in fact very neatly; it is the second part of the reaction, after addition of acryloyl chloride, which gives many impurities and lowers the final yield.

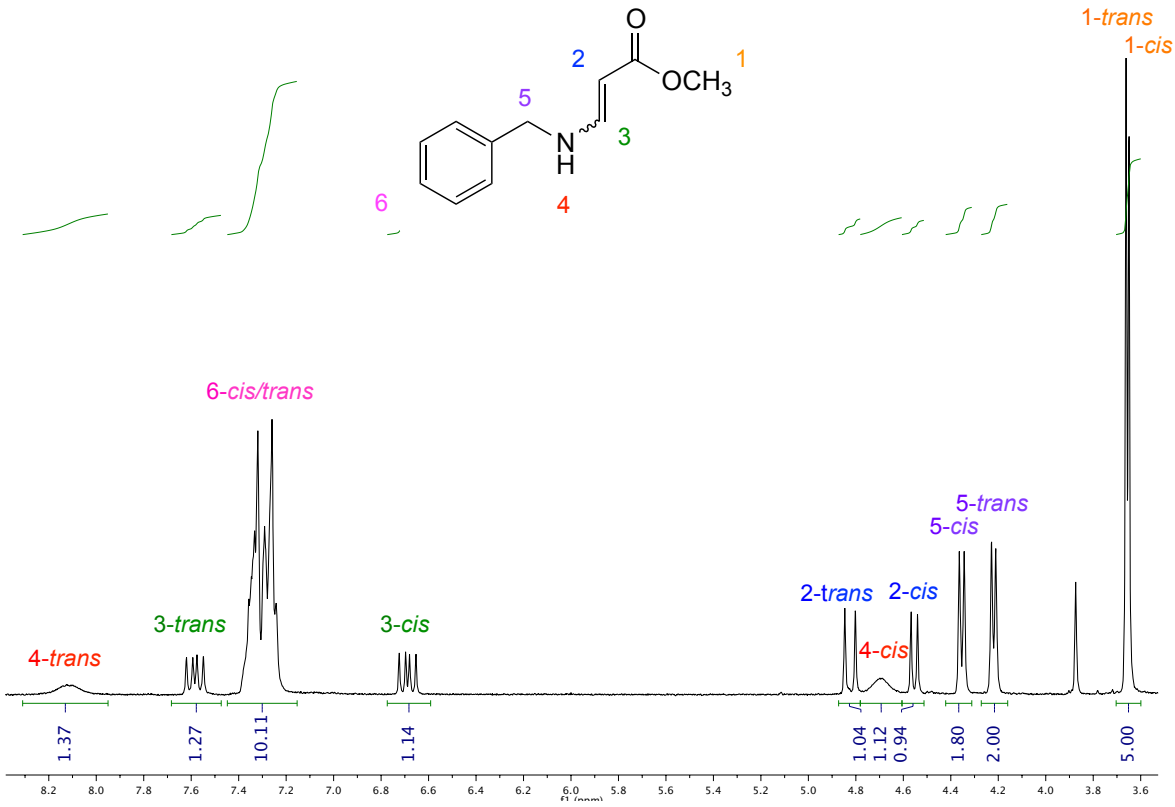

Fig. 2.1 enamine formed from conjugate addition of methyl propiolate **1** and benzylamine **2a**

The racemic ester **4a** has been generated by hydrogenation of compound **3a** in 95 % yield. This compound has been already studied by Gray *et al.*, using kinetic resolution, giving the enantio-enriched compounds in high yields.[4]

Compound **4a** was subsequently converted to the racemic alcohol **5a** using lithium borohydride, in 87 % yield and converted further to the iodo-derivative **6a** *via* a mesylate intermediate in 79 % yield over the two steps. This approach can also be substituted by the direct iodination (Appel reaction) of **5a**, affording **6a** after treatment with triphenylphosphine, imidazole and iodine, in toluene for 3 hours.[5] Compared to the two-step procedure, the latter is much quicker, but the purification of the desired compound from the side product triphenylphosphine oxide is difficult and, when successful, it gives lower yields (68 % versus 79 %).

An already exploited alternative technique of halogenation of compound **5a** is the direct bromination described in the literature by Gray and Gallagher which it

was not attempted in this project.[4]

A rapid intramolecular nucleophilic substitution was observed after treating **6a** with LHMDS, yielding **7a** in 86 %. Galeazzi and collaborators previously reported this type of intramolecular cyclisation, which they employed in the synthesis of *cis*-2-aminomethylcyclobutane carboxylic acid in both enantiomeric forms.[6] Compound **7a** is then deprotected under Birch conditions generating the bicyclic derivative **8** in 96 % yield. The three dimensional structure of **8** was confirmed by X-ray crystallography (Fig. 2.2).

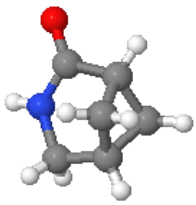

Fig. 2.2 X-ray crystal structure of bicyclic amide **8**

The Birch reduction is an excellent chemical reaction widely exploited in organic chemistry, which works in high yields and in short time with no need to further purify the product.

The mechanism (Scheme 2.3) involves a two-electron transfer, where the transfer of one electron is alternated with the uptake of H^+ to protonate the radical anion.

A metal, lithium or sodium, is dissolved in liquid ammonia releasing an electron. This "solvated electron" has a characteristic "royal blue"/black colour, depending on the concentration. An alcohol, usually *tert*-butanol, is needed as proton donor and is used in stoichiometric amount.[7]

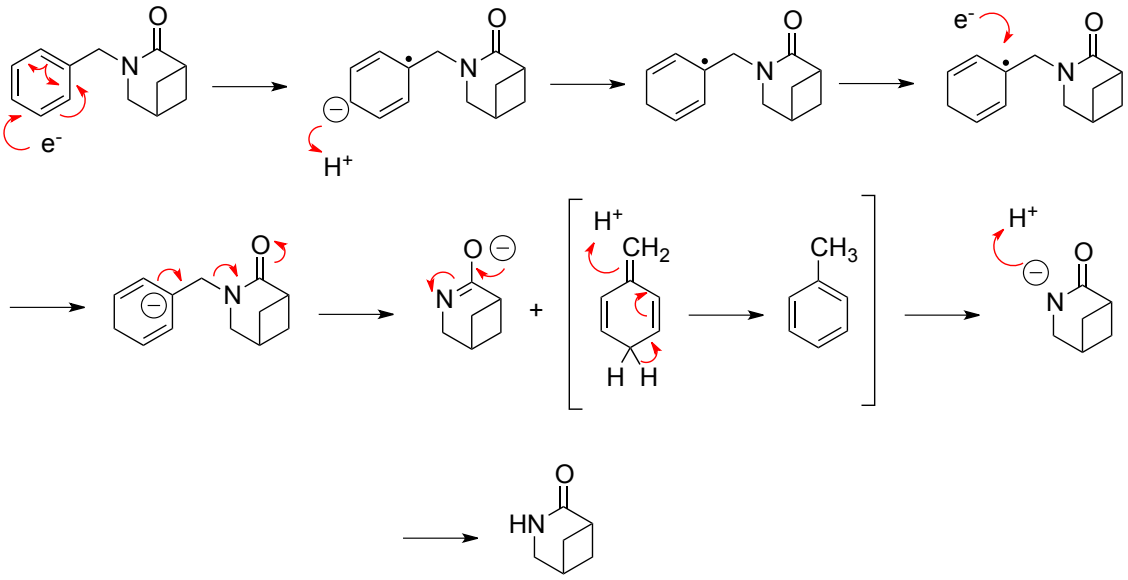

Scheme 2.3 mechanism of Birch reduction

The conditions just described, required from the reaction, are quite hazardous, due to the presence of ammonia (which has to be condensed from gas phase to liquid) and reactive flammable metals. Furthermore the reaction apparatus set up, illustrated in Fig. 2.3, is complex.

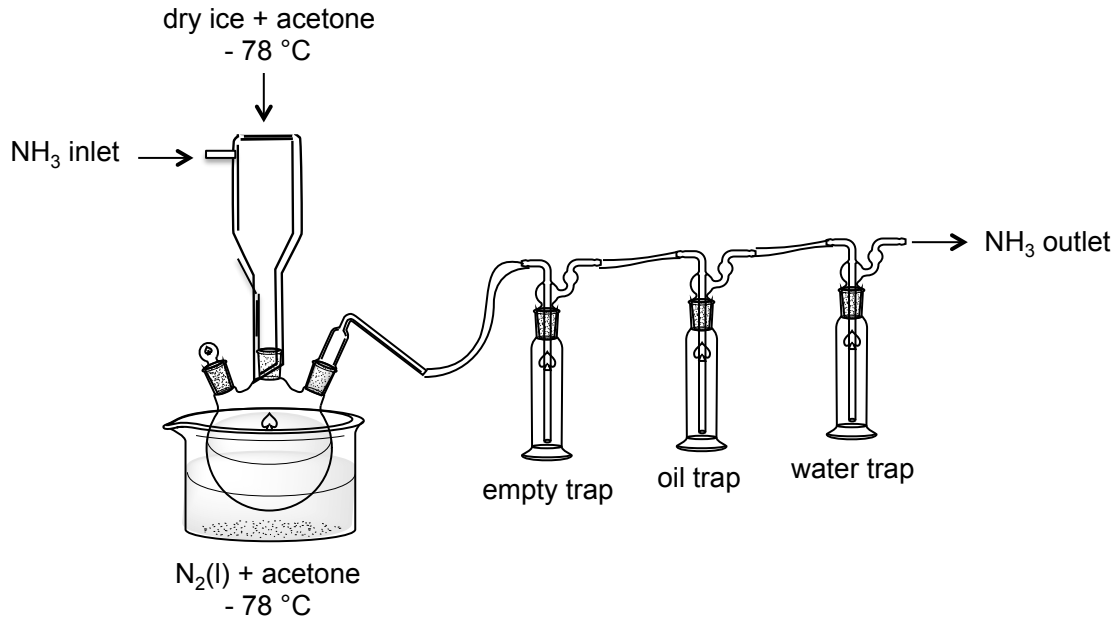

Fig. 2.3 apparatus set up for Birch reaction

Milder and safer conditions are used in the reaction with cerium ammonium nitrate (CAN). This oxidising compound is able to cleave *p*-methoxy-benzyl groups (PMB) but not benzyl groups. For this reason the synthesis of ACCA was also attempted using *p*-methoxy-benzyl amine **2b**.

As in the previous case, also this mechanism implicates the transfer of two electrons (Scheme 2.4).

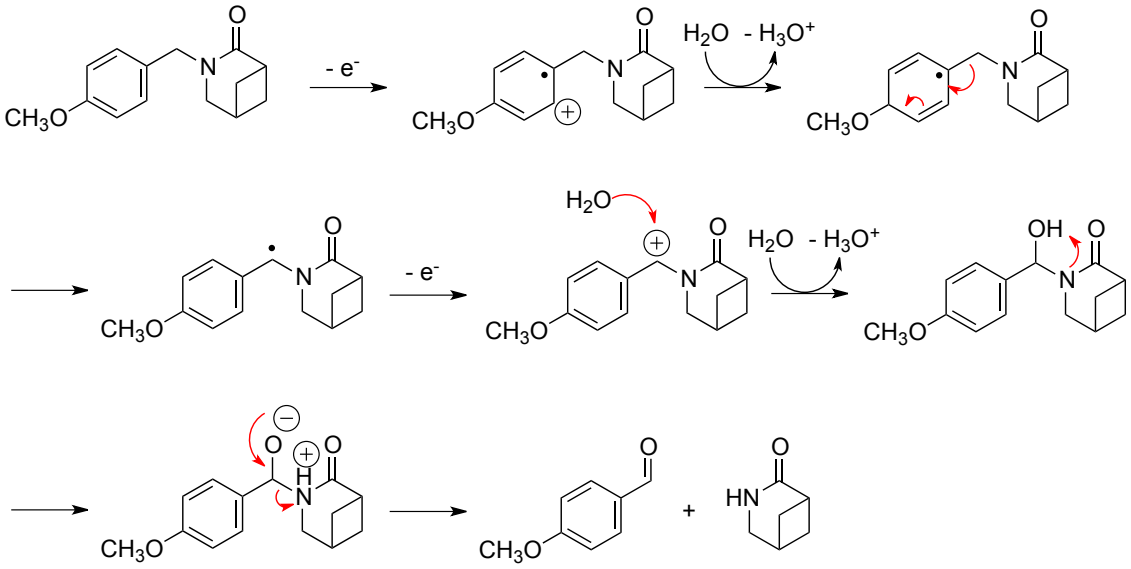

Scheme 2.4 mechanism of CAN oxidation

CAN is a very stable Ce (IV) compound and is reduced to Ce (III) after uptake of an electron from the PMB group. The PMB compound gains a water molecule and then looses a proton. This process is repeated a second time involving a second CAN molecule and generating the deprotected product **8** and PMB aldehyde.[8]

Several attempts were done with this alternative reaction for the deprotection of the lactam **7b**, but the yields were never as good as with the Birch reduction (50 % vs. 96 %) so the idea of substituting Birch conditions with CAN was abandoned, but it remains a good and green alternative.

Compound **8** was hydrolysed in acidic environment affording amino acid salt **9** as a brown solid in quantitative yield. The NMR spectrum at this stage looks clean with no need of purification (Fig. 2.4), but when Dowex 50wx8-200 resin

is used to purify the amino acid, the pure compound (95 % yield) appears like a pale beige solid, suggesting that probably some brown impurities, not detectable with NMR analysis, are present after the hydrolysis.

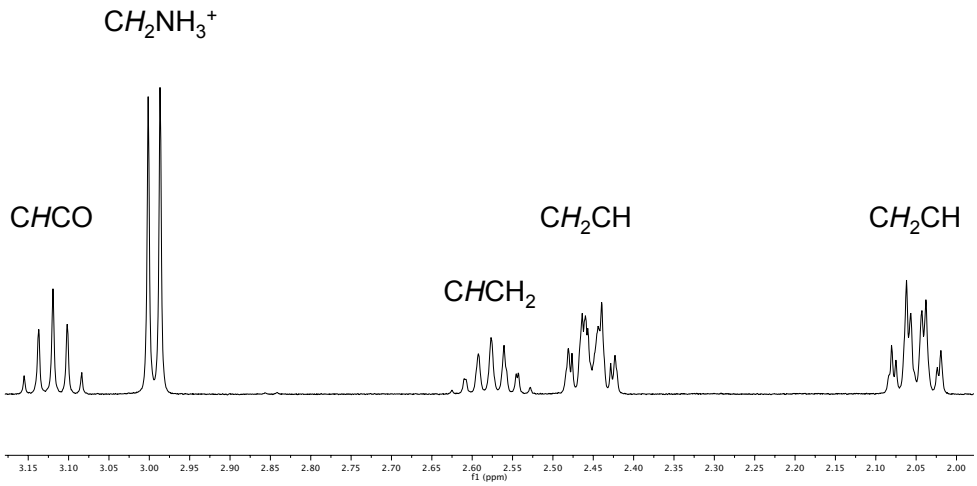

Fig. 2.4 ^{1}H-NMR spectrum of ACCA **9** with no purification

Looking at the "conformationally locked" nature of the cyclic precursor **8**, only the *cis* isomer is obtained. This is confirmed by spectroscopic analysis and by crystallographic data on the *t*-Boc protected derivative **12** (Fig. 2.5).

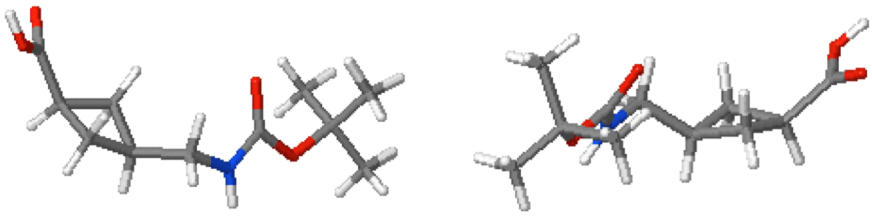

Fig. 2.5 X-ray crystal structure from two different angles of Boc protected ACCA **12**

To investigate further the possibility of epimerisation, amino acid **9** was also treated with a strong base (NaOH 2 M) and stirred overnight at 100 °C with no changes noticed in its ^{1}H-NMR spectrum, denoting a great stability of this compound. Another proof of ACCA *cis* conformation comes from the NOESY spectrum (Fig. 2.6).

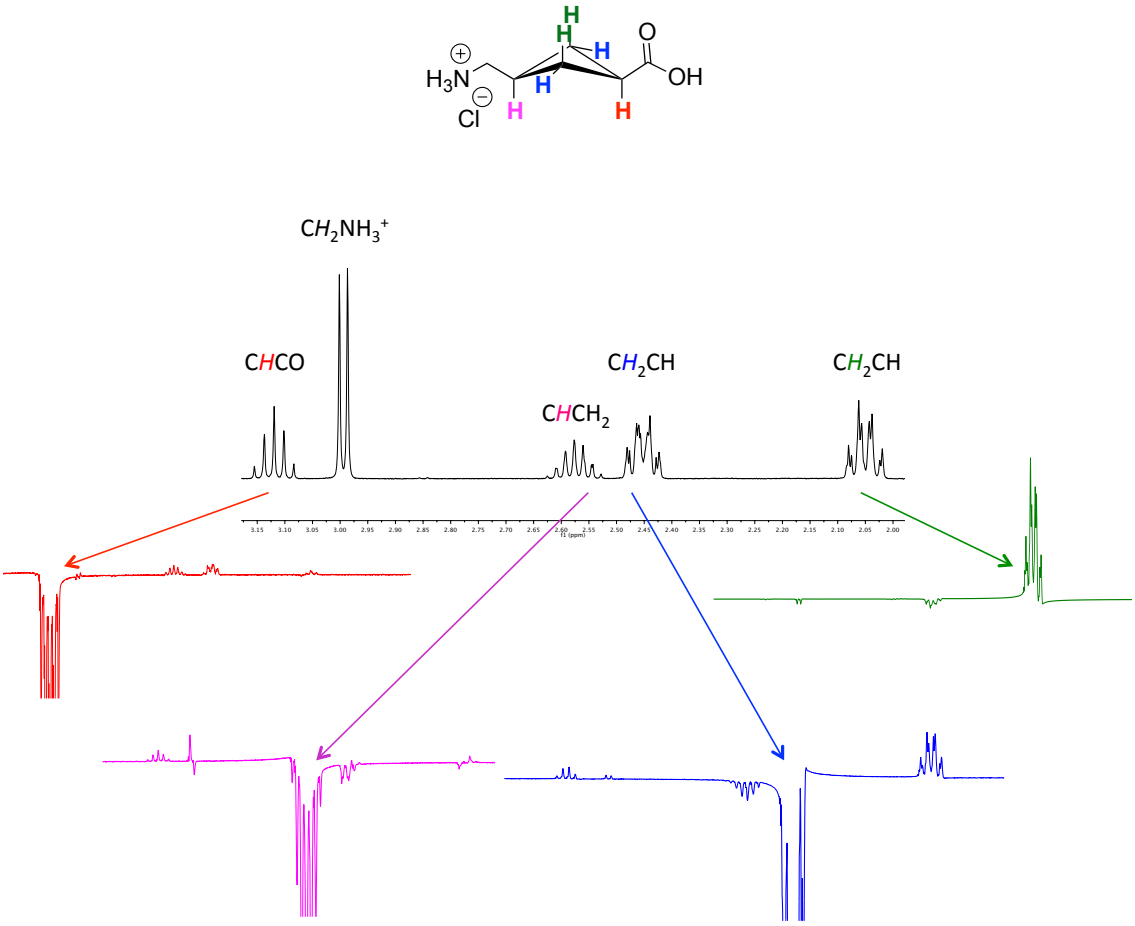

Fig. 2.6 NOESY spectrum of ACCA **9**

Is it possible to notice in fact, that after irradiation of the proton C*H*CO (red), no peak of C$H_2NH_3^+$ is visible in the spectrum, indicating that these two protons do not interact through space, because too distant from each other. This means that they are in a *trans* conformation and consequently the carboxylic group must be in the *cis* conformation with respect to $CH_2NH_3^+$.

2.2.2-Coupling of ACCA with other proteinogenic amino acids

A small library of dipeptides containing ACCA **9** and a proteinogenic amino acid **11a-c** was prepared.

To perform the coupling reaction, protection of the ACCA C-terminus and of the proteinogenic amino acid N-terminus needed to be carried out to avoid side products of unwanted coupling reactions.

The ACCA carboxylic acid moiety was protected through esterification.

The methyl ester was successfully synthesised using $SOCl_2$ in methanol, but ACCA methyl ester resulted to be unstable and easily hydrolysed back to the amino acid over time. Furthermore it appeared to be difficult to work with, due to solubility issues. Another esterification method was then adopted, generating the relative propyl ester. Successful esterification procedures are described in the literature using Lewis acids such as $TiCl_4$ and $ZrCl_4$; the technique here adopted was developed in a neighbouring group and therefore tried out in this project.[9,10]

A catalytic quantity of zirconium was found to be an effective catalyst for the esterification of amino acid **9**. The reaction proceeds with high efficiency in *n*-propanol yielding amino ester **10** in 89 % yield (Scheme 2.5).

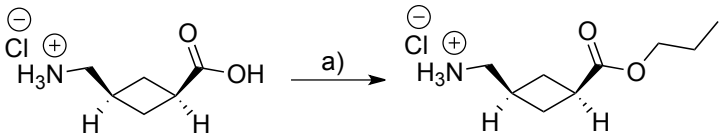

9 **10**

Scheme 2.5 esterification of ACCA **9**. *Reagents and conditions:* a) $ZrCl_4$ 20 % mol, *n*-propanol, 45 ˚C, 24 h, 89 %.

The protecting groups exploited for the N-terminus were *tert*-butyloxycarbonyl (^{t}Boc) or 9-fluorenylmethyloxycarbonyl (Fmoc). Amino acids already protected **11a-c** are commercially available.

The coupling between **10** and **11a-c** gives the protected dipeptides **12a-c** (Scheme 2.6).

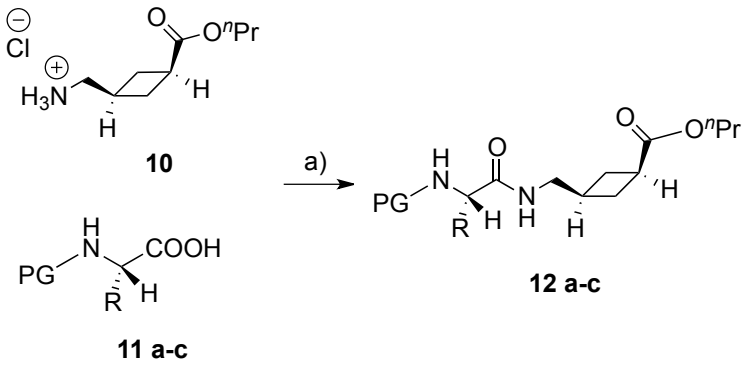

PG = Fmoc or Boc

R: a = CH_2Ph (PheACCA)
b = $CH(CH_3)_2$ (ValACCA)
c = H (GlyACCA)

Scheme 2.6 synthesis of protected ACCA dipeptides. *Reagents and conditions:* a) HATU, $^{i}Pr_2EtN$, CH_2Cl_2, 18 h, 76-92 %

The formation of the amide bond can be identified by nuclear magnetic resonance spectroscopy. In fact the amide bond is visible in the ^{1}H-NMR spectrum appearing as a small and broad peak around 5.5-6 ppm, as shown in the example for Boc-Phe-ACCA-Pr **12a** in Fig. 2.7.

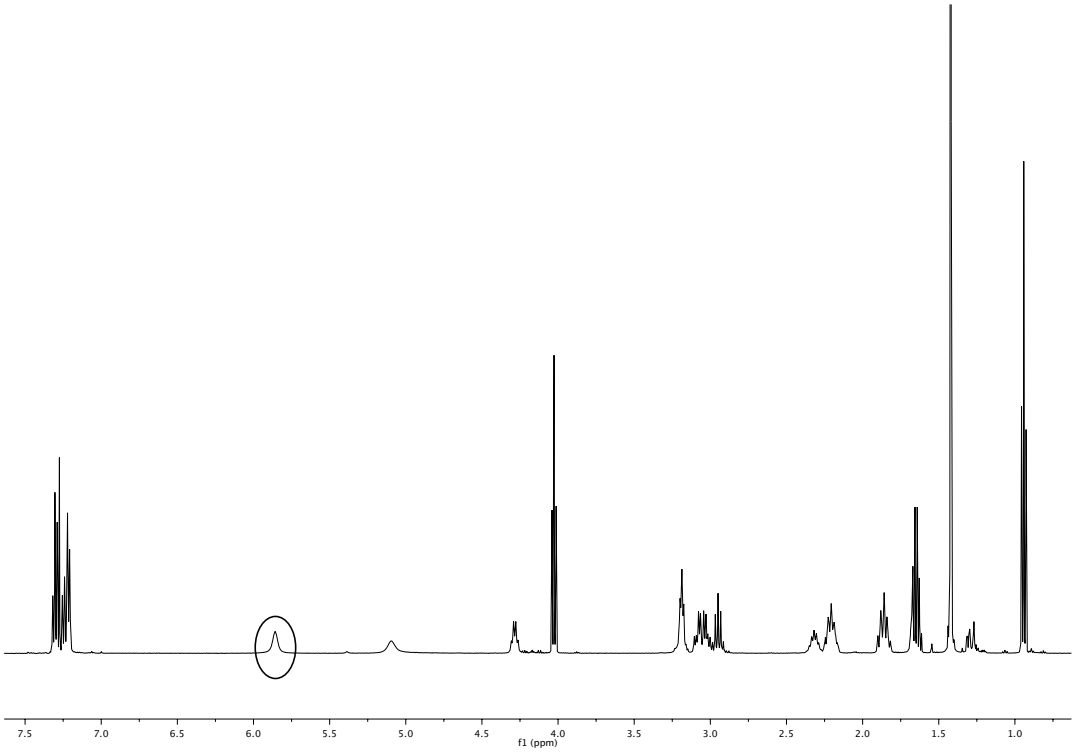

Fig. 2.7 ^{1}H-NMR spectrum of the protected dipeptide **11a**

In the case of the self-coupling product **14**, ACCA-Pr **10** was coupled with Boc-ACCA **13** (Scheme 2.7).

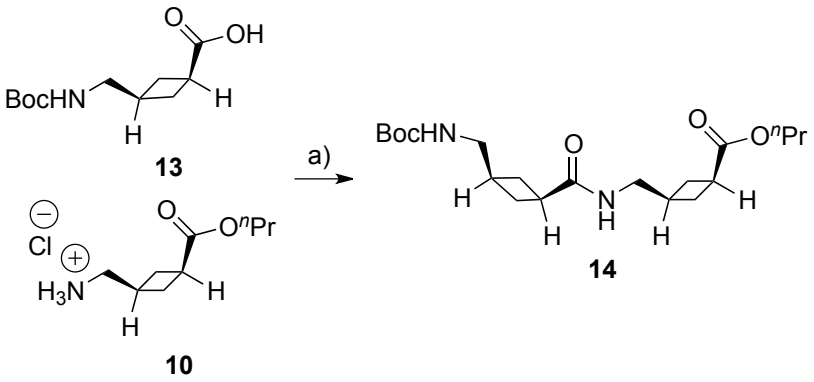

Scheme 2.7 synthesis of protected self-coupling dipeptide Boc-ACCA-ACCA-Pr. *Reagents and conditions:* a) HATU, $^{i}Pr_2EtN$, CH_2Cl_2, 18 h, 93 %

The amine protection of ACCA **9** was achieved reacting the deprotected amino acid with the anhydride di-*tert*-butyl-dicarbonate (Boc_2O) yielding compound **13** in 95 % yield as a brown solid (Scheme 2.8).

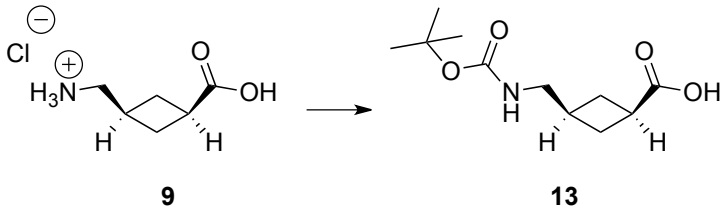

Scheme 2.8 synthesis of Boc-ACCA **13**. *Reagents and conditions:* a) Boc_2O, NaOH 2 M, dioxane/ water 2:1, 2 h, 95 %

First attempts for this reaction were carried out using *N,N'*-Diisopropylcarbodiimide (DIC, Fig 2.8), but it was not a reliable coupling agent for our purposes and best results were then achieved using O-(7-Azabenzotriazol-1-yl)-*N,N,N',N'*-tetramethyluronium hexafluorophosphate (HATU, Fig 2.8). This more modern coupling agent is part of the uranium reagents family and it is the most active.[11-13]

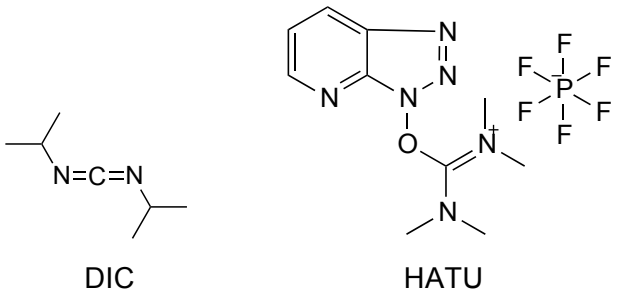

Fig. 2.8 peptide coupling agents

Carbodiimides are widely used in literature and their mechanism of action as coupling reagent is shown in Scheme 2.9.[14,15]

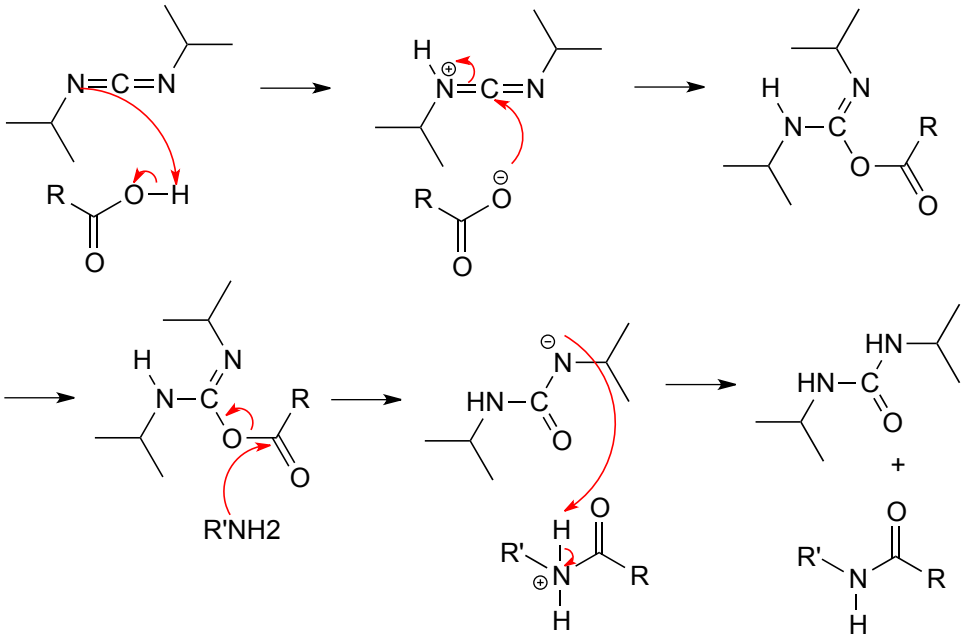

Scheme 2.9 mechanism of DIC

The mechanism of uronium salts is similar to the one for carbodiimides (Scheme 2.10). In both cases the nitrogen atom of the coupling reagent pulls the bonding electrons, generating a partial negative charge on the nitrogen and a partial positive charge on the carbon. This electrophilic carbon can be attacked from the nucleophilic deprotonated carboxylic acid.

The attack of the amine to the carboxylic acid is favoured more in the reaction with HATU due to the presence of a very good leaving group (triazole-pyridinolate), which renders the carboxylic acid more reactive.

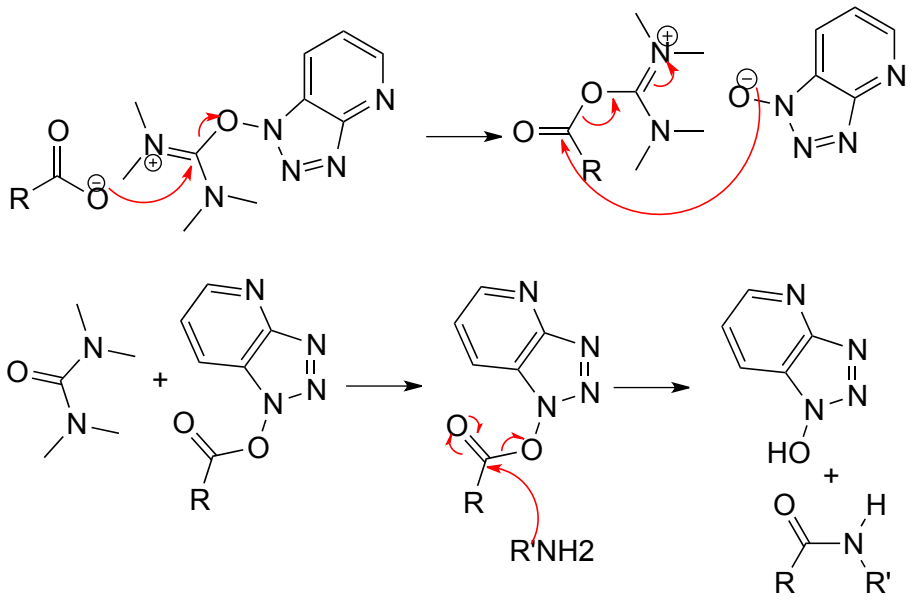

Scheme 2.10 mechanism of HATU

The two main steps in the coupling with uronium salt are therefore, activation and coupling. In the first step HATU reacts with the deprotonated carboxylic acid forming the active intermediate 7-azabenzotriazol-1-yl ester; in the second step the free amine attacks the active intermediate generating the amide bond. The rate of both steps depends on the characteristics of the amino group and carboxylic acid, so it may vary case by case.[16,17]

The carboxylic acid was deprotected through basic catalysis and that was the common denominator among all the deprotection procedures adopted for the different dipeptides. The N-terminus ^{t}Boc protecting group in **12a** was removed under standard acidic conditions. In the literature the Boc protecting group is often cleaved using trifluoro-acetic acid (TFA).[18,19] In our case the reaction with TFA/CH_2Cl_2 1:5 works in an hour at 25 °C (83 %), but hydrolysis with HCl/Et_2O was preferred (Scheme 2.11).

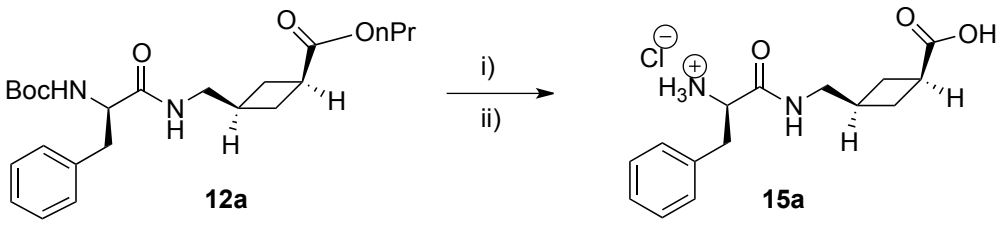

Scheme 2.11 deprotection of Boc-Phe-ACCA-Pr **12a**. *Reagents and conditions:* (i) NaOH 2 M, CH_3CN, 45 ºC, 3 h, 95 %; (ii) HCl/Et_2O, CH_2Cl_2, 4 h, 95 %

For the latter reaction, the non-aqueous environment allowed for the precipitation of the deprotected amino acid product **15a** as an off white solid with 95 % yield, making the work up significantly easier.

The cleavage of the N-terminus Fmoc protecting group was expected to take place under basic conditions used for the ester cleavage, namely hydrolysis in NaOH. Unfortunately, when this procedure was attempted with Gly-ACCA (**15c**), an unexpected behaviour was noted. The ^{1}H-NMR spectrum showed a splitting of all the signals (Fig. 2.9), which was initially thought to be due to epimerisation of the compound. Two-dimensional NMR studies could not explain what the second compound was, but it was clear that neither diasteromers nor rotamers were involved in the phenomenon.

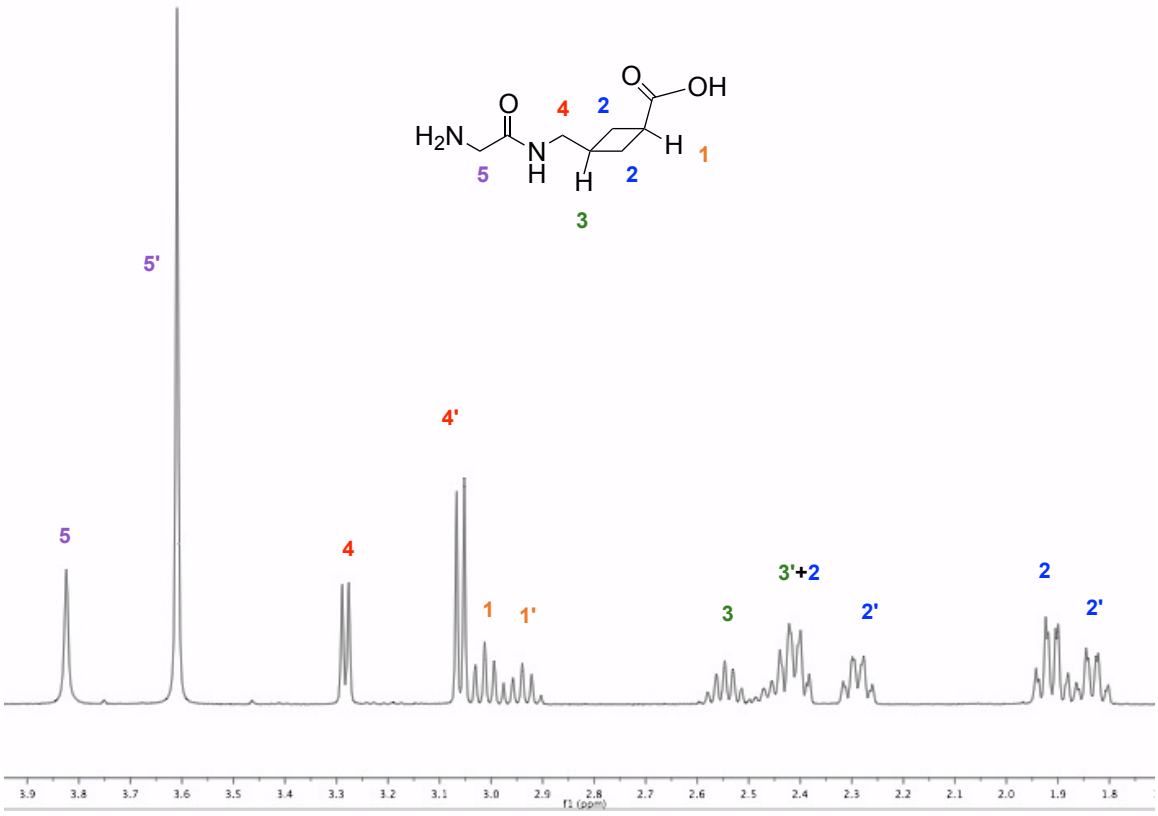

Fig. 2.9 ^{1}H-NMR spectrum of Gly-ACCA 12c deprotected using hydrolysis in NaOH

To make sure that the unwanted behaviour was not due to the Fmoc protecting group, the reaction was tested on FmocVal. When **12b** was hydrolysed in NaOH (Scheme 2.12), both NH_2 and COOH were cleved at the same time providing a clean spectrum in 90 % yield.

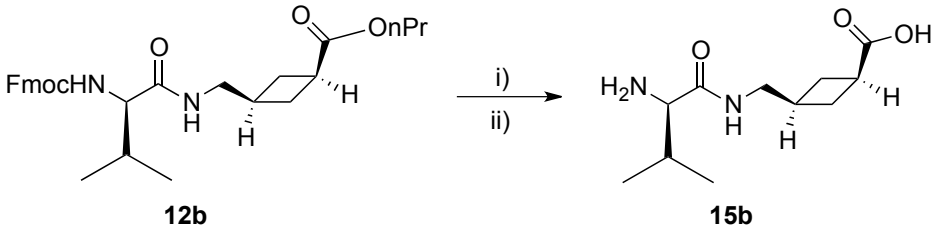

12b **15b**

Scheme 2.12 deprotection of Fmoc-Val-ACCA-Pr **12b**. *Reagents and conditions:* NaOH 2 M, dioxane/water 7:3, 45 °C, 3 h, 90 %

Once it was proved that the Fmoc was not the responsible for the unexpected behaviour observed with **11c**, a different approach was investigated. A stepwise deprotection protocol was employed, using a milder base for the first step. Initially piperidine was attempted for the selective cleavage of the Fmoc group, but the product could not be isolated with a sufficient degree of purity. Triethylamine (TEA) proved to be the best choice, even if a longer reaction time was needed. Compound **14c** was achieved after refluxing it overnight and followed by purification with 50wx8-200 ion exchange chromatography with excellent yields. The ion exchange resin purification step was sufficient to catalyse the hydrolysis of the ester protecting group, affording the free carboxylic acid in 90 % yield (Scheme 2.13).

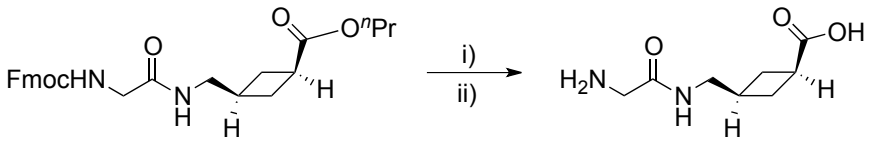

12c **15c**

Scheme 2.13 deprotection of Fmoc-Gly-ACCA-Pr **12c**. *Reagents and conditions:* CH_2Cl_2/TEA 1:1, 45 ºC, 24 h, 90 %

This hydrolysis technique was previously described in the literature.[20,21]

For the deprotection of the self-coupling product **14**, the procedure already employed for **12a** was used, yielding compound **16** in 81 % yield over the two deprotection steps (Scheme 2.14).

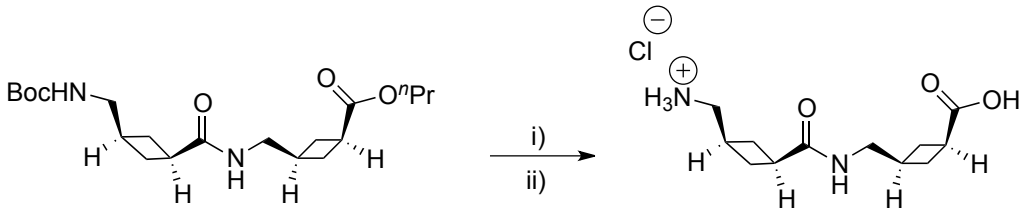

14 **16**

Scheme 2.14 deprotection of Boc-ACCA-ACCA-Pr **14**. *Reagents and conditions:* (i) NaOH 2 M, CH_2CN, 45 ºC, 3 h, 90 %; (ii) HCl/Et_2O, CH_2Cl_2, 4 h, 90 %

2.3-Conclusions

An efficient route has been developed for the synthesis of *cis*-3-(amino-methyl)cyclobutane carboxylic acid (ACCA), a novel non-proteinogenic δ-amino acid. The overall procedure gives ACCA in 23 % yield.

The main interesting characteristics of this achiral molecule are the cyclobutane core and its conformational rigidity. Due to the synthetic strategy employed, only the *cis* isomer is formed upon hydrolysis. NMR and X-ray crystallography data prove that no epimerisation of the amino acid occurs under the reaction conditions used.

This conformationally constrained δ-amino acid can find applications in the field of peptidomimetics and can also be widely exploited as synthetic building block.

Finally, a small library of dipeptides has been synthesised through HATU assisted coupling of ACCA with the proteinogenic amino acids Phe, Val, Gly. The dipeptide of ACCA coupled with itself was also synthesised.

2.4-Experimental

General Methods:

HATU and FmocVal were purchased from IRIS Biotech GmbH; all the other chemicals were purchased from Sigma Aldrich unless otherwise stated. Dry solvents were obtained from a Puresol Grubbs Speciality Chemicals and Stream. When necessary, all reactions were performed under an atmosphere of nitrogen using oven-dried glassware. Oxygen-free nitrogen was obtained from BOC gases and used without further drying.

Proton and carbon nuclear magnetic resonance spectra (^{1}H and ^{13}C-NMR respectively) were recorded on 400 MHz (operating frequencies: ^{1}H, 399.75 MHz; ^{13}C, 101.00 MHz), 500 MHz (operating frequencies: ^{1}H, 499.72 MHz; ^{13}C, 125.65 MHz) and 600 MHz (operating frequencies: ^{1}H, 599.78 MHz; ^{13}C, 150.82 MHz) FT spectrometers. ^{1}H-NMR spectra are herein reported, while ^{13}C-NMR spectra are in appendix 1. Tetramethylsilane (δ = 0.00 ppm) was used as an internal reference in the deuterated chloroform ($CDCl_3$) for ^{1}H NMR spectra. The middle $CDCl_3$ solvent peak was referenced to 77.16 ppm for ^{13}C NMR spectra. The residual solvent peak in deuterated methanol (CD_3OD) was referenced to 3.31 ppm and 49.00 ppm for ^{1}H NMR and ^{13}C NMR spectra respectively. The residual solvent peak in deuterated water (D_2O) was referenced to 4.79 ppm for ^{1}H NMR. The coupling constants (*J*) are in Hz and the chemical shifts (δ) are given in parts per million. High resolution mass spectra were obtained on a Waters/Micromass instrument, optical rotations were measured at 20 °C on a Perkin-Elmer 241 polarimeter and melting points were measured on a Stuart^{TM} melting point apparatus SMP 10. Evaporation *in vacuo* refers to the removal of solvent on a Büchi rotary evaporator with an integrated vacuum pump. Thin-layer chromatography (TLC) was carried out on aluminium backed 60 F254 silica gel.

Compounds **3** and **4** were prepared as described in the work of Cook and colleagues, with minor adjustments.[3]

Methyl 1-benzyl-6-oxo-1,4,5,6-tetrahydropyridine-3-carboxylate (3a):

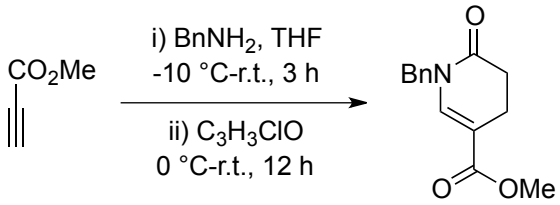

1 **3a**

$BnNH_2$ **2a** (9.27 g, 86.50 mmol) was added to a stirred solution of methyl propiolate **1** (8.00 g, 95.16 mmol) in THF (250 mL) at -10 °C. The solution was allowed to warm slowly to room temperature and stirred for 3 hours. The mixture was brought again to 0 °C and acryloyl chloride (7.70 mL, 95.15 mmol) was added. The reaction was allowed to warm slowly to room temperature and was stirred for 12 hours. The precipitate was filtered off and the solution was washed with saturated aqueous $NaHCO_3$ (200 mL). The organic layer was separated and the aqueous layer was extracted with Et_2O (100 mL x 3). The organic layers were combined, dried over $MgSO_4$ and concentrated *in vacuo.* The crude oil was purified by silica gel column chromatography (cyclohexane/Et_2O, 70:30) to give **3a** (9.2 g, 43 %) as a yellow oil. (Rf = 0.36, Cyclohexane/EtOAc, 50:50). δH (600 MHz; $CDCl_3$) 7.37-7.21 (6H, m, PhH and NCH) 4.74 (2H, s, $PhCH_2$), 3.71 (3H, s, OCH_3), 2.64 (4H, s, $COCH_2CH_2$). δC (151 MHz; $CDCl_3$) 169.6, 166.6, 139.4, 136.5, 128.8, 127.8, 127.6, 108.9, 51.5, 49.9, 30.7, 19.8. m/z (ES+) 246.1119 ($M+H^+$ $C_{14}H_{16}NO_3$ requires 246.113).

The reaction of *p*-methoxybenzyl amine **2b** gave **3b** in 56 % yield as a yellow oil. (Rf = 0.58, Cyclohexane/EtOAc, 50:50). δH (400 MHz; $CDCl_3$) 7.28 (1H, s, NCH), 7.18 (2H, d, CH_3OPhH) 6.88 (2H, d, $PhHCH_2N$) 4.67 (2H, s, $PhCH_2$), 3.80 (3H, s, CH_3OPh), 3.72 (3H, s, OCH_3), 2.62 (4H, s, $COCH_2CH_2$); δC (101 MHz; $CDCl_3$) 169.7, 166.8, 159.3, 139.5, 129.3, 128.6, 114.1, 108.8, 55.4, 51.7, 49.3, 30.7, 19.8. m/z (ES+) 298.1055 ($M+Na^+$ $C_{15}H_{17}NO_4Na$ required 298.1068).

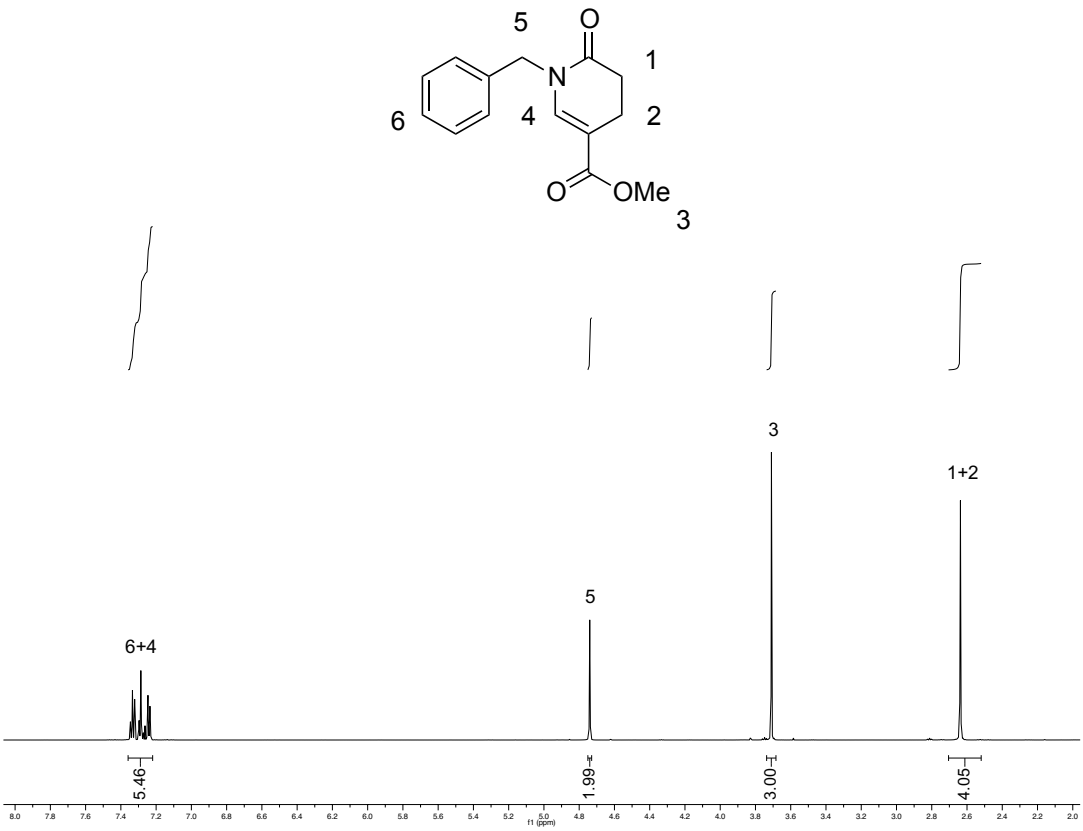

Preparation of (±) Methyl 1-benzyl-6-oxopiperidine-3-carboxylate (4a)

Method 1:

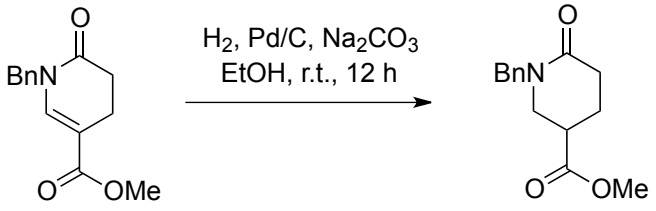

3a **4a**

A solution of **3a** (8.60 g, 35.09 mmol), Na_2CO_3 (11.15 g, 105.27 mmol) and 10 % Pd/C (3.71 g, 10 mol %) in EtOH (55 mL) was stirred under an atmosphere of H_2 for 12 hours. The solids were removed by filtration and the mixture was concentrated *in vacuo.* The crude oil was purified by silica gel column chromatography (cyclohexane/EtOAc, 60:40) to give **4a** (8.42 g, 95% yield) as a clear oil. (Rf = 0.10, Cyclohexane/EtOAc, 50:50). δH (400 MHz; $CDCl_3$) 7.38-7.18 (5H, m, PhH), 4.68 (1H, d, *J* = 14.6 Hz, $PhCH_2$), 4.53 (1H, d, *J* = 14.6 Hz,

$PhCH_2$), 3.65 (3H, s, OCH_3), 3.48-3.35 (2H, m, NCH_2), 2.83-2.74 (1H, m, C*H*CO_2CH_3), 2.60 (1H, dt, *J* = 17.7 and 4.4, $COCH_2$), 2.53-2.42 (1H, m, $COCH_2$), 2.18-2.1 (1H, m, $COCH_2CH_2$), 2.06-1.95 (1H, m, $COCH_2CH_2$). δC (101 MHz; $CDCl_3$) 172.6, 169.0, 136.8, 128.6, 128.1, 127.5, 52.1, 50.2, 48.0, 39.1, 30.7, 23.9. m/z (ES+) 248.1275 ($M+H^+$ $C_{14}H_{18}NO_3$ requires 248.1287).

The reaction of **3b** gave **4b** as a clear oil in 95 % yield. (Rf = 0.20, Cyclohexane/EtOAc, 50:50). δH (500 MHz; $CDCl_3$) 7.20 (2H, d, *J* = 8.6 Hz, CH_3OPhH), 6.86 (2H, d, *J* = 8.6 Hz, Ph*H*CH_2N), 4.63 (1H, dd, *J* = 14.5 and 4.0 Hz, $PhCH_2$), 4.44 (1H, dd, *J* = 14.5 and 3.8 Hz, $PhCH_2$), 3.80 (3H, s, OCH_3), 3.66 (3H, s, CH_3OPh), 3.44-3.35 (2H, m, NCH_2), 2.79-2.72 (1H, m, C*H*CO_2CH_3), 2.61-2.55 (1H, m, *J* = 17.8 and 5.4 Hz, $COCH_2$), 2.49-2.42 (1H, m, $COCH_2$), 2.16-2.10 (1H, m, $COCH_2CH_2$), 2.02-1.94 (1H, m, $COCH_2CH_2$). δC (75 MHz; $CDCl_3$) 169.6, 166.1, 159.2, 139.1, 129.0, 128.6, 114.2, 108.6, 55.2, 51.5, 49.2, 30.8, 19.8. m/z (ES+) 300.1212 ($M+H^+$ $C_{15}H_{19}NO_4Na$ requires 300.1223).

Method 2 (ammonium formate):

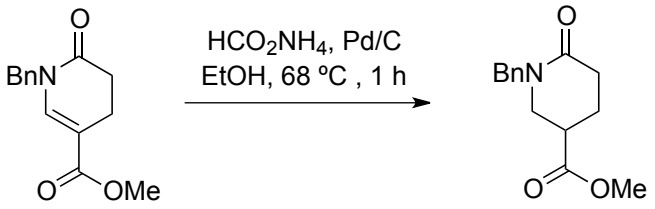

3a **4a**

A solution of **3a** (4.5 g, 18.36 mmol) was dissolved in EtOH (100 mL) with 10 % Pd/C (2.00 g, 1.84 mmol). Ammonium formate was added (11.8 g, 187 mmol) and the reaction was refluxed at 68 ˚C for 1 hour. The solids were removed by filtration and the mixture was concentrated *in vacuo.* The crude oil was purified by silica gel column chromatography (cyclohexane/EtOAc, 50:50) to give **4a** (4.13 g, 91 % yield) as a clear oil.

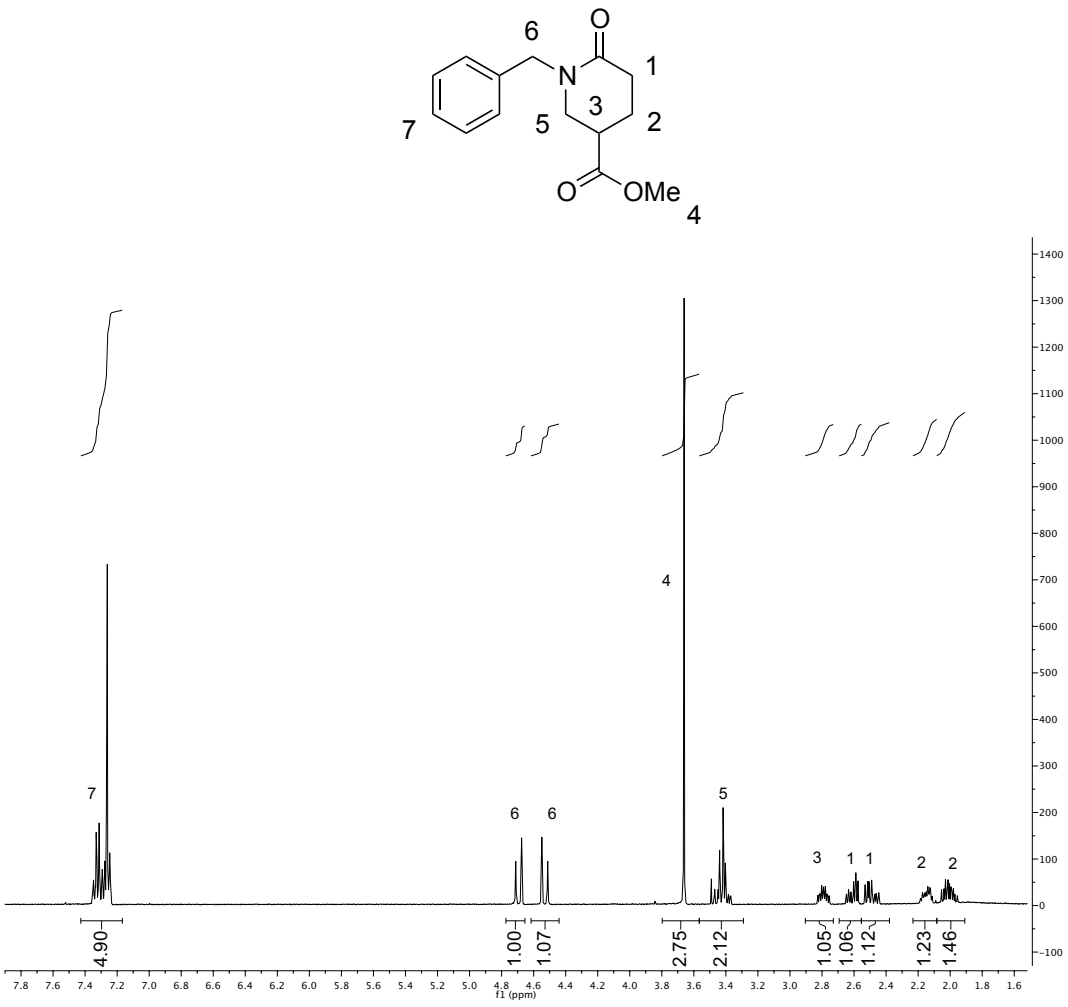

Preparation of (±)1-Benzyl-5-(hydroxymethyl)piperidin-2-one (5a):

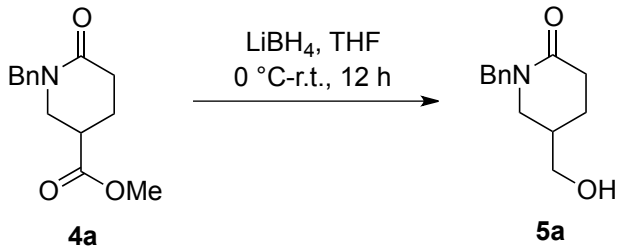

4a **5a**

(±)**4a** (5.23 g, 23.85 mmol) was dissolved in anhydrous THF (35 mL) and cooled to 0 °C. $LiBH_4$ (1.04 g, 47.70 mmol) was added and the solution was allowed to warm to room temperature and stirred overnight. The reaction was quenched at 0 °C with water (20 mL) and then with 10 % HCl. The organic layer was separated and the aqueous layer was extracted with EtOAc (20 mL x 4).

The organic layers were combined, dried over $MgSO_4$ and concentrated *in vacuo.* The crude oil was purified by silica gel column chromatography (cyclohexane/EtOAc, 60:40) to give (±)**5** (4.03 g, 87 % yield) as a clear oil. (Rf = 0.11, EtOAc, 50:50). δH (600 MHz; $CDCl_3$) 7.33-7.18 (5H, m, PhH), 4.59 (1H, d, *J* = 14.6 Hz, $PhCH_2$), 4.53 (1H, d, *J* = 14.6 Hz, $PhCH_2$), 3.53 (1H, dd, *J* = 10.7 and 5.6 Hz, C*H*$_2$OH), 3.44 (1H, dd, *J* = 10.7 and 7.2 Hz, C*H*$_2$OH), 3.30 (1H, dd, *J* = 12.2, 5.2 Hz, NCH_2), 2.99 (1H, dd, *J* = 12.2 and 10.1 Hz, NCH_2), 2.92 (1H, br s, OH), 2.51 (1H, ddd, *J* = 17.8, 5.8 and 3.4 Hz, $COCH_2$), 2.39 (ddd, *J* = 17.8, 11.3 and 6.5 Hz, $COCH_2$), 2.04-1.95 (1H, m, C*H*CH_2OH), 1.89-1.82 (1H, m, $COCH_2$C*H*$_2$), 1.54-1.46 (1H, m, $COCH_2$C*H*$_2$). δC (151 MHz; $CDCl_3$) 170.0, 137.0, 128.5, 127.9, 127.3, 64.3, 50.3, 49.8, 36.4, 31.1, 23.8. m/z (ES+) 220.1329 ($M+H^+$ $C_{13}H_{18}NO_2$ requires 220.1338).

The reaction of **4b** gave (±)**5b** as a clear oil in 85 % yield. (Rf = 0.5, EtOAc 100 %). δH (400 MHz; $CDCl_3$) 7.18 (2H, d, *J* = 8.6 Hz, CH_3OPh*H*), 6.86 (2H, d, *J* = 8.6 Hz, Ph*H*CH_2N), 4.52 (1H, s, $PhCH_2$), 3.79 (3H, s, CH_3OPh), 3.60-3.56 (1H, dd, *J* = 10.6 and 5.6 Hz, C*H*$_2$OH), 3.51-3.46 (1H, dd, *J* = 10.6 and 7.2 Hz, C*H*$_2$OH), 3.33-3.29 (1H, dd, *J* = 5.2 and 1.3 Hz, NCH_2), 3.02-2.96 (1H, dd, *J* = 10.0 and 12.0 Hz, NCH_2), 2.57-2.55 (1H, ddd, *J* = 17.8, 6.0 and 3.5 Hz, $COCH_2$), 2.46-2.37 (ddd, *J* = 17.7, 11.2 and 6.5 Hz, $COCH_2$), 2.06-1.96 (1H, m, C*H*CH_2OH), 1.92-1.85 (1H, m, $COCH_2$C*H*$_2$), 1.56-1.46 (1H, m, $COCH_2$C*H*$_2$). δC (101 MHz; $CDCl_3$) 170.1, 159.4, 130.0, 129.7, 114.4, 65.1, 55.7, 50.1, 49.9, 36.9, 31.3, 24.3. m/z (ES+) 250.1443 ($M+H^+$ $C_{14}H_{20}NO_3$ requires 250.1454).

Preparation of (±) 1-Benzyl-5-(iodomethyl)piperidin-2-one (6a):

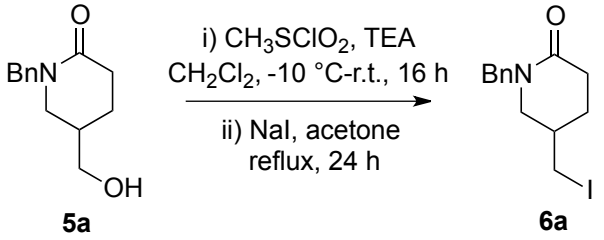

5a **6a**

(±)**5a** (3.92 g, 13.18 mmol) was dissolved in anhydrous CH_2Cl_2 (25 mL). The solution was cooled to -10 °C and TEA (2.0 g, 19.77 mmol) was added, followed by the slow addition of CH_3SO_2Cl (1.81 g, 15.19 mmol). The solution was allowed to warm slowly to room temperature and stirred overnight. The organic layer was concentrated *in vacuo* and dissolved in acetone (50 mL) and NaI (3.98 g, 26.58 mmol) was added to the stirring solution. The mixture was stirred under reflux for 24 hours. The organic solvent was removed *in vacuo* and H_2O (40 mL) was added along with EtOAc (50 mL) the organic layer was separated and the aqueous layer was extracted with EtOAc (20 mL x 5). The

organic layers were combined, washed with brine, dried over $MgSO_4$ and concentrated *in vacuo.* The crude oil was purified by silica gel column chromatography (cyclohexane/EtOAc, 70:30) to give (±)**6a** (3.36 g, 79 % yield) as a yellow/orange oil. (Rf = 0.12, Cyclohexane/EtOAc, 50:50). δH (500 MHz; $CDCl_3$) 7.3-7.22 (5H, m, PhH), 4.63 (1H, d, *J* = 14.7 Hz, $PhCH_2$), 4.54 (1H, d, *J* = 14.7 Hz, $PhCH_2$), 3.34 (1H, m, NCH_2), 3.08 (2H, m, CH_2I), 2.97 (1H, dd, *J* = 12.0 and 9.5 Hz, NCH_2), 2.56 (1H, ddd, *J* = 17.7, 6.2 and 3.6 Hz, $COCH_2$), 2.45 (1H, ddd, *J* = 17.7, 11.2 and 6.2 Hz, $COCH_2$), 2.06-1.95 (2H, m, $COCH_2CH_2$), 1.66-1.54 (1H, m, $CHCH_2I$). δC (126 MHz; $CDCl_3$) 169.0, 136.8, 128.5, 128.0, 127.4, 52.3, 50.1, 35.9, 30.7, 27.7, 7.9. m/z (ES+) 329.0273 ($M+H^+$. $C_{13}H_{16}INO$ requires 329.0277).

The reaction in two steps of **5b** gave (±)**6b** as a dark yellow oil in 77 % yield. (Rf = 0.32, EtOAc 100%). δH (400 MHz; $CDCl_3$) 7.21 (2H, d, *J* = 8.5 Hz, CH_3OPhH), 6.87 (2H, d, *J* = 8.5 Hz, $PhHCH_2N$), 4.59 (1H, d, *J* = 14.4 Hz, $PhCH_2$), 4.46 (1H, d, *J* = 14.4 Hz, $PhCH_2$), 3.80 (1H, s, CH_3OPh), 3.37-3.32 (1H, m, NCH_2), 3.13-3.05 (2H, m, CH_2I), 2.98-2-93 (1H, dd, *J* = 12.0 and 9.6 Hz, NCH_2), 2.59-2.52 (1H, ddd, *J* = 17.8, 6.0 and 3.6 Hz, $COCH_2$), 2.49-2.40 (1H, ddd, *J* = 17.4, 11.0 and 6.3 Hz, $COCH_2$), 2.05-1.95 (2H, m, $COCH_2CH_2$), 1.65-1.54 (1H, m, $CHCH_2I$); δC (101 MHz; $CDCl_3$) 169.5, 159.5, 130.0, 129.5, 114.5, 55.7, 52.7 50.1, 36.5, 31.3, 28.3, 8.4. m/z (ES+) 360.0469 ($M+H^+$. $C_{14}H_{19}INO_2$ requires 360.0461).

Direct iodination:

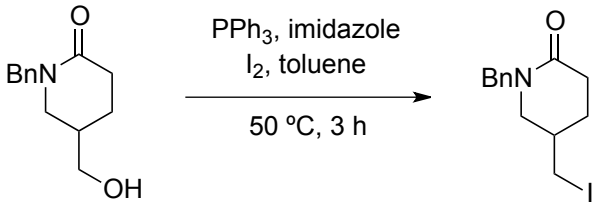

5a **6a**

Racemic alcohol (±)**5a** (0.42 g, 1.9 mmol) was dissolved in toluene (19 mL). Ph_3P (0.55 g, 2.1 mmol), I_2 (0.53 g, 4.18 mmol) and imidazole (0.29 g, 4.29mmol) were added. The mixture was refluxed at 90 °C for 3 hours. Na_2CO_3 saturated water was added to the reaction mixture, toluene was separated and the aqueous layer was extracted with EtOAc (15 mL x 3). The organic layers were combined, dried over $MgSO_4$ and concentrated *in vacuo*. The crude oil was purified by alumina gel column chromatography (CH_2Cl_2/cyclohexane 70:30) yielding (±) 1-benzyl-5-(iodomethyl)piperidin-2-one (±)**6a** (0.43 g, 68% yield) as a yellow/orange oil.

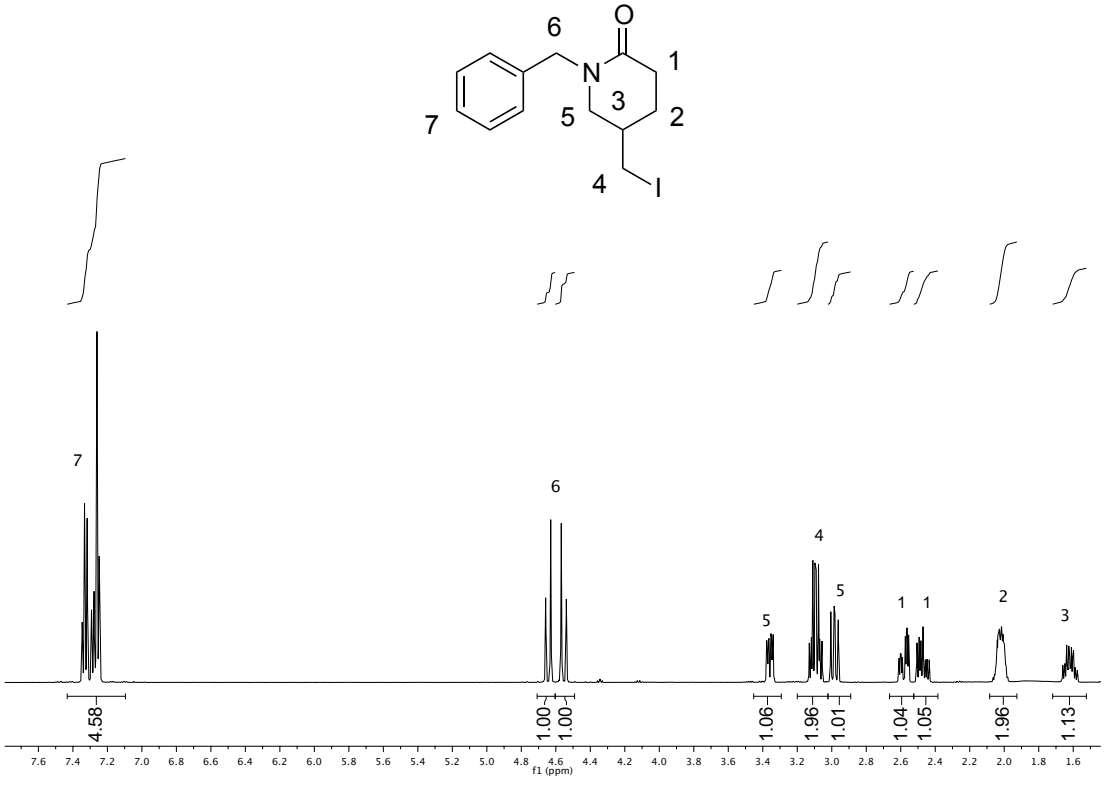

Preparation of 3-Benzyl-3-aza-bicyclo[3.1.1]heptan-2-one (7a):

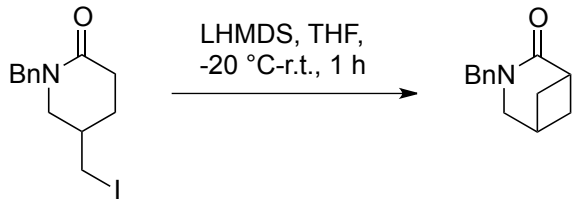

6a **7a**

(±)**6a** (3.2 g, 9.72 mmol) was dissolved in anhydrous THF (50 mL) and LHMDS (1M soln./THF, 9.72 mL) was added at -20 °C. The solution was stirred for one hour before being quenched with H_2O (15 mL). EtOAc (20 mL) was added and the organic layer was separated. The aqueous layer was extracted with EtOAc (15 mL x 3). The organic layers were combined, dried over $MgSO_4$ and concentrated *in vacuo.* The crude oil was filtered through a short silica column (cyclohexane/EtOAc, 2:1) to give **7a** (1.82 g, 86 % yield) as a yellow/orange oil. (Rf = 0.24, Cyclohexane/EtOAc, 50:50). δH (500 MHz; $CDCl_3$) 7.36-7.22 (5H, m, PhH), 4.61 (2H, s, $PhCH_2$), 3.26 (2H, d, *J* = 1.5 Hz, NCH_2), 2.84 (1H, q, *J* = 5.7 Hz, COCH), 2.72-2.65 (1H, m, NCH_2CH), 2.38-2.28 (2H, m, $COCH(CHH)_2$), 1.73-1.63 (2H, m, $COCH(CHH)_2$). δC (126 MHz; $CDCl_3$) 175.7, 137.4, 128.5, 128.0, 127.2, 50.0, 48.0, 41.1, 33.2, 30.9. m/z (ES+) 202.1222 ($M+H^+$ $C_{13}H_{16}NO$ requires 202.1232).

The reaction of **6b** gave **7a** as a crude oil was filtered through a short silica column (cyclohexane/EtOAc, 70:30) in 84 % yield as a yellow/orange oil. (Rf = 0.39, Cyclohexane/EtOAc, 50:50). δH (500 MHz; $CDCl_3$) 7.19 (2H, d, *J* = 8.6 Hz, CH_3OPhH), 6.86 (2H, d, *J* = 8.6 Hz, $PhHCH_2N$), 4.54 (2H, s, $PhCH_2$), 3.79 (1H, s, CH_3OPh), 3.25 (2H, d, *J* = 2.5 Hz, NCH_2), 2.85-2.81 (1H, q, *J* = 5.8 Hz, COCH), 2.70-2.66 (1H, m, NCH_2CH), 2.35-2.28 (2H, m, $COCH(CHH)_2$), 1.67-1.62 (2H, m, $COCH(CHH)_2$). δC (126 MHz; $CDCl_3$) 175.9, 159.1, 129.8, 129.7, 114.2, 55.5, 50.1, 47.7, 41.4, 33.5, 31.2. m/z (ES+) 254.1157 ($M+Na^+$ $C_{14}H_{17}NO_2Na$ requires 254.1668).

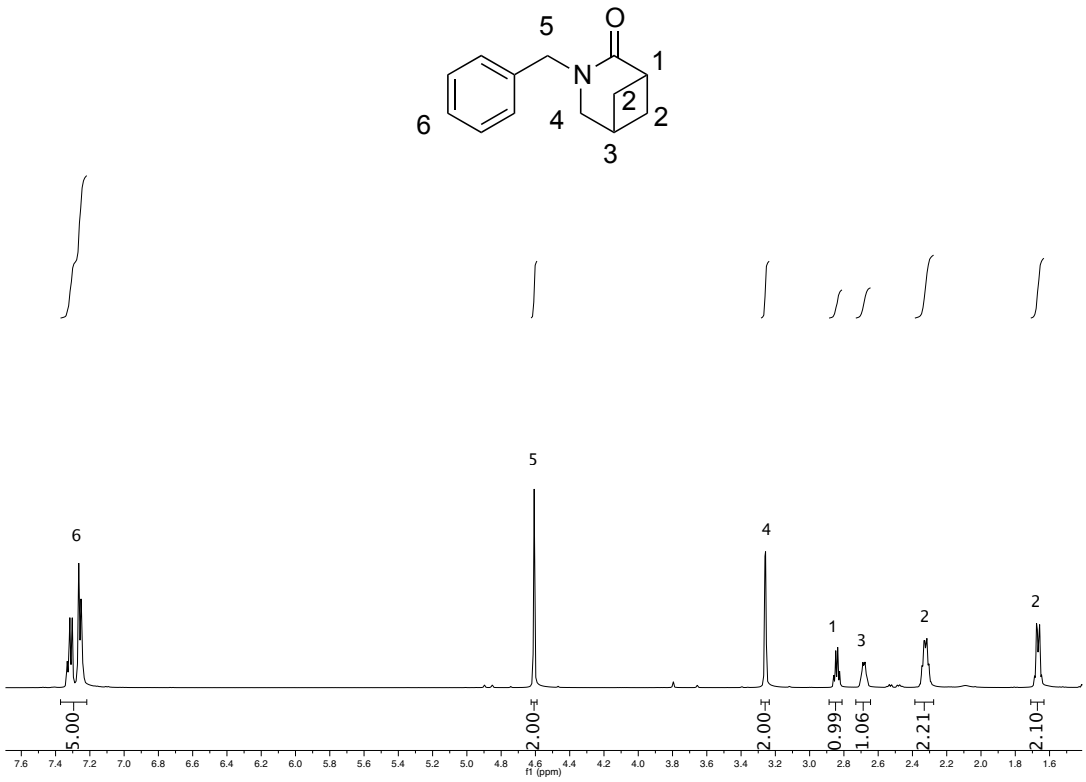

Preparation of 3-aza-bicyclo[3.1.1]heptan-2-one (8) from 7a:

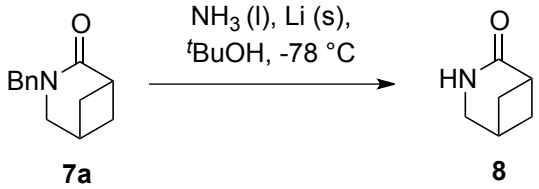

7a **8**

7a (1.5 g, 7.45 mmol) was dissolved in anhydrous THF/^{t}BuOH, 10:1 (10 mL) and the mixture was added to a stirring liquid ammonia at -78 °C. Metallic Li pellets were added slowly to the stirring solution until a constant blue/black colour was observed. The reaction was then quenched by the addition of solid ammonium chloride. After removal of the NH_3, EtOAc (30 mL) and H_2O (8 mL) was added. The organic layer was separated and the aqueous layer was extracted with EtOAc (15 mL x 3). The organic layers were combined, dried over $MgSO_4$ and concentrated *in vacuo.* The crude oil was filtered through a short silica column (cyclohexane/EtOAc, 1:1) to give **8** (800 mg, 96 % yield) as

a yellow oil. (Rf = 0.1, EtOAc, 50:50). δH (500 MHz; CD_3OD) 7.46-7.13 (1H, m, NH) 3.43 (2H, d, *J* = 2.0 Hz, NCH_2), 2.81-2.71 (1H, m, NCH_2CH), 2.60 (1H, q, *J* = 5.6 Hz, COCH), 2.48-2.37 (2H, m, $COCH(CHH)_2$), 1.70-1.62 (2H, m, $COCH(CHH)_2$). δC (126 MHz; CD_3OD) 181.5, 46.3, 42.0, 34.3, 31.4. m/z (ES+) 111.0684 ($M+H^+$ C_6H_9NO requires 111.0684).

Preparation of 3-aza-bicyclo[3.1.1]heptan-2-one (8) from 7b:

7b (0.51 g, 2.2 mmol) was dissolved in CH_3CN/H_2O, 3:2 (25 mL) and ammonium cerium nitrate (CAN, 4.2 g, 7.7 mmol) was added to the solution. The reaction was left under stirring for 4.5 hours. CH_3CN was then removed *in vacuo* and the water phase was extracted with CH_2Cl_2 (15 mL x 5). The organic layers were combined, dried over $MgSO_4$ and concentrated *in vacuo* to give **8** with no need of purification (122 mg, 50 % yield) as a yellow oil.

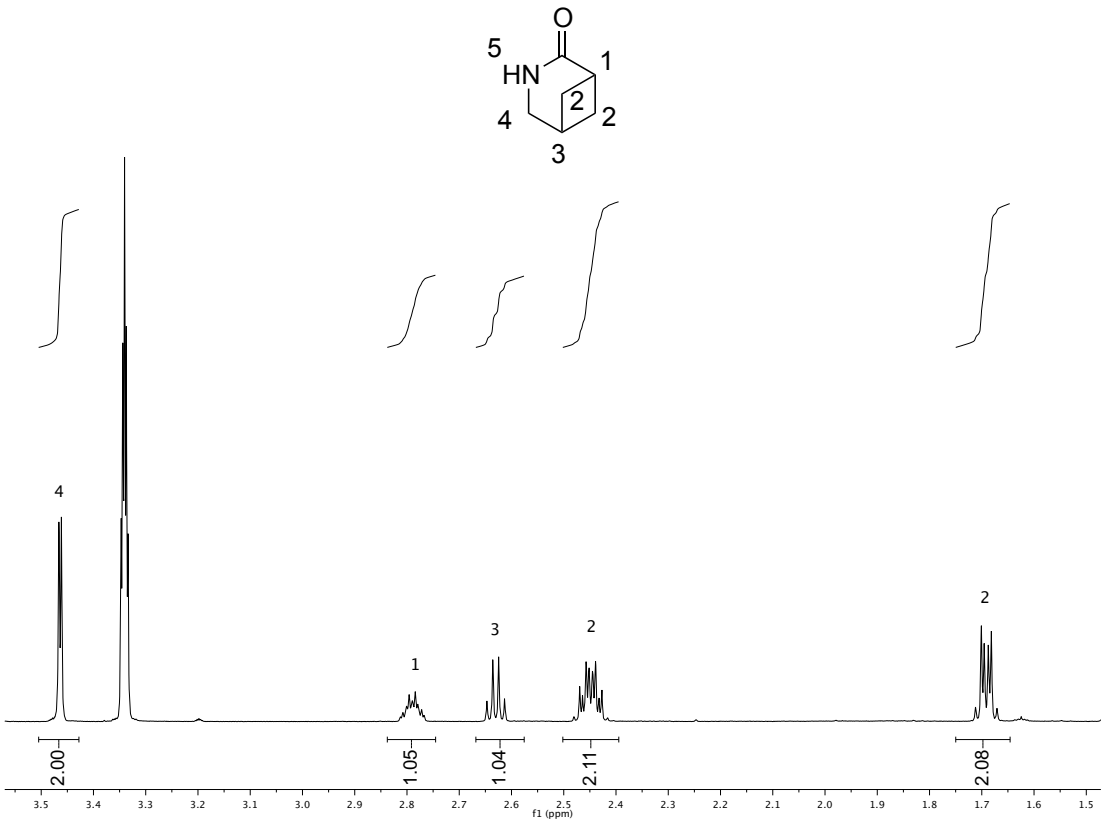

Preparation of *cis*-3-(Aminomethyl)cyclobutane carboxylic acid (ACCA, 9):

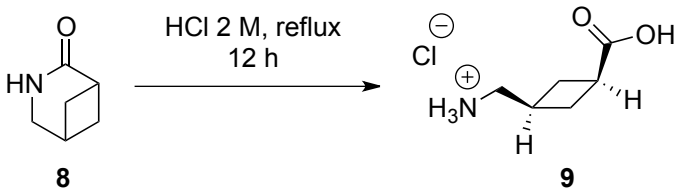

8 **9**

8 (220 mg, 1.98 mmol) was refluxed in 2 M HCl (10 mL) overnight. The H_2O was removed *in vacuo* to give **9** (328 mg, quantitative yield) as a beige solid with no further purification required. Mp: 169-170 °C. δH (500 MHz; CD_3OD) 3.18-3.08 (1H, p, *J* = 8.9 Hz, COCH), 2.96 (2H, d, *J* = 7.4 Hz, NCH_2), 2.63-2.51 (1H, m, NCH_2CH), 2.46-2.37 (2H, m, $COCH(CHH)_2$), 2.02 (2H, m, $COCH(CHH)_2$); δC (126 MHz; CD_3OD) 176.8, 45.5, 34.9, 30.2, 29.9. m/z (ES+) 130.0863 ($M+H^+$ $C_6H_{12}NO_2$ requires 130.0868).

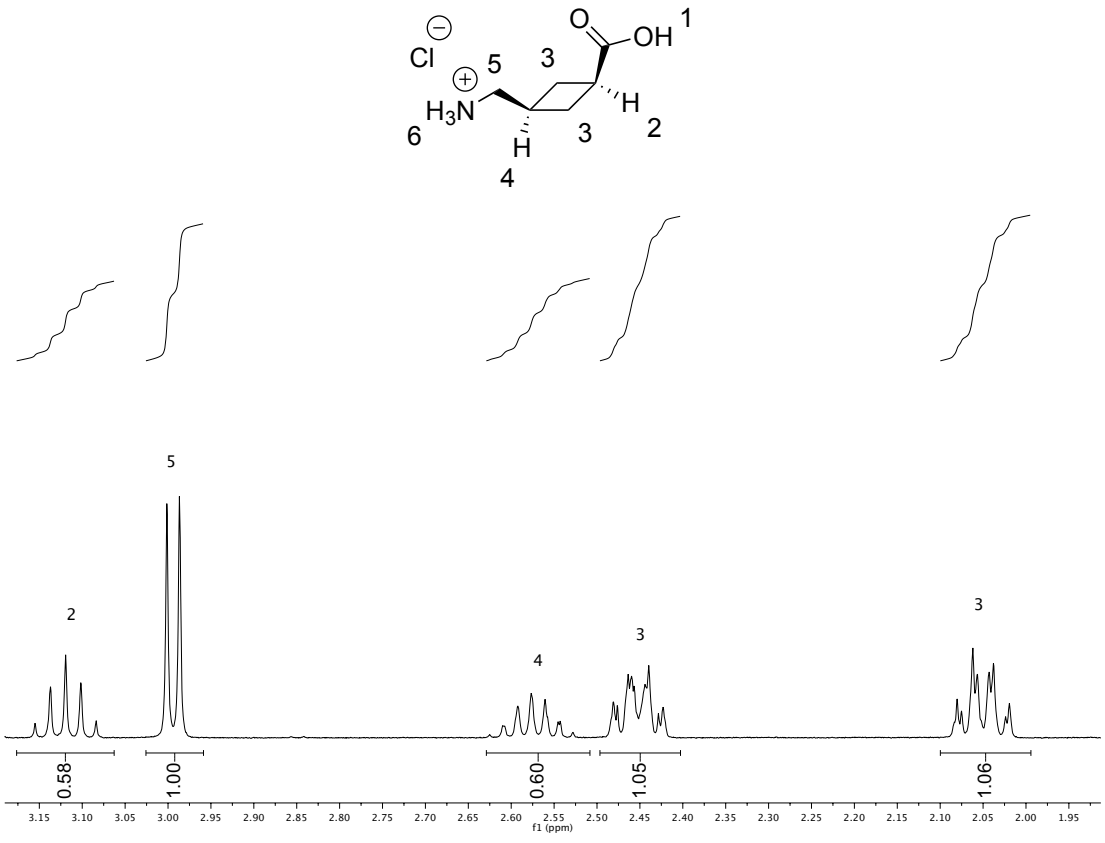

Preparation of (3-(Propoxycarbonyl)cyclobutyl)methanaminium chloride (ACCA-Pr, 10):

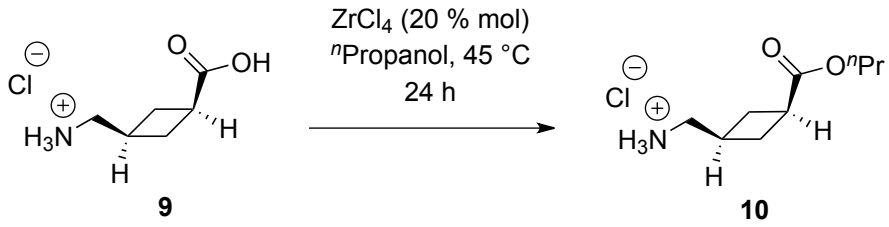

9 (370 mg, 2.86 mmol) was dissolved in *n*-propanol (10 mL) and $ZrCl_4$ (133 mg, 0.572 mmol, 20 mol %) was added. The solution was refluxed for 24 hours before being concentrated *in vacuo.* The crude oil was dissolved in $CHCl_3$ (2 mL) and left overnight. The precipitate was filtered off and the solution concentrated *in vacuo* to give **10** (570 mg, 89 % yield) as an off-white solid. **10** could also be purified using silica gel column chromatography (EtOAc/CH_3OH, from 100:0 to 80:20) with same yield. Mp: 159-161 °C. δH (400 MHz; CD_3OD) 3.46 (2H, t, *J* = 6.7 Hz, C*H*$_2$CH$_2$CH$_3$), 3.08 (1H, m, COCH), 2.93 (2H, d, *J* = 7.4 Hz, NCH$_2$), 2.60-2.49 (1H, m, NCH$_2$C*H*), 2.43-2.33 (2H, m, COCH(C*H*H)$_2$), 1.98 (2H, ddd, *J* = 18.7, 9.3 and 2.4 Hz, C=OCH(CH*H*)$_2$), 1.56-1.43 (2H, m, C*H*$_2$CH$_3$), 0.88 (3H, t, *J* = 7.4 Hz, CH$_2$C*H*$_3$); δC (101 MHz; CD_3OD) 176.7, 64.7, 45.4, 34.8, 30.1, 29.9, 26.6, 10.5. m/z (ES+) 172.1342 (M+H$^+$ $C_9H_{18}NO_2$ requires 172.1338).

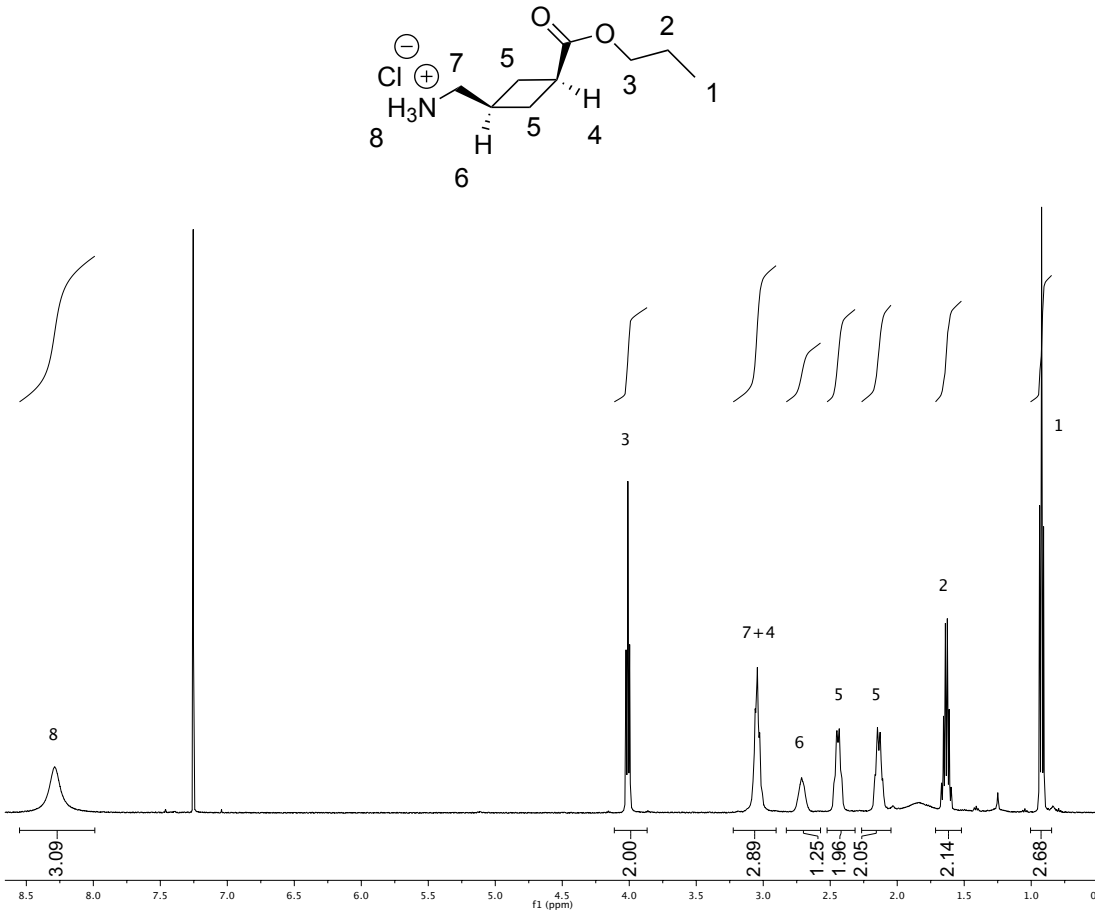

Preparation of 3-(((*tert*-butoxycarbonyl)amino)methyl)cyclobutane carboxylic acid (Boc-ACCA, 13):

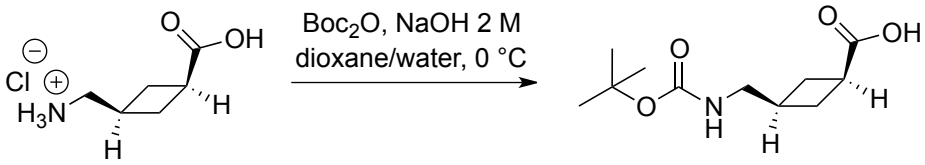

9 **13**

9 (150 mg, 0.9 mmol) was dissolved in dioxane and water 2:1 (12 mL) and cooled to 0 ºC. 2 M NaOH solution (5 mL) was added and the solution was stirred for 10 min before adding 2 eq of bis-*tert*-butyl dicarbonate (390 mg, 1.8 mmol). The reaction was left under stirring for 3 hours and then the solvent was removed *in vacuo.* The aqueous layer was extracted with Et_2O (15 mL x 2) and adjusted to pH 3 by the addition of 1 M HCl. The acidified aqueous layer was extracted with CH_2Cl_2 (15 mL x 5) and the combined CH_2Cl_2 layers were dried

over $MgSO_4$ and concentrated *in vacuo* to give **13** (227 mg, 95 % yield) as a brown solid. No further purification was required. (Rf = 0.28, EtOAc/CH_3OH 90:10). Mp: 63-65 °C. δH (400 MHz; $CDCl_3$) 5.99 (1H, br s, COOH), 4.61 (1H, br s, NH), 3.13 (2H, s, NCH_2), 3.07-2.98 (1H, quin, *J* = 8.9 Hz, C=OCH), 2.51-2.36 (1H, m, NCH_2CH), 2.37-2.25 (2H, m, C=OCH(CHH)$_2$, 2.00-2.09 (2H, m, C=OCH(CHH)$_2$, 1.44 (9H, s, $C(CH_3)_3$); δC (101 MHz; $CDCl_3$) 180.8, 156.5, 79.5, 45.7, 34.5, 31.4, 28.8, 28.4. m/z (ES+) 252.1212 ($M+Na^+$ $C_{11}H_{19}NO_4Na$ requires 252.1212).

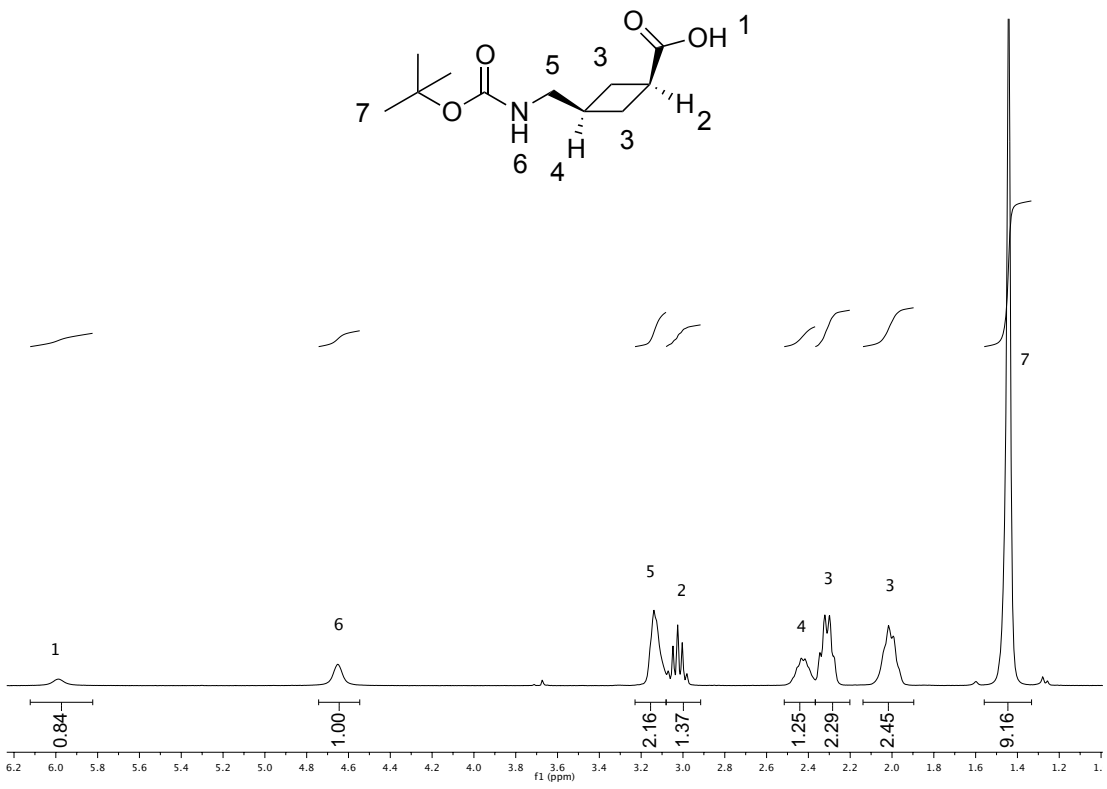

General method: coupling of protected dipeptides

9, the *N*-protected amino acid (**10a-c** and **13**), and O-(7-Azabenzotriazol-1-yl)-*N,N,N',N'*-tetramethyluronium hexafluorophosphate (HATU, 1 eq) were dissolved in anhydrous CH_2Cl_2 (20 mL). The solution was cooled to 0 °C and *N,N*-diisopropylethyl amine (3 eq) was added. The reaction was stirred at room temperature overnight. The solvent was evaporated *in vacuo* and the crude oil dissolved in CH_2Cl_2 (15 mL) and washed with $NaHCO_3$ (15 mL), acetic acid 10 % (15 mL x 2) and brine (15 mL). The combined organic layers were dried over $MgSO_4$ and concentrated *in vacuo*.

Preparation of propyl (*S*)-3-((2-((*tert*-butoxycarbonyl)amino)-3-phenyl propanamido)methyl)cyclobutane carboxylate (Boc-Phe-ACCA-Pr, 12a):

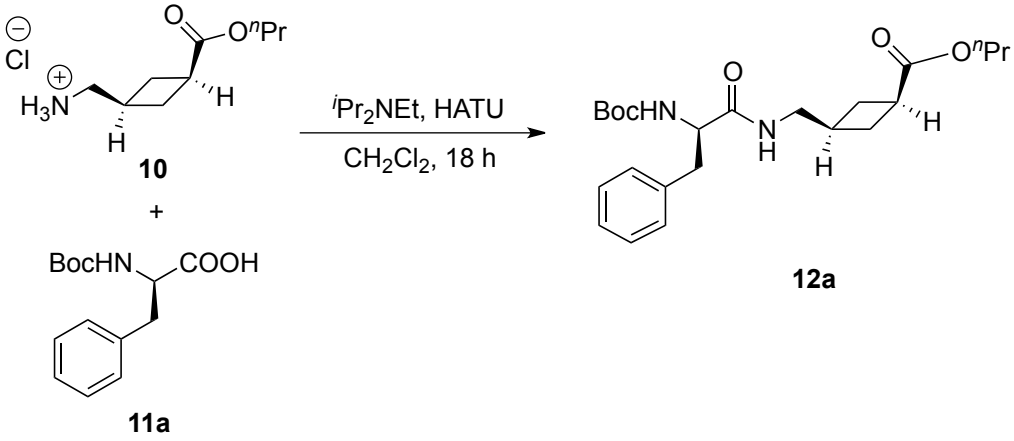

12a was prepared following the general procedure, by reacting **9** (300 mg, 1.45 mmol) with *N*-Boc-L-Phenylalanine **11a** (500 mg, 1.89 mmol). The crude oil was purified by silica gel column chromatography (cyclohexane/EtOAc, 100:0 then 70:30) to give **12a** as a white solid (557 mg, 92 % yield). (Rf = 0.65, cyclohexane/EtOAc, 50:50). $[\alpha]_D^{20}$: +1.6° (c $13 \cdot 10^{-3}$ $CHCl_3$). Mp: 106-108 °C. δH (500 MHz; $CDCl_3$) 7.33-7.17 (5H, m, PhH), 5.85 (1H, s, N*H*COCH), 5.08 (1H, s, NHBoc), 4.27 (1H, dd, *J* = 14.6, 7.3 Hz, C*H*CH_2Ph), 4.02 (2H, t, *J* = 6.7 Hz, C$H_2$$CH_2CH_3$), 3.26-3.12 (2H, dd, *J* = 12.8 and 6.5 Hz, NCH_2), 3.11-3.04 (1H, dd, *J* = 6.5 and 13.6 Hz, CH_2Ph), 3.04-2.98 (1H, dd, *J* = 7.7 and 13.6 Hz, CH_2Ph), 2.97-2.88 (1H, m, COCH), 2.34-2.27 (1H, m, NCH_2C*H*), 2.25-2.12 (2H, m, COCH(C*H*H)$_2$), 1.93-1.79 (2H, m, COCH(CH*H*)$_2$), 1.68-1.61 (2H, m, C$H_2$$CH_3$), 1.41 (9H, s, C($CH_3$)$_3$), 0.93 (3H, t, *J* = 7.4 Hz, CH_2CH_3). δC (125.65

MHz; $CDCl_3$) 175.2, 171.6, 155.7, 137.3, 129.7, 128.9, 127.1, 80.2, 66.2, 56.4, 45.0, 39.4, 34.4, 30.8, 29.1, 28.8, 22.3, 10.6. m/z (ES+) 417.2370 ($M+H^+$. $C_{23}H_{33}N_2O_5$ requires 417.2389).

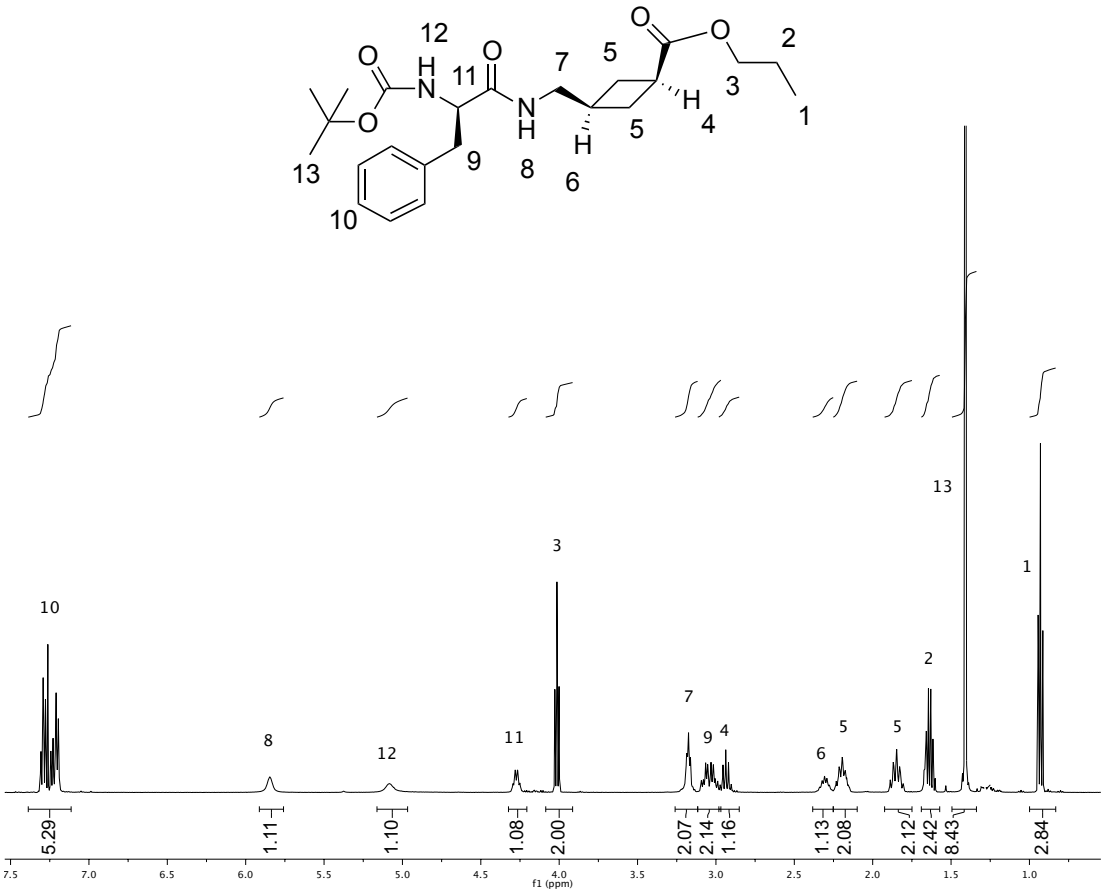

Preparation of propyl (*S*)-3-((2-((((9*H*-fluoren-9-yl)methoxy)carbonyl) amino)-3-methylbutanamido)methyl)cyclobutane carboxylate (Fmoc-Val-ACCA-Pr, 12b):

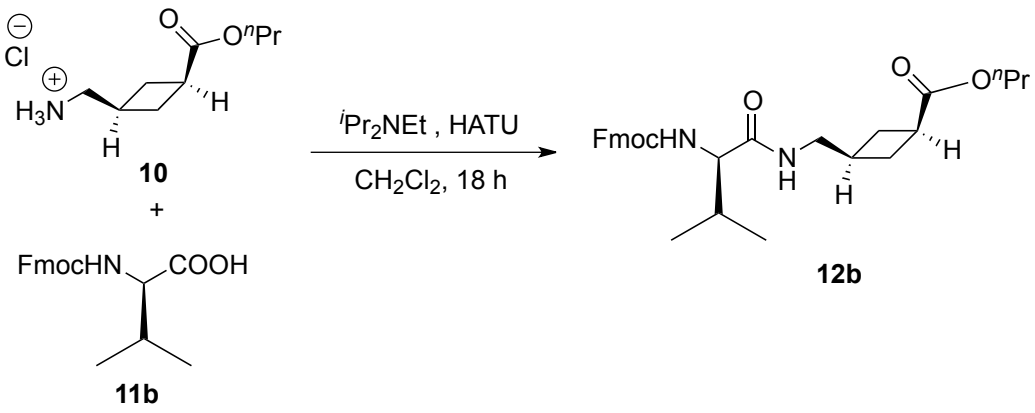

12b was prepared according to general procedure, by reacting **9** (180 mg, 0.86 mmol) with *N*-Fmoc-L-Valine **11b** (580 mg, 1.7 mmol). The crude oil was purified through a silica gel column chromatography (cyclohexane/EtOAc from 100:0 to 40:60) giving **12b** as a yellow solid (155 mg, 76 % yield). (Rf = 0.86, EtOAc). $[\alpha]_D^{20}$: -13.0° (c $10.2 \cdot 10^{-3}$ $CHCl_3$). Mp: 152-154 °C. δH (500 MHz; $CDCl_3$) 7.75 (2H, d, *J* = 7.5 Hz, Ar), 7.58 (2H, d, *J* = 7.4 Hz, Ar), 7.39 (2H, t, *J* = 7.4 Hz, Ar) 7.29 (2H, m, Ar), 6.29 (1H, s, N*H*COCH), 5.57 (1H, d, *J* = 8.2 Hz, NHFmoc), 4.43-4.39 (1H, m, CH_2Fmoc), 4.35-4.32 (1H, m, CH_2Fmoc), 4.19 (1H, t, *J* = 7.0 Hz, FmocCH), 4.01 (2H, t, *J* = 6.7 Hz, C*H*$_2$$CH_2CH_3$), 3.96-3.94 (1H, m, C*H*$CH(CH_3)_2$), 3.36-3.27 (1H, m, NCH_2), 3.27-3.18 (1H, m, NCH_2), 3.05-2.93 (1H, m, COCH), 2.53-2.38 (1H, m, NCH_2C*H*), 2.29-2.24 (2H, m, COCH(C*H*H)$_2$), 2.16-2.07 (1H, m, C*H*$(CH_3)_2$), 2.01-1.90 (2H, m, COCH(CH*H*)$_2$), 1.68-1.56 (2H, m, C*H*$_2$$CH_3$), 0.92 (6H, m, CH(C*H*$_3$)$_2$ and 3H, t, *J* = 7.4 Hz, CH_2C*H*$_3$). δC (125.65 MHz; $CDCl_3$) 175.5, 171.4, 156.6, 144.0, 141.6, 128.2, 127.4, 125.3, 120.1, 67.3, 66.3, 60.8, 47.3, 44.2, 34.0, 31.1, 30.7, 28.8, 28.7, 22.2, 19.4, 18.1, 10.6 m/z (ES+) 515.2521 ($M+Na^+$. $C_{29}H_{36}N_2O_5Na$ requires 515.2522).

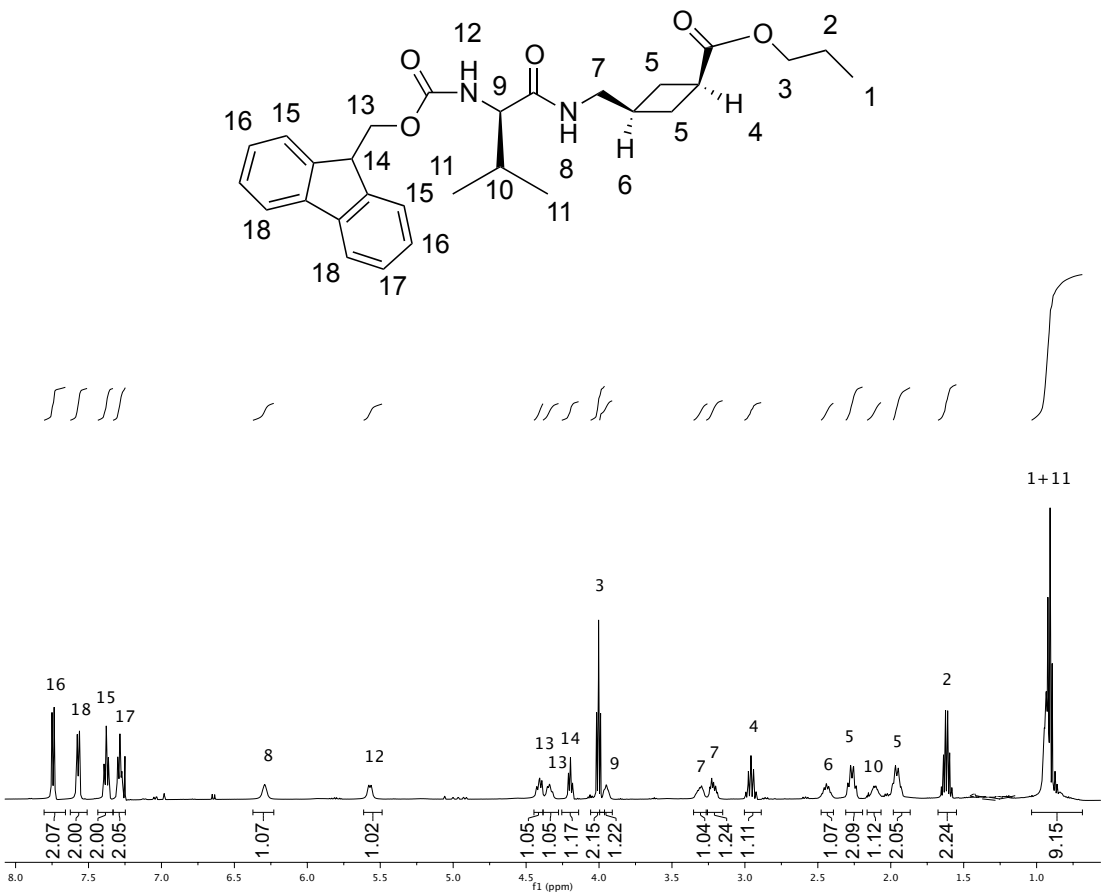

Preparation of propyl 3-((2-((((9*H*-fluoren-9-yl) methoxy)carbonyl)amino) acetamido)methyl)cyclobutane carboxylate (Fmoc-Gly-ACCA-Pr, 12c):

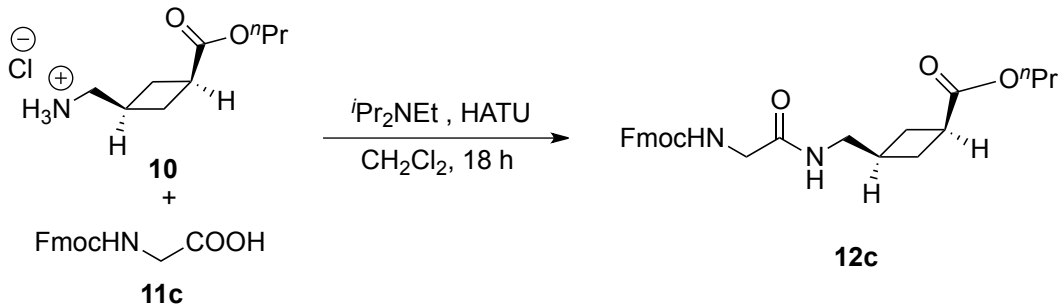

12c was prepared according to General Procedure, by reacting **9** (240 mg, 1.15 mmol) with *N*-Fmoc-Glycine **11c** (350 mg, 1.18 mmol). The crude oil was purified through a silica gel column chromatography (cyclohexane/EtOAc from 100:0 to 20:80) giving **12c** as a white solid (437 mg, 0.97 mmol, 84 % yield). (Rf

= 0.75, EtOAc/CH_3OH, 90:10). Mp: 111-113°C. δH (500 MHz; $CDCl_3$) 7.79-7.75 (2H, d, *J* = 7.6 Hz, Ar), 7.61-7.6 (2H, d, *J* = 7.4 Hz, Ar), 7.41-7.38 (2H, t, *J* = 7.5 Hz, Ar), 7.34-7.29 (2H, m, Ar), 6.15 (1H, s, N*H*$COCH_2$), 5.49 (1H, s, NHFmoc), 4.44 (1H, d, *J* = 6.9 Hz, CH_2Fmoc), 4.23 (1H, t, *J* = 6.9 Hz, CHFmoc), 4.02 (1H, t, *J* = 6.7 Hz, C*H*$_2CH_2CH_3$), 3.86 (2H, d, *J* = 4.6 Hz, NHC*H*$_2CO$), 3.30 (2H, t, *J* = 6.1 Hz, NCH_2), 3.03-2.96 (1H, quin, *J* = 8.8 Hz, C=OCH), 2.53-2.44 (1H, m, NCH_2C*H*), 2.35-2.26 (2H, m, COCH(C*H*H)$_2$), 2.02-1.92 (2H, m, COCH(CH*H*)$_2$), 1.67-1.60 (2H, m, CH_2C*H*$_2CH_3$), 0.92 (3H, t, *J* = 7.4 Hz, CH_2C*H*$_3$). δC (125.65 MHz; $CDCl_3$) 175.5, 169.0, 143.6, 141.6, 127.7, 127.2, 125.5, 120.0, 67.3, 66.2, 47.4, 44.3, 44.0, 34.2, 30.7, 28.4, 21.8, 10.3. m/z (ES+) 473.2033 ($M+Na^+$. $C_{26}H_{30}N_2O_5Na$ requires 473.2052).

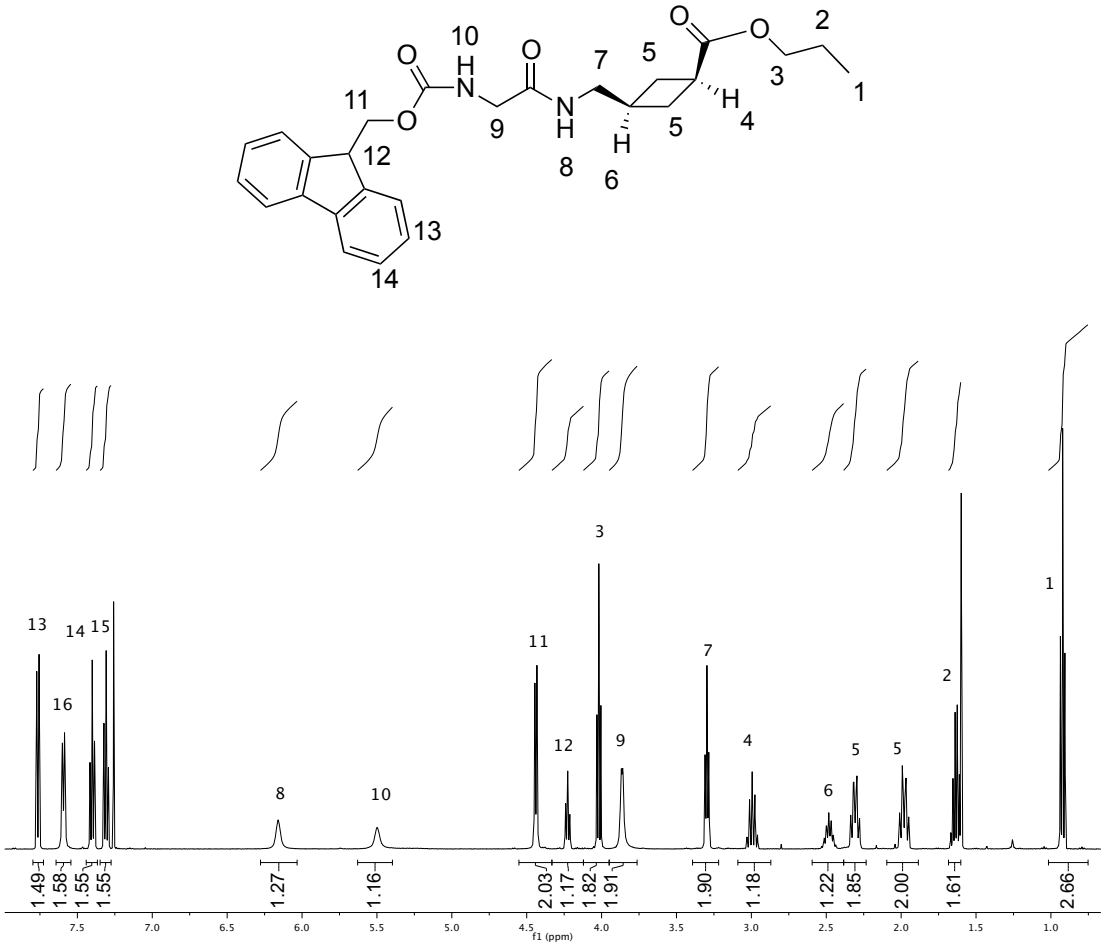

Preparation of propyl 3-((3-(((*tert*-butoxycarbonyl)amino)methyl) cyclobutanecarboxamido)methyl)cyclobutane carboxylate (Boc-ACCA-ACCA-Pr, 14):

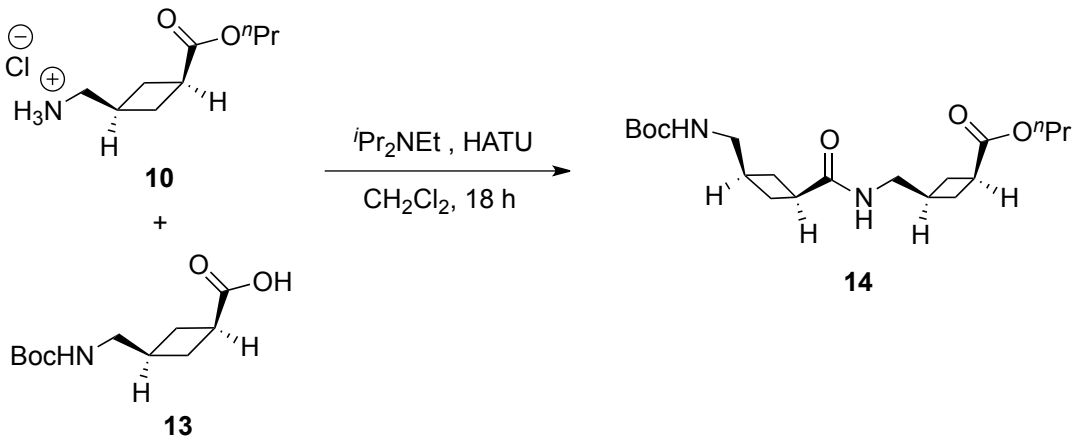

14 was prepared according to General Procedure, by reacting **9** (181 mg, 0.87 mmol) with **13** (195 mg, 0.85 mmol). The crude oil was purified through a silica gel column chromatography (cyclohexane/EtOAc from 100:0 to 0:100) giving **14** as a clear yellow solid (194 mg, 58 % yield). (Rf = 0.13, EtOAc/cyclohexane, 50:50). Mp: 62-64 °C. δH (400 MHz; $CDCl_3$) 5.60 (1H, s, N*H*C=OCH), 4.72 (1H, s, N*H*Boc), 4.02 (2H, t, *J* = 6.5 Hz, C*H*$_2$CH$_2$CH$_3$), 3.25 (2H, t, *J* = 5.9 Hz, NCH$_2$), 3.13-3.11 (2H, m, BocNCH$_2$), 3.04-2.95 (1H, m, C*H*COO^{n}Pr), 2.92-2.79 (1H, m, CHCON), 2.55-2.37 (2H, m, NCH$_2$C*H* and BocNCH$_2$C*H*), 2.33-2.21 (4H, m, OCOCH(C*H*H)$_2$ and NCOCH(C*H*H)$_2$), 2.01-1.92 (4H, m, OCOCH(CH*H*)$_2$ and NCOCH(CH*H*)$_2$), 1.69-1.60 (2H, m, C*H*$_2$CH$_3$), 1.44 (9H, s, C(CH$_3$)$_3$), 0.92 (3H, t, *J* = 7.4 Hz, CH$_2$C*H*$_3$). δC (101 MHz; $CDCl_3$) 175.7, 175.4, 156.4, 79.6, 66.5, 45.9, 44.6, 36.6, 34.4, 31.2, 28.9, 28.8, 22.4, 10.7. m/z (ES-) 381.2408 (M-H$^-$ $C_{20}H_{33}N_2O_5$ requires 381.2389).

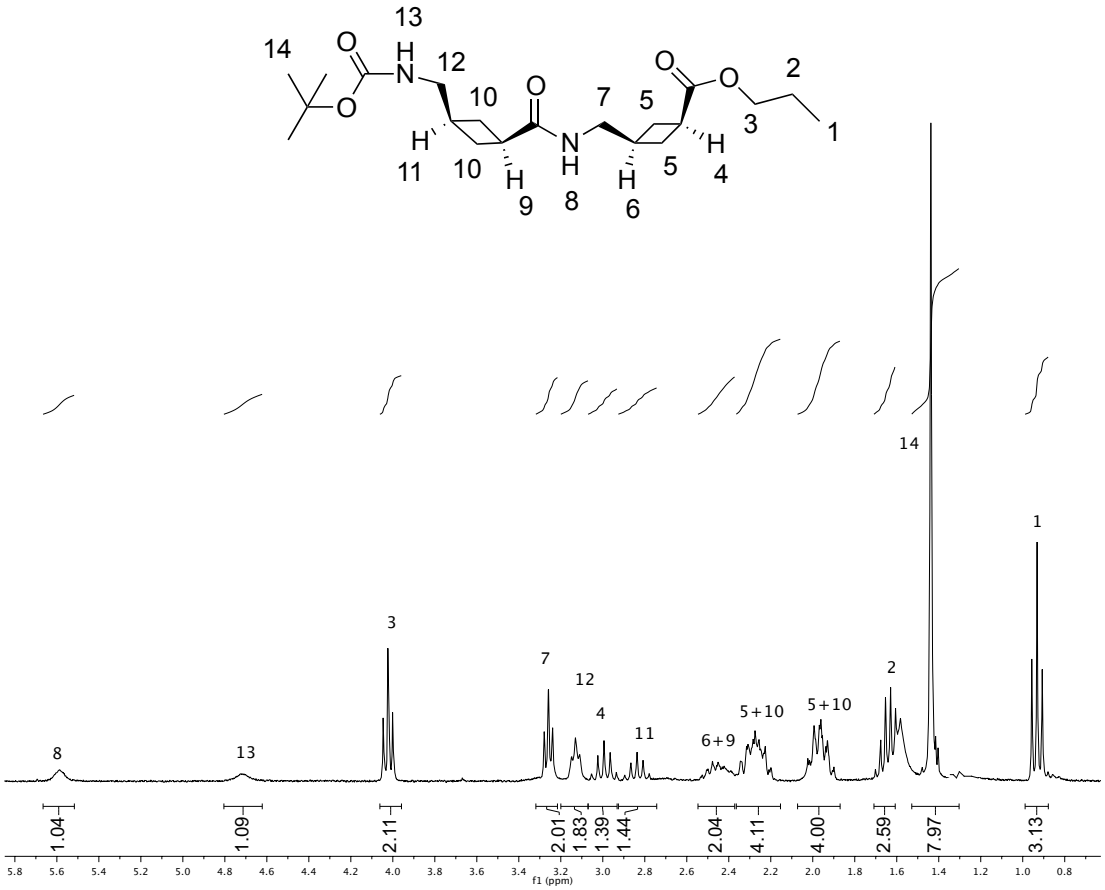

Preparation of (*S*)-1-(((3-carboxycyclobutyl)methyl)amino)-1-oxo-3-phenylpropan-2-aminium chloride (Phe-ACCA, 15a):

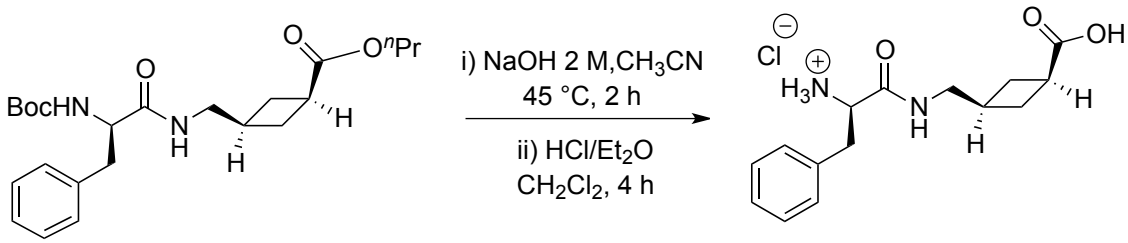

12a **15a**

12a (550 mg, 1.31 mmol) was dissolved in 20 mL of CH_3CN and NaOH 2 M (8 mL) was added. The reaction was left under stirring for 2 hours at 45 °C before bringing the solution to pH 3 with HCl 1 M and extracting it with CH_2Cl_2 (15 mL x 5). The organic layers were combined, dried over $MgSO_4$ and concentrated *in*

vacuo. The white solid obtained was dissolved in CH_2Cl_2 (20 mL) and HCl in Et_2O 3 M (0.4 mL) was added at 0 °C. The reaction was stirred for 4 hours. The white precipitate was filtered off and washed with Et_2O (190 mg, 0.69 mmol) with an overall yield (over the two steps) of 53 %. (Rf = 0.08, EtOAc/CH_3OH 90:10). $[\alpha]_D^{20}$: +26.0° (c $7.6 \cdot 10^{-3}$ CH_3OH). Mp: 170-172 °C. δH (400 MHz; CD_3OD) 7.46-7.18 (5H, m, PhH), 4.08 (1H, t, *J* = 7.4 Hz, C*H*CH_2Ph), 3.253.15 (2H, m, NCH_2) 3.12-3.05 (2H, m, CH_2Ph), 3.05-2.93 (1H, m, COCH), 2.45-2.26 (1H, m, NCH_2C*H*), 2.28-2.15 (2H, m, COCH(C*H*H)$_2$), 1.90-1.81 (2H, m, COCH(CH*H*)$_2$). δC (101 MHz; CD_3OD) 177.1, 169.6, 135.7, 130.6, 129.9, 128.7, 55.8, 45.4, 38.6, 34.7, 31.8, 29.9. m/z (ES+) 277.1552 ($M+H^+$ $C_{15}H_{21}N_2O_3$ requires 277.1552).

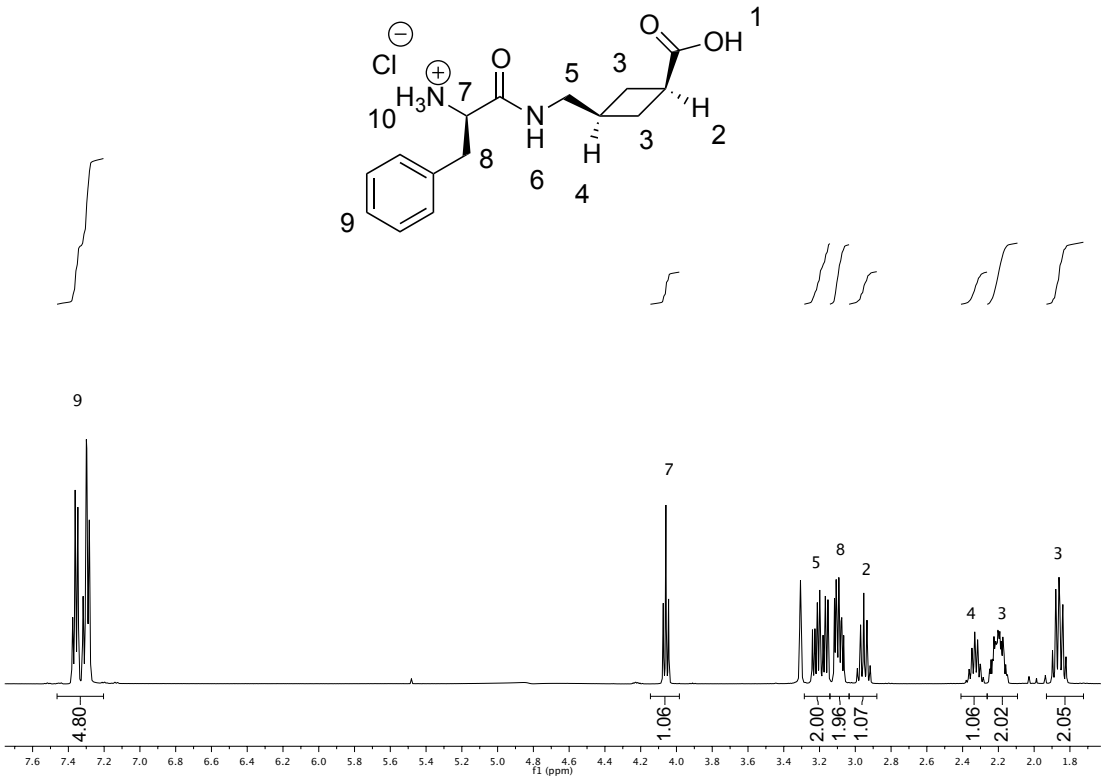

Preparation of (*S*)-3-((2-amino-3-methylbutanamido)methyl)cyclobutane carboxylic acid (Val-ACCA, 15b):

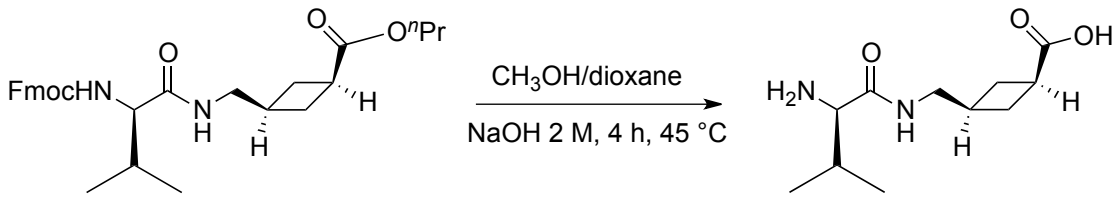

12b **15b**

12b (48 mg, 0.09 mmol) was dissolved in dioxane/ methanol 7:3 (7 mL) and NaOH 2 M (2 mL) was added. The reaction was left under stirring for 4 hours at 45 °C. The solution was concentrated *in vacuo*, and the water layer was extracted with Et_2O (10 mL) and CH_2Cl_2 (10 mL x 2). The aqueous layer was neutralised with HCl 1 M and purified with DOWEX 50WX8-200 ion exchange column affording **15b** as a yellow solid (18 mg, 0.078 mmol, 90 % yield). (Rf = 0.55, CH_3OH). Mp 195-196 °C. $[\alpha]_D^{20}$: +118.0° (c $0.5 \cdot 10^{-3}$ CH_3OH). δH (500 MHz, CD_3OD) 3.50 (1H, s, C*H*$CH(CH_3)_2$), 3.23 (1H, d, *J* = 6.2 Hz, NCH_2), 2.90 (1H, quint, *J* = 8.9 Hz, COCH), 2.50-2.39 (1H, m, NCH_2CH), 2.35-2.20 (2H, m, $COCH(CHH)_2$), 2.08-2.16 (1H, m, $CH(CH_3)_2$), 1.99-1.92 (2H, m, $COCH(CHH)_2$), 1.06-0.98 (6H, dd, *J* = 6.8, 3.9 Hz, $CH(CH_3)_2$). δC (125.65 MHz; CD_3OD) 180.1, 169.4, 60.4, 45.3, 37.1, 31.8, 30.4, 30.2, 19.2, 18.2. m/z (ES+) 229.1546 ($M+H^+$ $C_{11}H_{21}N_2O_3$ requires 229.1552).

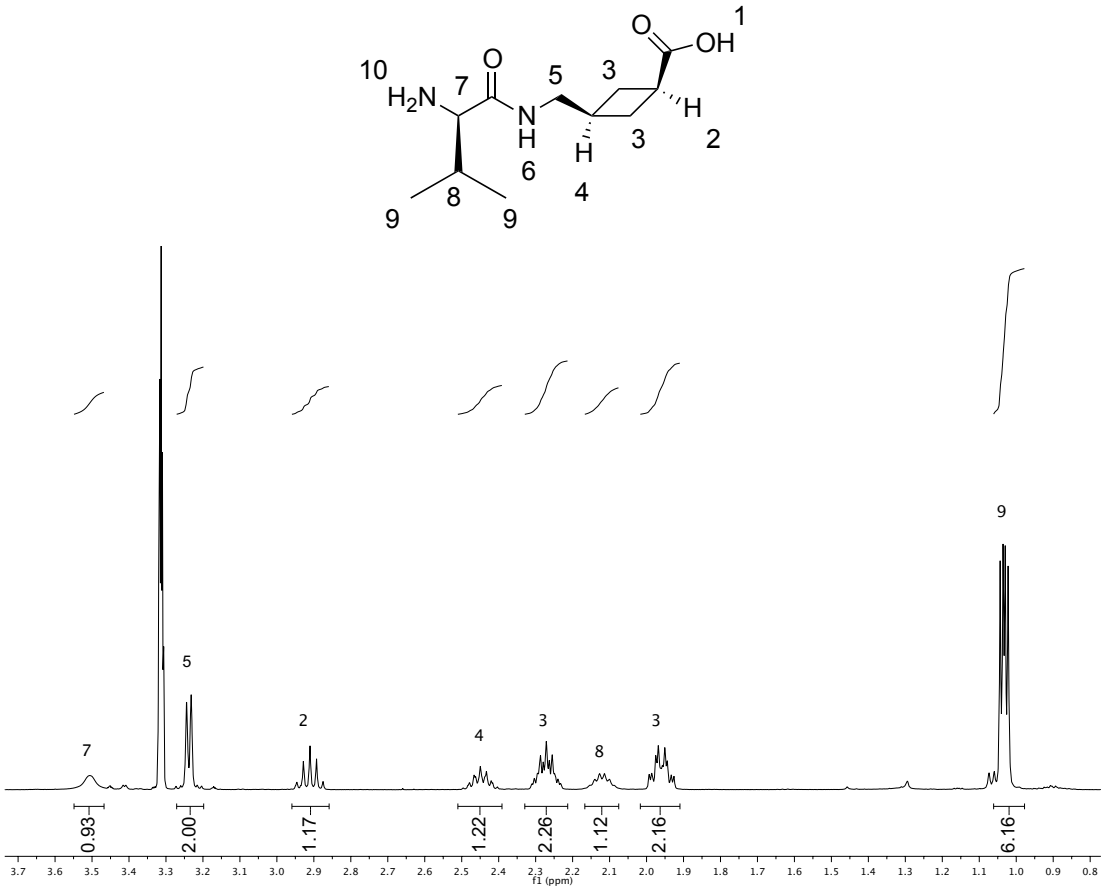

Preparation of *cis*-3-((2-aminoacetamido)methyl)cyclobutane carboxylic acid (Gly-ACCA, 15c):

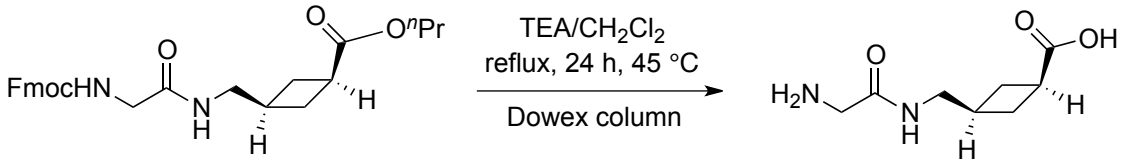

12c **15c**

12c (185 mg, 0.41 mmol) was dissolved in CH_2Cl_2/triethylamine 1:1 (20 mL). The reaction was left under stirring for 24 hours at 45 °C. The white precipitate was filtered off and washed with acetonitrile. The filtrate solution was concentrated *in vacuo* and the crude yellow solid was purified with DOWEX 50WX8-200 ion exchange column, affording **15c** as white solid (69 mg, 0.37 mmol, 90 % yield). (Rf = 0.3, CH_3OH). Decomposition temperature: 200 °C. δH

(500 MHz; D_2O) 3.87 (2H, br s, NHC*H*$_2$CO), 3.30 (2H, d, *J* = 6.4 Hz, NCH_2), 3.00-2.92 (2H, m, COCH), 2.52-2.42 (1H, m, NCH_2C*H*), 2.33-2.27 (3H, m, COCH(C*H*H)$_2$), 1.88-1.81 (2H, m, COCH(CH*H*)$_2$). δC (125.65 MHz; D_2O) 184.9, 166.8, 44.2, 40.5, 36,5, 29.5, 29.3. m/z (ES+) 187.1082 ($M+H^+$ $C_8H_{15}N_2O_3$ requires 187.1083).

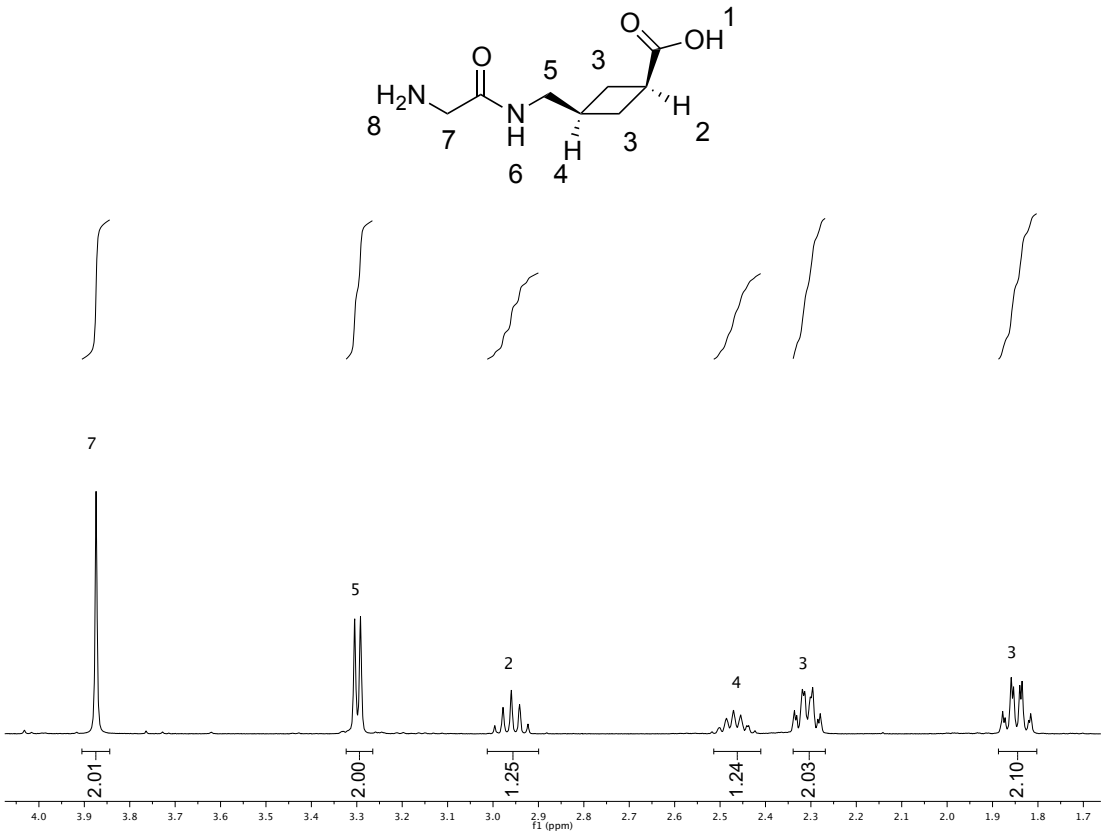

Preperation of (3-(((3-carboxycyclobutyl)methyl)carbamoyl)cyclobutyl) methanaminium chloride (ACCA-ACCA, 16):

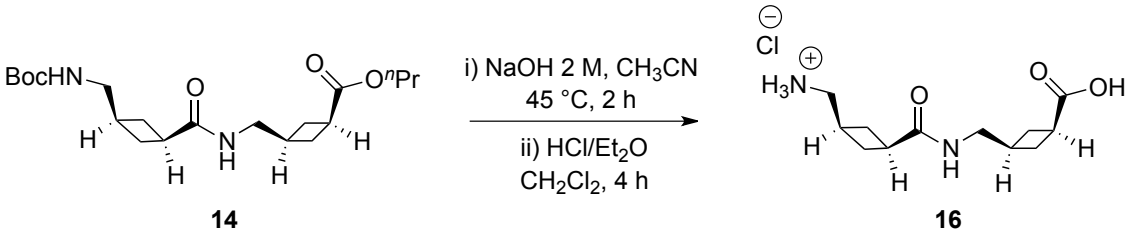

14 (180 mg, 0.47 mmol) was dissolved in CH_3CN (15 mL) and NaOH 2 M (5 mL) was added. The reaction was left under stirring for 2 hours at 45 °C before bringing the solution to pH 3 with HCl 1 M and extracting it with CH_2Cl_2 (15 mL x 5). The organic layers were combined, dried over $MgSO_4$ and concentrated *in vacuo* giving to give a dark yellow oil, 84 mg (0.25 mmol) of which was dissolved in CH_2Cl_2 (10 mL). HCl in Et_2O 5 M (0.1 mL) was added and the reaction was stirred for 4 hours. The clear yellow precipitate was filtered off and washed with Et_2O (38 mg, 0.14 mmol) affording **16** in an overall yield (over the two steps) of 56 %. (Rf = 0.025, EtOAc/CH_3OH 90:10). Mp: 156-158 °C. δH (500 MHz; CD_3OD) 3.17 (2H, d, *J* = 6.5 Hz, CONHC*H*$_2$), 3.06-2.94 (4H, m, COCH, NCOCH, CH_2N), 2.60-2.50 (1H, m, CONCH_2C*H*), 2.48-2.39 (1H, m, NCH_2C*H*), 2.37-2.32 (2H, m, OCOCH(C*H*H)$_2$), 2.29-2.23 (2H, m, NCOCH(C*H*H)$_2$), 2.03-1.92 (4H, m, OCOCH(CH*H*)$_2$ and NCOCH(CH*H*)$_2$). δC (101 MHz; CD_3OD) 177.2, 176.9, 45.3, 45.0, 36.3, 34.9, 32.2, 29.9, 29.7, 29.6. m/z (ES+) 241.1564 ($M+H^+$ $C_{12}H_{21}N_2O_3$ requires 241.1552).

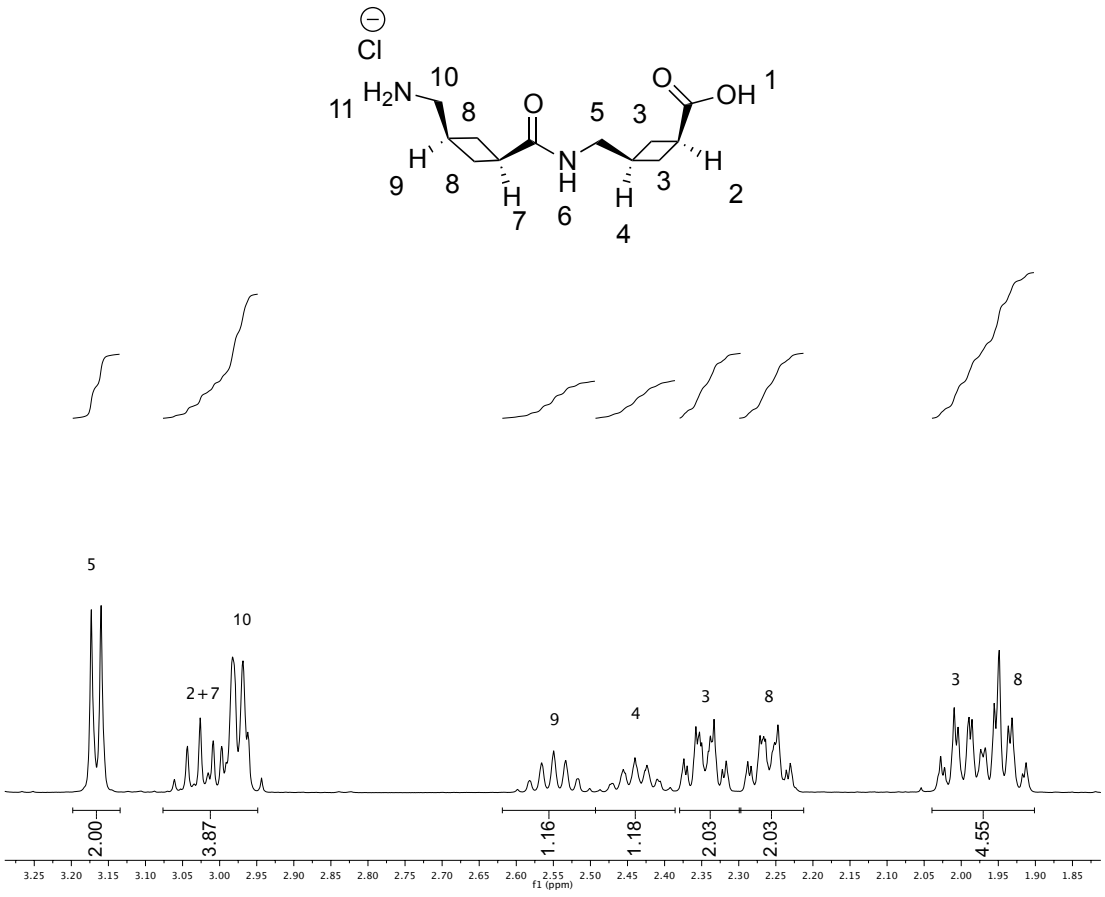
Cl
H2N
OH
O
N
H
5
10
2+7
9
4
3
8
2.00
3.87
1.16
1.18
2.03
2.03
4.55
f1 (ppm)

2.5-Bibliography

(1) O'Reilly, E.; Pes, L.; Paradisi, F.: From amines to diketopiperazines: a one-pot approach. *Tetrahedron Letters* **2010**, *51*, 1696-1697.

(2) O'Reilly, E.; Balducci, D.; Paradisi, F.: A stereoselective synthesis of alpha-deuterium-labelled (S)-alpha-amino acids. *Amino Acids* **2010**, *39*, 849-858.

(3) Cook, G. R.; Beholz, L. G.; Stille, J. R.: Construction of Hydroxylated Alkaloids (+/-)-Mannonolactam, (+/-)-Deoxymannojirimycin, and (+/-)-Prosopinine through Aza-Annulation. *The Journal of Organic Chemistry* **1994**, *59*, 3575-3584.

(4) Gray, D.; Gallagher, T.: A Flexible Strategy for the Synthesis of Tri- and Tetracyclic Lupin Alkaloids: Synthesis of (+)-Cytisine, (+/-)-Anagyrine and (+/-)-Thermopsine. *Angewandte Chemie International Edition in English* **2006**, *45*, 2419-2423.

(5) Garegg, P. J.; Samuelsson, B.: Novel reagent system for converting a hydroxy-group into an iodo-group in carbohydrates with inversion of configuration. Part 2. *Journal of the Chemical Society, Perkin Transactions 1* **1980**, 2866-2869.

(6) Galeazzi, R.; Mobbili, G.; Orena, M.: From pyrrolidin-2-ones to 3-aza-2-oxobicyclo[3.2.0]heptanes. Synthesis of both enantiomers of cis-2-aminomethylcyclobutane carboxylic acid, a conformationally restricted analogue of GABA. *Tetrahedron* **1999**, *55*, 261-270.

(7) Birch, A. J.: 212. Reduction by dissolving metals. Part II. *Journal of the Chemical Society (Resumed)* **1945**, 809-813.

(8) LukaÏc, M.; Smolarikova, E.; Lacko, I.; Devinsky, F.: the methoxybenzyl ethers as useful protecting groups for hydroxy compounds: methods of deprotection. *Acta Facult. Pharm. Univ. Comenianae* **2005**, *52*, 31-45.

(9) Shang, Y. M.; Li, J.; Song, Z. G.; Li, Y. G.; Huang, H. M.: *Chemical Research in Chinese Universities* **2007**, *23*, 430-432.

(10)Singh, S.; Duffy, C. D.; Shah, S. T. A.; Guiry, P. J.: $ZrCl_4$ as an Efficient Catalyst for a Novel One-Pot Protection/Deprotection Synthetic Methodology. *The Journal of Organic Chemistry* **2008**, *73*, 6429-6432.

(11) Albericio, F.; Bofill, J.; El-Faham, A.; Kates, S.: Use of onium salt-based coupling reagents in peptide synthesis. *Journal of Organic Chemistry* **1998**, *63*, 9678-9683.

(12) Carpino, L. A.; Henklein, P.; Foxman, B. M.; Abdelmoty, I.; Costisella, B.; Wray, V.; Domke, T.; El-Faham, A.; Mugge, C.: The Solid State and Solution Structure of HAPyU. *The Journal of Organic Chemistry* **2001**, *66*, 5245-5247.

(13) Carpino, L. A.; Imazumi, H.; El-Faham, A.; Ferrer, F. J.; Zhang, C.; Lee, Y.; Foxman, B. M.; Henklein, P.; Hanay, C.; Mügge, C.; Wenschuh, H.; Klose, J.; Beyermann, M.; Bienert, M.: The Uronium/Guanidinium Peptide Coupling Reagents: Finally the True Uronium Salts. *Angewandte Chemie International Edition* **2002**, *41*, 441-445.

(14) Nakajima, N.; Ikada, Y.: Mechanism of amide formation by carbodiimide for biconjugation in aqueous media. *Biconjugate Chemistry* **1995**, *6*, 123–130.

(15) Montalbetti, C. A. G. N.; Falque, V.: Amide bond formation and peptide coupling. *Tetrahedron* **2005**, *61*, 10827-10852.

(16) Joullie', M. M.; Lassen, K. M.: Evolution of amide bond formation. *ARKIVOC: Online Journal of Organic Chemistry* **2010**, 189-250.

(17) Li, P.; Xu, J. C.: The development of highly efficient onium-type peptide coupling reagents based upon rational molecular design. *Journal of Peptide Research* **2001**, *58*, 129-139.

(18) Isidro-Llobet, A.; Alvarez, M.; Albericio, F.: Amino Acid-Protecting Groups. *Chemical Reviews* **2009**, *109*, 2455-2504.

(19) Babu, K. N.; Kunze, K. L.; Nelson, W. L.: Metabolism of Diltiazem: A Short Efficient Synthesis of *N,N*-Didesmethyldiltiazem - An Important Product of *N*-Demethylation. *Synthesis* **2011**, *4*, 553-554.

(20) Basu, M. K.; Sarkar, D. C.; Ranu, B. C.: A mild and Selective Method of Ester Hydrolysis. *Synth. Commun.* **1989**, *19*, 627-631.

(21) Qureshi, M.; Qureshi, S.; Singhal, S. C.: An ion exchange method for the determination of aliphatic amides and esters. *Analytical Chemistry* **1968**, *40*, 1781-1783.

Chapter 3

Biological investigation of ACCA and its dipeptides

3.1-Introduction

Glutamate is a key player not only in maintaining a healthy nervous system, but it also plays a fundamental role in a wide number of neuronal diseases. For this reason, many research groups are working on the development of new glutamate analogues.

The considerable flexibility of the glutamate molecule (Glu) allows several conformations very close in energy to each other and therefore, Glu can assume different shapes and binds differently to the active sites of transporters, receptors and enzymes.[1] This characteristic makes the discovery of analogues more challenging. It is essential to exploit constrained structures to better target specific proteins and specific binding sites successfully. In fact, the most promising pharmacological drug candidates are the ones showing significant selectivity.

One of the techniques often employed to give constriction is the insertion of cyclic moieties. The presence of cyclobutane in the structure and its similarity with glutamate render ACCA a good candidate as glutamate analogue.

3.2-Results and discussion

In this thesis the neural activity of ACCA (**9**), its ester (**10**) and its dipeptides (**15a-c**), described in chapter 2 (Table 3.1) were examined as glutamate analogues, focusing on the interaction with glutamate transporter proteins in glial cells.

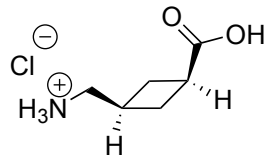 **9**	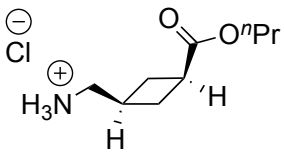 **10**	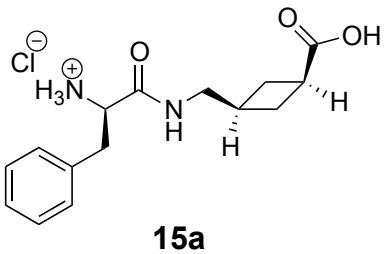 **15a**
ACCA	ACCA-Pr	Phe-ACCA

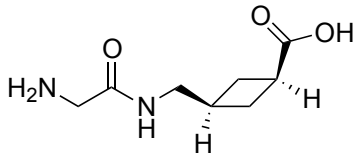 **15b**	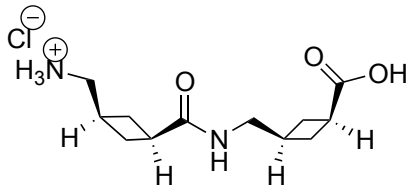 **15c**
Gly-ACCA	ACCA-ACCA

Table 3.1: ACCA (**9**), ACCA-Pr (**10**), Phe-ACCA (**15a**), Gly-ACCA (**15b**) and ACCA-ACCA (**15c**) chemical structures

The similarity of ACCA with the main neurotransmitters in the mammalian CNS, glutamic acid and GABA (Fig. 3.1), renders this novel amino acid very interesting for possible applications in the treatment of neuronal injuries and diseases. In particular, we will focus our attention on the study of the compounds listed in table 3.1 as glutamate analogues, even if it would also be interesting to test them as analogues of GABA.

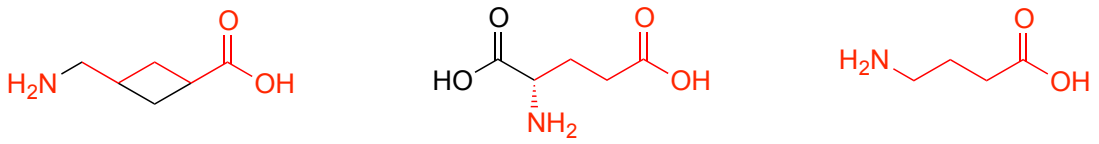

ACCA glutamic acid GABA

Fig. 3.1: ACCA and main excitatory (glutamic acid) and inhibitory (GABA) neurotransmitters in the mammalian CNS; the similarities in the backbones are highlighted in red

ACCA has never been synthesised and investigated before, but in the literature the neural activity of compounds with similar structures is described (see paragraph 1.3.5.1, pag. 44).

The ester (**10**) and the dipeptides (**15a-c**) are less hydrophilic than ACCA and therefore it is more likely for them to go through cell membranes, for instance the blood brain barrier. For this reason it is interesting to study their biological activity. Furthermore some dipeptides or structures containing amide bonds have been found active as glutamate analogues in recent years, such as the compounds reported in Fig. 3.2.[2-4]

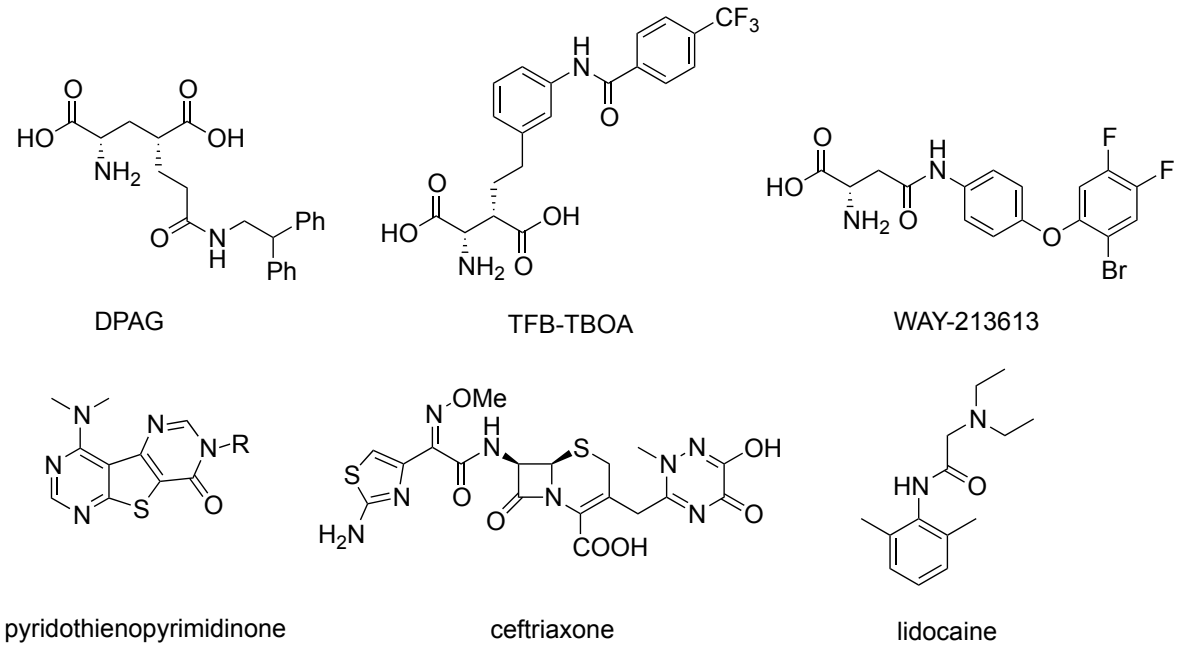

DPAG TFB-TBOA WAY-213613

pyridothienopyrimidinone ceftriaxone lidocaine

Fig. 3.2: glutamate analogues containing amidic bond, where DPAG = (2*S*,4*R*)-2-amino-4-(3-((2,2-diphenylethyl)amino)-3-oxopropyl)pentanedioic acid, TFB-TBOA = (2*S*,3*S*)-3-[3-[4-(trifluoromethyl) benzoylamino]benzyloxy]aspartate, WAY-213613 = (*S*)-2-amino-4-((4-(2-bromo-4,5-difluorophenoxy)phenyl)amino)-4-oxobutanoic acid

Even more glutamate analogues containing amide bonds were discovered only in the last year, such as Esaprazol, IKM-159 and argiotoxin-636 to name a few (Fig. 3.3).[5-7] It is possible that the amide moiety helps the interaction with the binding sites being both a H-donor and acceptor in hydrogen bonding.

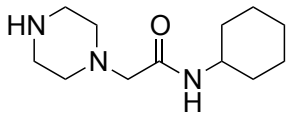

Esaprazol

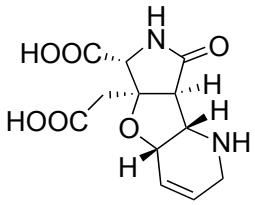

IKM-159

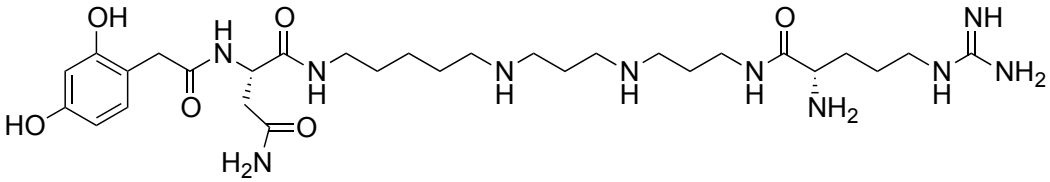

argiotoxin-636

Fig. 3.3: new glutamate analogues containing the amide moiety, where IKM159 = (4a*S*,5a*R*,6*R*,8a*S*,8b*S*)-5a-(carboxymethyl)-8-oxo-2,4a,5a,6,7,8,8a,8b-octahydro-1*H*-pyrrolo[3',4':4,5]furo[3,2-*b*]pyridine-6-carboxylic acid

In our case, the simple Gly and the more hindered Phe were chosen to couple with ACCA because they are involved in neurotransmission: phenylalanine is a part of the molecule 1-3-4-dihydroxy-phenylalanine (L-DOPA), precursor of the important neurotransmitter dopamine, while glycine is directly involved in the inhibitory neurotransmission.

All the efforts towards the cure of defects in glutamate-mediated neurotransmission diseases in the last decades unfortunately have provided very few positive results. The majority of the work done was developed mainly on Glu receptors therefore, more recently, more laboratories moved their attention towards EAATs.[3]

The C6 glioma cell line (Fig. 3.4), which derives from rat brain tumour induced by *N*-nitrosomethyl-urea, endogenously expresses the EAAC1 (orthologue of human EAAT3) subtype of glutamate high affinity transporter. They also express the X_c^- cystine-glutamate exchanger.[8] Gliomas are cancer cells developed in the supportive cells of the brain, the astrocytes. They behave similarly to neurons, but they are easier to culture. For all these reasons, C6 GLIOMA cells were chosen as a model system for the study of glutamate transport in the experiments herein described.[9]

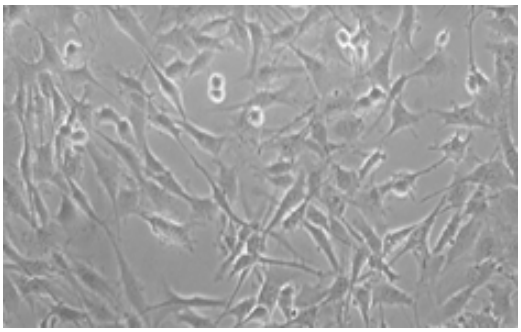

Fig. 3.4: rat C6 GLIOMA cells in DMEM medium

Glial cells, as neuronal cells, are fundamental for the control of extracellular glutamate concentration in the CNS, through sodium dependent transporters. It is recognised that a number of transporters is regulated by protein kinase C and phosphatidylinositol 3-kinase and among them is EAAC1.[9] Considering the important role of these transporter proteins in maintaining the glutamate level and their involvement in neurodegenerative diseases, their regulation is a topic of great interest in research.

Glial cells not only express EAATs, but also the cystine/glutamate exchanger (X_c^-, Fig. 3.5) so it is interesting to study the behaviour of our drugs with both types of transport.

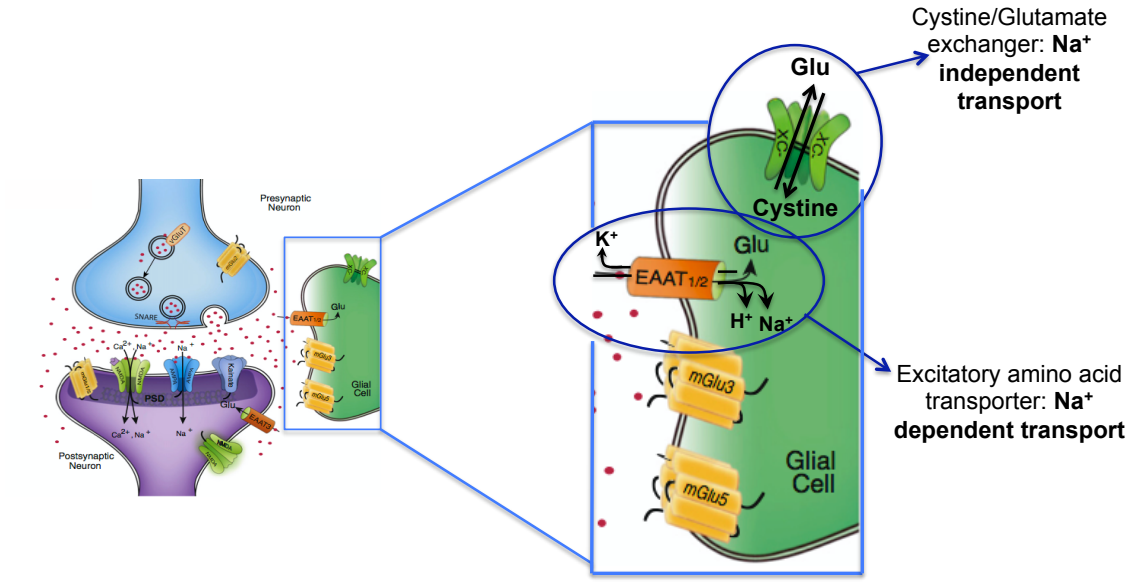

Fig. 3.5: neuronal synaptic cleft and enlargement of a glial cell with its protein transporters[†]

For these experiments, high concentrations of Glu are used (up to 200 μM), forcing the cystine-glutamate exchanger to work in a reverse mode and to take up glutamate instead of cystine. A standard amount of radioactive ^{3}H-labeled glutamate is added to the samples to monitor the glutamate uptake in C6 glioma cells exploiting its radioactivity (scintillation counts).

Experimental procedures are explained in detail in paragraph 3.4 and all the data are presented as percentage of control, where control refers to a C6 glioma cell suspension, in only media, with no drug present.

[†]Reprinted from Pharmacology & Therapeutics, Vol. 132, Issue 3, C. Pittenger, M. H. Bloch, K. Williams, "Glutamate abnormalities in obsessive compulsive disorder: Neurobiology, pathophysiology, and treatment", pag. 318, copyright 2011, with permission from Elsevier

3.2.1-Trypan blue dye exclusion toxicity assay

The first set of experiments executed was the Trypan blue dye exclusion toxicity assay. Trypan blue (Fig. 3.6) is a stain designed to only enter dead cells.

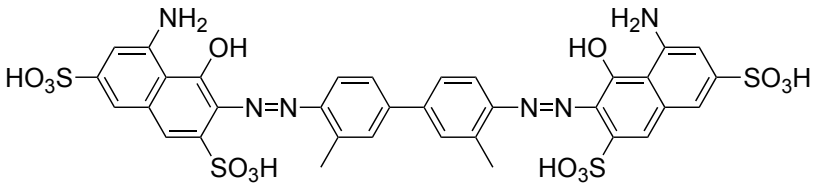

Fig. 3.6: trypan blue chemical structure

Viable cells are very selective for molecules that can cross the cell membrane, thus big molecules such as trypan blue can not go into the cytoplasm. In the case of dead cells, the membrane is compromised, therefore their selectivity is lost and the dye is no longer stopped (plasma membrane permeability is one of the early indicators of cell death). Dead cells with the dye inside appear blue, due to the presence of the dye in their cytosol, while viable cells appear white under the microscope so they are easily distinguishable (Fig. 3.7). In this way the trypan blue dye exclusion assay permits one to count the number of viable cells in a cell suspension.[10]

Fig. 3.7: trypan blue treated cells seen under the microscope

After incubating the cells free from the drugs (control) and with the drugs in DMEM culture medium (enhanced with 10 % foetal bovine serum, 1 % penicillin/streptomycin and 2 mM L-glutamine) for 24 hours at 37 ºC (80-90 % confluency), the toxicity assay was performed. Each drug was seeded three times and each experiment was repeated in triplicate for different concentrations: 10, 50, 100 and 200 μM (Fig. 3.8). The viable cells were counted using Invitrogen Countess automated cell counter.

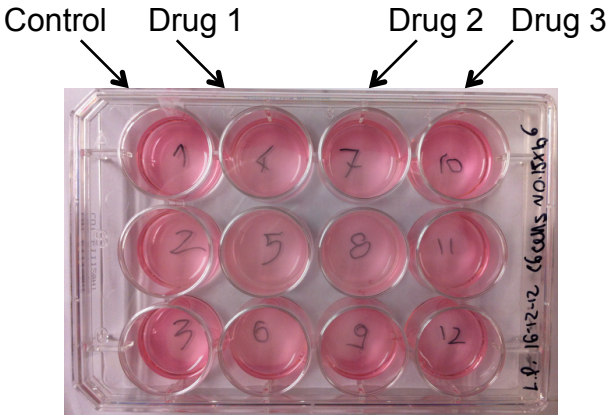

Fig. 3.8: C6 glioma cells in DMEM medium seeded into 12 well dishes ready for trypan blue dye exclusion assay

Firstly, cell morphology was checked to see whether the drugs have an influence on it. In the case of the drugs used for these experiments the morphology was unchanged, as shown in Table 3.2.

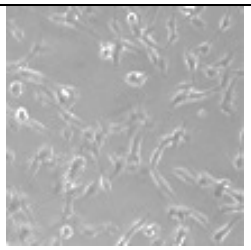	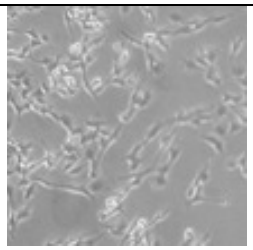	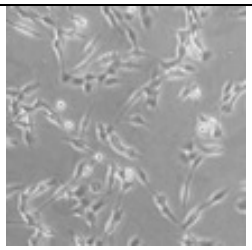
control (cells only)	cells + ACCA	cells + Phe-ACCA
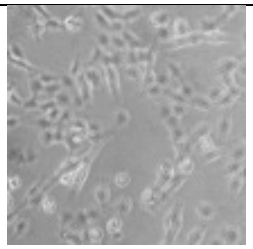	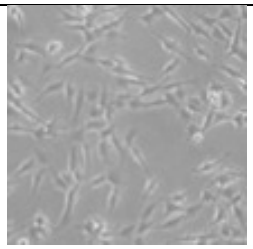	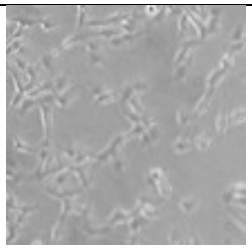
cells + Gly-ACCA	cells + PrACCA	cells + ACCA-ACCA

Table 3.2: C6 glioma cells, seeded for 24 hours with the different drugs; no change in morphology is registered compared to the control

The results of the toxicity assay, represented below, show no toxicity up to 200 μM concentration of the drugs. At this concentration, ACCA, Phe-ACCA and Gly-ACCA all showed a reduction in cell viability after 24 h incubation, as it is suggested from the registered decrease in viable cells number, but only for ACCA this data was statistically significant (Fig. 3.9).

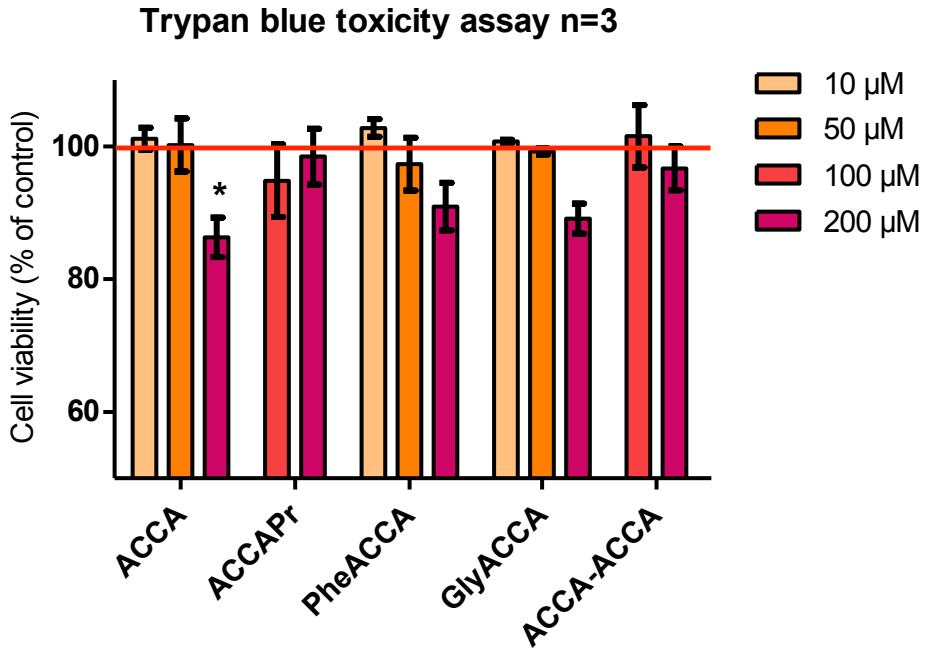

Fig. 3.9: trypan blue dye exclusion assay for C6 glioma cell line in presence of different drugs at different concentrations, reported in % of control, where the control is set at 100 % and is represented by the red line

In conclusion, these results showed that the drugs are not toxic for the cells up to 200 μM concentration, which states the higher limit for the glutamate uptake assays that will be explained later.

Through the counter it was also possible to record the size of the cells. Dead cells, as expected, are much smaller in size compared to viable cells, as shown in the example reported below (Fig. 3.10). However the size changes did not correlate with increasing concentrations of the drugs.

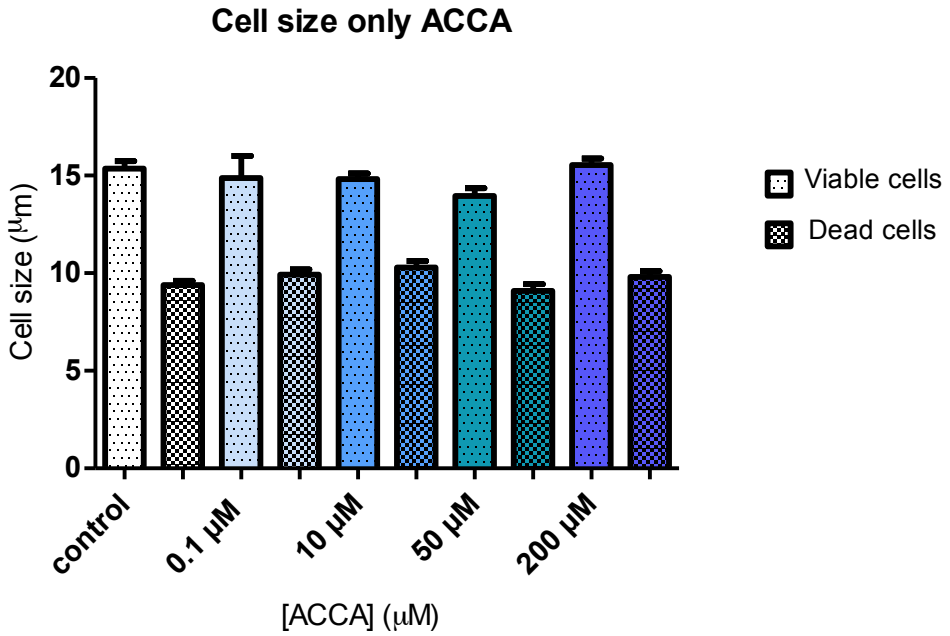

Fig. 3.10: comparison between size of viable and dead cells following incubation with increasing concentrations of ACCA (0.1-200 μM)

3.2.2-Analysis of L-[^{3}H]-glutamate transport in C6 glioma cells

After growing C6 glioma cells (in DMEM culture medium enhanced with 10 % foetal bovine serum, 1 % penicillin/streptomycin and 2 mM L-glutamine at 37 ºC) in 12 well plates for 24 hours as a monolayer, at a density of 0.2x10^6 cell/mL (80-90 % confluency), solutions of different concentrations of glutamate, mixed with a standard amount of ^{3}H-labelled glutamate, were given to the cells in triplicate. In order to verify the kinetics of the Glu transport in both the high affinity glutamate transporters (EAATs) and low affinity glutamate transporters (X_c^-), the experiments were performed in presence and also without Na^+. It was possible to estimate the Na^+ dependent transport subtracting the values of the sodium free transport (obtained from the samples without Na^+) from the total transport (obtained from the samples with Na^+). To understand the amount of Glu taken up at the different concentrations (0, 10, 25, 50, 200 μM), the cells were lysed with 0.25 M NaOH and the radioactivity (proportional to the amount of Glu in the cells) was measured *via* scintillation counter and corrected for the protein concentration, which was estimated with Bradford protein assay.[11]

Kinetic studies indicated a linear uptake for the sodium independent transport up to 200 μM and a Michaelis-Menten kinetic for the sodium dependent transport, with a K_m value of 5.3 μM and a V_{max} of 504.4 pmol·mg^{-1}·min^{-1} (Fig. 3.11). The K_m value obtained is comparable to the ones reported by Davis and co-workers (K_m = 16.8 μM and V_{max} = 567 pmol·mg^{-1}·min^{-1}) and Robinson and Dowd (K_m = 13 μM and V_{max} = 430 pmol·mg^{-1}·min^{-1}) for the same cell line.[9,12] This difference could be caused by different experimental factors, such as higher cell passage number and different radiolabelled isotope stock.

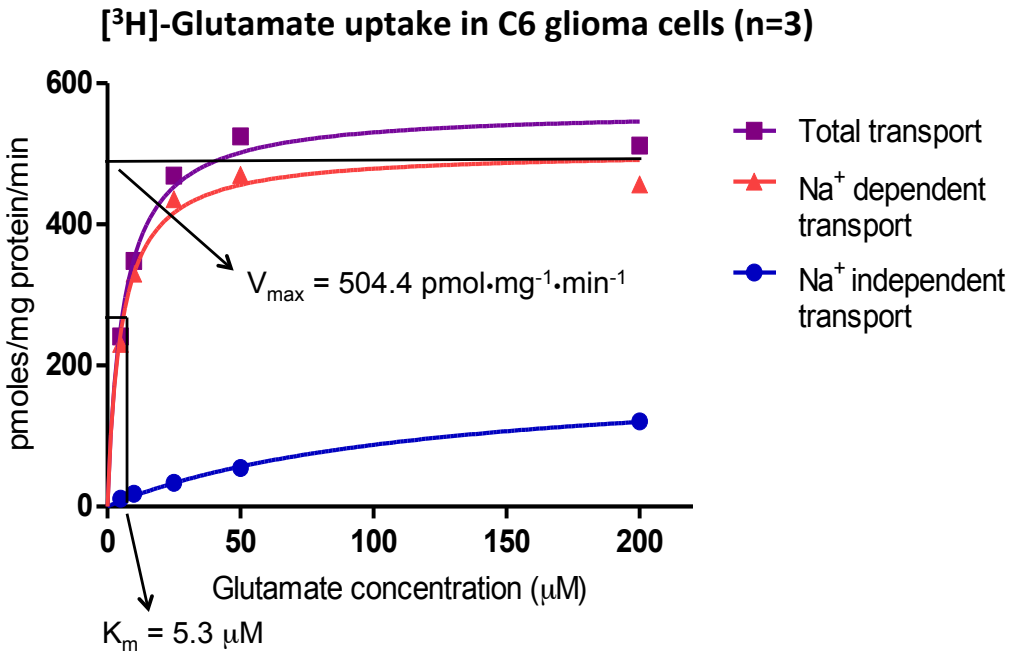

Fig. 3.11: kinetic studies through Glu uptake in C6 glioma cells for sodium dependent and independent transport

For the protein concentration determination, Bradford reagent was used. The Bradford protein assay is a colorimetric assay performed using a dye (Coomassie Brilliant Blue G-250, Fig. 3.12) which changes colour from red to blue when bound to proteins.[11]

In this way it is possible to understand how much protein is contained in each sample, measuring the absorbance of the lysate mixed with the dye and comparing the result with a calibration curve, calculated using known concentrations of the standard protein, bovine serum albumin (BSA).

The concentration of protein in each well was calculated from the absorbance data directly from the spectrometer using the standard curve slope. The values were then corrected for the appropriate dilution factor.

From the kinetic experiments it was possible to decide the experimental conditions to use in the next uptake assays. For the Na^+ dependent transport, 10 μM seemed to be a suitable choice, in between the K_m value and the saturation concentration (maximum Glu transport activity). Na^+ independent transport has low affinity for glutamate and therefore it is slow and does not reach saturation in the experimental conditions used, but it is possible to choose a high enough concentration of glutamate so that it is still possible to detect (200 μM).

These concentrations were kept constant for the uptake experiments in presence of the different drugs, while the drugs concentration was increased from 0 μM (control) to 200 μM.

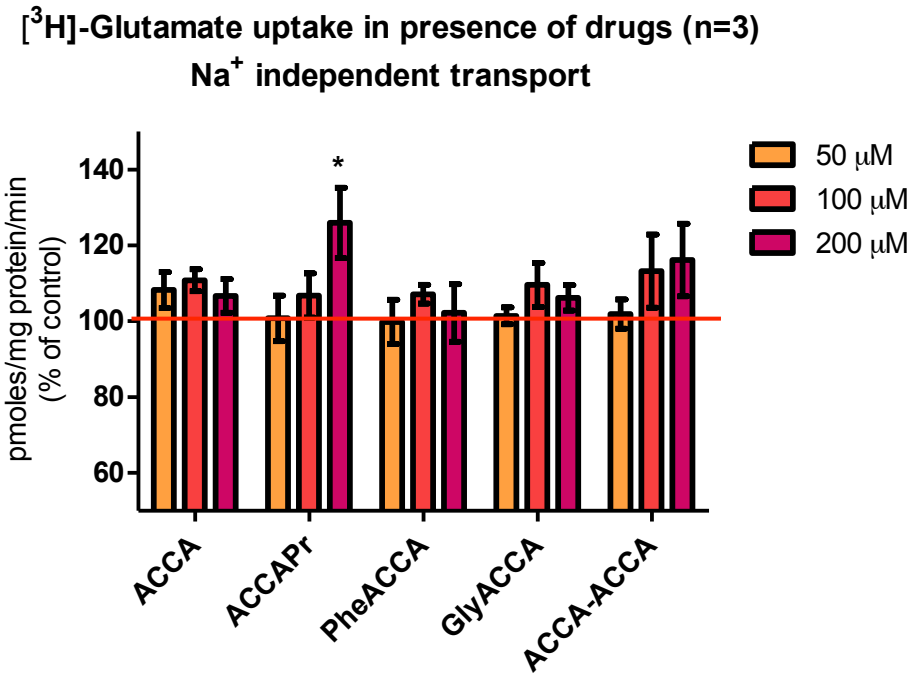

a)

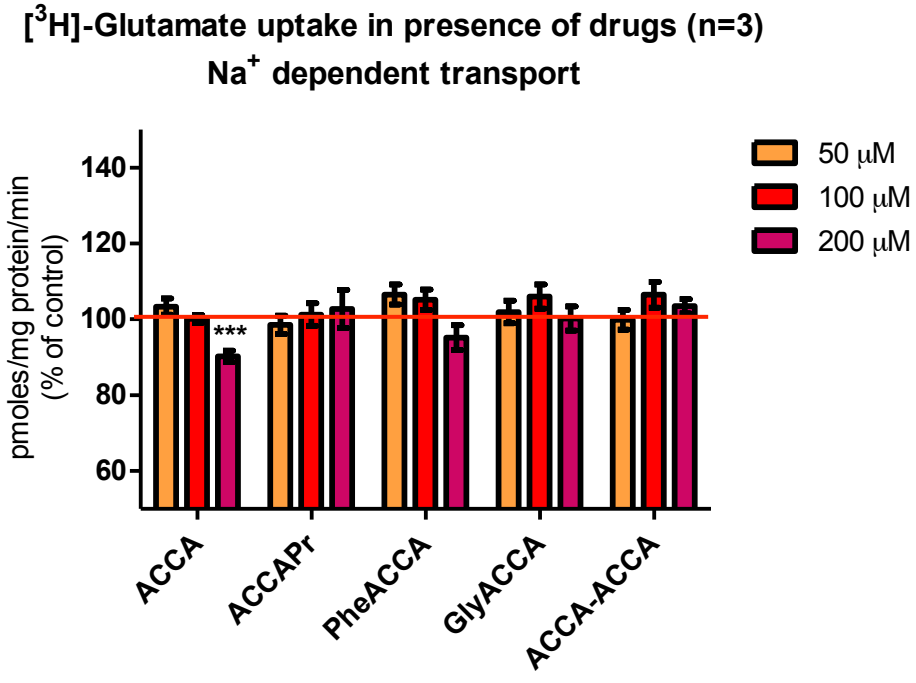

b)

Fig. 3.13: Glu uptake experiments: (a) in presence of the drugs for Na^+ independent transport ([Glu] = 200 μM) and (b) for Na^+ dependent transport ([Glu] = 10 μM); results are expressed as % of control, where the control is set at 100 % and is represented by the red line

The results obtained are shown in Fig. 3.13. For the sodium independent transport, representing the cystine-glutamate exchanger, there is only one significant value, ACCA-Pr ester, which showed an increase in the amount of Glu taken up by the antiporter at 200 μM concentration. This is a very interesting result, even more considering that we expected the opposite behaviour, given its similarity with Glu inhibitors already studied in the literature, some of which are described in the introduction (paragraph 1.3.5.1, pag. 44). ACCA instead seems to act as inhibitor for the sodium dependent uptake (EAAC1) at 200 μM, but unfortunately it is not possible to rely on the data due to the toxicity shown before at that concentration. In conclusion for this part of experiments, only 200 μM ACCA-Pr showed some neural activity.

To investigate the drugs further, a new set of glutamate uptake experiments was performed, pre-incubating the drugs with the cells for 18 hours. The concentration of Glu was maintained the same as before and the concentration of each drug was kept at 100 μM (Fig. 3.14).

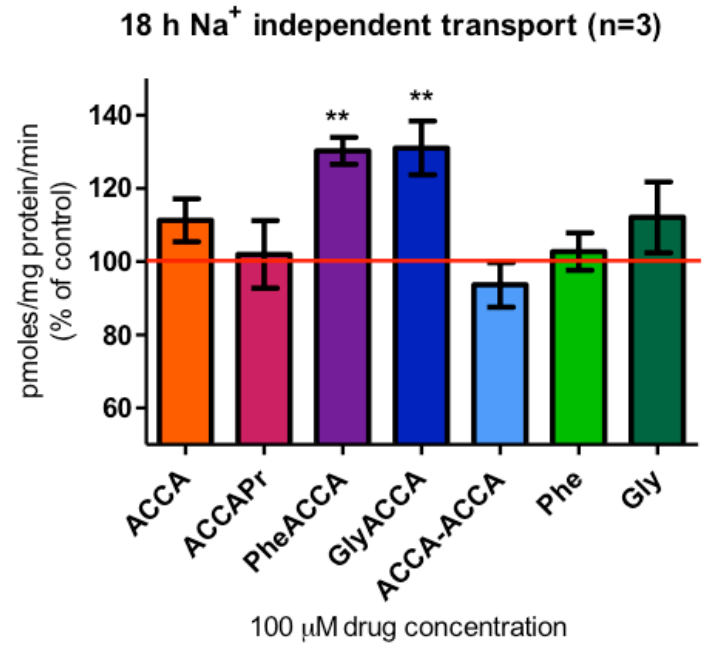

a)

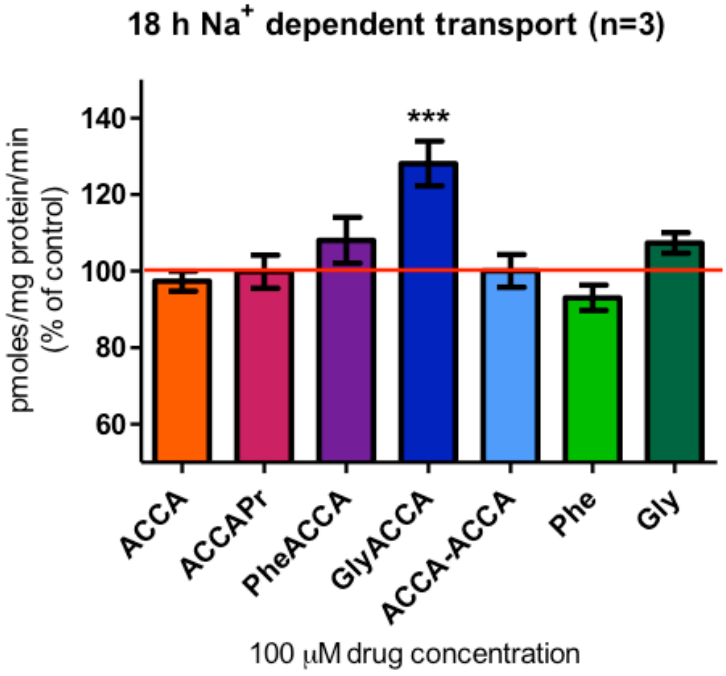

b)

Fig. 3.14: 18 h pre-incubation Glu uptake experiments: (a) at 100 μM drug concentration, for Na^+ independent transport ([Glu] = 200 μM) and (b) for Na^+ dependent transport ([Glu] = 10 μM); results are expressed as % of control, where the control is set at 100 % and is represented by the red line

The results obtained in this case were more interesting. For the sodium independent transport, the two drugs Phe-ACCA and Gly-ACCA significantly increased the glutamate uptake and the same behaviour was registered for Gly-ACCA in the sodium dependent transport. The fact that Gly-ACCA is active in both Na^+ dependent and independent transport, while Phe-ACCA is active only in the case of Na^+ independent transport, means that the latter is selective towards only one of the two glutamate transport mechanisms present in glial cells, making it even more interesting and potentially more important from a pharmaceutical point of view.

To make sure that the effect wasn't due to Phe and Gly alone (degradation of the dipeptides by peptidases was considered only as an extreme possibility), the uptake experiments were performed also with these two amino acids, but as expected no activity was found (Fig. 3.14).

Measurement at 50 and 100 μM concentration of Phe-ACCA and Gly-ACCA for 24 h pre-incubation were also executed to see whether the same trend was evident with a longer pre-incubation time and with half of the drug concentration previously used (Fig. 3.15).

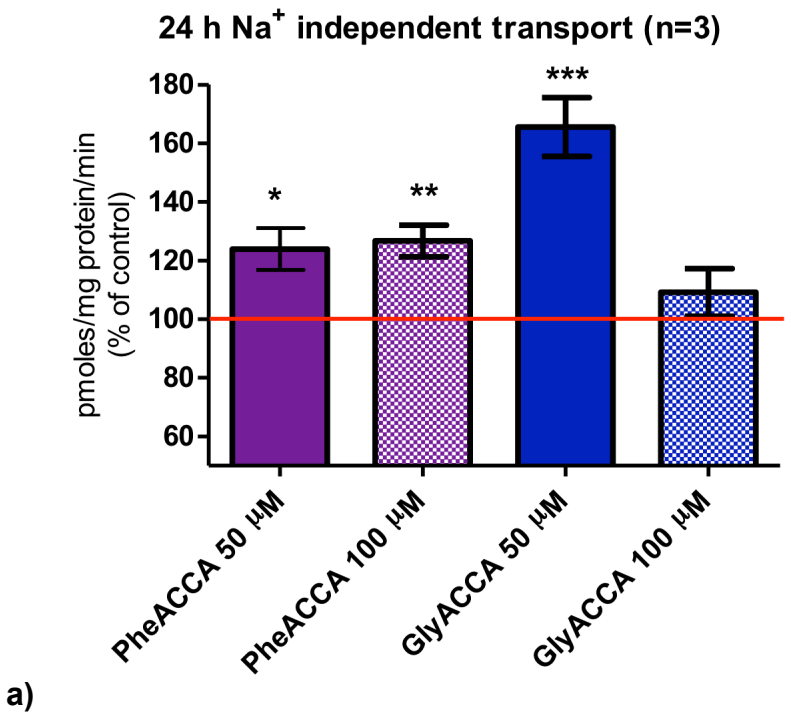

a)

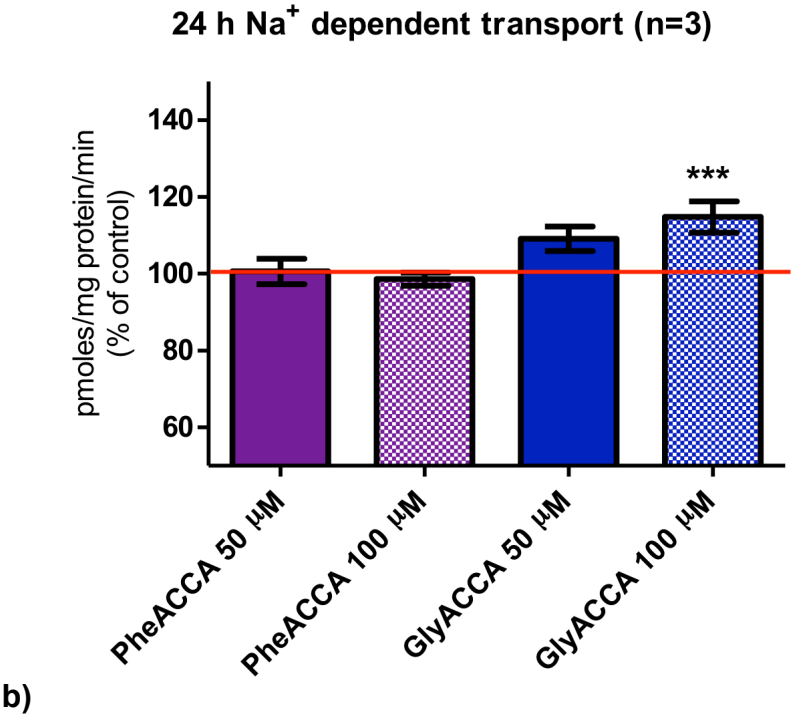

b)

Fig. 3.15: 24 h pre-incubation Glu uptake experiments at 50 and 100 μM concentration of Phe-ACCA and Gly-ACCA: (a) for Na^+ independent transport ([Glu] = 200 μM) and (B) for Na^+ dependent transport ([Glu] = 10 μM) (b); results are expressed as % of control, where the control is set at 100 % and is represented by the red line

After 24 h pre-incubation, Phe-ACCA was still active at both 50 and 100 μM for sodium independent transport, while Gly-ACCA only at 50 μM concentration. In the case of sodium dependent transport, only Gly-ACCA at 100 μM was statistically relevant. This suggests an experimental error for the measurement of Gly-ACCA activity at 100 μM for the sodium independent uptake, considering that it seems to be more active that Phe-ACCA. Another set of experiments should have been repeated in this case.

In light of the reported results, the same trend observed after 18 hours incubation was maintained after 24 hours; the two dipeptides tested are more active in increasing glutamate uptake *via* sodium independent transport compared to the sodium dependent one, meaning a better interaction with the cystine-glutamate exchanger compared to EAATs.

Another interesting result is the fact that, overall, Gly-ACCA is more effective than Phe-ACCA, but it is less selective, while Phe-ACCA is less effective, but more selective towards the exchanger.

Considering the similar behaviour previously observed for ACCA-Pr in the sodium independent transport, it would be interesting to test in the future if that increase persists in pre-incubation experiments.

The up-regulation of the protein transporters measured can occur in two possible different ways: increase of the transporter activity through direct interaction or increase of the number of transporters available.

In the majority of the cases, when a drug enhances the glutamate uptake after pre-incubation, the mechanism of action is not a direct interaction but it rather takes place at a transcriptional, translational or posttranslational level increasing the transporter expression.

In order to prove this theory, protein expression by immunodetection (Western Blot) experiments need to be done to measure the transporters protein concentration in presence of the active drugs compared to the transporter alone.

It would also have been interesting to synthesise and test the dipeptide with cysteine (Cys-ACCA), considering that cystine is a substrate for the X_c^- exchanger.

3.3-Conclusions

Herein ACCA and some derivatives have been tested as glutamate analogues. We can affirm that the 5 drugs analysed have minimal cytotoxicity profiles on C6 glioma cells when incubated for 24 h, but among them only 3 were active: ACCA-Pr in sodium independent transport at a concentration of 200 μM, Phe-ACCA at 100 μM in sodium independent transport after 18 h pre-incubation and finally Gly-ACCA at 100 μM in both sodium independent and sodium dependent transport after 18 h pre-incubation. A similar trend was registered after 24 h pre-incubation. The activity observed was not the inhibitory effect expected, but a very interesting behaviour as transporter enhancement was found.

Recently it has become increasingly clear how much glutamate transporter proteins (EAATs and X_c^-) are involved in neurological disorders and injuries and for this reason they are good drug targets.

Glutamate receptors have been widely studied in this context, but little improvements have been made recently, therefore research of new drugs candidates targeting glutamate transporters should be the way to go for the future.

A number of neuronal dysfunction is due to high extracellular glutamate concentrations and limited glutamate uptake or malfunctioning of the protein transporters. In these cases, drugs able to increase the Glu uptake enhancing the transporters activity could be beneficial.

In light of the consideration just made, ACCA-Pr, Phe-ACCA and Gly-ACCA could find pharmaceutical application as glutamate transport enhancer drugs.

3.4-Experimental

Cell behaviour is influenced by the environment in which they live, in particular, biochemical and physiological properties depend on interactions with the culture medium (namely a synthetic material designed to support the growth of cells with the addition of a serum, which is needed to promote cells growth). Different batch of medium and serum can affect the experimental reproducibility.[13]

Materials: Bradford dye reagent, glutamate sodium salt, HEPES, BSA, glucose, NaOH, choline chloride, KCl, $MgCl_2$, NaCl, $CaCl_2$, were purchased from Sigma Aldrich. Dulbecco's modified Eagle's medium (DMEM) was purchased from Lonza, trypsin and PBS from Invitrogen, ^{3}H-glutamate from Perkin Elmer (NET 490, 250 μCi, 9.25 MBq), Ecosint A scintillator cocktail from National Diagnostics.

Cells culture conditions:
Rat C6 glioma cells (obtained from American Type Culture Collection) were grown in Dulbecco's modified Eagle's medium (DMEM) enhanced with 10 % foetal bovine serum, 1 % penicillin/streptomycin and 2 mM L-glutamine in T75 cell culture flasks at 37 ºC in a humidified incubator at 5 % CO_2 and 95 % air. Cells were grown as a monolayer and regularly harvested twice weekly.

Experiments involving the drugs were executed starting from stock solutions: 10 mM in deionised water and DMSO in ratio 1:1 for ACCA, ACCA-Pr, ACCA-Phe and ACCA-ACCA and 2 M in water for ACCA-Gly The stock solutions were stored in the fridge. Control experiments included the appropriate percentage of DMSO.

Viability analysis with Trypan Blue Assay:
C6 glioma cells were seeded at a density of $0.1x10^6$ cell/mL in 12 well plates and grown overnight under normal cell culture conditions. When 80-90 % confluency was reached, solutions of the drugs were prepared from a 10 mM

stock solution at 10, 50, 100, 200 μM concentrations in fresh medium, adding a DMSO vehicle of 0.5 %.

The old cell medium was discarded and 2 mL of each drug solution were added to the cells in triplicate. The cells were then placed back into the incubator for 6 and 24 h. At the assay endpoint the medium from each well was removed to labelled Eppendorf tubes. The cells were washed with 500 µL of pre-warmed sterilized phosphate buffered saline solution (PBS, containing NaCl, KCl, Na_2HPO_4, KH_2PO_4) and 200 µL of 0.05 % trypsin/EDTA was added to each well. Following cell detachment, the cells from each well were re-suspended in the original cell culture medium pertaining to that well. The cell solutions were spun at 1200 RPM for 4 min using a SIGMA 2-5 bench top centrifuge. The supernatant was removed and the cells were re-suspended in 200 μL of serum free media and 200 µL of 0.4 % trypan blue solution was mixed together. Viable cells were then counted using Invitrogen Countess automated cell counter. The viability results were expressed as percentage of the control value (cell suspension in culture medium with no drug added).

L-[^{3}H]-Glutamate uptake assay:

C6 glioma cells were seeded at a density of $0.2x10^6$ cell/mL in 12 well plates and grown for 24 h under normal cell culture conditions.

Solutions of L-glutamate 0, 50, 100 and 200 μM combined with L-[^{3}H]-glutamate 0.5 μM were prepared in Krebs-HEPES buffers Na^+ free (KHB-F: 10 mM HEPES, 120 mM choline chloride, 3 mM KCl, 2 mM $MgCl_2$, 2 mM $CaCl_2$ and 2.2 mM glucose adjusted to pH 7.4) and Krebs-HEPES buffers Na^+ plus (KHB-P: 10 mM HEPES, 120 mM NaCl, 3 mM KCl, 2 mM $MgCl_2$, 2 mM $CaCl_2$ and 2.2 mM glucose adjusted to pH 7.4). Each well from one of the two 12 well plates was washed with 1 mL of warm KHB-F, after removing the medium. The assay was started by replacing the buffer from the first well with 1 mL of the first test L-glutamate solution. After 20 seconds the next well was treated in the same way. Each solution was tested in triplicate before moving to the next concentration. The kinetic analysis of L-glutamate transport activity was monitored for exactly 5 min, thereafter 1 mL of a solution 20 mM of unlabelled ice-cold L-glutamate in KHB-F was added to stop the transporter action and therefore the uptake. Each

well was washed one more time with the ice-cold glutamate solution and 500 µL of NaOH 0.25 mM was added to lyse the cells overnight. The same procedure was repeated with the second 12 well plate using KHB-P instead of KHB-F.
The cell lysates were subjected to liquid scintillation counting for determination of radioactivity and values were adjusted to protein content, calculated with Bradford assay. All results were expressed as percentage of the control value, as specific transport of L-[^{3}H]-glutamate (pmol/mg protein/min).

Radioactivity determination by scintillator counter:
400 µL of the cell lysates were transferred to scintillation vials containing 4 mL of Ecosint A scintillator cocktail. Determination of radioactivity levels was carried on with a Beckman LS60001C Scintillation counter.

Protein Determination by Bradford Assay:
10 µl of each cell lysate were mixed with 40 µL of Bradford reagent and 150 µL of deionised water in triplicate in a 96 well plate. The absorbance was read at A_{595} for each well using a Spectra Max 190 spectrometer from Molecular Devices. A protein standard curve was prepared using lyophilized bovine serum albumin (BSA), reconstituted with deionised water to yield a 0.1 mg/mL solution (Fig. 3.16). The absorbance of samples ranging from 0.25-2.5 µg/mL concentration of BSA was used to construct the standard curve. Samples from cells typically had an A_{595} in the range of 0.01 to 0.06 (approximately 50-70 µg protein per well).

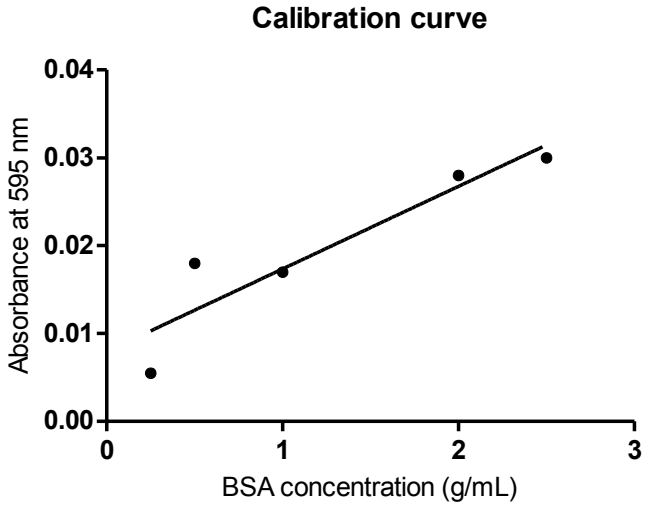

Fig. 3.16: example of standard curve for Bradford protein assay; linear fit: y = A + Bx, where A = 0.00809 and B = 0.009331; $R^2 = 0.85$

Statistical analysis

Graph Pad Prism software (San Diego, CA) was used for the analysis of the data. All the experiment results are presented as mean ± SEM and are analysed statistically by one-way analysis of variance (ANOVA), followed by the Newman-Keuls multiple comparison test. Values of $P < 0.05$ were considered to be significant.

Data for the measurement of L-[^{3}H] Glutamate uptake were analysed using non-linear regression by applying the Michaelis-Menten equation and representing the V_{max} and K_m.

3.5-Bibliography

(1) Koch, H. P.; Kavanaugh, M. P.; Esslinger, C. S.; Zerangue, N.; Humphrey, J. M.; Amara, S. G.; Chamberlin, A. R.; Bridges, R. J.: Differentiation of Substrate and Nonsubstrate Inhibitors of the High-Affinity, Sodium-Dependent Glutamate Transporters. *Molecular Pharmacology* **1999**, *56*, 1095-1104.

(2) Brumfield, S.; Korakas, P.; Silverman, L. S.; Tulshian, D.; Matasi, J. J.; Qiang, L.; Bennett, C. E.; Burnett, D. A.; Greenlee, W. J.; Knutson, C. E.; Wu, W.-L.; Sasikumar, T. K.; Domalski, M.; Bertorelli, R.; Grilli, M.; Lozza, G.; Reggiani, A.; Li, C.: Synthesis and SAR development of novel mGluR1 antagonists for the treatment of chronic pain. *Bioorganic & Medicinal Chemistry Letters* **2012**, *22*, 7223-7226.

(3) Bunch, L.; Erichsen, M. N.; Jensen, A. A.: Excitatory amino acid transporters as potential drug targets. *Expert Opinion on Therapeutic Targets* **2009**, *13*, 719-731.

(4) Varano, F.; Catarzi, D.; Colotta, V.; Poli, D.; Filacchioni, G.; Galli, A.; Costagli, C.: Synthesis and Biological Evaluation of a New Set of Pyrazolo[1,5-c]quinazolines as Glycine/N-Methyl-D-aspartic Acid Receptor Antagonists. *Chemical and Pharmaceutical Bulletin* **2009**, *57*, 826-829.

(5) Kelly, N. M.; Wellejus, A.; Elbrond-Bek, H.; Weidner, M. S.; Jorgensen, S. H.: Synthesis and biological evaluation of Esaprazole analogues showing œÉ1 binding and neuroprotective properties in vitro. *Bioorganic & Medicinal Chemistry* **2013**, *21*, 3334-3347.

(6) Juknaite, L.; Sugamata, Y.; Tokiwa, K.; Ishikawa, Y.; Takamizawa, S.; Eng, A.; Sakai, R.; Pickering, D. S.; Frydenvang, K.; Swanson, G. T.; Kastrup, J. S.; Oikawa, M.: Studies on an (*S*)-2-Amino-3-(3-hydroxy-5-methyl-4-isoxazolyl)propionic Acid (AMPA) Receptor Antagonist IKM-159: Asymmetric Synthesis, Neuroactivity, and Structural Characterization. *Journal of Medicinal Chemistry* **2013**, *56*, 2283-2293.

(7) Poulsen, M. H.; Lucas, S.; Bach, T. B.; Barslund, A. F.; Wenzler, C.; Jensen, C. B.; Kristensen, A. S.; Stromgaard, K.: Structure-activity Relationship Studies of Argiotoxins: Selective and Potent Inhibitors of Ionotropic Glutamate Receptors. *Journal of Medicinal Chemistry* **2013**, *56*, 1171-1181.

(8) Matthaes, S.; McBean, G.: The cystine-glutamate exchanger in 1321N1 human astrocytoma cells. *Irish Journal of Medical Science* **2011**, *180*, 43-43.

(9) Davis, K. E.; Straff, D. J.; Weinstein, E. A.; Bannerman, P. G.; Correale, D. M.; Rothstein, J. D.; Robinson, M. B.: Multiple Signaling Pathways Regulate Cell Surface Expression and Activity of the Excitatory Amino Acid Carrier 1 Subtype of Glu Transporter in C6 Glioma. *The Journal of Neuroscience* **1998**, *18*, 2475-2485.

(10) Strober, W.: Trypan blue exclusion test of cell viability. *Current protocols in immunology / edited by John E. Coligan ... [et al.]* **2001**, *Appendix 3*, 3B-Appendix 3B.

(11) Bradford, M. M.: Rapid and sensitive method for quantitation of microgram quantities of protein utilizing principle of protein-dye binding. *Analytical Biochemistry* **1976**, *72*, 248-254.

(12) Sheldon, A. L.; Robinson, M. B.: The role of glutamate transporters in neurodegenerative diseases and potential opportunities for intervention. *Neurochemistry International* **2007**, *51*, 333-355.

(13) Wolfe, R. A.; Sato, G. H.; McClure, D. B.: Continuous culture of rat C6 glioma in serum-free medium. *The Journal of Cell Biology* **1980**, *87*, 434-441.

Chapter 4

Synthesis of a tetrapeptide-like macrocycle incorporating ACCA

4.1-Introduction

Considering the recent interest in macrocyclic molecules as peptidomimetics and their advantages already described (paragraphs 1.3 and 1.4), we decided to take advantage of ACCA *cis* locked conformation for the generation of a cyclopeptide-like molecule.

In fact, one of the tricks usually adopted in order to facilitate the challenging macrocyclisation reaction is the introduction of constrained molecules.

Furthermore, ACCA, being a non-proteinogenic amino acid, can not be recognised by endo- and exopeptidases, and therefore it can be a good candidate as metabolic stable drug.

Before building the macrocycle, an accurate research of the possible commercially available linkers was conducted. *p*-Aminomethyl benzoic acid (AMBA) was chosen as best candidate because it possess the amino and carboxylic acid functional groups to build a peptide-like molecule and in addition to this it contains a benzene ring, which could be exploited for π-stacking.

In collaboration with Dr. Andrew Phillips we also decided to carry out computational studies to understand the overall rigidity of such macrocyclic molecule and to analyse its ability in complexing cations.

4.2-Results and discussion

4.2.1-Synthesis of the tetrapeptide-like macrocycle

The synthesis of the macrocyclic compound **25** has been performed following a series of protection, coupling and deprotection reactions using a [2+2] approach. [2+2] approach means that two dipeptide-like compounds formed by ACCA and a linker are coupled together to give the tetrapeptide-like final product, rather than coupling the four units of the macrocycle one by one. The retrosynthetic pathway is shown in Scheme 4.1.

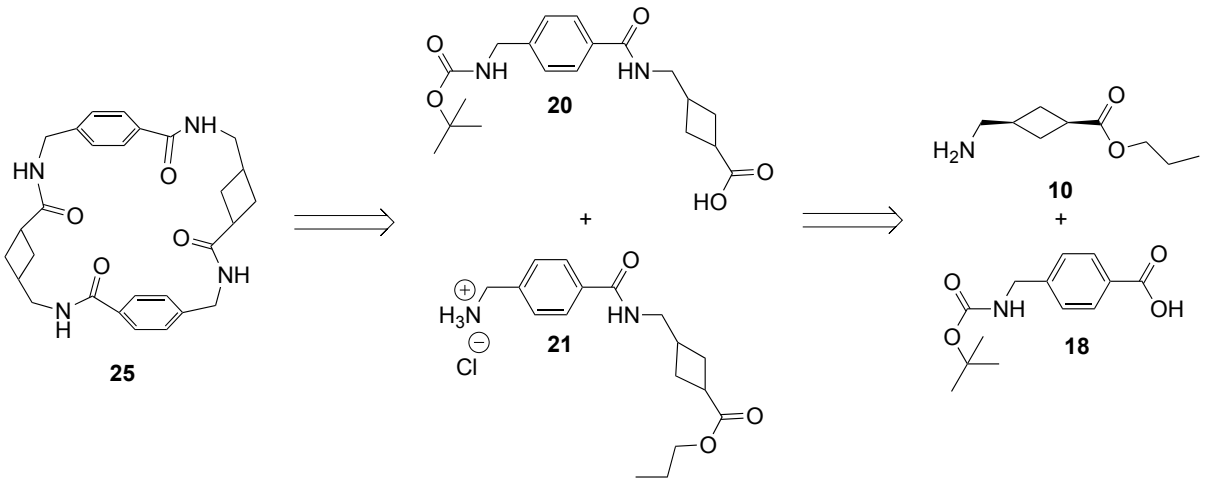

Scheme 4.1 retrosynthetic route to the macrocyclic compound **25**

ACCA was thought to be ideal to incorporate in macrocycles exploiting its *cis*-constrained configuration and, because of its δ-amino acid structure, an amide formation approach was chosen to connect the building blocks. Compound **25** is formed by four units, two ACCA and two linker molecules alternated. The linker selected as best candidate was *p*-aminomethyl-benzoic acid (AMBA, **18**, Fig. 4.1).

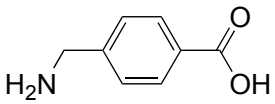

Fig. 4.1 AMBA chemical structure

AMBA is commercially available at low cost and contains both an amine and a carboxylic acid functional groups, which are needed to carry out the peptide coupling; it contains also a benzene ring, useful for π-stacking, which could help with the cyclisation.

Generally, the term amino acid is used to describe an α-amino acid, where the N-terminus is separated from the C-terminus by only one carbon. In our case neither ACCA nor AMBA are amino acids under this definition, but they could be defined as non-natural δ- and ε-amino acids respectively (4 and 5 carbons in between –NH and -COOH) so their peptide derivatives are not proper peptides, but peptide-like structures. For simplicity, from now on they will be referred to as peptides.

ACCA propyl ester **10** is synthesised as already described in chapter 1. AMBA is easy to protect at the amine functional group with Boc, using the same procedure employed previously for the 'ACCA-natural amino acid' dipeptides (Scheme 4.2).

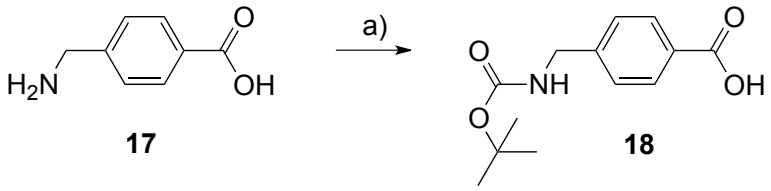

Scheme 4.2 synthesis of Boc-AMBA **18**. *Reagents and conditions:* (a) Boc_2O, NaOH 2 M, dioxane/H_2O, 0 ºC-r.t., 2 h, 70 %

Boc-AMBA **18** was then coupled with ACCA-Pr **10** in good yields, using HATU as coupling reagent (Scheme 4.3).

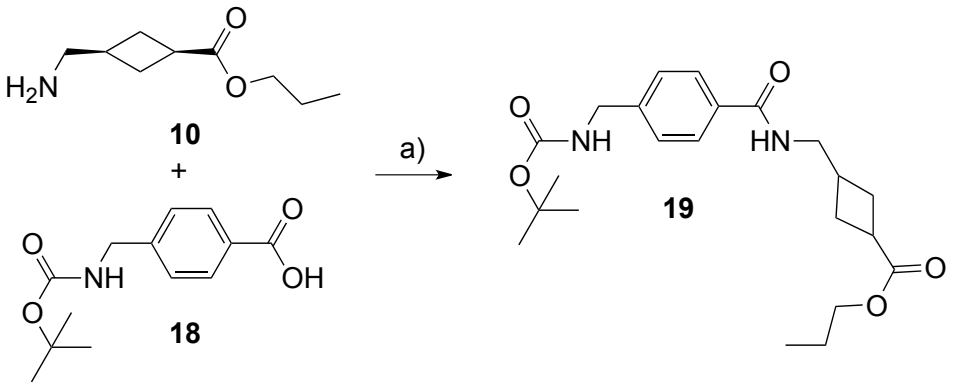

Scheme 4.3 synthesis of Boc-AMBA-ACCA-Pr **19**. *Reagents and conditions:* (a) HATU, $^{i}Pr_2EtN$, dry THF, 18 h, 85 %

Once the dipeptide **19** was synthesised, half was deprotected through basic hydrolysis to free the carboxylic acid (**20**, Scheme 4.4) and the other half was deprotected under acidic conditions to free the amine (**21**, Scheme 4.5). Both reactions proceeded with high yields.

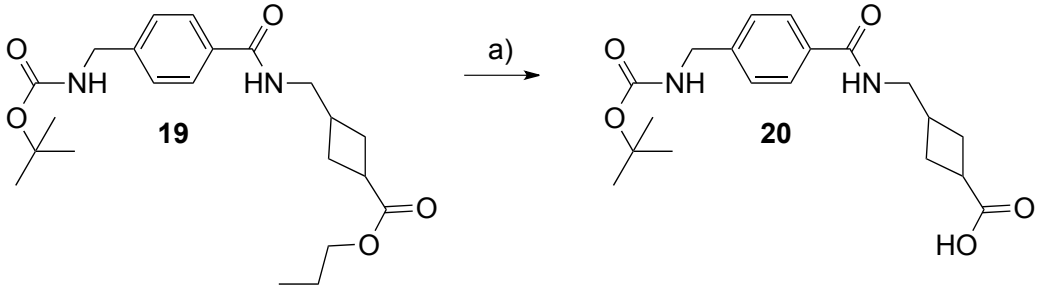

Scheme 4.4 synthesis of Boc-AMBA-ACCA-OH **20**. *Reagents and conditions:* (a) NaOH 2 M, CH_3CN, 45 °C, 3 h, 90 %

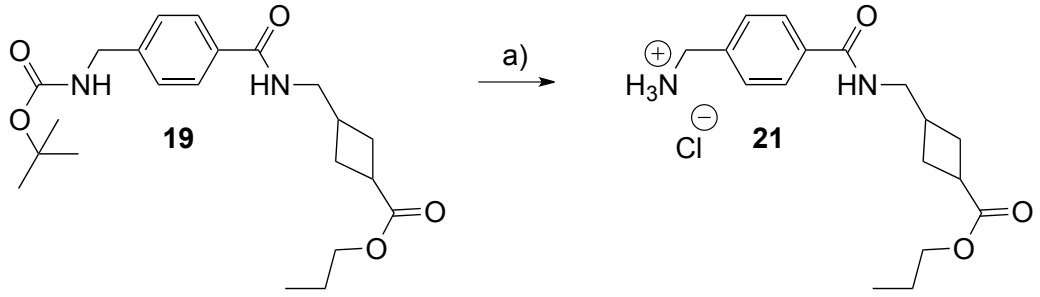

Scheme 4.5 synthesis of $ClNH_3$-AMBA-ACCA-Pr **21**. *Reagents and conditions:* (a) HCl/Et_2O, CH_2Cl_2, 3 h, 93 %

In the latter reaction the product precipitated out making the work up significantly easier as the product could be recovered through simple filtration.
20 and **21** were coupled again using the usual HATU reagent (Scheme 4.6).

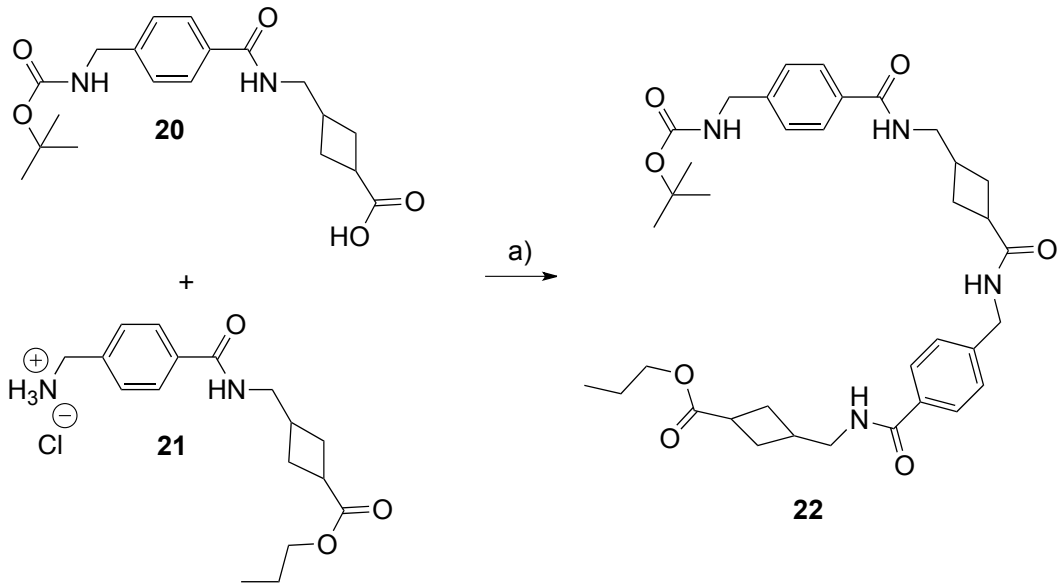

Scheme 4.6 synthesis of Boc-AMBA-ACCA-AMBA-ACCA-Pr **22**. *Reagents and conditions:* (a) HATU, $^{i}Pr_2EtN$, dry THF, 18 h, 67 %

The reaction proceeded successfully, even though with lower yield (67 %) comparing to the previous couplings. This might be due to the fact that the molecules involved are now bigger and steric hindrance can interfere.
To allow for the cyclisation of the linear peptide, the propyl ester and the Boc protecting groups had to be removed, in this order, respectively in basic and acidic conditions (Scheme 4.7 and Scheme 4.8).

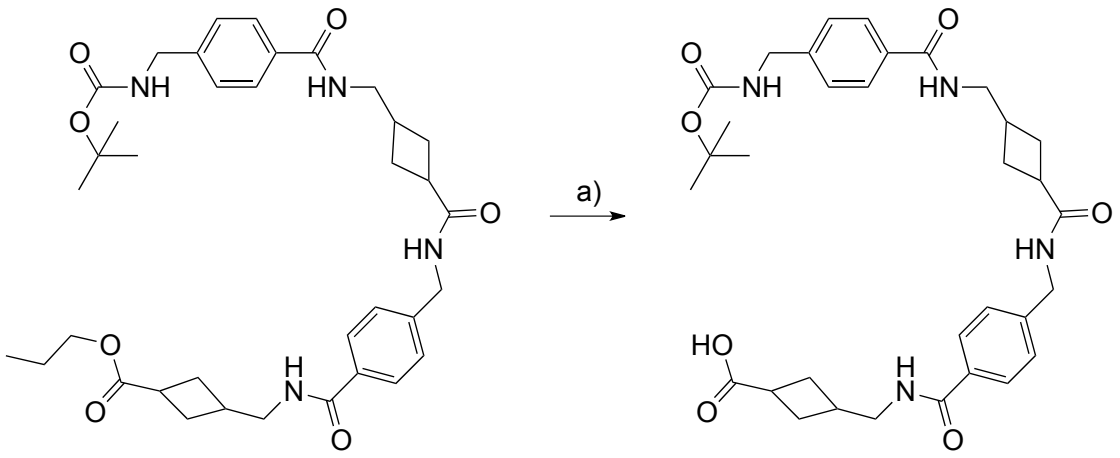

22 **23**

Scheme 4.7 synthesis of Boc-AMBA-ACCA-AMBA-ACCA-OH **23**. *Reagents and conditions:* (a) NaOH 2 M, CH_3CN, 45 °C, 3 h

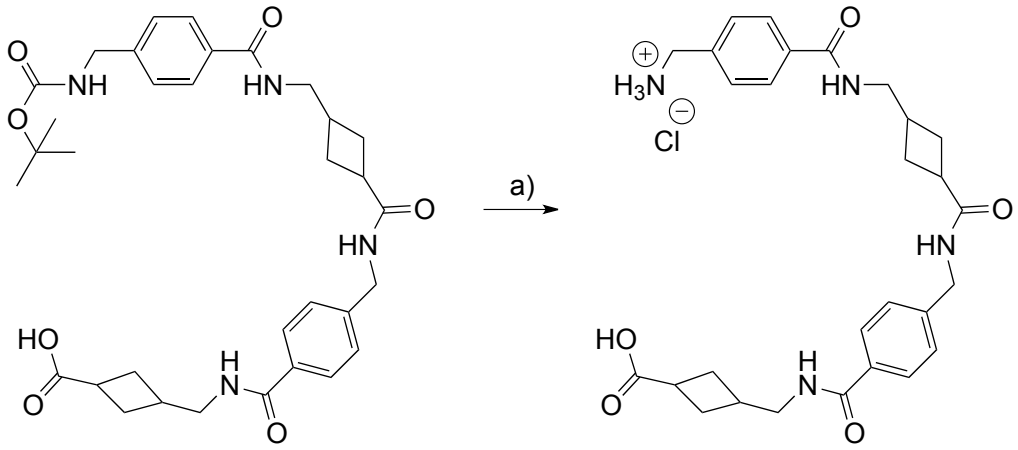

23 **24**

Scheme 4.8 synthesis of $ClNH_3$-AMBA-ACCA-AMBA-ACCA-Pr **24**. *Reagents and conditions:* (a) HCl/Et_2O, CH_2Cl_2, 2 h, 68 % over two steps

Both the protected tetrapeptide **22** and the half deprotected tetrapeptide **23** dissolved only partially in the solvents used, forming a suspension, but they were able to react and give the desired products despite the solubility issue. Especially in the cleavage of the Boc group, it was interesting to notice how the half deprotected tetrapeptide in suspension agglomerated as soon as the acid was added.

The solubility difficulties rendered the work up easier and avoided the need of purification techniques such as column chromatography or recrystallisation, but at the same time it was troublesome to find a suitable solvent to carry out the

reaction. After increasing the temperature to 40-50 °C, only methanol and DMSO were able to improve the solubility of the linear tetrapeptide. This behaviour made the characterisation procedure complicated, especially for ^{13}C-NMR.

The macrocycle closure, as expected, was the most delicate step. A number of problems came to our attention. The first concern arose from the big size of the molecule involved and its steric hindrance, a problem previously encountered in the formation of the protected linear tetrapeptide. Secondly bringing the open tetrapeptide into solution resulted a particularly tricky job and finally the desired cyclisation product is not the most favourable one over polymerisation. Since it needs the free amine and the free carboxylic acid to be very close in space to react, this step required particular reaction conditions and care.

Both the building blocks of the linear peptide, ACCA and AMBA, are quite constrained so the free N-terminus and C-terminus should be closer to each other than in natural peptides, although, the presence of the four methylene bridges confer some flexibility to the molecule making dimerisation and polymerisation side reactions possible. To avoid this, some precautions needed to be applied. As discussed previously (paragraph 1.5), the most common technique used in cyclic peptide synthesis is the exploitation of extremely high dilution conditions. It is known in fact, that the more the reaction solution is diluted the more likely cyclisation will take place over polymerisation reactions. Very high dilution conditions require a minimal amount of compound (usually 50 mg) and a very large amount of solvent (half to one litre) to achieve submillimolar concentrations, which is not practical for various reasons. A smart way-out, originally described by Malesevic *et al*. in 2004[1] and then adopted successfully by different research groups,[2,3] is the concept of pseudo-high dilution. Adding a reasonably diluted solution of the linear peptide (0.01 M) and a solution of the coupling reagent to a stirring solution of the base, very slowly over time, high dilution conditions were reproduced without the need of inconveniently large amounts of solvent. This very slow addition (10 μL/min) is possible through a syringe-pump, so that only a drop of the solution of the linear tetrapeptide gets in contact with the reagents and has the time to react before the next drop is added (~ 0.01 mM). The reaction apparatus employed is shown

in Fig. 4.2: the syringe-pump is set so that the syringes are pushed at an addition rate of 10 μL/min and the needles are immersed into the reaction solution.

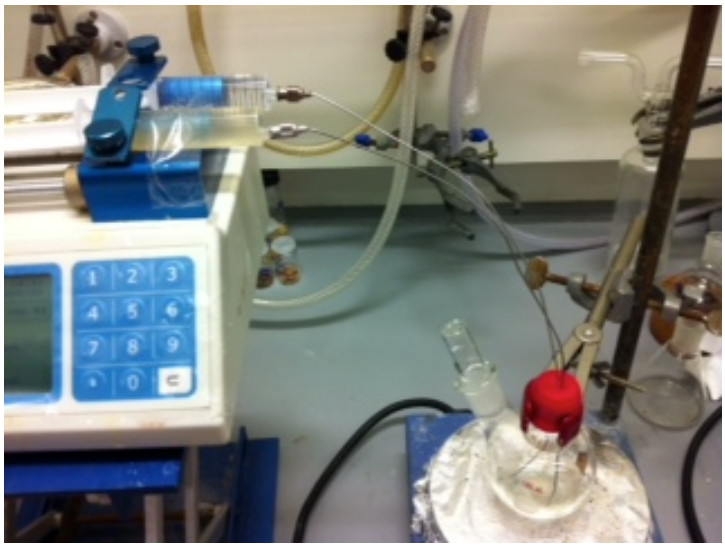

Fig. 4.2 tetrapeptide cyclisation reaction using a syringe-pump: pseudo-high dilution conditions

The complete addition of the open tetrapeptide and coupling reagent into the reaction solution was performed over 21 hours. The reaction was left stirring for a further night before the work up (Scheme 4.9).

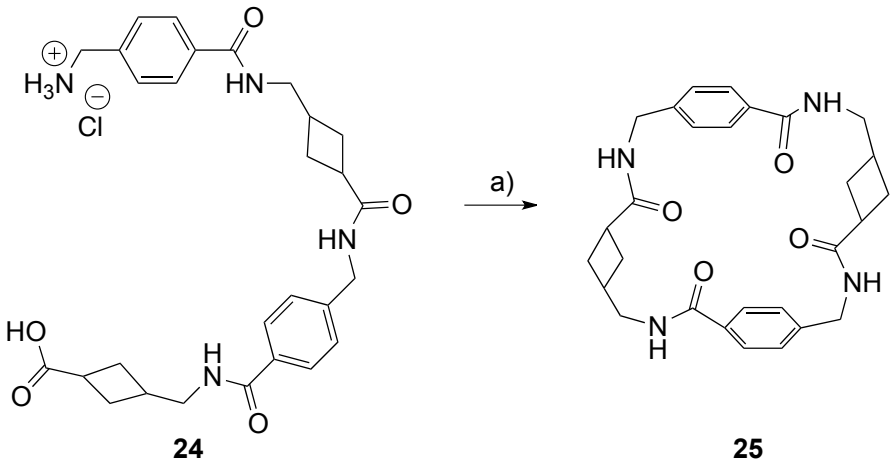

24 **25**

Scheme 4.9 synthesis of cyclo-(AMBA-ACCA-AMBA-ACCA)- **25**. *Reagents and conditions:* (a) HATU, $^{i}Pr_2EtN$, DMF/CH_3OH, 2 days.

The deprotected tetrapeptide was found to be soluble only in hot DMSO or hot methanol. Considering the difficulties in removing DMSO, methanol was chosen. HATU was not soluble in methanol so a small portion of DMF was added.

Unfortunately, only the starting material was recovered and a minimal amount of cyclisation product was identified through mass spectrometry. One of the possible reasons for the failure of the reaction is the poor solubility of the starting material. In fact, part of it precipitated out of the solution overnight, during the syringe addition.

To bring the reaction to completion, longer times might be needed or the temperature could be carefully increased (keeping in mind that sodium perchlorite is explosive at high temperatures). Another complication is the monitoring of the reaction advancement through TLC, because the base used ($^{i}Pr_2EtN$) covers the spot of the very polar linear tetrapeptide. Analytical HPLC seems to be a better way of monitoring the reaction.

Another interesting technique, that should minimise the inconvenience of polymerisation and favour the cyclisation and at the same time improve the solubility, is the use of a templating metal that, coordinating to the open peptide, brings the N- and C-termini close in space to react. The metal ion behaves as activating and catalytic agent.[4]

Usually for tetrapeptides cyclisation Li^+ salts as LiCl are used, but for our purposes a bigger cation such as Na^+ seemed to be a better choice considering that compound **24** is bigger than natural tetrapeptides, being formed by δ- and ε-amino acids.

The templating metal technique was previously used by Robey with a non-protected octadecapeptide from the C4 domain of HIV-1 gp120, before performing the cyclisation step. For 10 mg of the linear peptide in 10 mL of DMF, 1.5 g of LiCl were needed to bring the compound in solution.[5] Liu and colleagues tried different metals as templating agent to cyclise penta- and heptapeptides. They found that the best ion for pentapeptides was Na^+, while heptapeptides needed a bigger ion such as Cs^+.[6]

Before trying the template metal procedure, solubility tests were initially performed with NaCl and KCl to see if compound **24** could be dissolved in methanol in presence of the salts. With KCl no improvement in solubility was noticed, while the compound went into solution with NaCl.

ESI mass spectra of the peptide in presence of the salts were collected and compared (Fig. 4.3): linear tetrapeptide MW ~ 507 g/mol, tetrapeptide + K^+ MW ~ 545 g/mol and tetrapeptide + Na^+ MW ~ 529 g/mol. It is possible to see a typical peptide fragmentation path, where some fragments as the whole tetrapeptide and the dipeptide were detected.

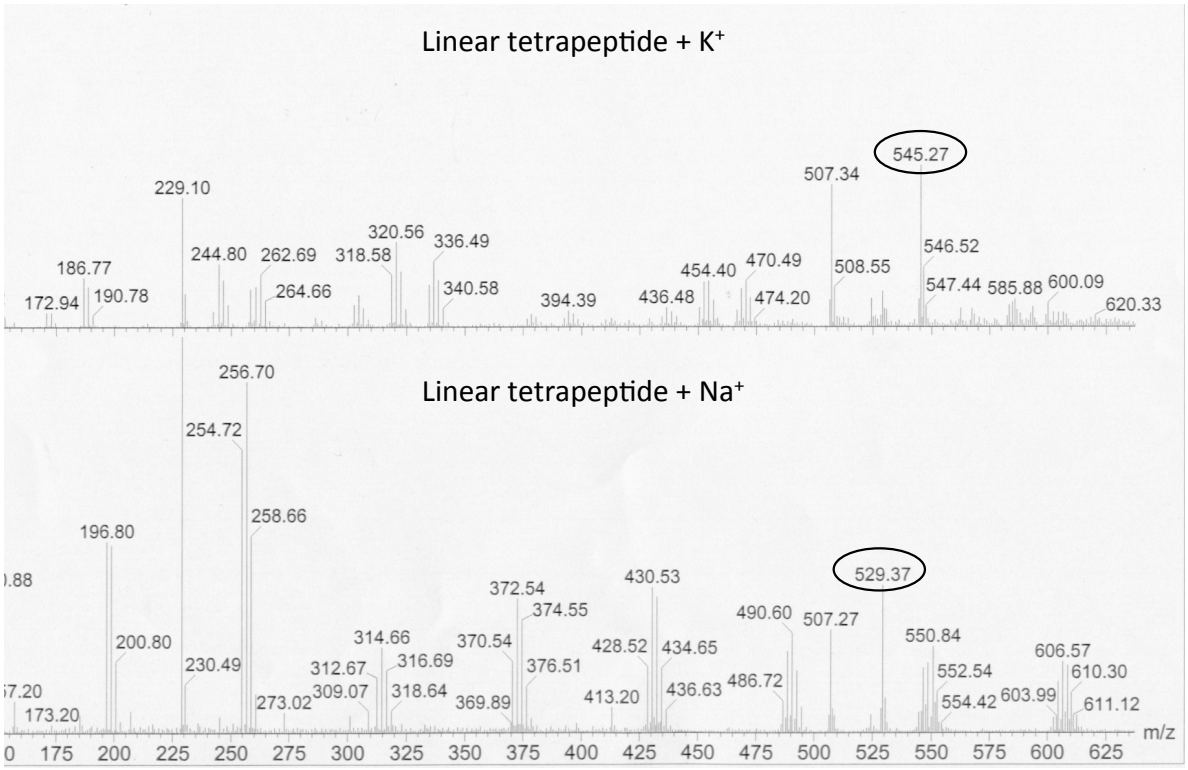

Fig. 4.3 ESI spectra of tetrapeptide **24** in presence of Na^+ (529 g/mol) and K^+ (545 g/mol) ions

For the experiment $NaClO_4$ was preferred to NaCl considering its good solubility in methanol. Keeping in mind its explosive nature, sodium perchlorate had to be handled carefully.

The purpose of the cation is to coordinate to the tetrapeptide (through the nitrogens or, more likely, through the carbonyls), bringing the free amine and the free carboxylic acid close to each other to react. Furthermore, once

coordinated to the metal, the peptide should be more soluble in organic solvents.

After dissolving compound **24** in methanol in presence of 1.5 equivalents of $NaClO_4$, the same procedure used for pseudo-high dilution conditions was followed (Scheme 4.10).

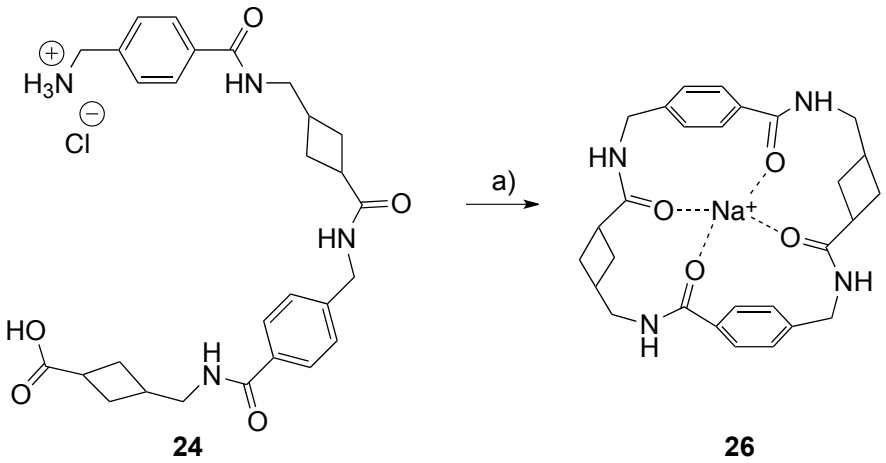

24 **26**

Scheme 4.10 synthesis of cyclo-(AMBA-ACCA-AMBA-ACCA)- **26** using a templating metal. *Reagents and conditions:* (a) HATU, $^{i}Pr_2EtN$, CH_3CN/CH_3OH, $NaClO_4$, 2 days.

It would have been interesting to use Ni^{2+} instead of Na^{+} since it changes its colour when coordinated, giving a colorimetric indication of the complexation reaction. Another possibility could be Zn^{2+} because of its high affinity for oxygen atoms. However, both Ni^{2+} and Zn^{2+} have small ionic radii (Table 4.1) so they might not be suitable for our molecule.

Ion	Radius (pm)
Ni^{2+}	55
Li^{+}	59
Zn^{2+}	60
Na^{+}	99
K^{+}	137
Cs^{+}	167

Table 4.1 Ionic radii of Ni^{2+}, LI^{+}, Zn^{2+}, Na^{+}, K^{+} and Cs^{+}[7]

After evaporating the solvent overnight, the solid was washed with acetonitrile and the 42 mg recovered were analysed through mass spectrometry, ^{1}H- and ^{13}C-NMR, to confirm the presence of the cyclotetrapeptide. Unfortunately the cyclisation product was not separated from the unreacted coupling reagent after silica gel column chromatography; the impure spectrum is reported in Fig. 4.4.

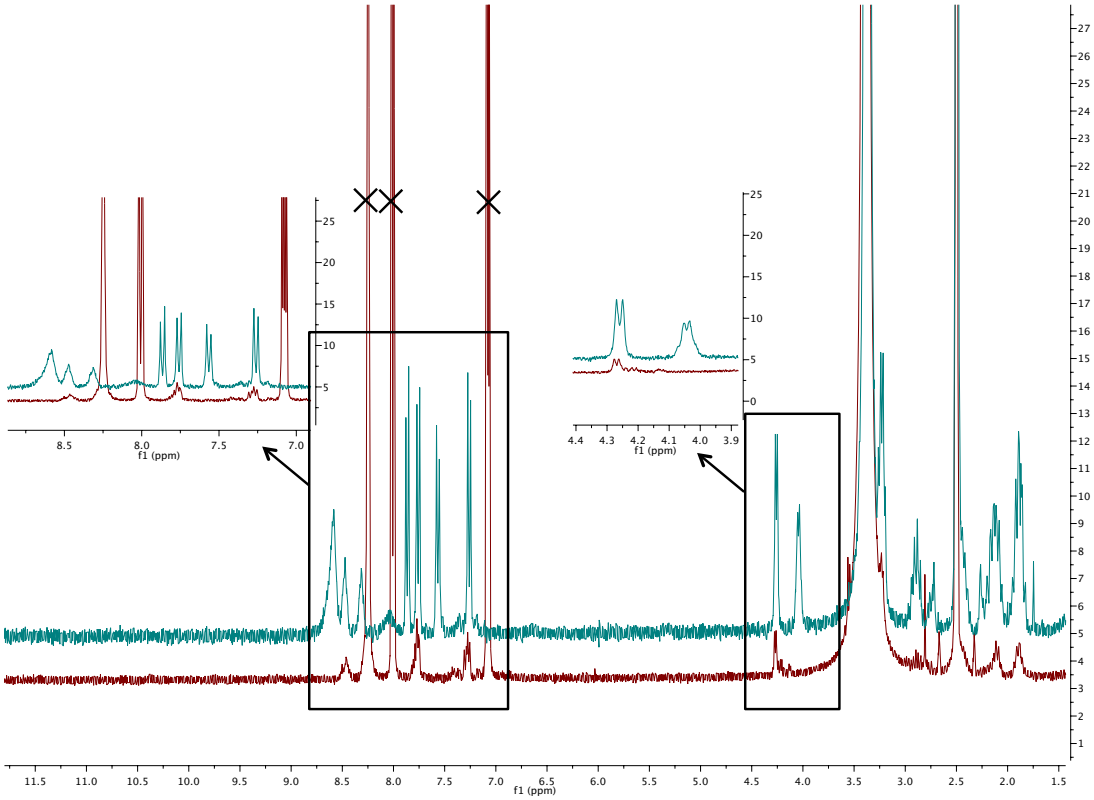

Fig. 4.4 spectrum of cyclotetrapeptide contaminated with un-reacted HATU; where the open tetrapeptide spectrum is in green and the cyclic peptide in red

As it is possible to notice from the ^{1}H-NMR, in the aromatic region (7-9 ppm) the four peaks referring to the two benzene rings in the starting material (green) become two in the product (red) and only one NH peak is visible while three peaks were visible before. Also the two doublets relative to the CH_2 in alpha to the benzene rings (4-4.5 ppm) become one. This behaviour means an increase in symmetry, as expected from the cyclic product.

To better understand the ratio of the product tetrapeptide compared to the unreacted coupling reagent, HPLC analysis will be performed.

The macrocyclisation reaction with template metal needs to be improved, especially in the purification step. In the latter, preparative HPLC should be preferred over chromatography column. Once enough material will be synthesised, it would be interesting to test its ability in complexing different metal ions in solution and comparing the results with the theoretical data (paragraph 4.2.2).

4.2.2-Computational studies

In collaboration with Dr. Andrew Phillips some computational studies on the cyclic peptide **25** were performed, in order to understand the feasibility of its complexation with alkali and earth-alkali metal ions. All calculations were performed in the gas phase, using density functional theory (DFT), which provides the most reliable results with the resources available.
Using the computational chemistry program Gaussview, the macrocyclic molecule was optimised to a minimum energy conformation, taking into account electron correlation and possible molecule conformations in gas phase (Fig. 4.5).

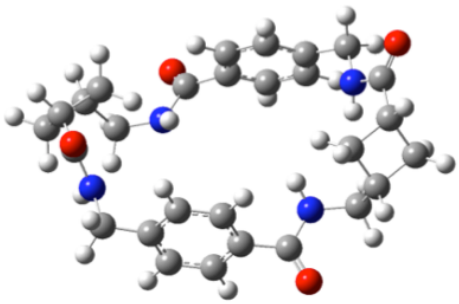

Fig. 4.5 minimum energy conformation for macrocycle **25**

Surprisingly, the theoretical calculations showed significant flexibility in the molecule. Such a result was not expected considering ACCA *cis*-locked conformation and the presence of two cyclobutane and two benzene rings in the core structure. The only possible points of mobility are the four methylene bridges. This flexibility, although unexpected, does not represents a negative

characteristic; it is instead a key feature of the macrocycle since it allows it to adapt to the metal ion to better allocate it into the cavity and form the complex.
The optimised coordination pattern is the one where the cyclic peptide binds to the metal through the four carbonyl groups in a tetrahedral geometry.
Different alkali and earth-alkali cations were measured and, interestingly, all the binding energy (intended as the ΔE in Scheme 4.11) resulted to be exothermic, namely $\Delta G < 0$.

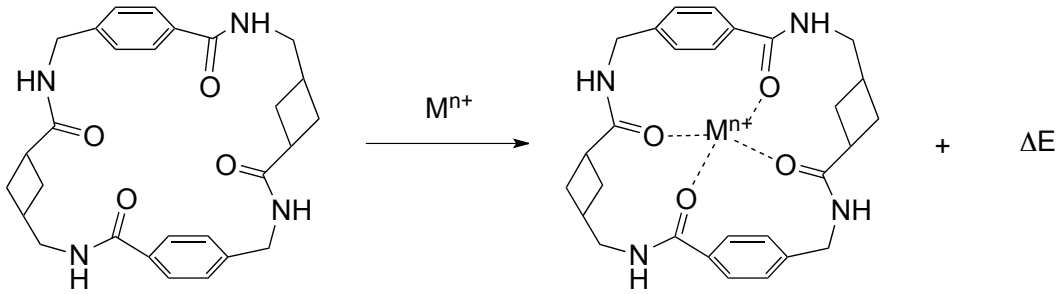

Scheme 4.11 macrocycle binding to different metal cations; where n = 1 or 2 and ΔE = energy of reaction

The energies of binding are listed in Table 4.2 and are measured in hartree (1 hartree = 627.51 kcal/mol).[8]
The energies of the different complexes (macrocycle ligand coordinated to the metals, $E_{complex}$) are compared to the sum of the energy of the uncomplexed macrocycle (E_{ligand} = -1605.7318 hartrees) plus the energy of the free metal cation (E_{cation}). The difference of the two values for each metal gives the ΔE. The fact that all the ΔE are negative means that it takes less energy to form the complex than having the free metal and the free ligand. Therefore, the coordination of the macrocycle to the metal is a favourable process.

Cation	E_{cation} (hartree)	$E_{cation} + E_{ligand}$ (hartree)	$E_{complex}$ (hartree)	ΔE (hartree)	ΔE (kcal/mol)
Be^{2+}	**-13,652**	**-1619,382**	**-1620,107**	**-0,724**	**-454,592**
Mg^{2+}	**-199,227**	**-1804,959**	**-1805,489**	**-0,530**	**-332,704**
Ca^{2+}	**-676,866**	**-2282,598**	**-2282,991**	**-0,393**	**-246,629**
Sr^{2+}	-29,812	-1635,543	-1635,890	-0,346	-217,306
Ba^{2+}	-24,652	-1630,384	-1630,683	-0,300	-188,018
Rb^{+}	-23,606	-1629,338	-1629,539	-0,201	-126,383
Li^{+}	-7,285	-1613,016	-1613,211	-0,194	-121,849
Na^{+}	-162,081	-1767,813	-1767,964	-0,151	-94,7449
K^{+}	-599,724	-2205,456	-2205,570	-0,114	-71,622
Cs^{+}	-19,732	-1625,463	-1625,551	-0,088	-55,060

Table 4.2 Binding energies of the macrocycle with different cations; where E for the free ligand is -1605.7318 hartrees, E_{cation} refers to the energy of the free metal, $E_{cation} + E_{cation}$ refers to the sum of energies of free ligand and free cation, $E_{complex}$ refers to the energy of the ligand coordinated to the metal

It is also interesting to notice that, according to the theoretical calculations, the ligand shows selectivity towards the smallest cations, especially earth-alkali metals (M^{2+}) as beryllium, magnesium and calcium, which are highlighted in bold in Table 4.2. In Fig. 4.6 it is possible to better see the trend of the stabilisation energies, from the most to the least stable metal.

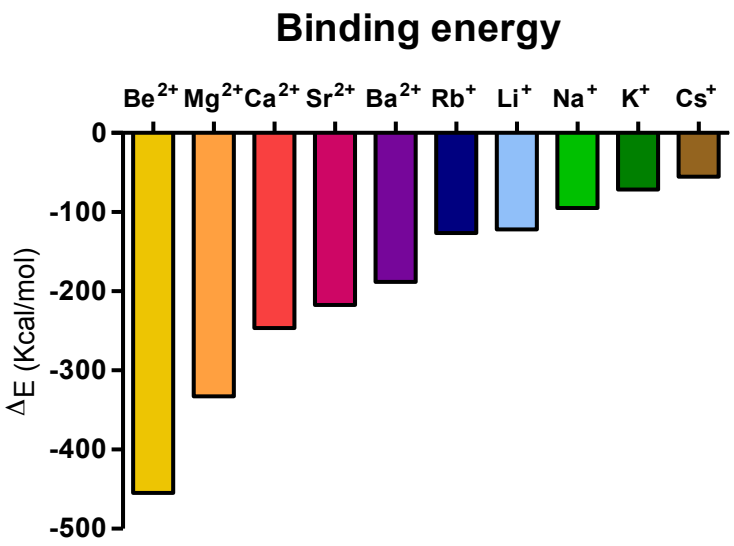

Fig. 4.6 ligand-cations binding stabilisation energy

The correlation between the stabilisation energy (ΔE) and the ionic radius of the cations is plotted in Fig. 4.7. The linear trend confirms that the best interaction of the macrocycle is obtained with the metals of the second group over the first group and is stronger with smaller metals. Only rubidium is an exception.

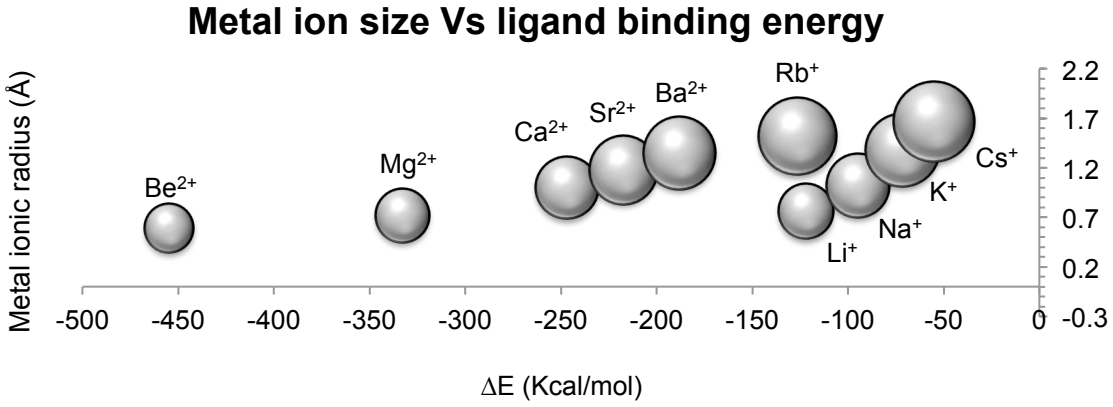

Fig. 4.7 cations size vs binding stabilisation energy

The ligand-metal interaction generally has an ionic character. In the case of Be^{2+} the distance between the carbonyl donor in the ligand and the cation is shorter and therefore the bond has more of a covalent character.

The macrocycle is able to adapt its structure considerably to accommodate the metals and bind them through the four amidic carbonyl groups with a tetrahedral geometry. The example shown in Fig. 4.8 represents the adaptation in structure of the ligand to bind Be^{2+}, which is the most drastic change among the metals studied.

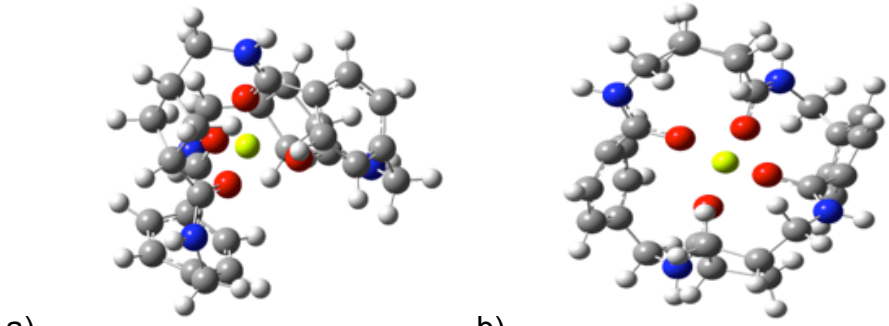

a) b)

Fig. 4.8 two different points of view of the complex macrocycle-Be^{2+}

As it is possible to see in Fig. 4.8a, the macrocycle folds almost in half to better bind Be^{2+}, while in Fig 4.8b it is possible to notice the tetrahedral geometry at the metal centre.

In contrast with the previous example, the one with Ba^{2+}, shown below in Fig. 4.9, is one of the less stable of the complexes tested.

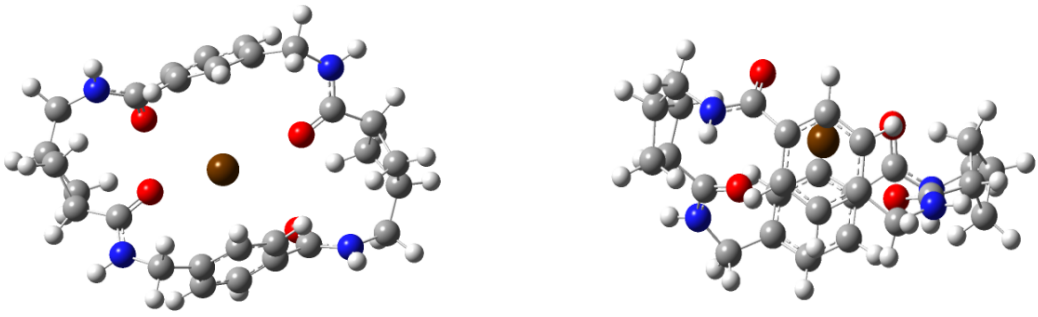

a) b)

Fig. 4.9 two different points of view of the complex macrocycle-Ba^{2+}

Compared to the previous case, here the macrocycle changes its conformation only marginally, without folding, but it stays almost planar and the distance between the amidic carbonyl groups and the metal is bigger.

The dipole moments of the ligand-metal complexes were also calculated theoretically and are reported in Table 4.3.

M^{n+} + Ligand	Dipole moment (debye)
Rb^{+}	5.08
Cs^{+}	5.06
Ba^{2+}	3.77
Sr^{2+}	3.32
Na^{+}	3.24
Ca^{2+}	2.37
Li^{+}	2.10
Mg^{2+}	1.01
Be^{2+}	0.41

Table 4.3 dipole moments of the ligand-metal complexes

The more the macrocycle has to adapt its structure in order to bind the metal, the lower the dipole moment of the complex is. This means that the most stable complexes with beryllium and magnesium should be soluble in organic solvents, given that the dipole moment of water is 1.85 debye.[9] The uncomplexed ligand resulted to be 1.526 debye and therefor is also partially soluble in organic solvents.
Considering the solubility problems encountered during the synthesis with the open tetrapeptide, this is a very interesting result.

All the characteristics found in the synthesised tetrapeptide-like macrocycle **25** are very attractive and promising for future applications. The ability of adapting its structure to accommodate earth alkali metals and its solubility properties make it a suitable candidate for phase transfer and ion carrier in organic solvents.
Phase transfer catalysts are of great interest in organic chemistry because they bring two reactants with different solubility together into a common solvent, making reactions possible that would not occur otherwise.

The concept of phase transfer catalysis (PTC) was born in the 1960s to perform reactions between water soluble reagents and organic molecules and it is still widely employed.[10]

Usually PTC molecules as quaternary onium salts bring anions into organic phase, but they are also exploited to transfer cations (e.g. crown ethers), free radicals and in certain cases full molecules.[11]

Crown ether derivatives are typical examples of cyclic molecule used as ion and molecule carrier. For instance Vladimirova and colleagues studied dibenzo-18-crown-6 (Fig. 4.10) as transfer of aminoglycoside antibiotics.

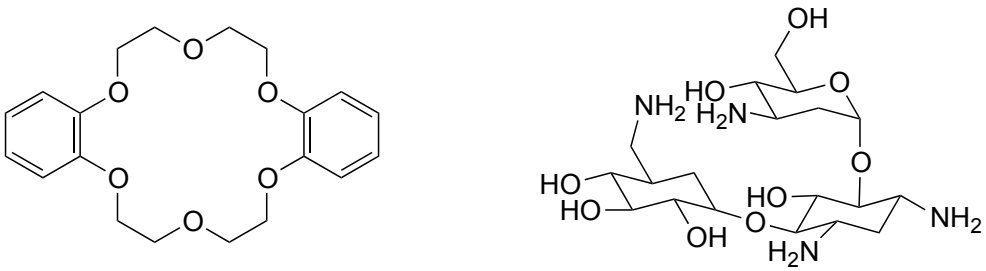

Fig. 4.10 dibenzo-18-crown-6 chemical structure and kanamycin A, an example of aminoglycoside antibiotic

Considering that macrocyclic ligands can form stable complexes with organic compounds, they decided to use it to detect aminoglycosidic drugs in aqueous solutions through voltammetry at the interface of two immiscible electrolyte solutions.[12]

An example more similar to compound **25**, used as efficient phase transfer catalyst, is the peptoid oligomer of N-substituted glycine reported in Fig. 4.11. As well as compound **25**, the coordination to the metal is gained through the carbonyls.

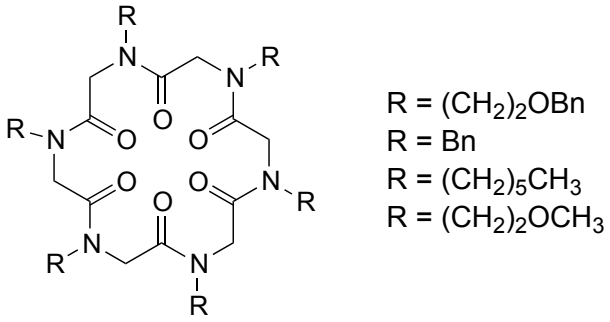

Fig. 4.11 peptoid oligomer of N-substituted glycine

Complex **25** could also be exploited for water purification, given its ability to bind cations.

Considering its characteristic adaptability to the metal ion hosts, it would also be interesting to study its binding with small molecules, which could be useful for drug delivery. Macromolecules as dendrimers and cyclodestrine are often studied in the literature to improve bioavailability and water solubility of small molecules for this purpose.[13]

4.3-Conclusions

The open tetrapeptide was synthesised in good yield after a series of protection/coupling/deprotection reactions, starting from ACCA propyl ester and Boc protected AMBA and using a [2+2] approach.

The synthesis of the tetrapeptide-like macrocycle **25** was challenging and was attempted through pseudo-high dilution and also through a metal template method, for which sodium was chosen as templating agent. Only the second technique allowed the accomplishment of the desired cyclic peptide product.

We can conclude that the cyclisation reaction of the linear tetrapeptide-like **24** worked only in the presence of a template metal as driving force. Intramolecular interactions such as H-bondings between amides, and π-π stacking between the benzene rings and π-cation interaction probably helped the macrocycle closure, as well as the *cis*-locked conformation of ACCA. The difficulties encountered, though, lead to believe that perhaps the flexibility of the open tetrapeptide, shown by theoretical calculation, exceeded the pre-organisational features.

Promising results were obtained with computational studies. Despite the constrained benzene ring and the cyclobutane moieties, the cyclic tetrapeptide seems to have enough flexibility to modify its structure to accommodate various metals. Highest complex stabilities were measured for smaller cations, especially with alkaline earth metals as Mg^{2+}, Ca^{2+} and Be^{2+}. This selectivity could be exploited for instance in water purification, considering the organic solvent solubility of compound **25** suggested from the dipole moment calculation.

The macrocycle could be also studied as ion carrier for medicinal applications such as drug delivery and as phase transfer catalysis.

Last but not least, an important application for peptide-like macrocycles is found in peptidomimetics, where the employment of non-proteinogenic amino acids and the cyclic framework render the peptide bonds not recognisable and therefore not hydrolysable by peptidases, increasing the bioavailability of these molecules.

Not only the apo cyclic peptide can be exploited in this field, but also when coordinated to metal ions.

4.4-Experimental

General Methods:

All chemicals were purchased from Sigma Aldrich. Dry solvents were obtained from a Puresol Grubbs Speciality Chemicals and Stream. When necessary, all reactions were performed under an atmosphere of nitrogen using oven-dried glassware. Oxygen-free nitrogen was obtained from BOC gases and used without further drying.

Proton and carbon nuclear magnetic resonance spectra (^{1}H and ^{13}C-NMR respectively) were recorded on 400 MHz (operating frequencies: ^{1}H, 399.75 MHz; ^{13}C, 101.00) and 500 MHz (operating frequencies: ^{1}H, 499.72 MHz; ^{13}C, 125.65) FT spectrometers. ^{1}H-NMR spectra are herein reported, while ^{13}C-NMR spectra are in appendix 1. Tetramethylsilane (δ = 0.00 ppm) was used as an internal reference in the deuterated chloroform ($CDCl_3$) for ^{1}H NMR spectra. The middle $CDCl_3$ solvent peak was referenced to 77.16 ppm for ^{13}C NMR spectra. The residual solvent peak in deuterated methanol (CD_3OD) was referenced respectively to 3.31 ppm and 49.00 ppm for ^{1}H NMR and ^{13}C NMR spectra, respectively and in deuterated DMSO to 2.50 ppm and 39.52 ppm for ^{1}H NMR and ^{13}C NMR. The coupling constants (*J*) are in Hz and the chemical shifts (δ) are given in parts per million. High resolution mass spectra were obtained on a Waters/Micromass instrument and melting points were measured on a Stuart^{TM} melting point apparatus SMP 10. Evaporation *in vacuo* refers to the removal of solvent on a Büchi rotary evaporator with an integrated vacuum pump. Thin-layer chromatography (TLC) was carried out on aluminium backed 60 F254 silica gel.

Preparation of 4-(((*tert*-butoxycarbonyl)amino)methyl) benzoic acid (Boc-AMBA, 18).

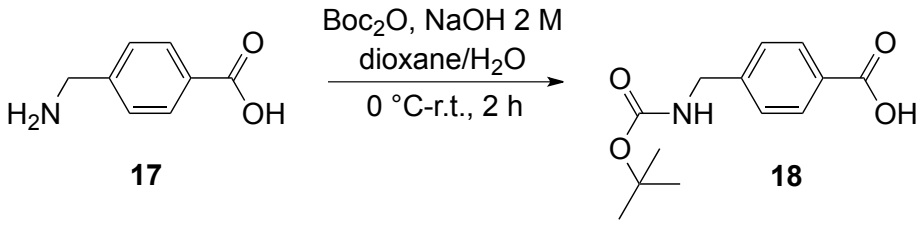

17 **18**

p-(aminomethyl)benzoic acid **17** (AMBA, 0.8 g, 5.25 mmol) was dissolved in dioxane/water 2:1 (35 mL) and NaOH 2 M (10 mL) was added. The solution was cooled to 0 °C and Boc_2O (2.5 g, 11.64 mmol) was added. After 2 hours dioxane was removed *in vacuo* and the aqueous phase was acidified with 1 M HCl to pH 3. The aqueous layer was was extracted with CH_2Cl_2 (20 mL x 3). The organic layers were combined, dried over $NaSO_4$ and concentrated *in vacuo* yielding Boc-AMBA **18** (0.39 g, 70 % yield) as a white powder. (Rf = 0.66, EtOAc/CH_3OH, 1:3). Mp: 162-164 °C. δH (400 MHz; $CDCl_3$) 8.06 (2H, d, *J* = 8.2 Hz, COPhH), 7.39 (2H, d, *J* = 8.2 Hz, CH_2PhH), 4.94 (1H, s, N*H*CH_2Ph), 4.39 (2H, d, *J* = 5.0, C*H*$_2$Ph), 1.47 (9H, s, $C(CH_3)_3$). (500 MHz; DMSO) 7.88 (2H, d, *J* = 8.2 Hz, COPhH), 7.44 (1H, t, *J* = 6.5 Hz, N*H*CH_2Ph), 7.35 (2H, d, *J* = 8.2 Hz, CH_2PhH), 4.18 (2H, d, *J* = 6.5, C*H*$_2$Ph), 1.33 (9H, s, $C(CH_3)_3$). δC (125.65 MHz, DMSO) 167.5, 156.0, 145.6, 129.3 (2 C), 126.8 (2 C), 77.9, 43.7, 28.2 (3 C). m/z (ES-) 250.1083 (M-H^+ $C_{13}H_{16}NO_4$ requires 250.1079).

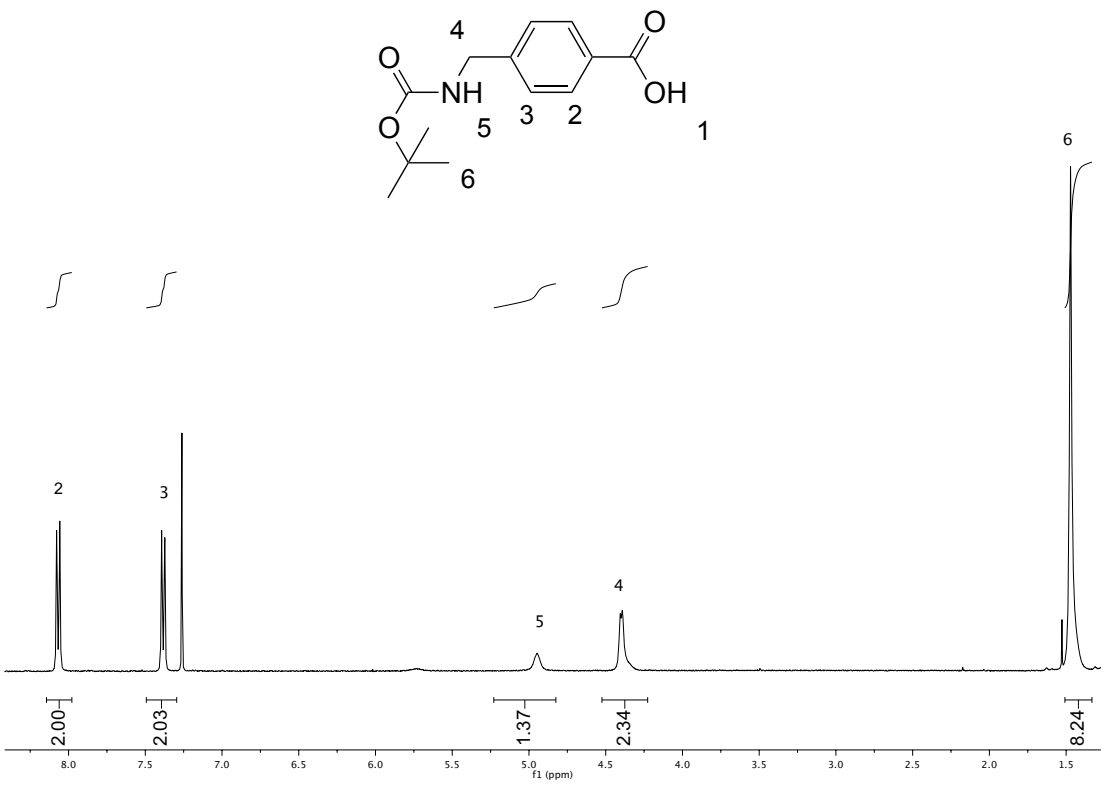

Preparation of propyl 3-((4-(((*tert*-butoxycarbonyl)amino)methyl) benzamido)methyl) cyclobutane carboxylate (Boc-AMBA-ACCA-Pr, 19)

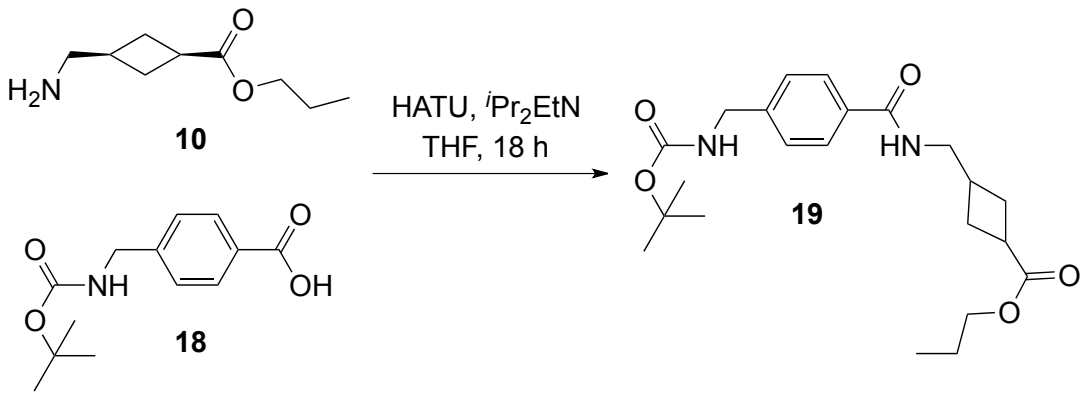

Boc-AMBA **18** (0.75 g, 3.6 mmol) and ACCA-Pr **10** (0.8 g, 3.2 mmol) were dissolved in dry THF (50 mL) and 1 eq of HATU (1.18 g, 3.2 mmol) was added. The solution was cooled to 0 °C and *N,N*-diisopropylethyl amine (3 eq) was added. The reaction was stirred at room temperature overnight. The solvent

was evaporated *in vacuo* and the crude oil dissolved in CH_2Cl_2 (20 mL) and washed with $NaHCO_3$ (20 mL), acetic acid 10 % (20 mL x 2) and brine (20 mL). The combined organic layers were dried over $MgSO_4$ and concentrated *in vacuo*. The crude yellow oil was purified by silica gel column chromatography (cyclohexane/EtOAc, from 90:10 to 50:50) yielding the pure product **19** as a white powder (1.10 g, 85 %). (Rf = 0.78, EtOAc/CH_3OH 3:2) Mp: 94-95 °C. δH (400 MHz, $CDCl_3$) 7.72 (2H, d, *J* = 8.2 Hz, COPhH), 7.35 (2H, d, *J* = 8.2 Hz, CH_2PhH), 6.34 (1H, br s, BocNH), 4.91 (1H, br s, PhCONH), 4.36 (2H, d, *J* = 5.7 Hz, CH_2Ph), 4.02 (2H, t, *J* = 6.7 Hz, $CH_2CH_2CH_3$), 3.47 (2H, t, *J* = 6.1 Hz, NCH_2CH), 3.03 (1H, q, *J* = 8.8 Hz, COCH), 2.60 (1H, m, NCH_2CH), 2.36 (2H, m, $COCH(CHH)_2$), 2.08 (2H, m, $COCH(CHH)_2$), 1.64 (2H, m, CH_2CH_3), 1.46 (9H, s, $C(CH_3)_3$), 0.92 (3H, t, *J* = 7.4 Hz, CH_2CH_3). δC (125 MHz, CD_3OD): 175.5, 167.7, 156.1, 142.7, 133.7, 127.9 (4 C), 79.9, 66.3, 44.8, 44.4, 34.1, 30.8, 28.8 (2 C), 28.5 (3 C), 22.1, 10.5. m/z (ES+) 427.2227 ($M\text{-}Na^+$ $C_{22}H_{32}N_2O_5$ requires 427.2209).

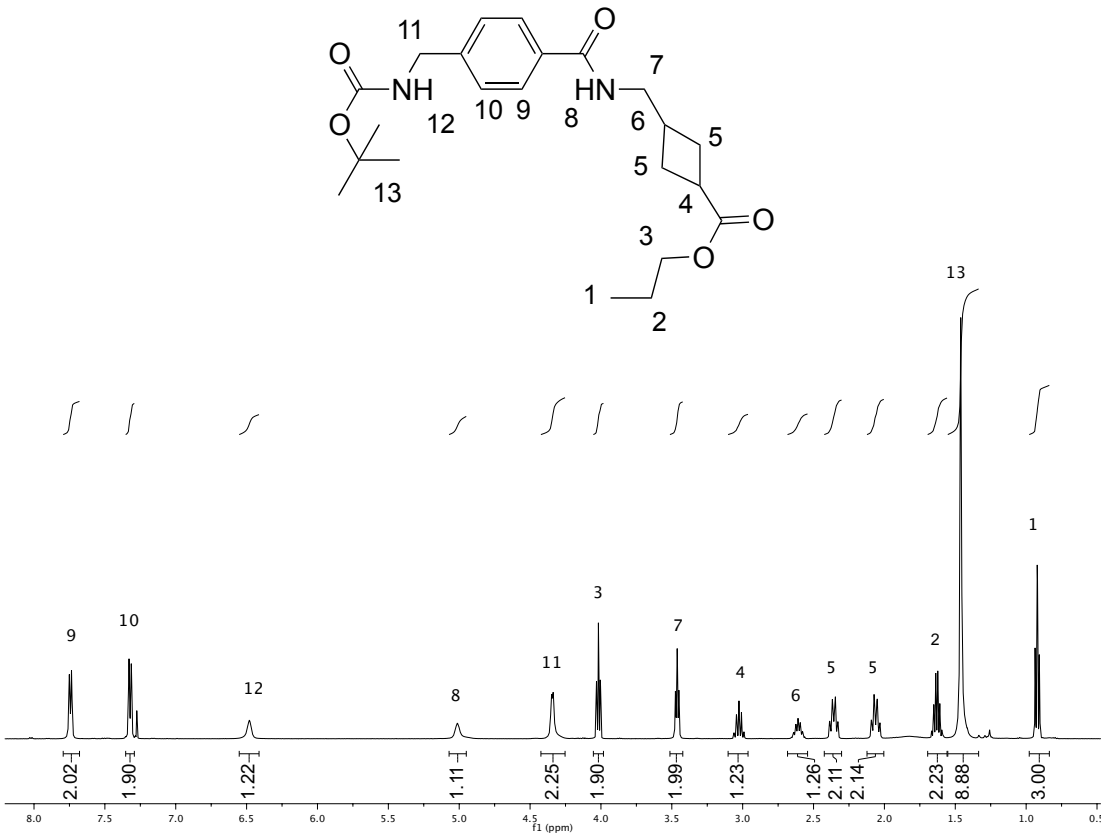

Preparation of 3-((4-(((*tert*-butoxycarbonyl)amino)methyl)benzamido) methyl) cyclobutane carboxylic acid (Boc-AMBA-ACCA-OH, 20)

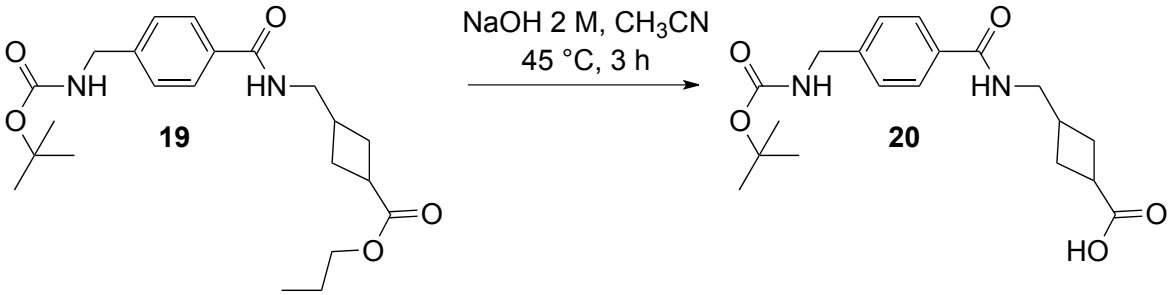

Boc-AMBA-ACCA-Pr **19** (0.55 g, 1.36 mmol) was dissolved in CH_3CN (30 mL) and NaOH 2 M was added (10 mL). The solution was left to stir at 45 °C for 4 hours. CH_3CN was removed *in vacuo*. The aqueous phase was acidified with 1 M HCl to pH 3. Brine (15 mL) was added and the aqueous phase was washed with CH_2Cl_2 (20 mL x 5). The organic layers were combined, dried over Na_2SO_4 and concentrated *in vacuo* yielding **20** (0.34 g, 90 %) as a white powder. (Rf = 0.66, EtOAc) Mp: 134-135 °C. δH (400 MHz, $CDCl_3$) 7.75 (2H, d, *J* = 7.3 Hz, COPhH), 7.32 (2H, d, *J* = 7.9 Hz, CH_2PhH), 6.54 (1H, br s, BocNH), 5.03 (1H, br s, PhCONH), 4.33 (2H, d, *J* = 5.5 Hz, CH_2Ph), 3.47 (2H, t, *J* = 6.5 Hz, NCH_2CH), 3.07 (1H, m, COCH), 2.65 (1H, m, NCH_2CH), 2.38 (2H, m, $COCH(CHH)_2$), 2.12 (2H, m, $COCH(CHH)_2$), 1.46 (9H, s, $C(CH_3)_3$). δC (101 MHz, $CDCl_3$): 174.4, 168.0, 156.2, 142.7, 133.6, 127.5 (4 C), 80.0, 44.7, 44.4, 38.7, 30.6, 28.5 (2 C), 28.4 (3 C). m/z (ES+) 385.1751 ($M\text{-}Na^+$ $C_{19}H_{26}N_2O_5$ requires 385.1751).

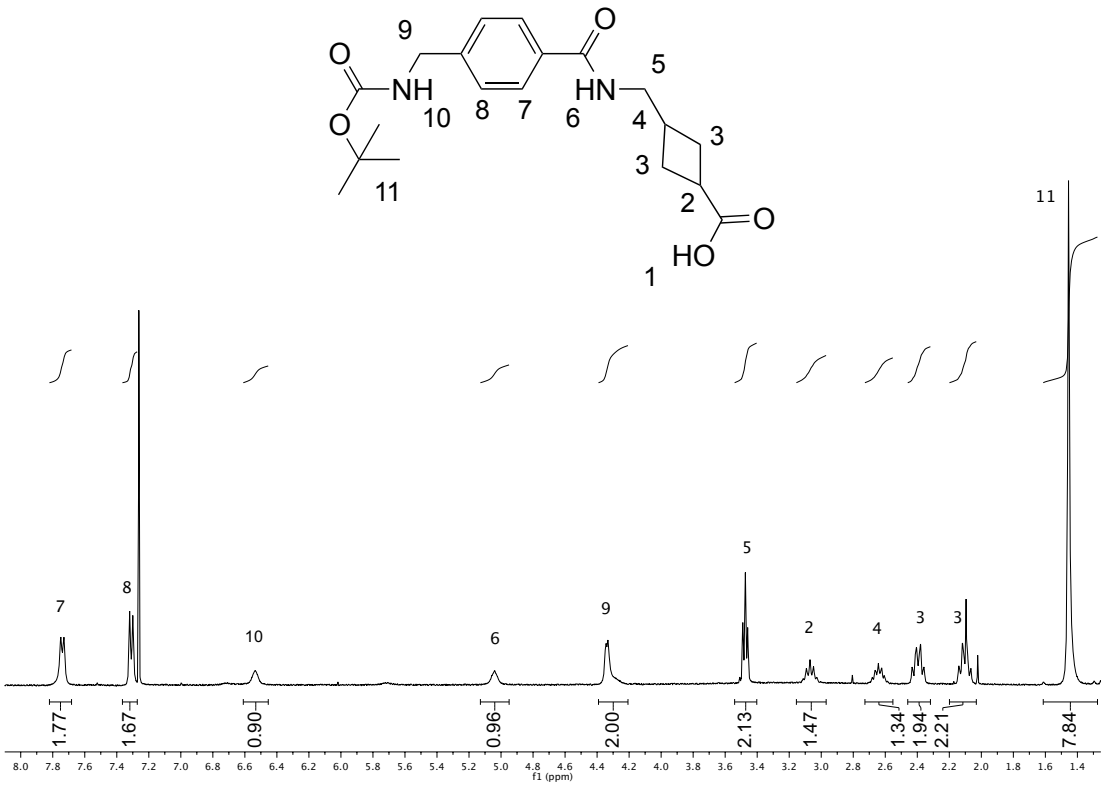

Preparation of propyl 3-((4-(aminomethyl)benzamido)methyl)cyclobutane carboxylate ($ClNH_3$-AMBA-ACCA-Pr, 21)

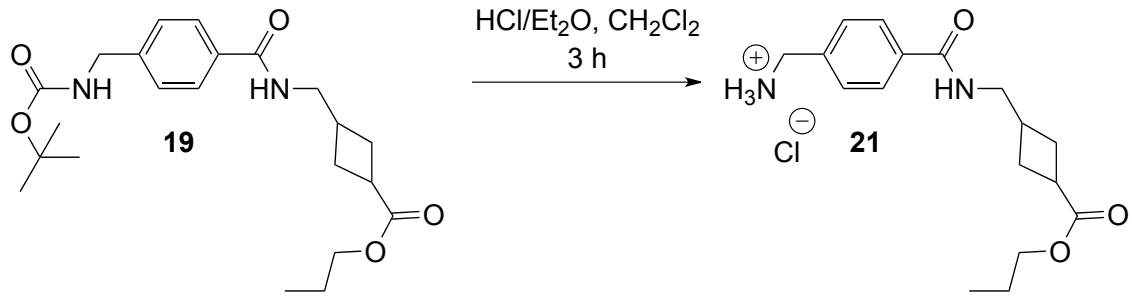

Boc-AMBA-ACCA-Pr **19** (0.57 g, 1.41 mmol) was dissolved in CH_2Cl_2 (15 mL) and HCl/Et_2O 2 M (1 mL) was added. The solution was left to stir at room temperature for 2 hours. The product precipitated out as a white powder, which was filtered and washed with Et_2O yielding **21** in 93 % (0.43 g) (Rf = 0.63, EtOAc). Mp: 235-236 °C. δH (400 MHz, CD_3OD) 7.88 (d, *J* = 8.2 Hz, 2H, COPhH), 7.56 (2H, d, *J* = 8.2 Hz, CH_2PhH), 4.18 (2H, s, CH_2Ph), 4.00 (2H, t, *J* = 6.6 Hz, $CH_2CH_2CH_3$), 3.39 (2H, d, *J* = 6.5 Hz, NCH_2CH), 3.04 (1H, m,

COCH), 2.60 (1H, m, NCH_2CH), 2.30 (2H, m, $COCH(CHH)_2$), 2.03 (2H, m, $COCH(CHH)_2$), 1.61 (2H, m, CH_2CH_3), 0.92 (3H, t, J = 7.4 Hz, CH_2CH_3). δC (101 MHz, CD_3OD): 176.8, 169.6, 137.7, 136.5, 130.0 (2 C), 129.1 (2 C), 67.1, 45.6, 43.8, 35.2, 35.0, 32.3, 29.9 (2 C), 23.0, 10.6. m/z (ES+) 327.1692 ($M\text{-}Na^+$ $C_{17}H_{24}N_2O_3$ requires 327.1685).

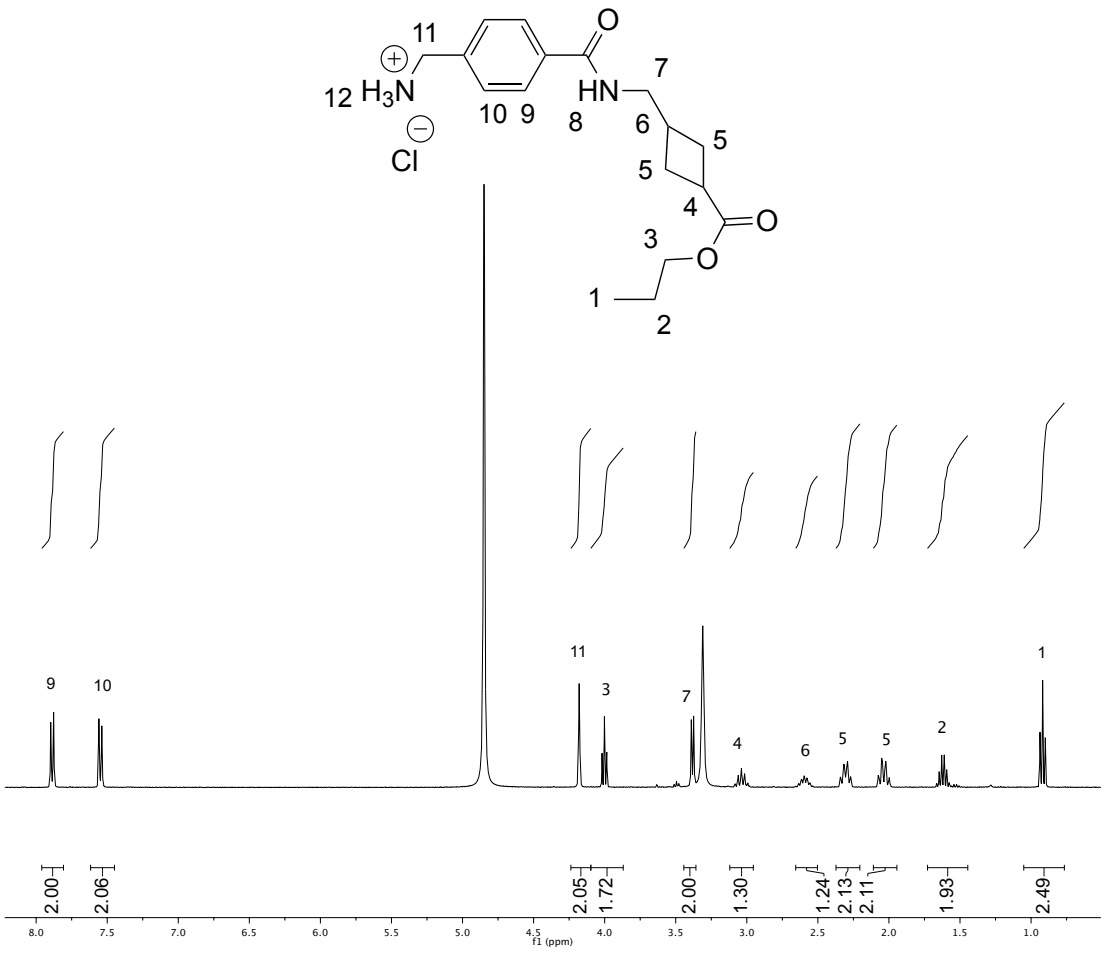

Preparation of propyl 3-((4-((3-((4-(((*tert*-butoxycarbonyl)amino)methyl) benzamido)methyl)cyclobutanecarboxamido)methyl)benzamido)methyl) cyclobutane carboxylic acid (Boc-AMBA-ACCA-AMBA-ACCA-Pr, 22)

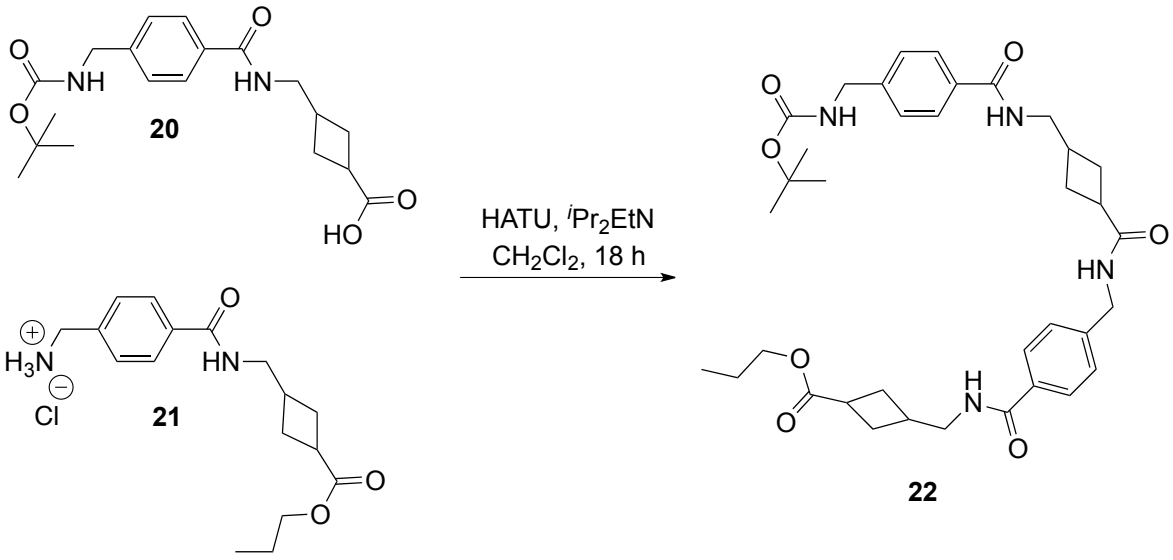

Boc-AMBA-ACCA-OH **20** (0.37 g, 1.02 mmol), $ClNH_3$-AMBA-ACCA-Pr **21** (0.45 g, 1.35 mmol) and HATU (0.58 g, 1.53 mmol) were dissolved in anhydrous CH_2Cl_2 (25 mL). The solution was cooled to 0 °C and $^{i}Pr_2EtN$ (0.5 mL, 3.0 mmol) was added. The mixture was allowed to warm to room temperature and stirred overnight. The product **22** precipitated out as a white powder, which was filtered and washed with CH_2Cl_2 giving 67 % yield (0.47 g) as a white powder. (Rf = 0.87, EtOAc/CH_3OH 3:2). Mp: burnt around 200 °C. δH (400 MHz, DMSO) 8.43 (2 H, m, NH), 8.25 (1H, t, *J* = 5.7 Hz, NH), 7.76 (4H, m, COPhH), 7.43 (1H, t, *J* = 6.0 Hz, NH), 7.28 (4H, m, CH_2PhH), 4.27 (2H, d, *J* = 5.9 Hz, CH_2Ph), 4.15 (2H, d, *J* = 6.1 Hz, CH_2Ph), 3.94 (2H, t, *J* = 6.6 Hz, $CH_2CH_2CH_3$), 3.23 (4H, m, NCH_2CH), 3.03-2.84 (2H, m, COCH), 2.50-2.40 (2H, m, NCH_2CH), 2.20-2.06 (4H, m, $COCH(CHH)_2$), 1.95-1.86 (4H, m, $COCH(CHH)_2$), 1.59-1.50 (2H, m, CH_2CH_3), 1.39 (9H, s, $C(CH_3)_3$), 0.85 (3H, t, *J* = 7.4 Hz, CH_2CH_3). δC (101 MHz, CD_3OD): 174.5, 173.9, 166.2 (2 C), 155.9 143.3, 142.9, 133.2, 127.2 (2 C), 126.8 (2 C), 126.6, 77.9, 65.2, 44.3, 44.0, 43.1, 41.7, 38.3, 34.7, 33.3, 30.7, 30.5, 28.6 (2 C), 28.3 (3 C), 21.4, 10.3. m/z (ES+) 671.3406 ($M\text{-}Na^+$ $C_{36}H_{48}N_4O_7$ requires 671.3421).

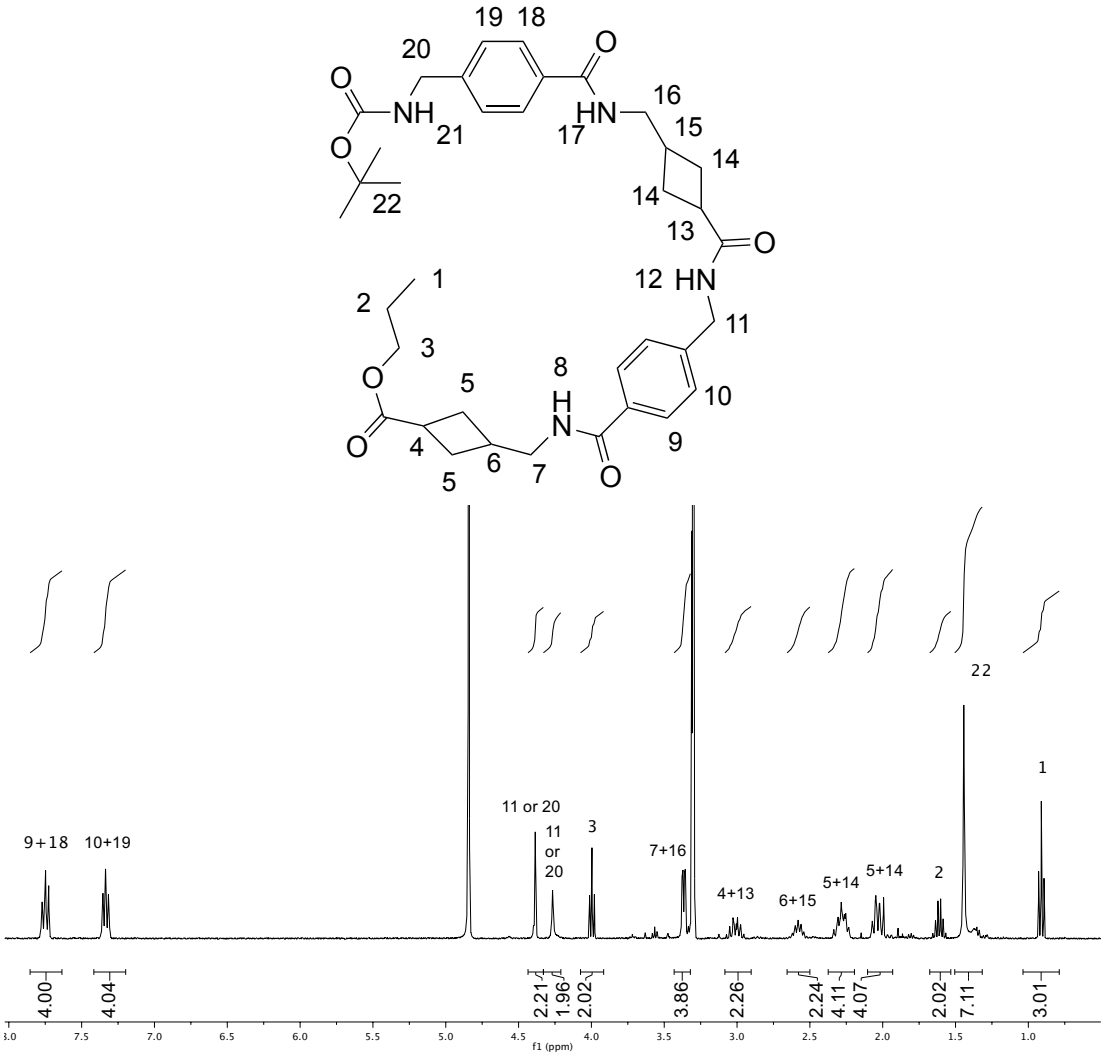
9+18
10+19
11 or 20
11
or
20
3
7+16
4+13
6+15
5+14
5+14
2
22
1
4.00
4.04
2.21
1.96
2.02
3.86
2.26
2.24
4.11
4.07
2.02
7.11
3.01
f1 (ppm)

Preparation of 3-((4-((3-((4-(((*tert*-butoxycarbonyl)amino)methyl) benzamido)methyl)cyclobutanecarboxamido)methyl)benzamido)methyl) cyclobutane carboxylic acid (Boc-AMBA-ACCA-AMBA-ACCA-OH, 23)

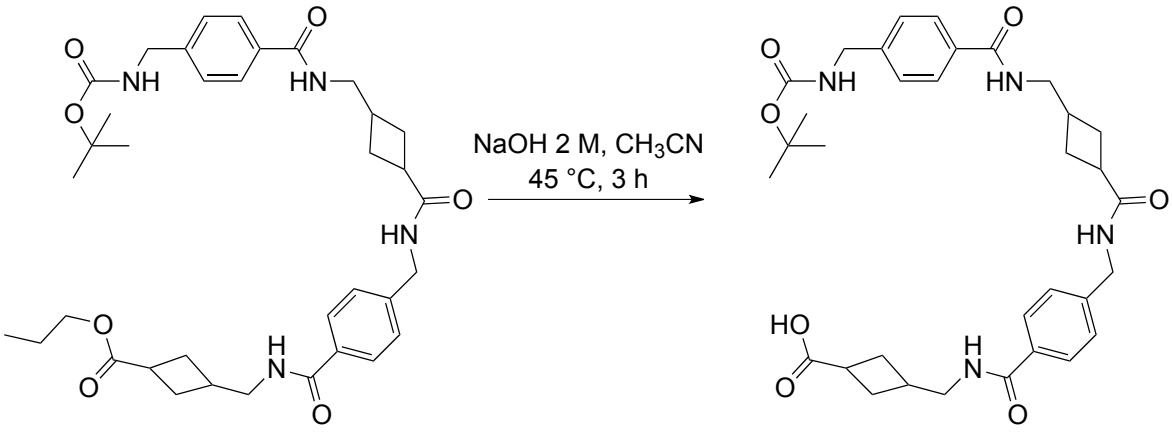

22 **23**

Boc-AMBA-ACCA-AMBA-ACCA-Pr **22** (0.124 g, 0.19 mmol) was dissolved in CH_3CN (15 mL) and NaOH 2 M was added (5 mL). The mixture was left to stir at 45 °C for 4 hours. CH_3CN was removed *in vacuo,* the aqueous phase was acidified with HCl 1 M to pH 3 and washed with CH_2Cl_2 (15 mL x 5). The organic layers were combined, dried over Na_2SO_4 and concentrated *in vacuo* to give compound **23** as a white powder. (Rf = 0.55, EtOAc). Mp: 135-136 °C. δH (400 MHz, DMSO) 8.45 (2 H, t, *J* = 8.6 Hz, 2 NH), 8.29 (1H, t, *J* = 5.9 Hz, NH), 7.78 (4H, m, COPhH), 7.74 (1H, t, *J* = 6.0 Hz, NH), 7.29, (4H, m, CH_2PhH), 4.29 (2H, d, *J* = 6.0 Hz, CH_2Ph), 4.17 (2H, d, *J* = 5.9 Hz, CH_2Ph), 3.26-3.22 (4 H, m, NCH_2CH), 2.96-2.85 (2 H, m, COCH), 2.48-2.41 (2H, m, NCH_2CH), 2.20-2.08 (4H, m, $COCH(CHH)_2$), 1.94-1.85 (4H, m, $COCH(CHH)_2$), 1.39 (9H, s, $C(CH_3)_3$). δC (101 MHz, DMSO): 176.1, 173.9, 166.2 (2 C), 155.8, 143.3, 142.9, 133.1, 127.2 (4 C), 126.8 (4 C), 126.6, 77.9, 44.3, 44.1, 43.1, 41.7, 34.7, 33.4, 30.5 (2), 28.6 (2 C), 28.5 (2 C), 28.3 (3 C). m/z (ES+) 629.2924 ($M\text{-}Na^+$ $C_{33}H_{42}N_4O_7$ requires 629.2951).

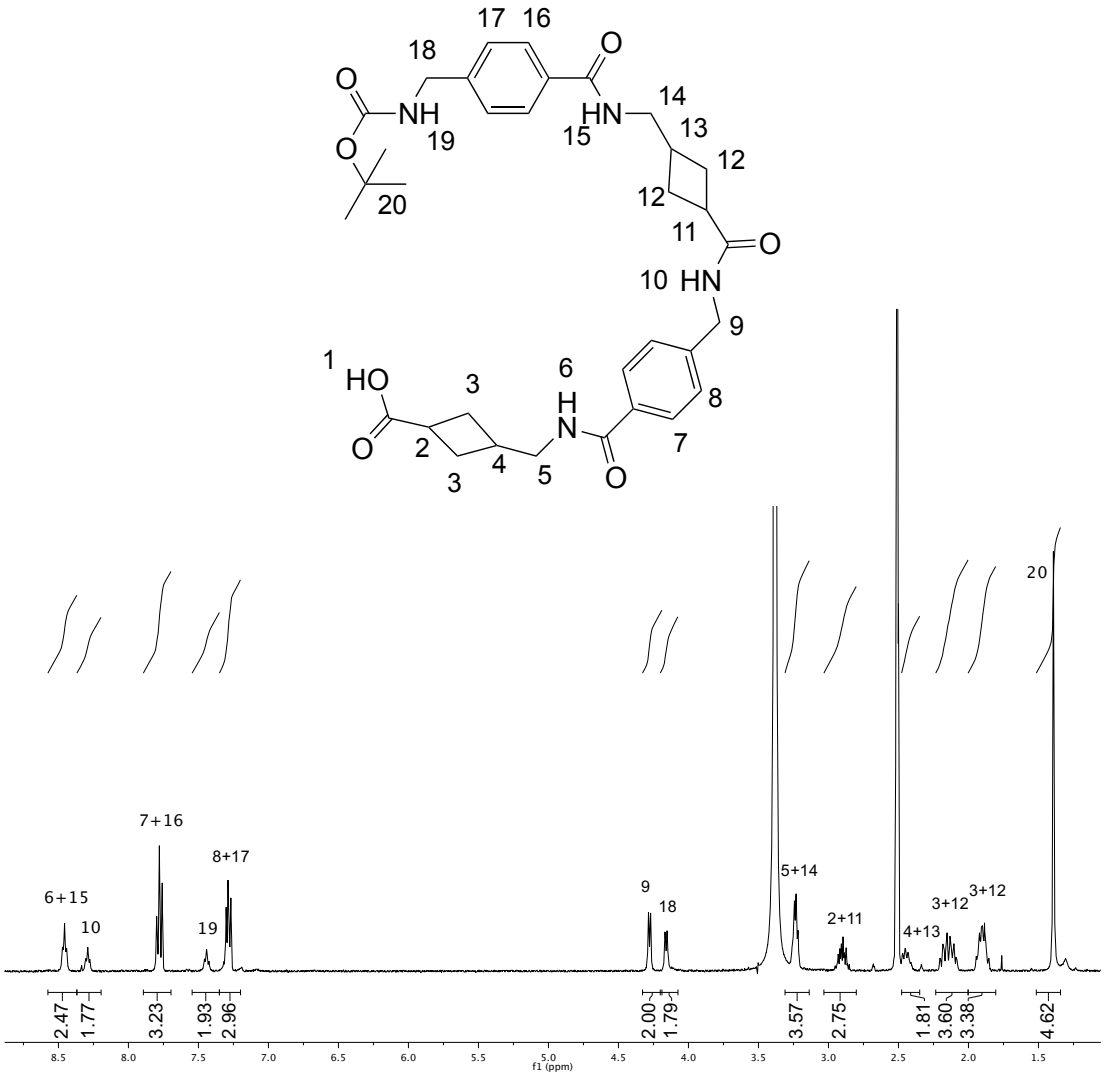
17 16
18
O
O
NH
19
O
20
HN
15
14
13
12
12
11
O
10 HN
9
1
HO
3
6
H
N
8
O
2
4
5
7
3
O
6+15
10
7+16
19
8+17
9
18
5+14
2+11
4+13
3+12
3+12
20
2.47
1.77
3.23
1.93
2.96
2.00
1.79
3.57
2.75
1.81
3.60
3.38
4.62
8.5
8.0
7.5
7.0
6.5
6.0
5.5
5.0
4.5
4.0
3.5
3.0
2.5
2.0
1.5
f1 (ppm)

Preparation of 3-((4-((3-((4-(aminomethyl)benzamido)methyl)cyclobutane carboxamido)methyl)benzamido)methyl)cyclobutane carboxylic acid ($ClNH_3$-AMBA-ACCA-AMBA-ACCA-OH, 24)

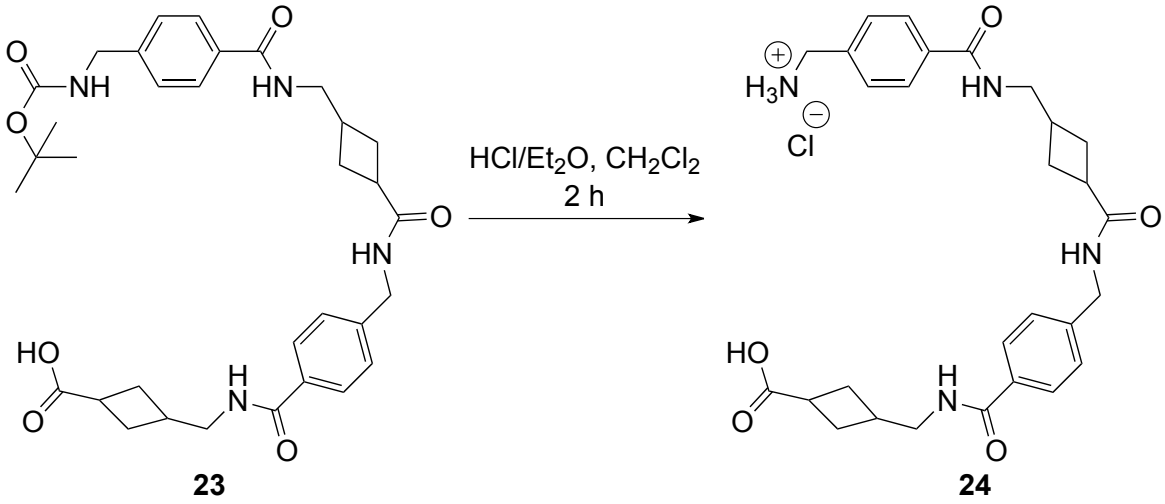

23 **24**

Boc-AMBA-ACCA-AMBA-ACCA-OH **23** (0.12 g, 0.19 mmol) was suspended in CH_2Cl_2 (10 mL) and HCl/Et_2O 2 M (1 mL) was added. As soon as the acid was added the compound in suspension agglomerated together. The mixture was left to stir for 2 hours affording **24** in 68 % over 2 steps (70 mg) as a white powder. (Rf = 0.22, EtOAc). Mp: burnt around 300 °C. δH (399.75 MHz; DMSO) 8.59 (3 H, br s, NH_3^+), 8.48 (2 H, br s, 2 NH), 8.32 (2 H, br s, 2 NH), 7.89 (2H, d, *J* = 8.2 Hz, COPhH), 7.78 (2H, d, *J* = 8.2 Hz, COPhH), 7.58 (2H, d, *J* = 8.2 Hz, CH_2PhH), 7.28 (2H, d, *J* = 8.2 Hz, CH_2PhH), 4.27 (2H, d, *J* = 5.9 Hz, CH_2Ph), 4.06 (2H, s, *J* = 6.2 Hz, CH_2Ph), 3.27-3.20 (4H, m, 2 NCH_2CH), 2.95-2.84 (1H, m, COCH), 2.84-2.81 (1H, m, COCH), 2.49-2.37 (2H, m, NCH_2CH), 2.37-2.06 (4H, m, $COCH(CHH)_2$), 2.00-1.83 (4H, m, $COCH(CHH)_2$). δC (101.00 MHz; DMSO) 174.88, 173.93, 166.20, 165.82, 142.90, 136.91, 134.45, 132.99, 128.71, 127.35, 127.20, 126.79, 51.32, 44.16, 41.73, 41.68, 34.61, 33.05, 30.60, 30.43, 28.58 (2C), 28.52 (2C). m/z (ES+) 507.2927 ($M\text{-}H^+$ $C_{28}H_{34}N_4O_5$ requires 507.2607).

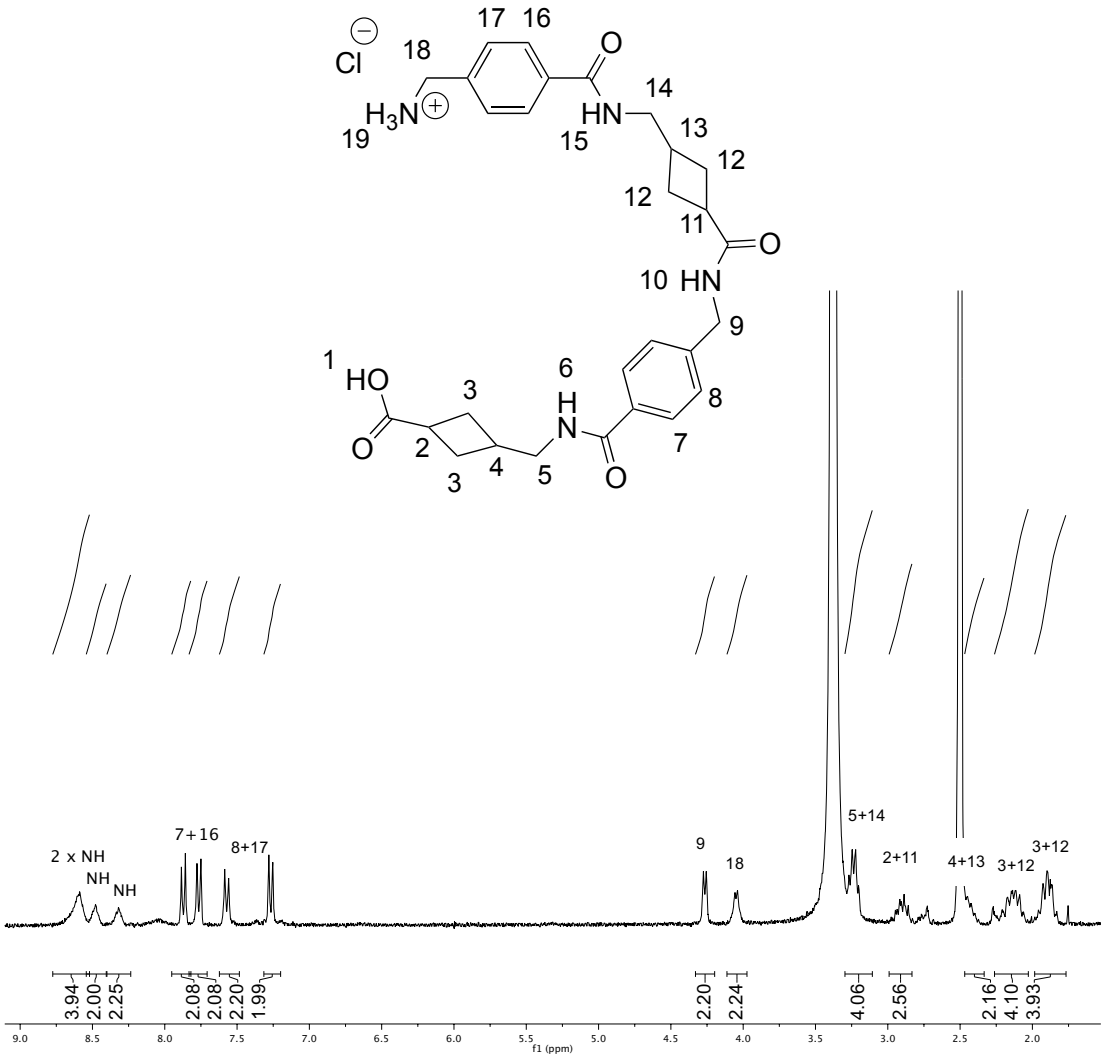
Cl
17 16
18
O
14
H_3N
HN
19
15
13
12
12
11
O
10 HN
9
1
HO
6
3
H
N
8
O
2
7
4
5
3
O
2 x NH
NH
NH
7+16
8+17
9
18
5+14
2+11
4+13
3+12
3+12
3.94
2.00
2.25
2.08
2.08
2.20
1.99
2.20
2.24
4.06
2.56
2.16
4.10
3.93
9.0
8.5
8.0
7.5
7.0
6.5
6.0
5.5
5.0
4.5
4.0
3.5
3.0
2.5
2.0
f1 (ppm)

Preparation of cyclo-[(4-(((benzamido)methyl)cyclobutane carboxamido) methyl)] (cyclo(AMBA-ACCA-AMBA-ACCA-), 25)

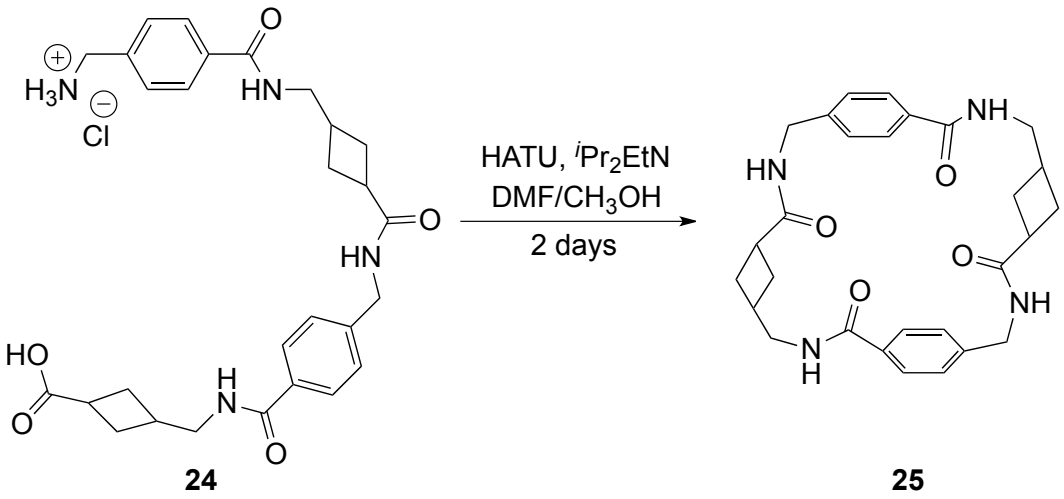

24 **25**

$ClNH_3$-AMBA-ACCA-AMBA-ACCA-OH **24** (54 mg, 0.1 mmol) was dissolved in hot CH_3OH (10 mL) and placed in a syringe. HATU (0.114 g, 0.3 mmol) was dissolved in DMF (10 mL) and placed in a second syringe. $^{i}Pr_2EtN$ (0.99 mL, 0.6 mmol) was dissolved in DMF (10 mL) and 0.3 eq of HATU were added (4 mg, 0.01 mmol). Through a syringe pump, **24** and HATU solutions were added to the $^{i}Pr_2EtN$ solution at a flow rate of 0.01 mL/min. After 2 days CH_3OH was concentrated *in vacuo* and the yellow solid was washed with chloroform and acetonitrile giving 37 mg of starting material.

Preparation of cyclo-[(4-(((benzamido)methyl)cyclobutane carboxamido) methyl)] (cyclo(AMBA-ACCA-AMBA-ACCA-)·Na^+, 26)

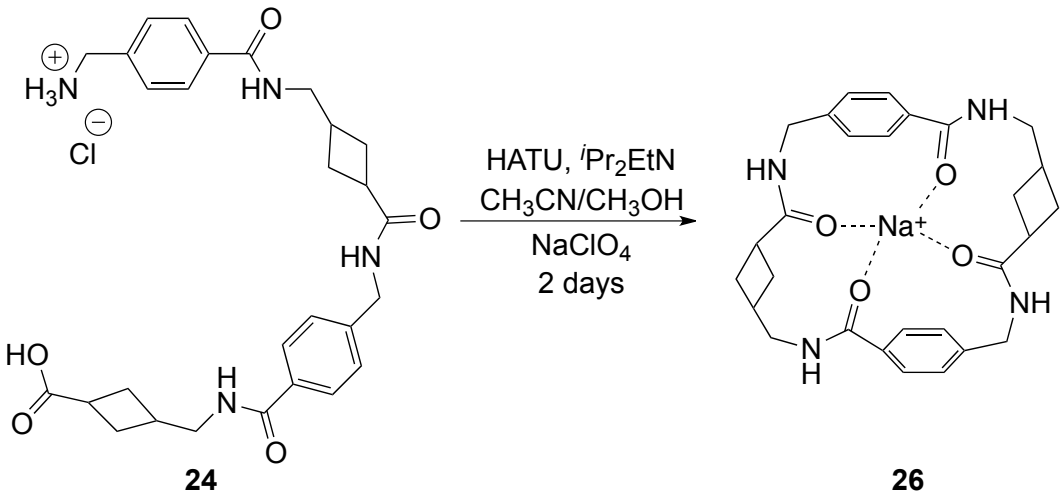

24 **26**

$NaClO_4$ (19 mg, 0.15 mmol) was dissolved in CH_3OH (10 mL) and $ClNH_3$-AMBA-ACCA-AMBA-ACCA-OH **24** (0.054 g, 0.1 mmol) was added and mixed until dissolved. The solution was placed in a syringe. HATU (0.114 g, 0.3 mmol) was dissolved in CH_3CN (3 mL), CH_3OH (7 mL) was added and the solution was placed in a second syringe. $^iPr_2EtN$ (0.99 mL, 0.6 mmol) was dissolved in CH_3OH (10 mL) and some HATU was added (4 mg, 0.01 mmol). Through a syringe pump, **24** and HATU solutions were added to the $^iPr_2EtN$ solution at a flow rate of 0.01 mL/min. The solution was then left to stir for two nights and the solvent was left evaporate overnight. The yellow solid was washed with acetonitrile, giving 42 mg of impure product. Silica gel column chromatography (EtOAc/CH_3OH from 100:0 to 80:20) was not able to separate **25** from the unreacted HATU. δH (399.75 MHz; DMSO) 8.44 (2H, br s, NH), 8.25 (2H, br s, NH) 7.78 (4H, m, COPhH), 7.29 (4H, m, CH_2PhH), 4.27 (2H, d, *J* = 6.1 Hz, CH_2Ph), 3.23 (4H, m, 2 NCH_2CH), 2.95-2.84 (1H, m, COCH), 2.84-2.81 (1H, m, COCH), 2.49-2.37 (2H, m, NCH_2CH), 2.37-2.06 (4H, m, $COCH(CHH)_2$), 2.00-1.83 (4H, m, $COCH(CHH)_2$).

4.5-Bibliography

(1) Malesevic, M.; Strijowski, U.; Baechle, D.; Sewald, N.: An improved method for the solution cyclization of peptides under pseudo-high dilution conditions. *Journal of Biotechnology* **2004**, *112*, 73-77.

(2) White, C. J.; Yudin, A. K.: Contemporary strategies for peptide macrocyclization. *Nature Chemistry* **2011**, *3*, 509-524.

(3) White, C. J.; Yudin, A. K.: A Versatile Scaffold for Site-Specific Modification of Cyclic Tetrapeptides. *Organic Letters* **2012**, *14*, 2898-2901.

(4) Beck, W.: Metal Complexes of Biologically Important Ligands, CLXXVI. Formation of Peptides within the Coordination Sphere of Metal Ions and of Classical and Organometallic Complexes and Some Aspects of Prebiotic Chemistry. *Zeitschrift Fur Anorganische Und Allgemeine Chemie* **2011**, *637*, 1647-1672.

(5) Robey, F. A.: Selective and facile cyclization of *N*-chloroacetylated peptides from the C4 domain of HIV Gp120 in LiCl/DMF solvent systems. *The Journal of Peptide Research* **2000**, *56*, 115-120.

(6) Liu, M.; Tang, Y. C.; Fan, K. Q.; Jiang, X.; Lai, L. H.; Ye, Y. H.: Cyclization of several linear penta- and heptapeptides with different metal ions studied by CD spectroscopy. *The Journal of Peptide Research* **2005**, *65*, 55-64.

(7) Dean, J. A.: *Lange's handbook of chemistry (chapter 4)*; 15th ed.; McGrawHill, Inc.: New york, 1999.

(8) Irikura, K. K.; Frurip, D. J.: *Computational Thermochemistry: Prediction and Estimation of Molecular Thermodynamics*; American Chemical Society: Washington, DC, 1998.

(9) Brey, W. S.: *Physical chemistry and its biological applications (p. 26)*; Academic Press, Inc.: New York, 1978.

(10) Pozzi, G.; Quici, S.; Fish, R. H.: Fluorous phase transfer catalysts: From onium salts to crown ethers. *Journal of Fluorine Chemistry* **2008**, *129*, 920-929.

(11) Stark, C. M.; Liotta, C.; Halpern, M.: *Phase transfer catalysis: Fundamentals, Applications and Industrial Perspective* 1st edition ed.; Chapman and Hall: New York, 1994.

(12) Vladimirova, E. V.; Dunaeva, A. A.; Petrukhin, O. M.; Shipulo, E. V.: Study of the transfer of aminoglycoside antibiotics through the phase boundary water/*o*-nitrophenyl octyl ether by voltammetry at the interface of two immiscible electrolyte solutions. *Journal of Analytical Chemistry* **2013**, *68*, 253-260.

(13) Hettiarachchi, G.; Nguyen, D.; Wu, J.; Lucas, D.; Ma, D.; Isaacs, L.; Briken, V.: Toxicology and Drug Delivery by Cucurbit n uril Type Molecular Containers. *Plos One* **2010**, *5*.

Conclusions

Conclusions

In conclusion, in this thesis work, the novel non-proteinogenic δ-amino acid *cis*-3-(aminomethyl)cyclobutane carboxylic acid (ACCA) has been investigated and proven to be a useful and versatile molecule as building block for organic synthesis, especially for the preparation of peptidomimetics.

Here, an efficient synthetic methodology leading to a small library of dipeptides containing the conformational constrained amino acid ACCA has been developed, using the effective coupling reagent HATU. The dipeptides synthesised (Phe-ACCA, Gly-ACCA, ACCA-ACCA), have been tested as glutamate neurotransmitter analogues, as well as ACCA and its ester ACCA-Pr.

The tests, effectuated on rat C6 glioma cells, demonstrated that the five compounds are not cytotoxic. Only ACCA-Pr, Phe-ACCA and Gly-ACCA showed activity as glutamate uptake enhancers, especially for the sodium independent transport (X_c^- exchanger). These results show interesting possibilities for the three molecules as drugs, for the treatment of brain diseases originated from limited activity of the transporter proteins.

Among the three active compounds, Gly-ACCA was the most effective, but it was not selective between the two transport mechanisms (EAATs and X_c^-).

Considering the increased glutamate uptake provoked by Phe-ACCA and Gly-ACCA only after pre-incubating them with the cells, it is very likely that their mechanism of action consists in up-regulating the transporter protein expression. In order to prove this, protein expression by immunodetection experiments (Western Blot) will be carried out.

ACCA has also been successfully exploited as building block for the synthesis of a macrocycle tetrapeptide-like molecule. Theoretical calculation on the ability of this macrocycle to form complexes with ion metals are promising and suggest possible applications as ion carrier, water purification and phase transfer agent.

It will be very interesting to test the effectiveness of the complex formation with different cations in solution and compare the results with the theoretical data.

Appendix 1

APPENDIX 1: **^{13}C-NMR spectra**

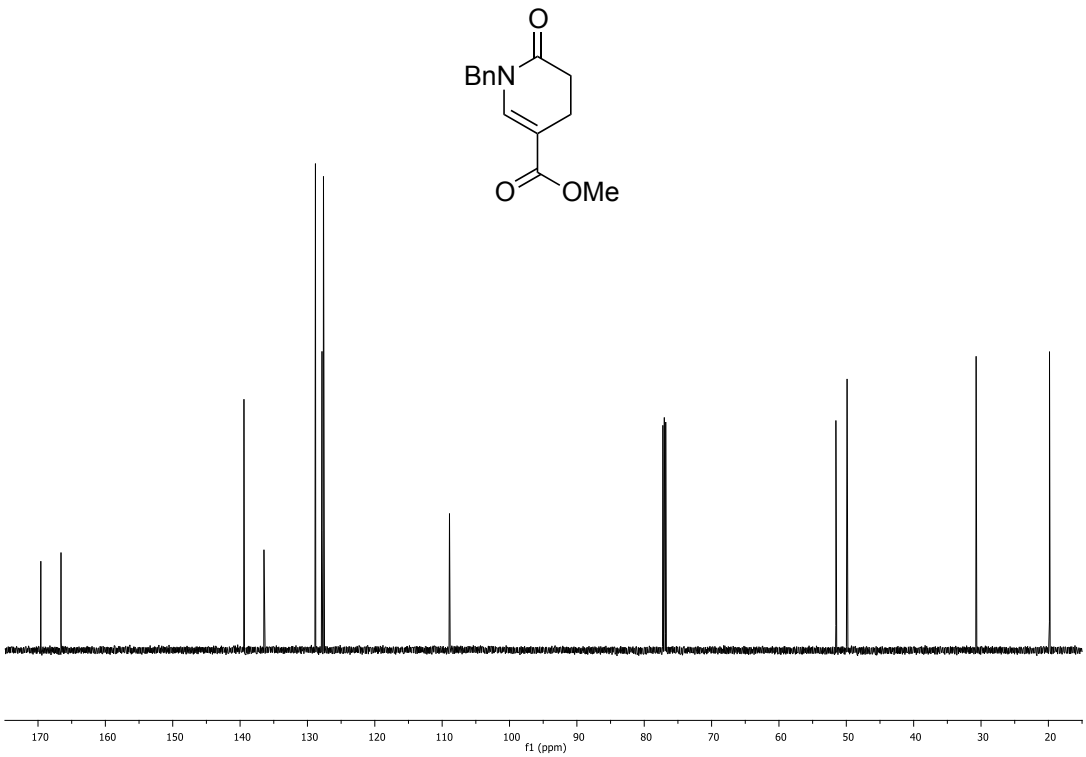

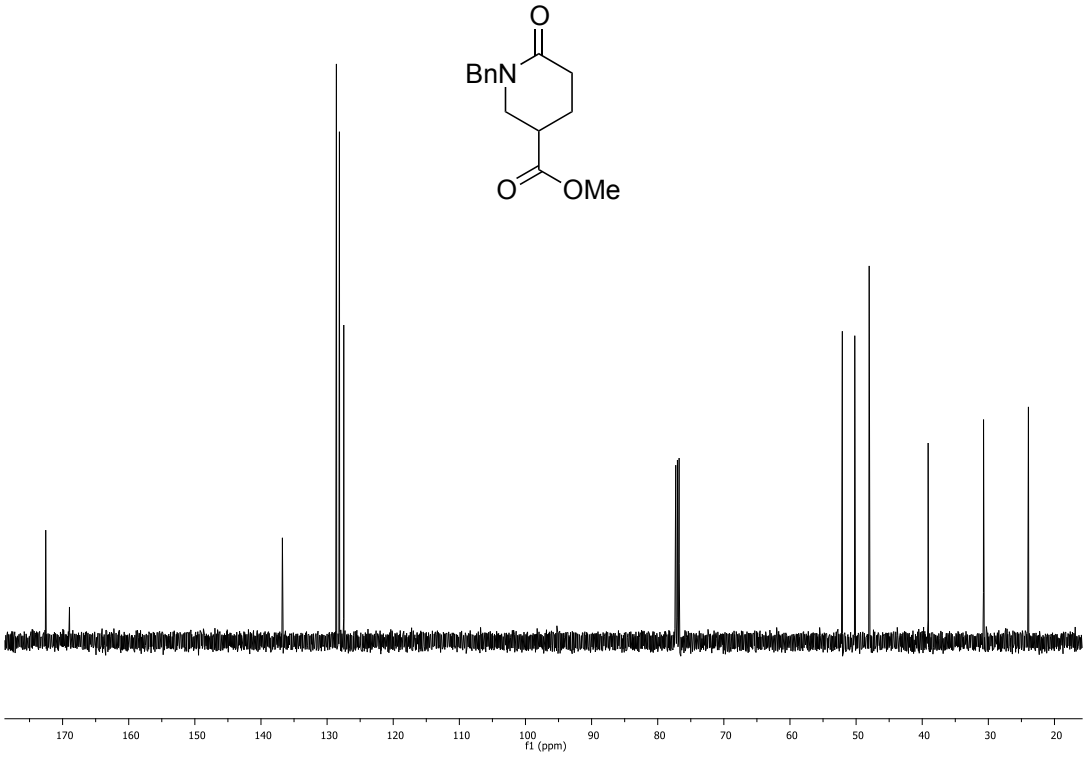

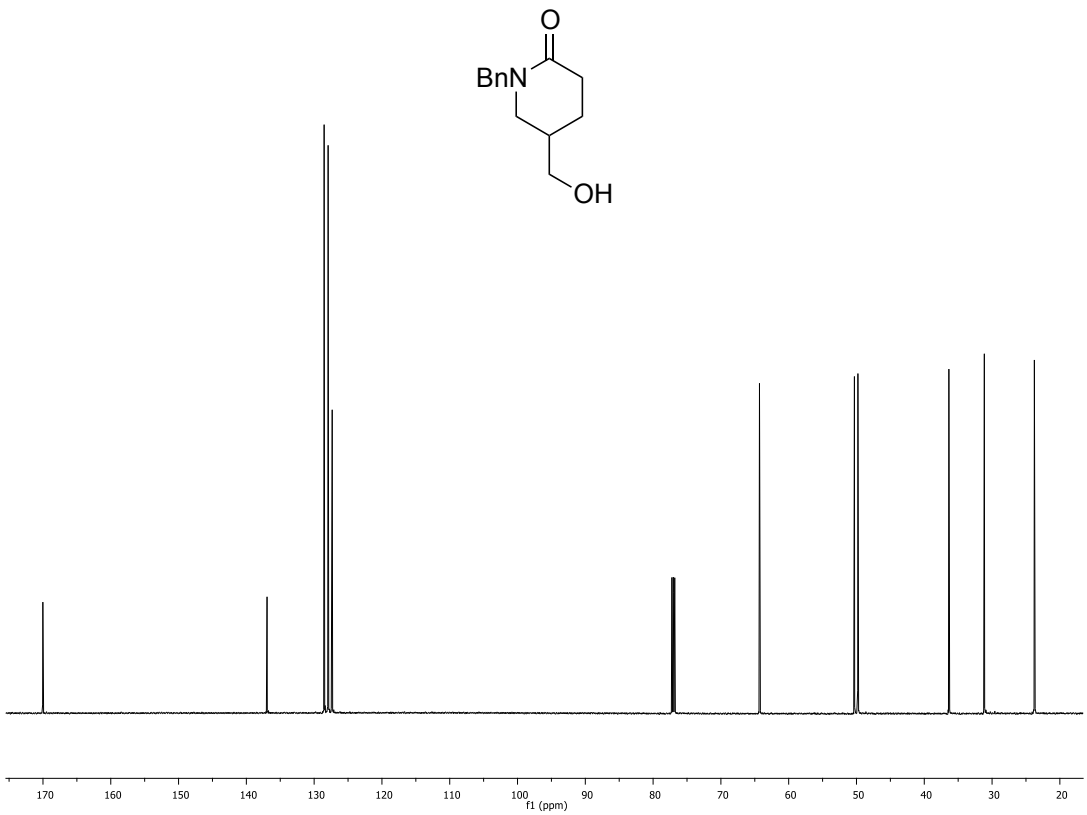
O
BnN
OH
170
160
150
140
130
120
110
100
90
80
70
60
50
40
30
20
f1 (ppm)

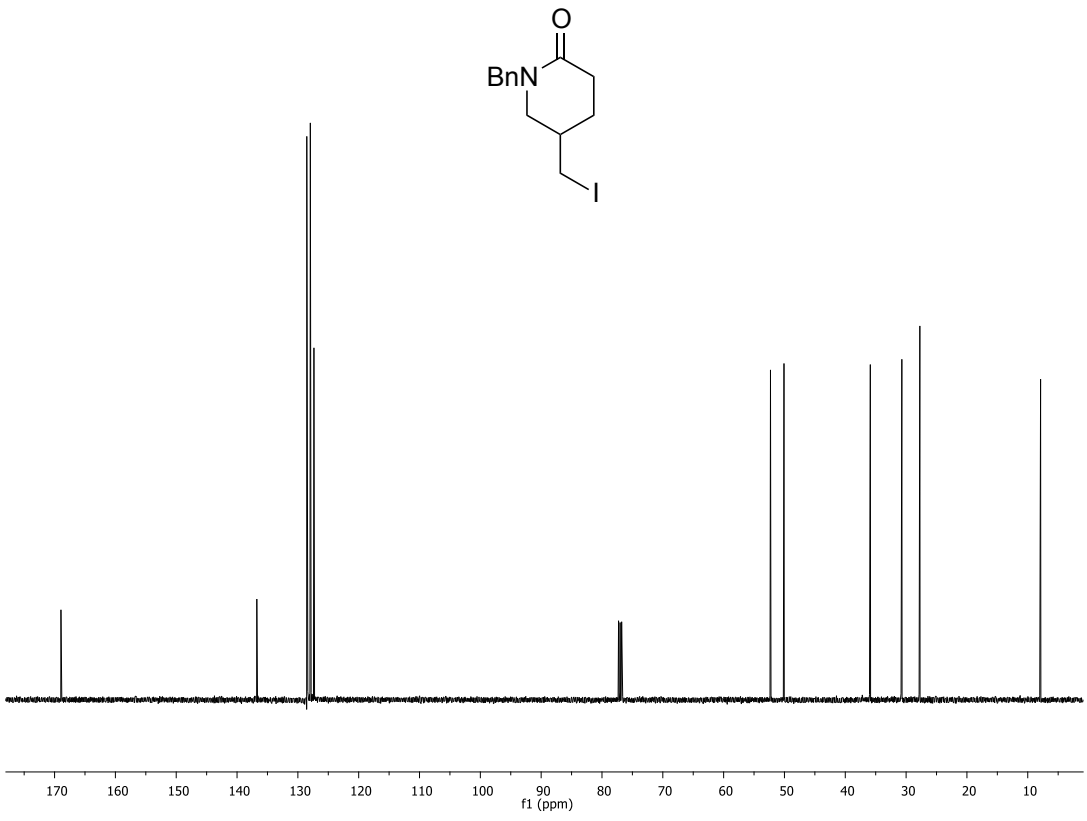
O
BnN
I
170
160
150
140
130
120
110
100
90
80
70
60
50
40
30
20
10
f1 (ppm)

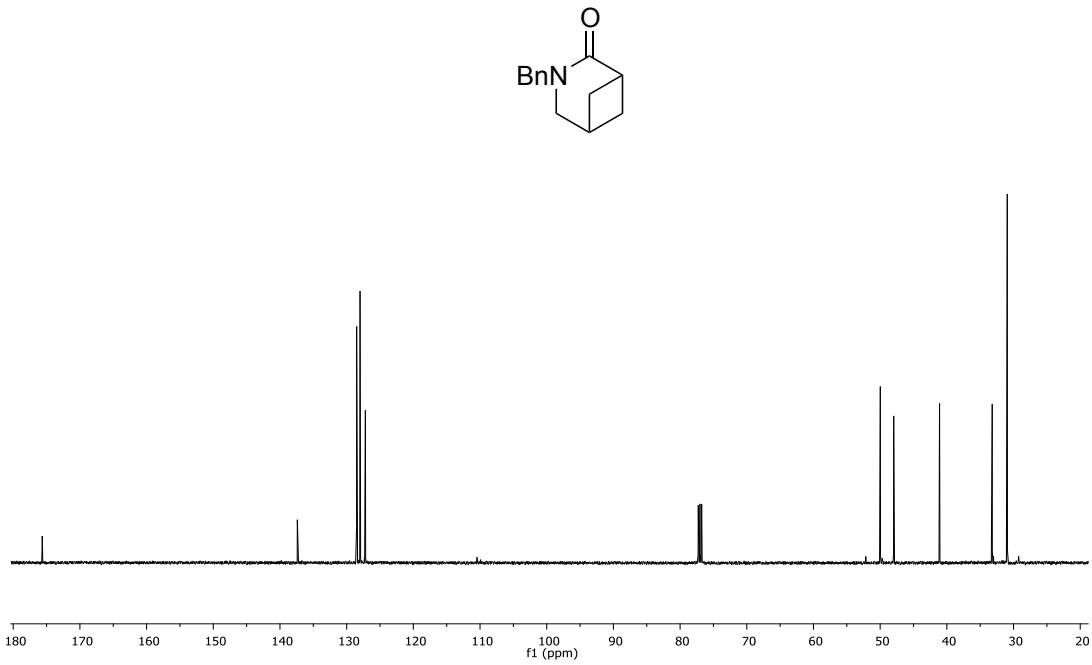
O
BnN
180
170
160
150
140
130
120
110
100
90
80
70
60
50
40
30
20
f1 (ppm)

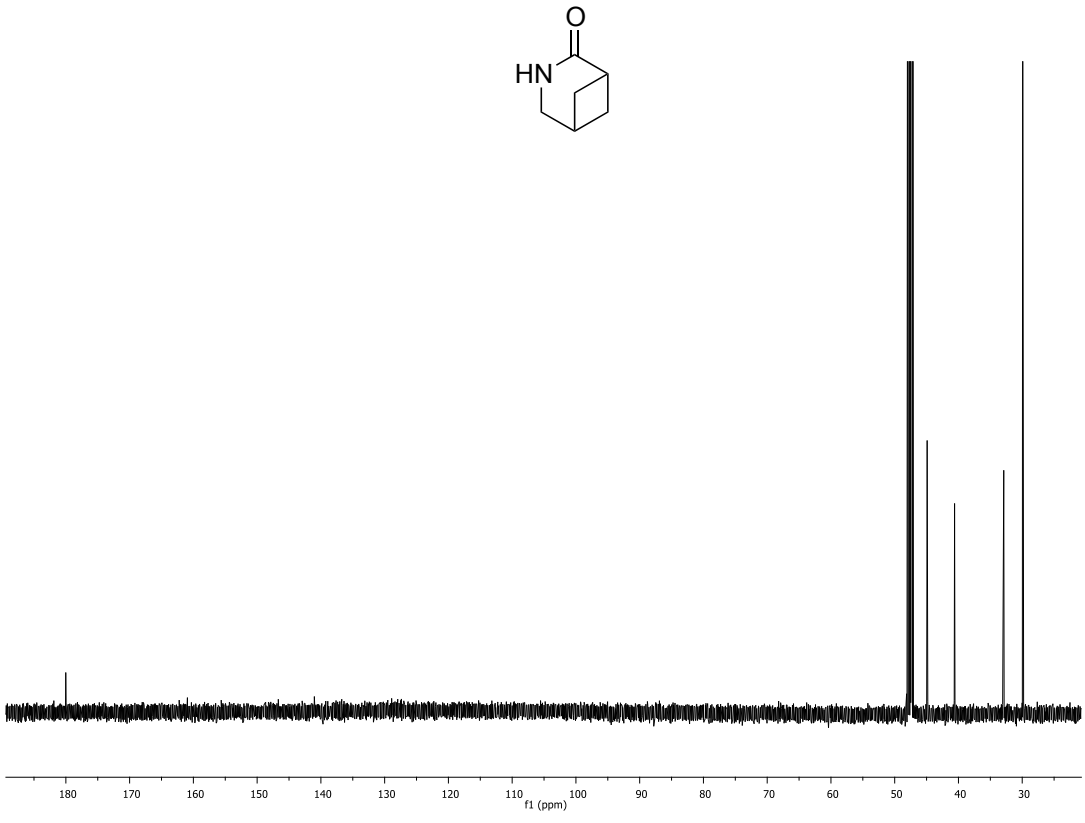
O
HN
180
170
160
150
140
130
120
110
100
90
80
70
60
50
40
30
f1 (ppm)

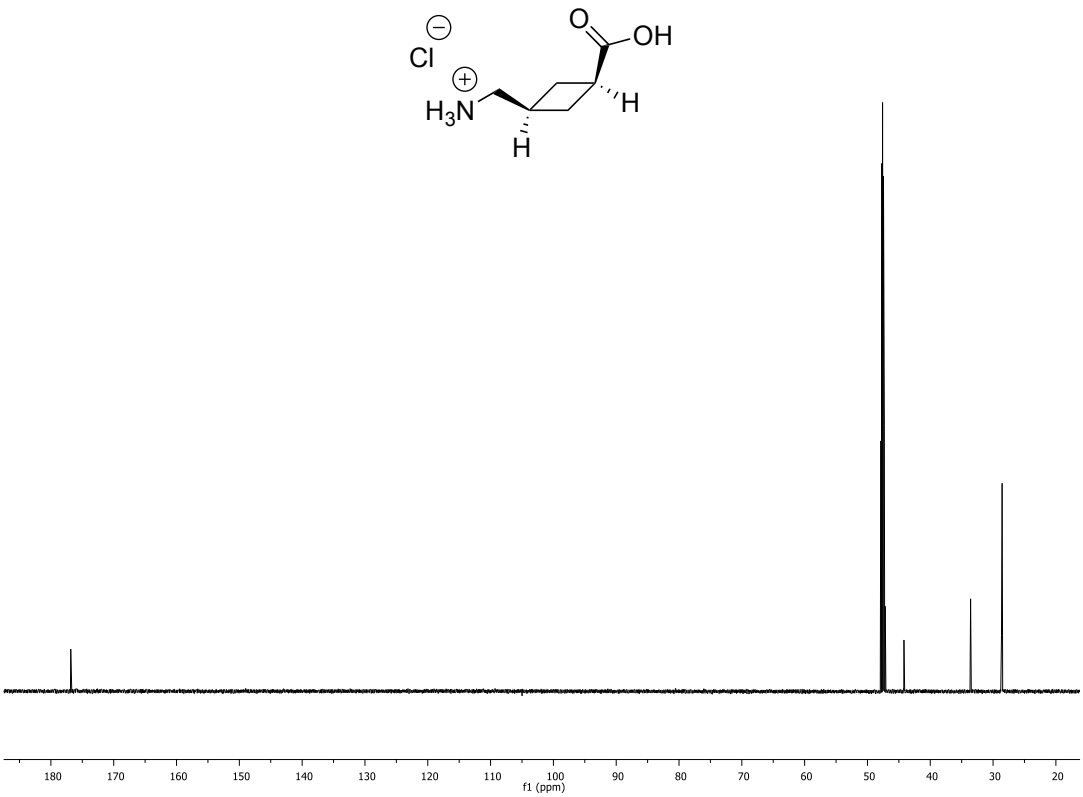
Cl
O
OH
H3N
H
H
180
170
160
150
140
130
120
110
100
90
80
70
60
50
40
30
20
f1 (ppm)

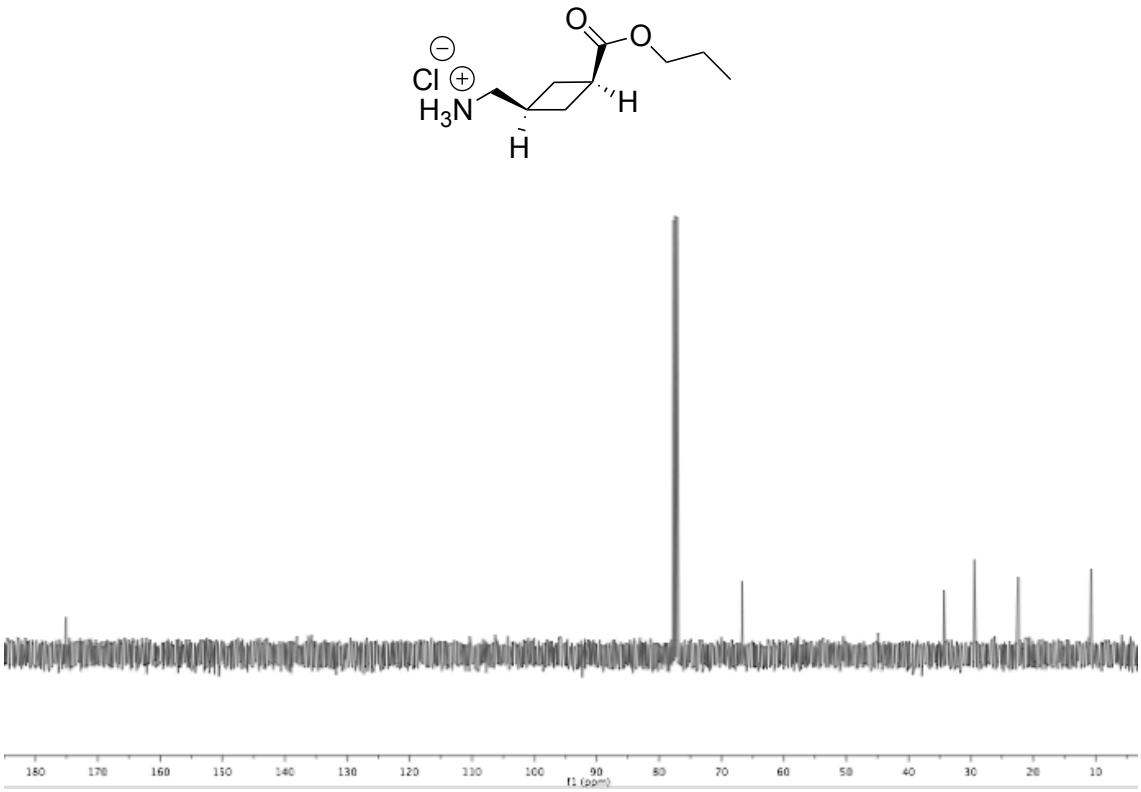
Cl
O
O
H3N
H
H
180
170
160
150
140
130
120
110
100
90
80
70
60
50
40
30
20
10
f1 (ppm)

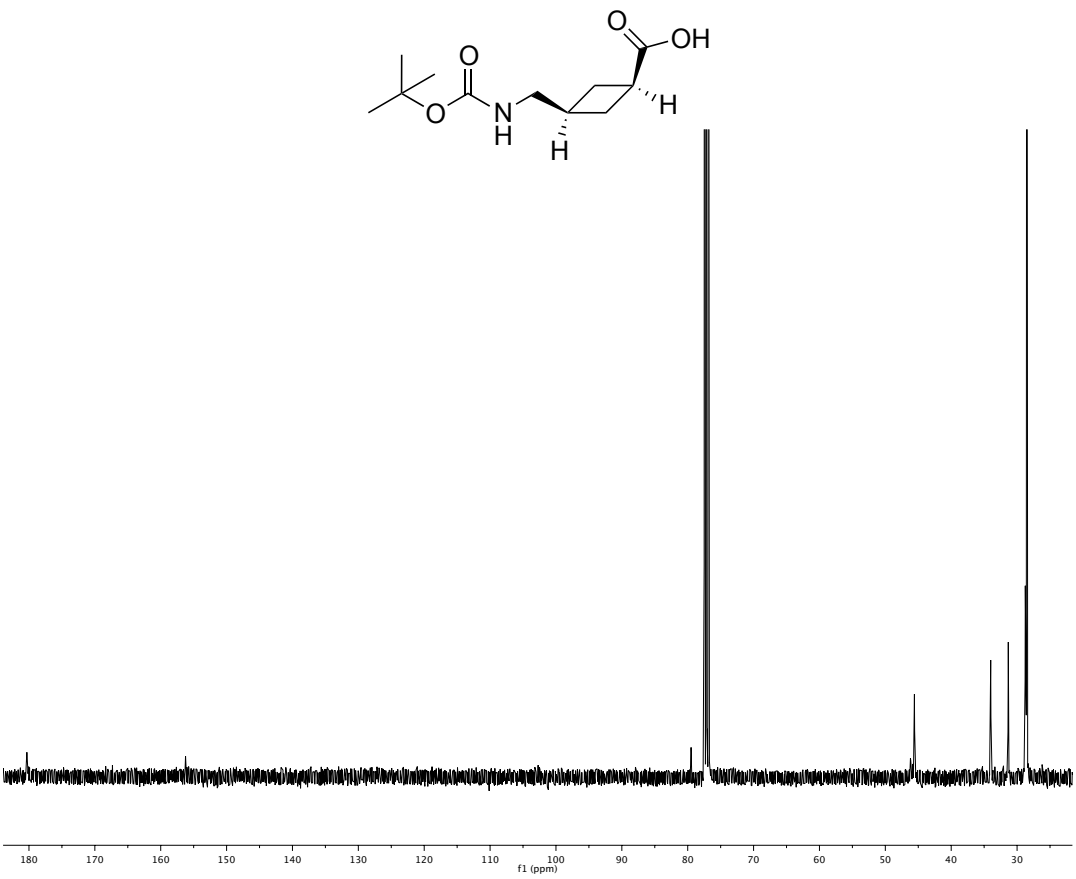
O
OH
O
O
N
H
H
H
180
170
160
150
140
130
120
110
100
90
80
70
60
50
40
30
f1 (ppm)

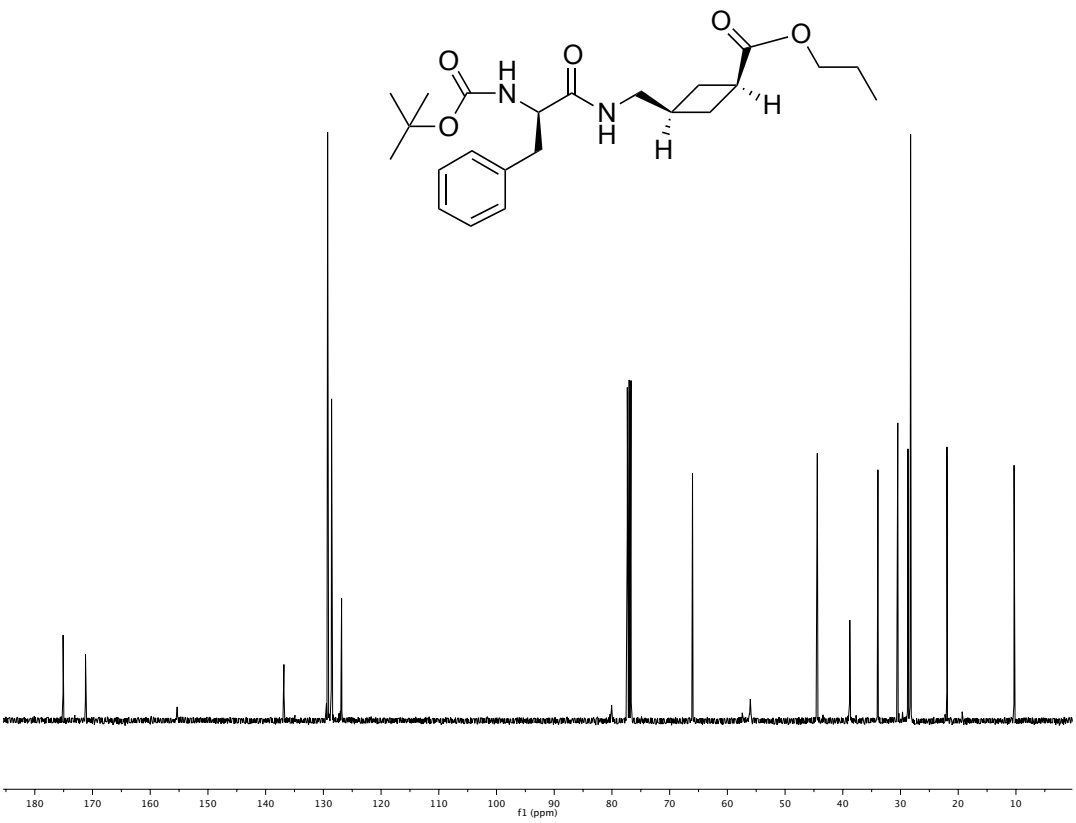
O
O
O
H
N
O
N
H
H
H
180
170
160
150
140
130
120
110
100
90
80
70
60
50
40
30
20
10
f1 (ppm)

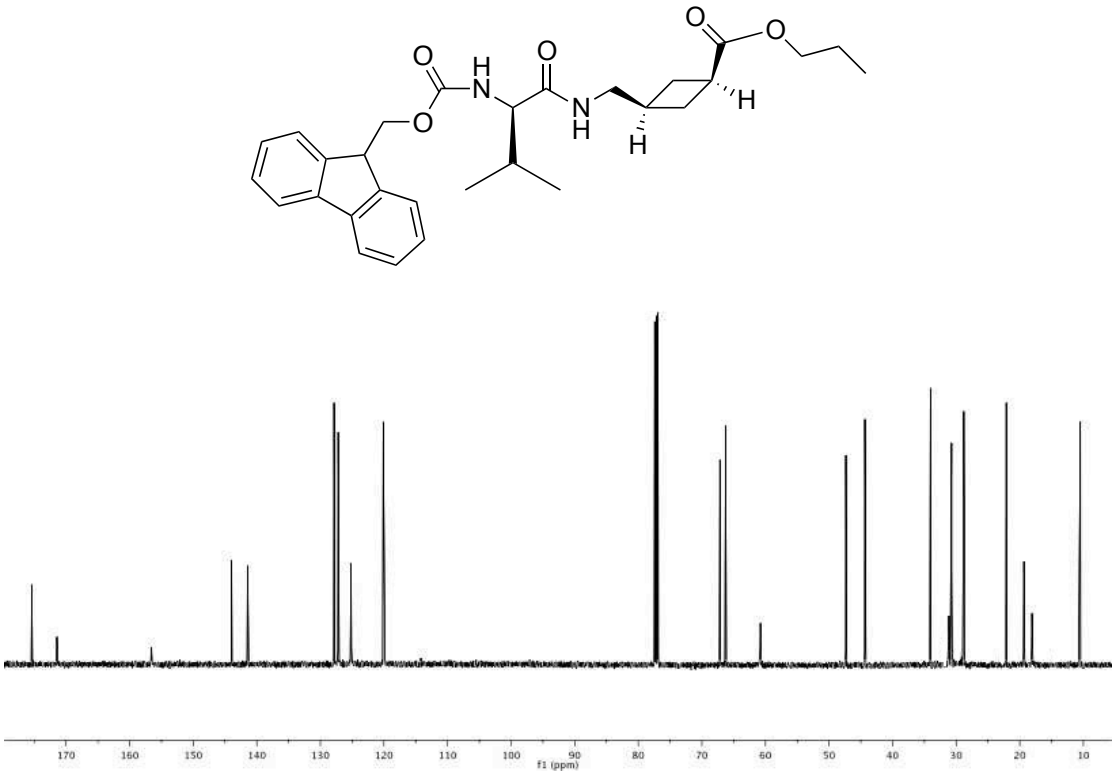
O
O
H
N
O
O
N
H
H
O
O
H
170
160
150
140
130
120
110
100
90
80
70
60
50
40
30
20
10
f1 (ppm)

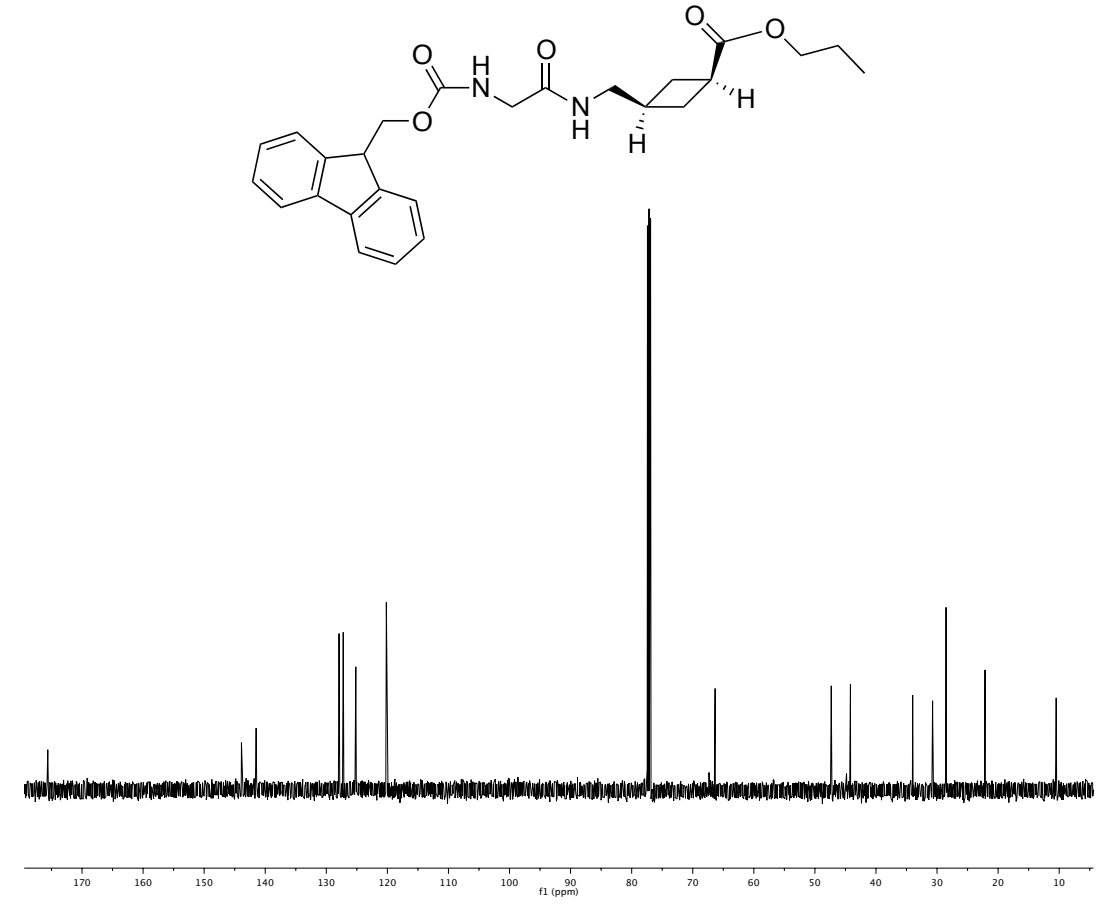
O
O
H
N
O
O
N
H
H
O
O
H
170
160
150
140
130
120
110
100
90
80
70
60
50
40
30
20
10
f1 (ppm)

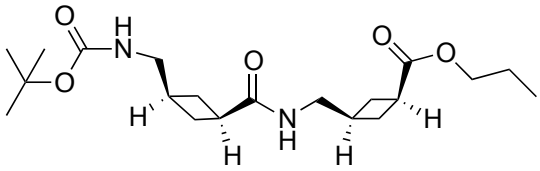
O
H
N
O
O
O
O
H
H
N
H
H
H

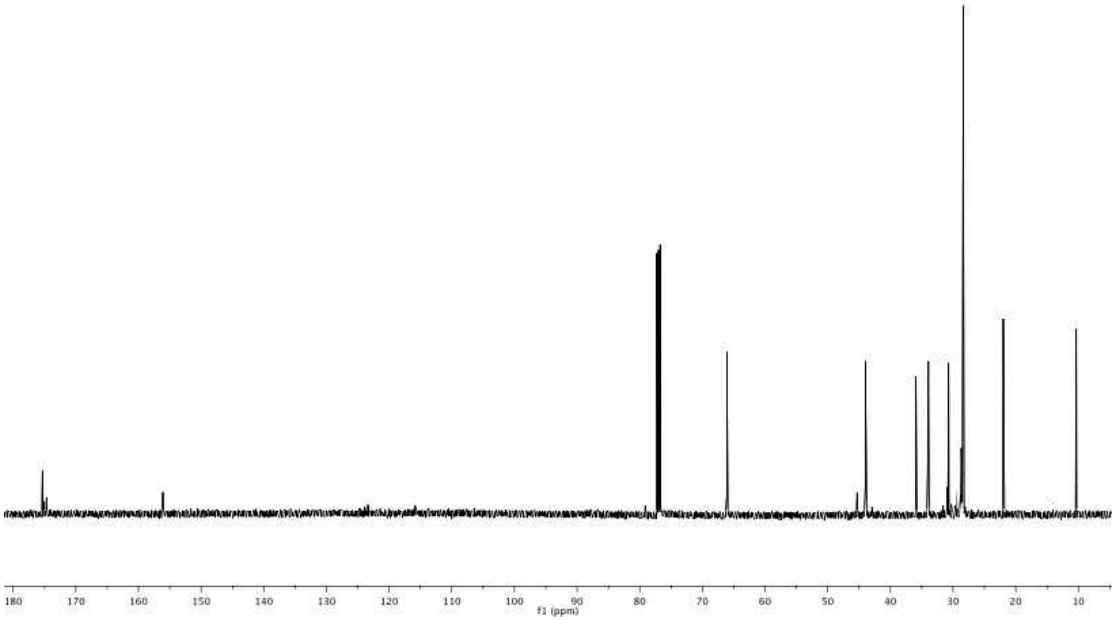
180 170 160 150 140 130 120 110 100 90 80 70 60 50 40 30 20 10
f1 (ppm)

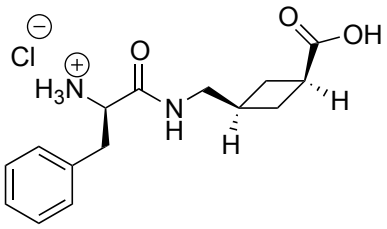
Cl
H3N
O
N
H
H
O
OH
H

180 175 170 165 160 155 150 145 140 135 130 125 120 115 110 105 100 95 90 85 80 75 70 65 60 55 50 45 40 35 30
f1 (ppm)

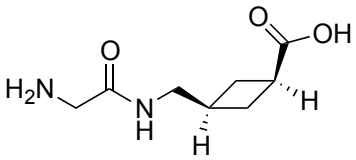
O
OH
O
H2N
N
H
H
H

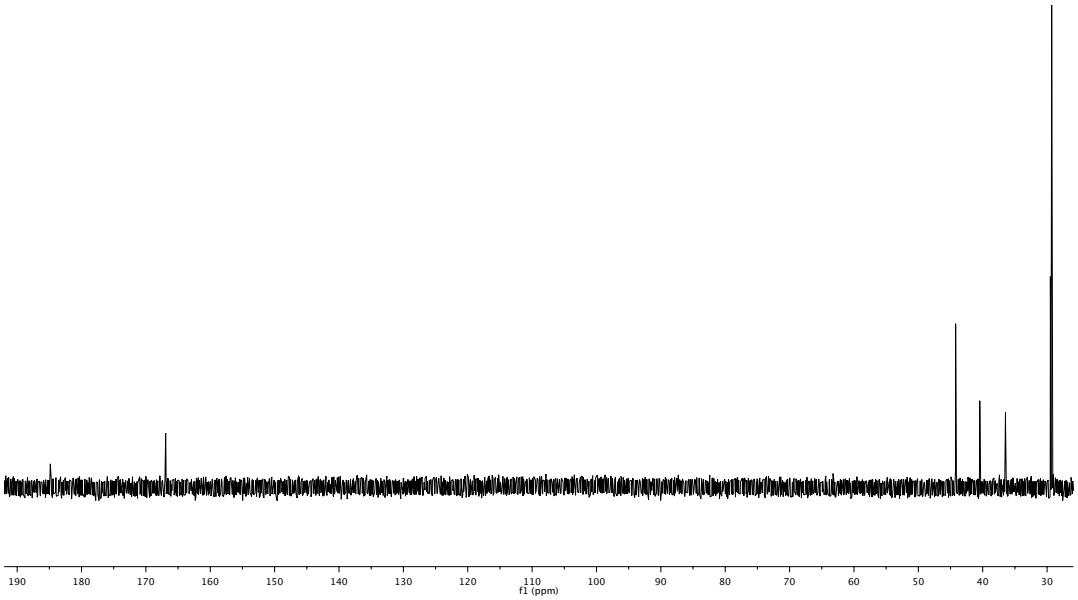
190 180 170 160 150 140 130 120 110 100 90 80 70 60 50 40 30
f1 (ppm)

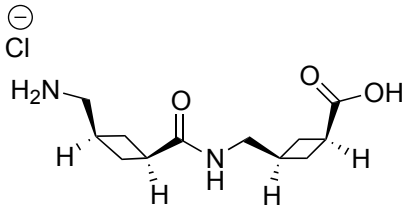
⊖
Cl
H2N
O
O
OH
H
N
H
H
H
H

180 175 170 165 160 155 150 145 140 135 130 125 120 115 110 105 100 95 90 85 80 75 70 65 60 55 50 45 40 35 30
f1 (ppm)

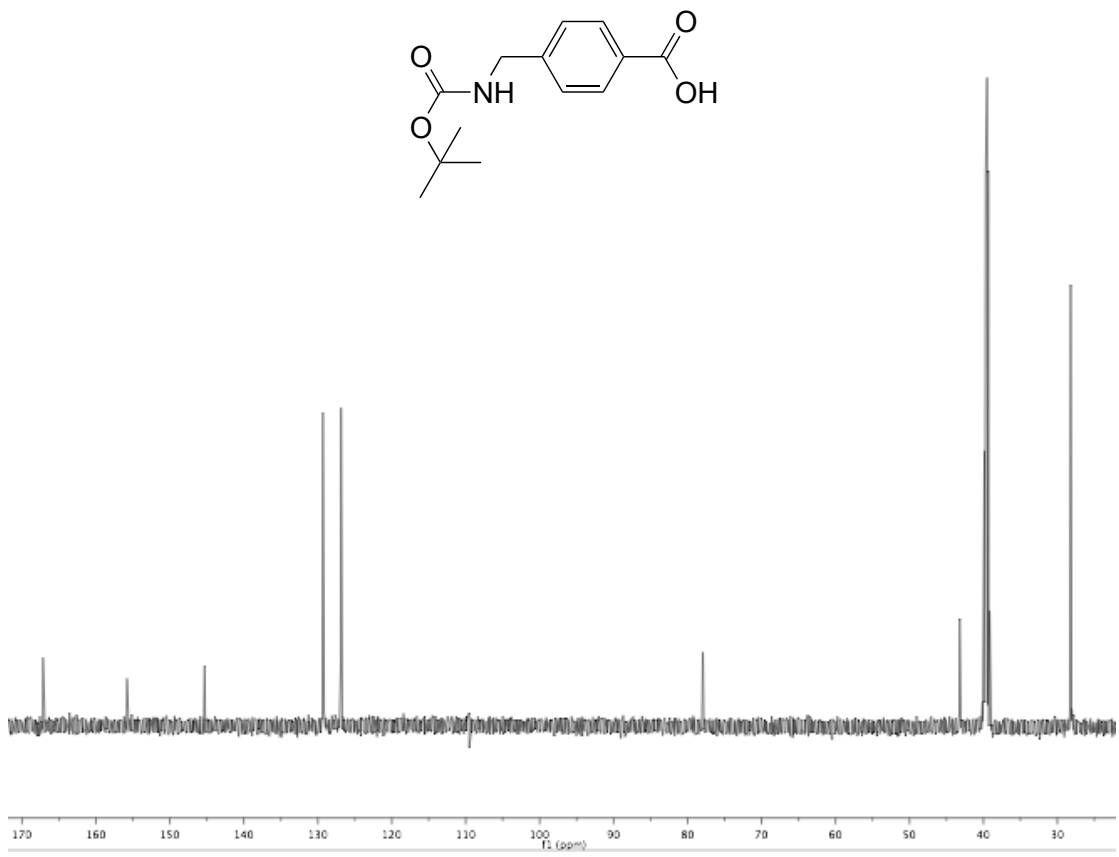
O
NH
O
O
OH
170
160
150
140
130
120
110
100
90
80
70
60
50
40
30
f1 (ppm)

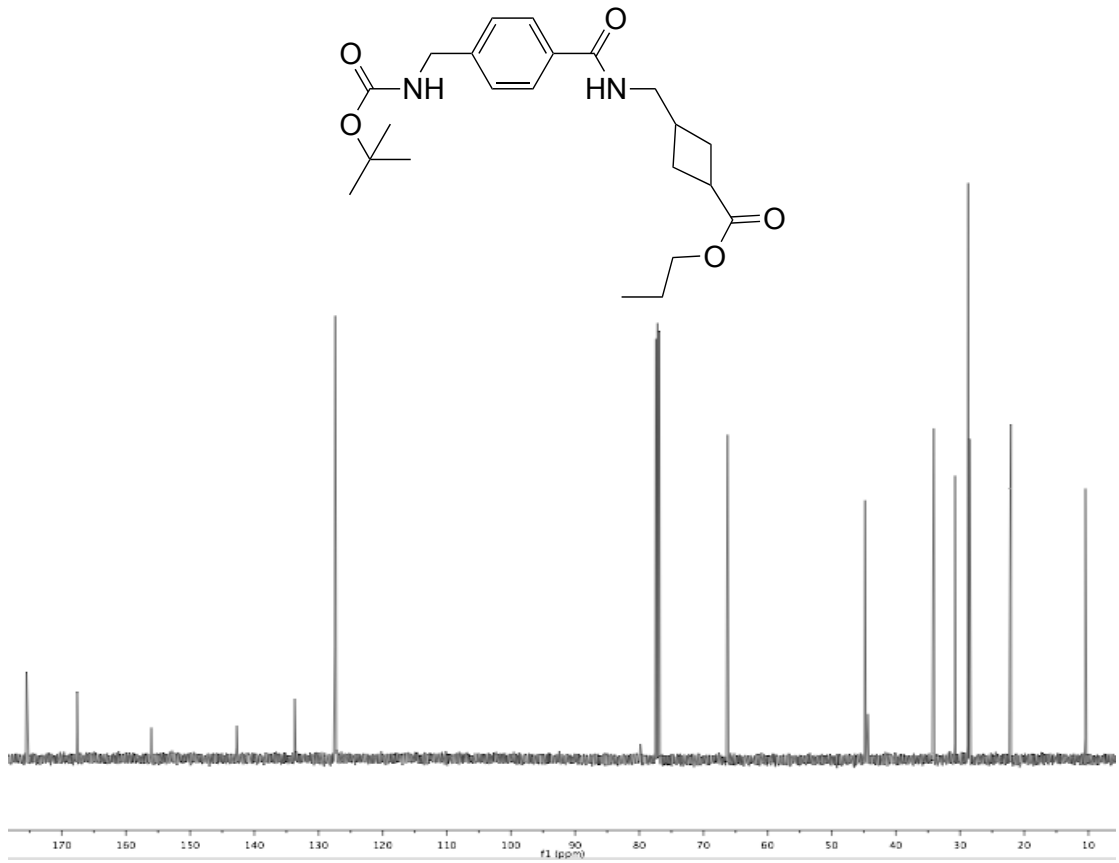
O
O
NH
O
HN
O
O
170
160
150
140
130
120
110
100
90
80
70
60
50
40
30
20
10
f1 (ppm)

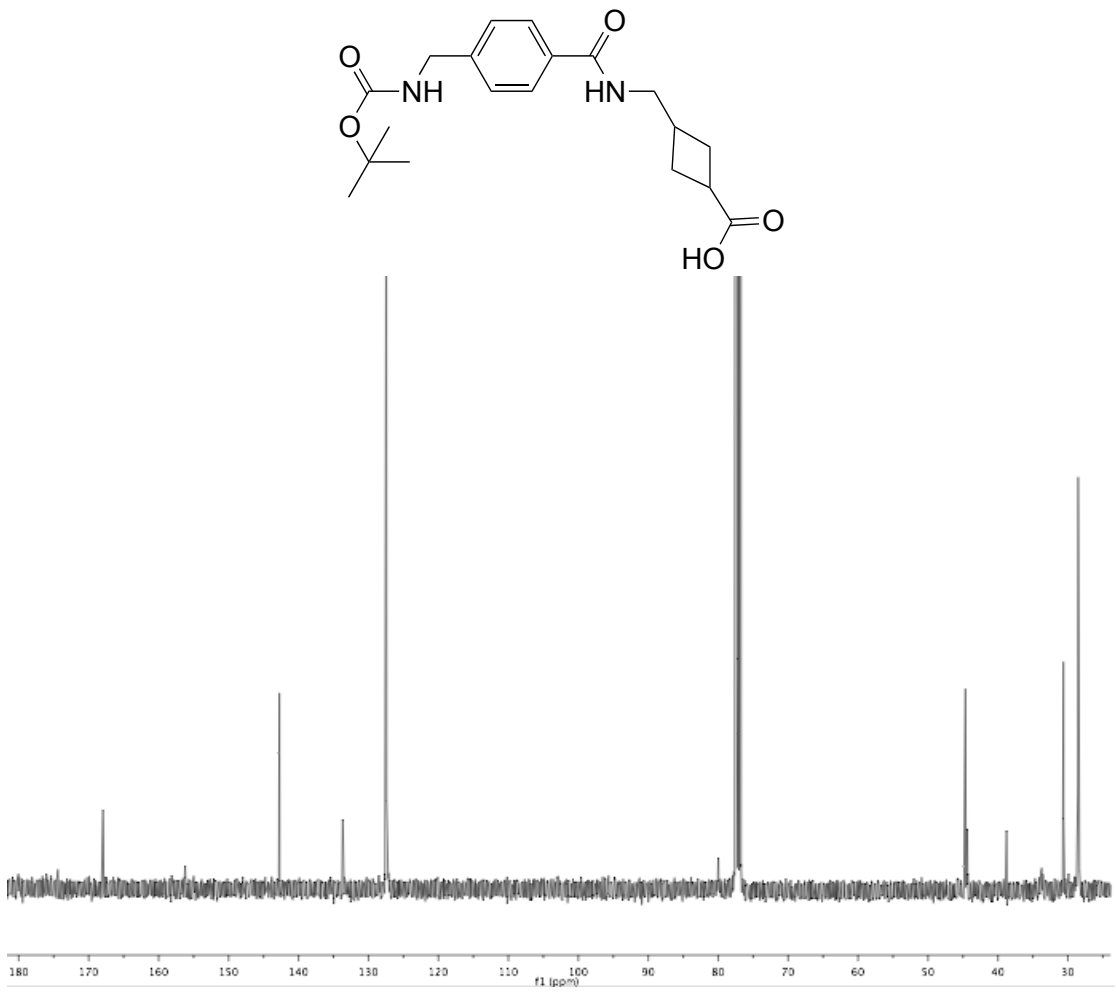
O
O
NH
O
HN
O
HO
180
170
160
150
140
130
120
110
100
90
80
70
60
50
40
30
f1 (ppm)

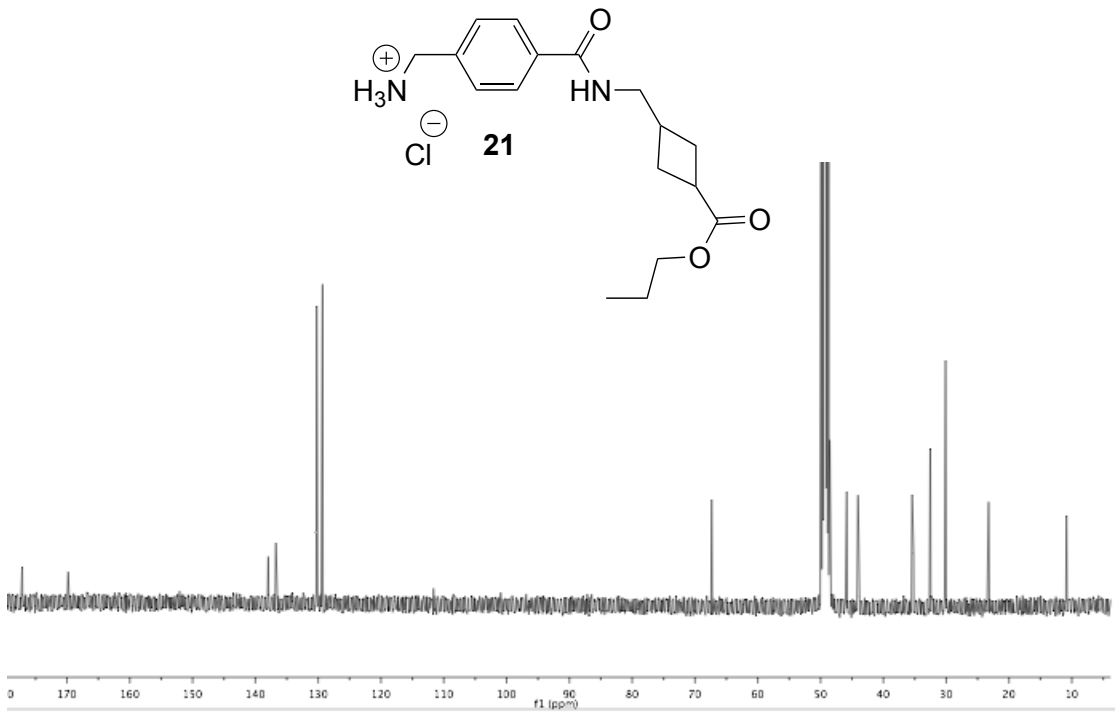
O
H3N
HN
Cl
21
O
O
0
170
160
150
140
130
120
110
100
90
80
70
60
50
40
30
20
10
f1 (ppm)

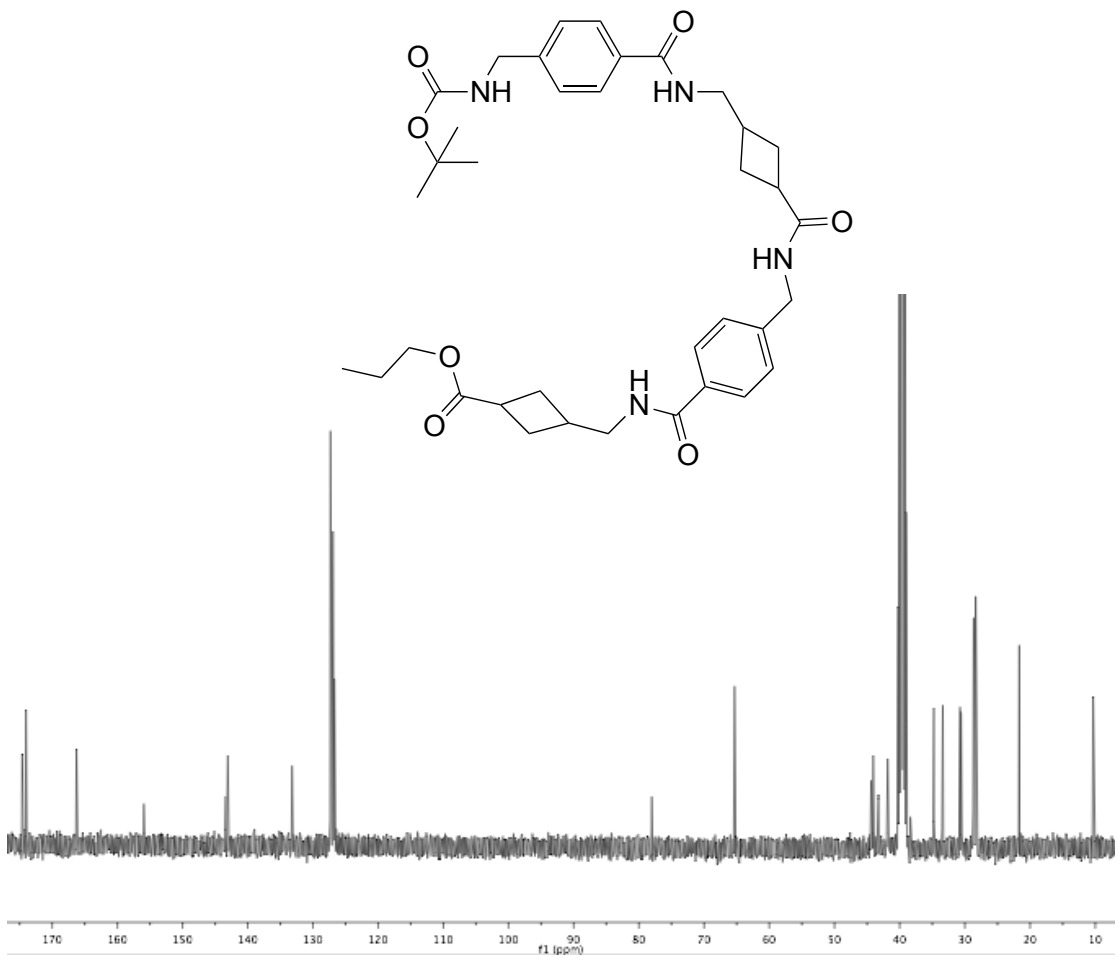
O
NH
O
HN
O
HN
O
O
H
N
O
170
160
150
140
130
120
110
100
90
80
70
60
50
40
30
20
10
f1 (ppm)

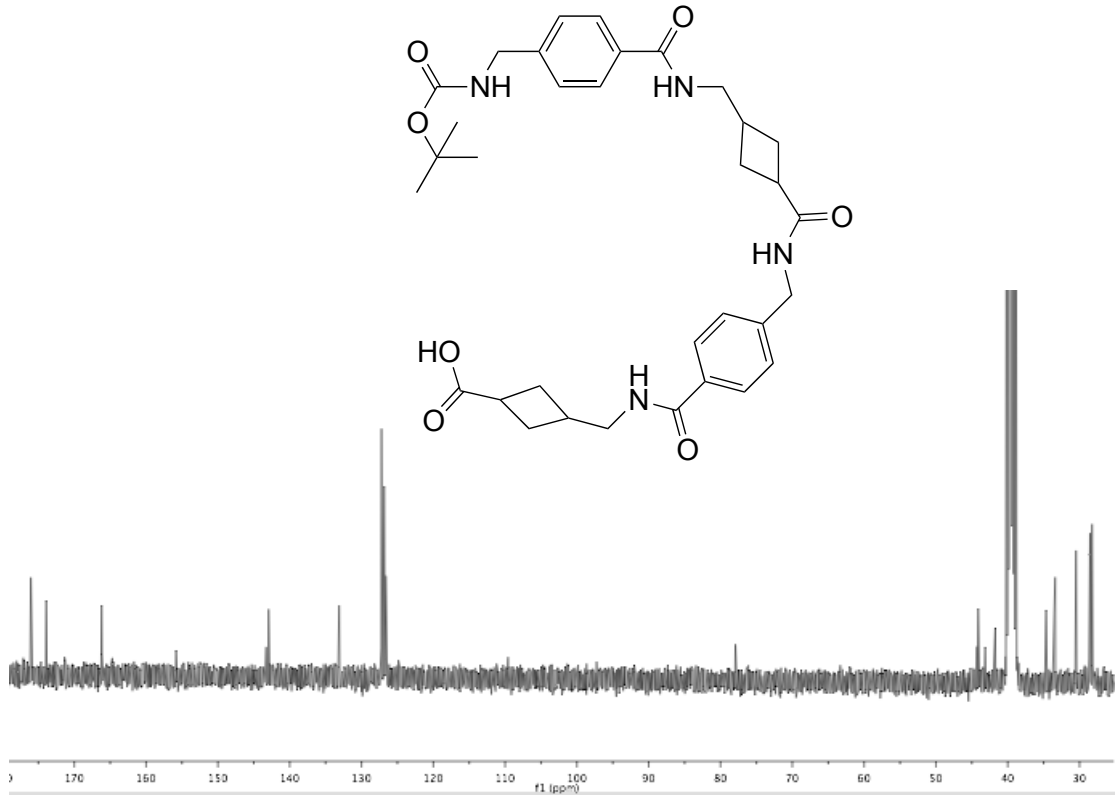
O
NH
O
HN
O
HN
HO
O
H
N
O
170
160
150
140
130
120
110
100
90
80
70
60
50
40
30
f1 (ppm)

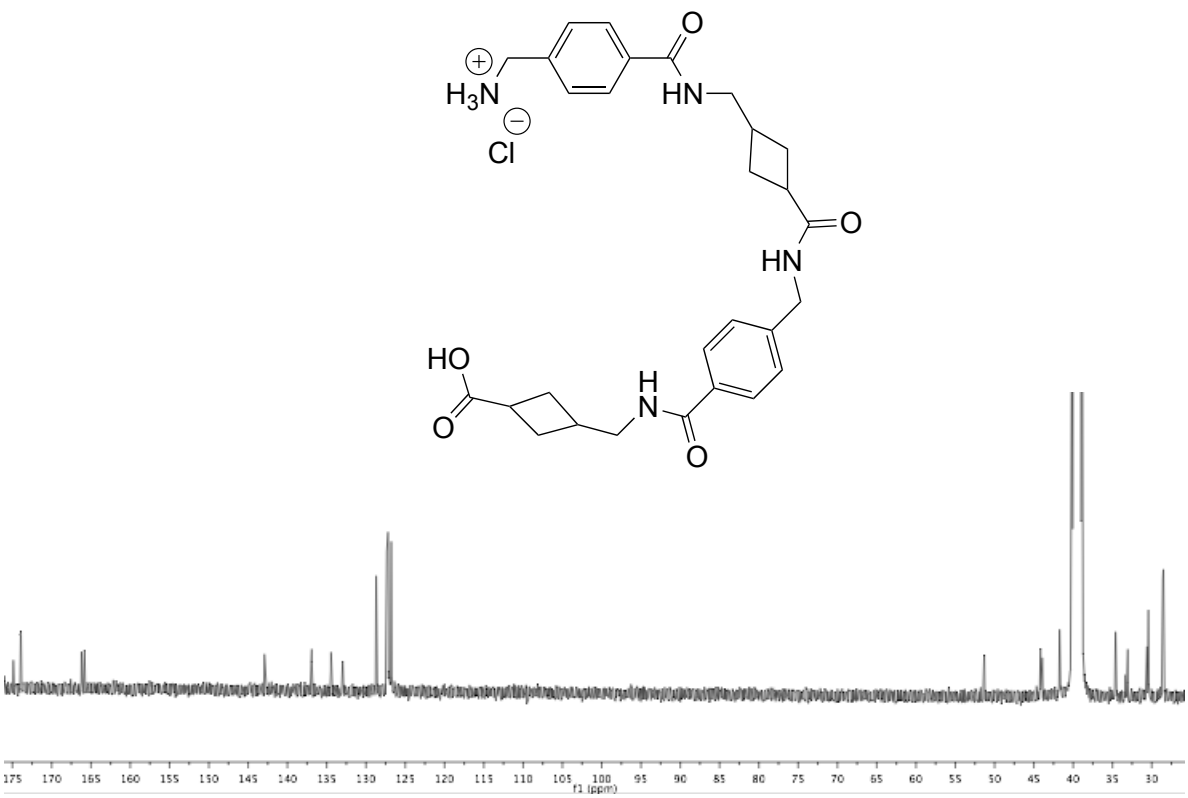
O
HN
H3N
Cl
O
HN
HO
O
H
N
O

175 170 165 160 155 150 145 140 135 130 125 120 115 110 105 100 95 90 85 80 75 70 65 60 55 50 45 40 35 30
f1 (ppm)

Appendix 2

APPENDIX 2: **Antibacterial activity evaluation of ACCA and its dipeptides**

In collaboration with Dr. Marta Martins (UCD Centre for Food Safety) antibacterial tests on ACCA (**9**), ACCA-Pr (**10**), Phe-ACCA (**15a**), Gly-ACCA (**15b**) and ACCA-ACCA (**15c**) were performed.

The compounds were tested against a series of antimicrobial resistant Gram-positive and Gram-negative bacteria as well as clinical isolates (E. coli 25922, E. coli 4, MRSA ATCC 43300, MRSA 06/04, Table. 1).

Strain	Type	Hospital/Isolation	Source	Resistant to
E. coli 25922	Reference	FDA strain Seattle 1946 [DSM 1103, NCIB 12210]	-	PEN; VAN; AMP; CLI; CL
E. coli 4	Clinical isolate	UCD Veterinary Hospital	Bovine	AMC; AMP; C; CIP; F; Fc; Gm; N; NAL; S; Su; TET; TMP
MRSA ATCC 43300	Reference	Kansas	Human	AMP; PEN; OXA; MET; AXO; CIP; LEVO; GAT; ERY; CLI
MRSA 06/04	Clinical isolate	-	Human	AMP; PEN; OXA; MET; AXO; CIP; LEVO; GAT; ERY

Table 1 the strains of bacteria used for antibacterial testing[1,2]

Antibiotics abbreviations: AMC - Amoxicillin-Clavulanic acid; C-Chloramphenicol; F-Furazolidone; Fc- Florfenicol Gm-Gentamycin; *N*-Neomycin; NAL-Nalidixic acid; S-Streptomycin; Su-Sulphonamides; TET- Tetracycline; TMP-Trimetoprim; AMP-ampicillin; PEN – penicillin; OXA – oxacillin; MET-methicillin; AXO – ceftriaxone; CIP-ciprofloxacin; LEVO-levofloxacin; GAT – gatifloxacin; ERY-erythromycin; CLI- clindamycin; CL- Cephalexin; Van-Vancomycin

An example of bacterial growth curve is reported in Fig. 1, where it is possible to notice that there was no difference in growth in the presence of the drugs up to 3.2 mg/mL.

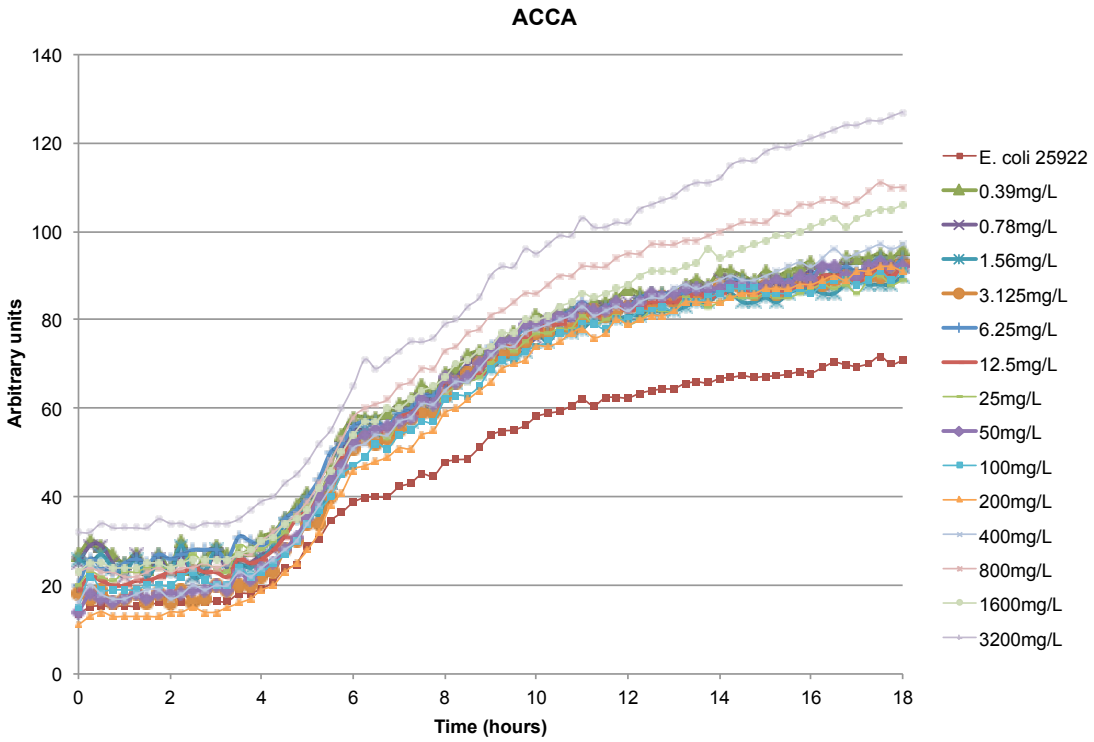

Fig. 1 example of bacterial growth curve for *E. coli* 25922 (reference strain) in presence of ACCA (**9**)

The Minimum Inhibitory Concentration (MIC) registered were all greater than 3.2 mg/mL against the bacteria tested, so none of the compounds investigated showed antibacterial activity.

Experimental

The experiments were carried out by Dr Marta Martins (UCD Centre for food safety).

A 96 well plate was made up as follows; 100 μL of Mueller-Hinton broth (MHB) were added to each well. 100 μL of the test compound (dissolved in sterile deionised water) were added to well 12 at a concentration double than the highest concentration to be tested, using a multichannel pipette. The solution and media were homogenised by repeated pipetting and 100 μL of the homogenised media solution mixture were transferred to well 11. This procedure was repeated until well 3, such that the concentration of test compound in each well was half that of the previous well. The bacteria to be tested against had been freshly incubated at 37 °C for 18 hours at 200 rpm and diluted to McFarland 0.5 standard by taking 50 μL of the overnight culture into 4.95 mL of Phosphate Buffered Saline (PBS) solution and vortexing well. From this, a second dilution was performed by taking 500 μL into 4.5 mL of PBS. The diluted culture was vortexed well and transferred into a reservoir. With a multichannel pipette, 5 μL were inoculated into each well of the plate. The plate was then incubated at 37 °C for 18 hours. The final make-up of the 96 well plate was as shown in table 2.

-	+	Test Wells										Compound
1	2	3	4	5	6	7	8	9	10	11	12	
												9
												10
												15a
												15b
												15c

Table 2 Diagram of 96 well plate

Well 1: 100 μL MHB (negative control).

Well 2: 100 μL MHB and 5 μL bacterial strain (positive control).

Wells 3-12: 100 μL of compounds diluted in MHB and 5 μL bacterial strain (test wells).

Materials

Bacteria were incubated using an Ominolog® automated incubator manufactured by Biolog Inc. 21124 Cabot Boulevard, Hayward, CA 94545, USA.

Mueller-Hinton broth was purchased from **Oxoid Limited** and phosphate buffered saline from Sigma.

Bibliography

(1) http://www.lgcstandards-atcc.org/
(2) Karczmarczyk, M.; Abbott, Y.; Walsh, C.; Leonard, N.; Fanning, S. *Applied and Environmental Microbiology* **2011**, *77*, 7104.

Appendix 3

APPENDIX 3: **published work**

The following article was published during the development of this thesis; the material treated is the one described in chapter 1.
Part of the results was achieved in collaboration with Dr. Elaine O'Reilly, who is therefore first shared author.

Appendix 4

APPENDIX 4: **Role of retinol in congenital diaphragmatic hernia**

Aside from my main research, I also collaborated with Dr. Balazs Kutasy and Prof. Prem Puri from the National Children's Research Centre, Our Ladys Children's Hospital, in a project on the role of retinol in congenital diaphragmatic hernia, where I contributed with all the samples analysis through High Performance Liquid Chromatography. Results have been presented to conferences (oral presentation in Annual Meeting of British Associated Paediatric Surgeons, Bournemouth, UK, 2013; poster presentation in Annual Meeting of American Academy of Paediatrics, Orlando, USA, 2013) and the two papers reported below have been submitted to the Journal of Paediatric Surgery. Two more papers are in preparation.

Paper 1: **Increased uptake of dietary retinoids at the maternal-fetal barrier in the nitrofen model of congenital diaphragmatic hernia**

Balazs Kutasy[1], Lara Pes[2], Florian Friedmacher[1], Francesca Paradisi[2], Prem Puri[1]

[1]The National Children's Research Center, Our Lady's Children's Hospital, Dublin, Ireland
[2]Centre for Synthesis & Chemical Biology, School of Chemistry & Chemical Biology, University College Dublin, Ireland

Abstract:

Background: It has been shown that retinol signalling pathway is disrupted in congenital diaphragmatic hernia (CDH). Since there is no fetal retinol synthesis, maternal retinol has to cross the placenta. Recently, we demonstrated that nitrofen interferes with retinol-RBP transfer pathway in CDH. However, in RBP knockout mice, retinol has been shown to be present. In that model increased uptake of maternal dietary retinoid-ester (RE) bounded in low-dense-lipoprotein (LDL) through low-density-lipoprotein-receptor (LRP1) and increased activity of RE hydrolysis by lipoprotein-lipase (LPL) have been found. The aim of this study was to investigate the RE transfer pathway in the nitrofen-CDH model.

Methods: Pregnant rats were treated with nitrofen or vehicle on gestational day (D9) and sacrificed on D21. Immunohistochemistry was performed to evaluate LRP1 and LPL protein expression. Serum LDL levels were measured by ELISA. Pulmonary and serum retinoids levels were measured using HPLC.

Results: Markedly increased trophoblastic and pulmonary LRP1 and LPL immunoreactivity were observed in CDH compared to controls. Significantly increased serum LDL and RE levels were observed in CDH compared to controls.

Conclusions: The increased uptake of dietary retinoids at the maternal-fetal barrier in the nitrofen-CDH model suggests that RE transfer pathway may be the main source of retinol in this model.

Keywords: Retinol, Placenta, Nitrofen, Congenital diaphragmatic hernia

Introduction:

Despite prenatal diagnosis and improved postnatal treatment strategies, the mortality rate of infants born with congenital diaphragmatic hernia (CDH) remains high [1]. The high mortality is mainly attributed to pulmonary hypoplasia (PH) and associated persistent pulmonary hypertension [2]. Much of the current understanding of pathogenesis of PH in CDH originates from experimental studies. Maternal exposure of nitrofen (2,4-dichlorophenyl-*p*-nitrophenyl ether) in rodents at specific gestational times results in a high rate of CDH and associated pulmonary hypoplasia to their fetuses, which is strikingly similar to the condition seen in humans [3]. However, the exact molecular mechanism by which nitrofen induces hypoplastic lung in this model still remains unclear.

It is well understood that retinoids, vitamin A and its derivates are essential for the morphogenesis of most developing organs and tissues, including lungs [4]. Human [5] and animal [6] studies have found that the retinoid signaling pathway is disrupted in CDH, contributing to PH. Recent work from our laboratory has shown that pulmonary retinol levels are significantly decreased in nitrofen-induced hypoplastic lungs during late lung morphogenesis, supporting the hypothesis that a disturbed retinol status is involved in the pathogenesis of CDH [6].

Within the maternal circulation, approximately 95-99% of retinol is bound to its sole specific carrier retinol-binding protein (RBP), which is the most abundant retinoid form [7]. It has been demonstrated that even in the fasting state there are always low concentrations of dietary retinyl ester (RE) associated with circulating low-density lipoprotein (LDL) and small amounts of circulating retinoid acid (RA) bound to albumin [8]. The placenta has a major role in the retinol homeostasis in fetal life [9]. Since there is no fetal retinol synthesis, the fetus relies on circulating maternal retinol that reaches the embryo through the maternal-fetal barrier in the placenta [8]. Recently, it has been demonstrated that maternal RBP does not cross the placental barrier [10]. Therefore, to enter the fetal circulation, maternal retinol bound to maternal RBP must be released at the maternal-fetal interface; and trophoblast have to produce their own RBP for retinol transfer from the placenta to the fetus [10, 11]. It has been shown that this is the primary retinol contributor to fetal development [10]. In human newborns with CDH, both retinol and RBP in serum has been reported to be

decreased, whereas maternal levels were comparable between mothers of CDH patients and mothers of healthy children in a case control study [5]. The above findings suggested that maternal-fetal retinol transport by placenta may be disrupted causing PH in CDH. Recently, we demonstrated that nitrofen alters the trophoblastic RBP expression in the nitrofen model of CDH [12]. However, in RBP knockout mice retinol has been shown to be present and this reflects the existence of an alternative pathway of retinol delivery to the fetus [7]. It has been demonstrated that maternal dietary RE bound in LDL through low-density lipoprotein-receptor (LRP1) can be transferred to the placenta [9]. The RE in the placenta can be either hydrolyzed into retinol and transferred to the fetal circulation by lipoprotein-lipase (LPL), or can be released to the fetus via scavenger-receptor class B-1 (SR-B1) receptor as LDL containing RE [8, 12]. In RBP knockout mice, increased placental activation of the alternative retinol transfer (increased LRP1 and LPL activation) has been found [12]. Moreover, it has been recently shown that lungs are able to take in retinol in RE formation from serum LDL through LRP1 receptor [13] and lungs can hydrolyze RE to retinol by LPL [14]. Therefore, we hypothesized that in nitrofen model of CDH during lung morphogenesis the alternative retinol transfer is activated in the placenta and then the lungs can take in dietary retinol for lung development. Thus, we designed this study to investigate the uptake of dietary retinoids at the maternal-fetal barrier in the nitrofen model of CDH.

Materials and methods:

Animals and drugs

Adult Sprague-Dawley rats were mated, and the females were checked daily for plugging. The presence of spermatozoids in the vaginal smear was considered as a proof of pregnancy; the day of observation determined gestational day 0 (term, 22 days). Pregnant female rats were then randomly divided into two groups. At 9 days (D9) of gestation, animals in the experimental group received intragastrically 100 mg of nitrofen (WAKO Chemicals, Osaka, Japan) dissolved in 1 ml of olive oil under short anesthesia, whereas those in the control group received only the vehicle. Fetuses were harvested by cesarian section on D21 of gestation and divided into two groups: control (n=8) and nitrofen with CDH (n=8). The Department of Health and Children approved the protocol of these

animal experiments (REC:668b) under the Cruelty to Animals Act, 1876; as amended by European Communities Regulations 2002 and 2005, all animals were treated according to the current guidelines of animal care.

Tissue collection

After sedation with isoflurane, term fetuses were harvested free from the dams. Placentas and lungs were dissected from each fetus. Blood was taken from the dams by intracardiac puncture for serum LDL and retinol determination. Freshly prepared serum samples for enzyme linked immunoassay (ELISA) and high-performance liquid chromatography (HPLC) were stored in aliquots at -80 °C after clotting for two hours and centrifugation for 10 minutes at 1000xg. Lung samples for reverse transcriptase–polymerase chain reaction (RT-PCR) were kept in TRIzol® reagent (Invitrogen, Carlsbad, CA) and stored at −20 °C until further analysis. Placenta and lung samples for immunohistochemistry were fixed in 4 % formalin and embedded in paraffin.

Immunohistochemistry

The paraffin-embedded lungs and placentas were sectioned at a thickness of 5 µm, and the sections were deparaffinized with xylene and then rehydrated through ethanol and distilled water. Tissue sections were immersed in target retrieval solution (DAKO Ltd, Cambridgeshire, UK) heated for 10 min at 121 °C followed by incubation in 0.03 % H_2O_2 for 30 min to block endogenous peroxidase activity. Sections were incubated overnight at 4 °C with a 1:100 dilution of rabbit monoclonal primary antibody against LRP1 (ab92544; Abcam, Cambridge, UK), 1:100 dilution of rabbit polyclonal primary antibody against SR-B1 (ab24603; Abcam, Cambridge, UK), and 1:50 dilution of rabbit polyclonal primary antibody against LPL (sc32885; Santa Cruz Biotechnology, USA). After intensively washing, sections were then incubated with horseradish peroxidase-labeled anti-rabbit secondary antibodies and then processed using a DAKO EnVision kit® (DAKO Ltd, Cambridgeshire, UK), developed with a diaminobenzidine–H_2O_2 substrate complex, and counterstained with hematoxylin.

High-performance liquid chromatography analysis

Preparation of samples for measurement of total retinol concentration (including retinol, retinyl-ester, retinoid acid and other metabolite of Vitamin A) was performed by modification of a previously described protocol [6]. Total retinol concentrations of lungs and serum were analysed by high-performance liquid chromatography provided with SPD-10A Shimadzu UV-Vis detector on 3.9x150 mm, 5mm reverse phase Resolve C18 column (Waters, Milford). The elution phase was acetonitrile/methanol/DMSO (90:10:1) and flow rate was 1.0 mL/min. Chromatograms were extracted at a wave lengths of 325 nm. The concentration of each sample was extrapolated from a calibration curve obtained with pure retinol samples (Sigma-Aldrich, Steinheim, Germany) between 0.1 and 10 *µ*g/mL in concentration.

Preparation of samples for simultaneous determination of retinol and retinyl-ester was performed by modification of a previously described protocol [15]. Retinol and RE concentrations of serum and lungs were analysed by high-performance liquid chromatography as described above.

RNA isolation and real-time reverse transcription polymerase chain reaction (PCR)

The total RNA of each lung derived from fetuses was isolated using TRIzol® reagent (Invitrogen, Carlsbad, CA) according to recommended protocol. Total RNA quantification was performed spectrophotometrically (NanoDrop ND-1000 UV-Vis Spectrophotometer). Total RNA (1 *µ*g) was reverse-transcribed using Transcriptor High Fidelity cDNA Synthesis Kit® (Roche Diagnostics, West Sussex, United Kingdom) according to manufacturer's instruction. Following reverse transcription at 44 °C for 60 minutes, polymerase chain reaction was performed using a LightCycler 480 SYBR Green I Master® (Roche Diagnostics) according to the manufacturer's protocol. Gene-specific primer pairs are listed in Table1.

Gene	Sequence	
b actin	Forward	5′-ttg ctg aca gga tgc aga ag-3′
	Reverse	5′-tag agc cac caa tcc aca ca-3
LRP1	Forward	5’-ctt tcg aag acc ctg agc ac-3’
	Reverse	5’-aca gag ccc aca ttt tcc ac-3’
LPL	Forward	5’- aca ctg gaa acg ctg ttg tg -3’
	Reverse	5’-ttc cgg ata aaa cgt tct cg-3’

Table 1 primers for quantitative real time PCR

After initial denaturation step of 5 minutes at 95 °C, 45 cycles of amplification for each primer pair were carried out. Each cycle included a denaturation step (10 seconds at 95 °C), an annealing step (15 seconds at 60 °C) and an elongation step (10 seconds at 72 °C). Final elongation temperature was 65°C for 1 minute. Relative levels of gene expression were measured using a LightCycler 480® (Roche Diagnostics) according to the manufacturer's instructions. The relative changes in the expression levels of LRP1 and LPL genes were normalized against the level of *β*-actin gene expression in each sample. Experiments were carried out at least in duplicate for each data point.

Enzyme linked immunoassay (ELISA)

Fetal serum LDL levels were measured with rat LDL ELISA kit (E91107RA, USCN, China) according to the manufacturer’s protocol. The results were measured at 450 nm with Synerg Mx microplate reader (BioTek) immediately after adding the stop solution. Experiments were carried out at least in duplicate for each data point.

Statistical analysis

All numerical data are presented as mean ± standard error of the mean (SEM). Differences between two groups at D21 were tested using an unpaired *t* test or *U* test, depending on the distribution of data. Statistical significance was accepted at *P* values <0.05.

Results:

Immunohistochemical staining of LRP1, LPL and SR-B1

Immunohistochemistry showed markedly increased LRP1, LPL and SR-B1 immunoreactivity in CDH placenta compared to controls (Figure 1).

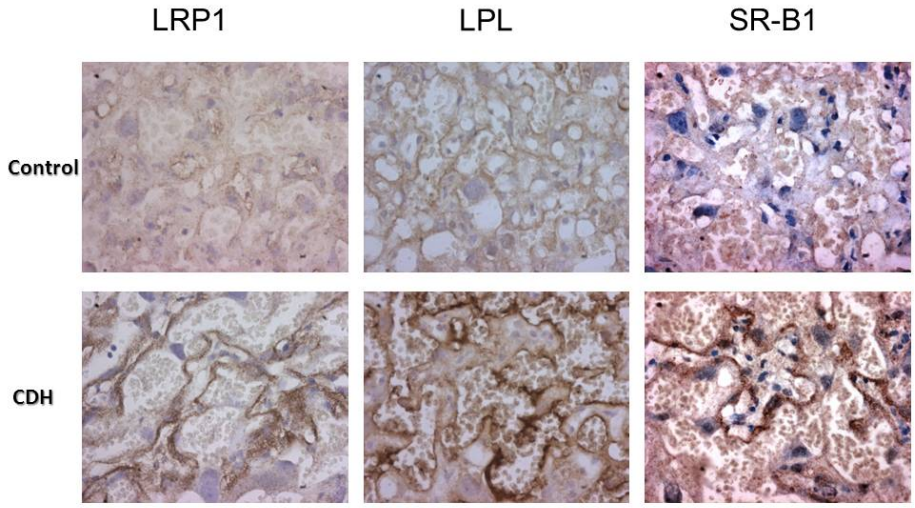

Figure 1 trophoblastic LRP1, LPL and SR-B1 expression (40x)

Markedly increased immunoreactivity of LRP1 and LPL were observed in nitrofen-induced hypoplastic lungs of CDH fetuses compared to control lungs (Figure 2).

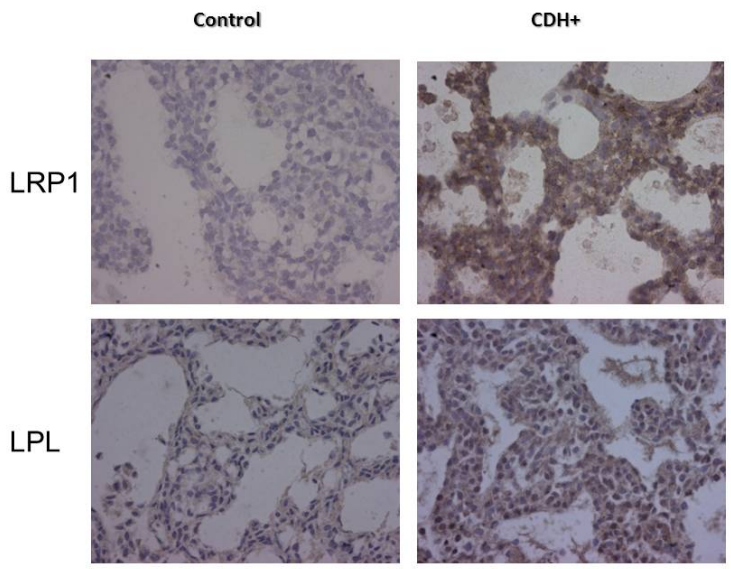

Figure 2 pulmonary LRP1 and LPL expression (40x)

Relative mRNA expression levels of LRP1 and LPL in fetal lungs

The relative mRNA expression levels of LRP1 and LPL genes were significantly up-regulated in CDH lungs (68.12 ± 3.39 and 4.05 ± 0.7) compared to controls (48.93 ± 5.09 and 1.94 ± 0.4, $p<0.05$) (Table 2).

RT PCR	Control (n=8)	CDH (n=8)
LRP1	48.93±5.09	68.12±3.39*
LPL	1.94±0.4	4.05±0.7*

*: vs Control, $p<0.05$

Table 2 relative mRNA expression levels of LRP1 and LPL in fetal lungs

Retinol levels

In the fetal serum, significantly increased total retinol levels were detected in CDH group compared to controls (0.198±0.008 vs 0.0897±0.002 *μM/*g, $p<0.05$).

With simultaneous detection of retinol and retinyl-ester in serum, significantly decreased retinol level (0.0151±0.003 vs 0.0872±0.001 *μM/*g, p<0.05) and increased RE level (0.1829±0.005 vs 0.00245±0.002 *μM/*g, p<0.05) were measured in CDH group compared to controls (Table 3).

Serum	Control (n=8)	CDH (n=8)
Total retinol μM/g)	0.0897±0.002	0.198±0.008*
Retinol (μM/g)	0.0872±0.001	0.0151±0.003*
Retinyl-ester (μM/g)	0.00245±0.002	0.1829±0.005*

*: vs Control, p<0.05

Table 3 fetal serum retinol levels

Significantly decreased total pulmonary retinol levels were measured in CDH fetuses compared to controls (0.77 ± 0.05 vs 0.51 ± 0.01*μM/*g, p<0.05) (Table 4).

Pulmonary	Control (n=8)	CDH (n=8)
Total retinol (μM/g)	0.7772 ± 0.05	0.5133 ± 0.01*
Retinol (μM/g)	0.0816 ± 0.01	0.0717 ± 0.01
Retinyl-ester (μM/g)	0.69 ± 0.03	0.44 ± 0.02*

*: vs Control, p<0.05

Table 4 pulmonary retinol levels

There were no significant differences in pulmonary retinol levels between CDH group (0.08 ± 0.01 *μM/*g) and control group (0.07 ± 0.01*μM/*g). The retinyl-ester levels were significantly decreased in CDH lungs (0.44 ± 0.02 *μM/*g) compared to control lungs (0.69 ± 0.03 *μM/*g, $p<0.05$).

Serum LDL levels

There were no significant differences in maternal serum LDL levels between nitrofen-exposed mothers (n = 4, 24.4 ± 2.5 ng/mL) and control mothers (n = 4, 29.0± 2.1 ng/mL). Significantly increased serum LDL levels were detected in CDH group (19.5 ± 1.4 ng/mL) compared to controls (14.9 ± 1.9 ng/mL, $p<0.05$).

Discussion:

It is well understood that retinoids, vitamin A and its derivates are essential for the morphogenesis of most developing organs and tissues, including lungs [4]. All retinoids are derived from diet either as preformed vitamin A from animal products (retinol, RE and very small amount of RA) or as carotenoids from vegetables and fruits [8]. Within the intestinal mucosa the retinol, regardless of its dietary origins, is re-esterified with long-chain fatty acids primarily [8]. Together with other dietary lipids, the newly synthesized REs are packaged into chylomicrons and secreted into the lymphatic system [8]. Once in the general circulation, lipoprotein lipase (LPL), which is bound to the luminal surface of the vascular endothelium, catalyzes the lipolysis of triglycerides to generate free fatty acids and chylomicron remnants [8]. After chylomicron remnants acquire apolipoprotein E, either in plasma or in the space of Disse, approximately 75 % of chilomycron remnant-RE is cleared by the liver, the major site of retinol storage and metabolism [8]. Once taken up by the hepatocytes, REs are hydrolyzed again to retinol either to be transferred to stellate cells and then re-esterified for storage; or retinol can bind to its sole specific serum transport protein, RBP to be secreted into the bloodstream [7]. The major function of RBP is to mobilize hepatic retinoid stores and deliver retinol to peripheral tissues such as embryos [7]. In the fasting circulation, retinol-RBP accounts for

approximately 95-99 % of all serum retinoids [8]. However, even in the fasting state there are always low concentrations of RE associated with circulating lipoproteins [8].

Since there is no de novo fetal synthesis of retinol, to meet its requirement for retinoids, the developing mammalian embryo relies on circulating maternal retinol that reaches the embryo through the maternal-fetal barrier [8]. Quadro et al [16] have demonstrated that two major retinoid forms can be identified in the maternal bloodstream: retinol bound to RBP secreting from liver stores and RE packaged in chylomicrons upon dietary retinol intake. It has been shown in mice that maternal RBP does not cross the placenta [10]. Therefore, to enter the fetal circulation, maternal retinol bound to maternal RBP must be released at the maternal-fetal interface; and trophoblast have to produce their own RBP for retinol transfer from placenta to fetus [10]. However, recently Quadro et al [16] have shown that in RBP knockout mice retinol is present and this suiggests the existence of an alternative pathway of retinol delivery. It has been demonstrated that maternal dietary RE bounded in LDL through LRP1 can be transferred to the placenta [9]. These RE in the placenta can be either hydrolyzed into retinol and transferred to the fetal circulation by LPL, or can be released it to the fetus via SR-B1 receptor as LDL containing RE [8]. In RBP knockout mice, increased placental activation of LRP1 and LPL has been found [9]. Therefore, Spiegler et al [8] have concluded that under normal circumstances the retinol-RBP pathway is the primary contributor to fetal development, while in mice lacking retinol-RBP, the RE levels incorporated in maternal circulating chylomicron remnants provides the embryos with sufficient amounts of retinol for survival.

Several authors have shown that the retinoid signaling pathway is disrupted in both humans and animal models of CDH, and decreased pulmonary retinol levels have been associated with the development of PH in CDH [5, 6]. Beurskens *et al.* [5] have found decreased serum RBP and retinol levels in human newborns with CDH compared to controls whereas mothers of both have comparable levels of RBP and retinol. These authors concluded that the maternal-fetal transport may be disrupted, leading to CDH and PH. The importance of the retinoid signaling pathway during fetal development and especially in lung morphogenesis is further supported by a study showing that RA administration attenuates the development of PH in the nitrofen-induced

CDH model [17]. The nitrofen CDH model is one of the most widely used animal models to study the pathogenesis of PH in CDH [18, 19]. However, the exact molecular mechanism underlying nitrofen-induced PH in CDH still remains unclear. It has recently been reported that nitrofen does not directly interfere with RA signaling but induces a dose-dependent apoptosis [20]. Clugston et al demonstrated that the level of nitrofen estimated to reach the embryo would be too low to induce apoptosis directly [21]. Recently we demonstrated that nitrofen disturbs trophoblastic RBP expression, resulting in PH in the nitrofen CDH model [12].

There are conflicting findings in serum retinol levels in CDH between human and animal studies [5, 6, 22]. Significantly decreased serum retinol levels have been found in human newborns with CDH [5, 22]. In contrast both our previous work [6] and current study have found significantly increased serum total retinol levels in CDH in rats. This difference may be due to the different detection methods employed. Beurskens et al [5] and Major et al [22] measured only the retinol levels and they did not investigate RE levels in CDH. However, in our study we used that detection method which measured retinol as well as RE and RA. In the current study using simultaneous measurement of retinol and RE, we demonstrated that the serum retinol level is significantly decreased in nitrofen induced CDH fetuses. Moreover, we found that the most of the circulating retinoids in CDH are RE. At the same time significantly increased serum LDL levels were observed suggesting that the circulating RE is bound to LDL. It has been shown that the lungs are able to take in retinol in RE form from serum LDL through LRP1 receptor [13] and lungs can hydrolyze RE to retinol by LPL [14]. The increased pulmonary activation of LRP1 receptor may suggest that nitrofen induced hypoplastic lungs increase their RE uptake. The comparable pulmonary retinol levels in CDH and controls, together with the increased pulmonary LPL activation in CDH, suggests that CDH lung hydrolyze RE into retinol during lung morphogenesis. Therefore, it is tempting to speculate that the RE pathway is the main source of retinol in CDH during lung morphogenesis in nitrofen model.

References

1. Colvin J, Bower C, Dickinson JE, Sokol J: Outcomes of congenital diaphragmatic hernia: a population-based study in Western Australia. *Pediatrics* 2005, 116(3):e356-363.
2. Robinson PD, Fitzgerald DA: Congenital diaphragmatic hernia. *Paediatr Respir Rev* 2007, 8(4):323-334; quiz 334-325.
3. Montedonico S, Nakazawa N, Puri P: Congenital diaphragmatic hernia and retinoids: searching for an etiology. *Pediatr Surg Int* 2008, 24(7):755-761.
4. Clagett-Dame M, DeLuca HF: The role of vitamin A in mammalian reproduction and embryonic development. *Annu Rev Nutr* 2002, 22:347-381.
5. Beurskens LW, Tibboel D, Lindemans J, Duvekot JJ, Cohen-Overbeek TE, Veenma DC, de Klein A, Greer JJ, Steegers-Theunissen RP: Retinol status of newborn infants is associated with congenital diaphragmatic hernia. *Pediatrics*, 126(4):712-720.
6. Nakazawa N, Montedonico S, Takayasu H, Paradisi F, Puri P: Disturbance of retinol transportation causes nitrofen-induced hypoplastic lung. *J Pediatr Surg* 2007, 42(2):345-349.
7. Quadro L, Hamberger L, Colantuoni V, Gottesman ME, Blaner WS: Understanding the physiological role of retinol-binding protein in vitamin A metabolism using transgenic and knockout mouse models. *Molecular aspects of medicine* 2003, 24(6):421-430.
8. Spiegler E, Kim YK, Wassef L, Shete V, Quadro L: Maternal-fetal transfer and metabolism of vitamin A and its precursor beta-carotene in the developing tissues. *Biochimica et biophysica acta* 2012, 1821(1):88-98.
9. Wassef L, Quadro L: Uptake of dietary retinoids at the maternal-fetal barrier: in vivo evidence for the role of lipoprotein lipase and alternative pathways. *The Journal of biological chemistry* 2011, 286(37):32198-32207.
10. Quadro L, Hamberger L, Gottesman ME, Colantuoni V, Ramakrishnan R, Blaner WS: Transplacental delivery of retinoid: the role of retinol-binding protein and lipoprotein retinyl ester. *American journal of physiology Endocrinology and metabolism* 2004, 286(5):E844-851.
11. Sapin V, Ward SJ, Bronner S, Chambon P, Dolle P: Differential expression of transcripts encoding retinoid binding proteins and retinoic acid receptors during placentation of the mouse. *Dev Dyn* 1997, 208(2):199-210.
12. Kutasy B, Gosemann JH, Doi T, Fujiwara N, Friedmacher F, Puri P: Nitrofen interferes with trophoblastic expression of retinol-binding protein and transthyretin during lung morphogenesis in the nitrofen-induced congenital diaphragmatic hernia model. *Pediatr Surg Int* 2012, 28(2):143-148.
13. Roebroek AJ, Reekmans S, Lauwers A, Feyaerts N, Smeijers L, Hartmann D: Mutant Lrp1 knock-in mice generated by recombinase-mediated cassette exchange reveal differential importance of the NPXY motifs in the intracellular domain of LRP1 for normal fetal development. *Molecular and cellular biology* 2006, 26(2):605-616.
14. Blaner WS, Obunike JC, Kurlandsky SB, al-Haideri M, Piantedosi R, Deckelbaum RJ, Goldberg IJ: Lipoprotein lipase hydrolysis of retinyl ester. Possible implications for retinoid uptake by cells. *The Journal of biological chemistry* 1994, 269(24):16559-16565.
15. Moulas AN ZI, Taitzoglou IA, Tsantarliotou MP, Botsoglou NA.: Simultaneous determination of retinoic acid, retinol, and retinyl palmitate in ram plasma by liquid chromatography. *J Liq Chromatogr* 2003, 26:559–572.
16. Quadro L, Hamberger L, Gottesman ME, Wang F, Colantuoni V, Blaner WS, Mendelsohn CL: Pathways of vitamin A delivery to the embryo: insights from a new tunable model of embryonic vitamin A deficiency. *Endocrinology* 2005, 146(10):4479-4490.
17. Montedonico S, Nakazawa N, Puri P: Retinoic acid rescues lung hypoplasia in nitrofen-induced hypoplastic foetal rat lung explants. *Pediatr Surg Int* 2006, 22(1):2-8.
18. Doi T, Hajduk P, Puri P: Upregulation of Slit-2 and Slit-3 gene expressions in the nitrofen-induced hypoplastic lung. *J Pediatr Surg* 2009, 44(11):2092-2095.
19. Doi T, Puri P: Up-regulation of Wnt5a gene expression in the nitrofen-induced hypoplastic lung. *J Pediatr Surg* 2009, 44(12):2302-2306.

20. Kling DE, Cavicchio AJ, Sollinger CA, Schnitzer JJ, Kinane TB, Newburg DS: Nitrofen induces apoptosis independently of retinaldehyde dehydrogenase (RALDH) inhibition. *Birth Defects Res B Dev Reprod Toxicol*, 89(3):223-232.
21. Clugston RD, Zhang W, Greer JJ: Early development of the primordial mammalian diaphragm and cellular mechanisms of nitrofen-induced congenital diaphragmatic hernia. *Birth Defects Res A Clin Mol Teratol*, 88(1):15-24.
22. Major D, Cadenas M, Fournier L, Leclerc S, Lefebvre M, Cloutier R: Retinol status of newborn infants with congenital diaphragmatic hernia. *Pediatr Surg Int* 1998, 13(8):547-549.

Paper 2: **Nitrofen increases total retinol levels in placenta during lung morphogenesis in the nitrofen model of congenital diaphragmatic hernia**

Balazs Kutasy[1], Lara Pes[2], Florian Friedmacher[1], Francesca Paradisi[2], Prem Puri[1]

[1]The National Children's Research Center, Our Lady's Children's Hospital, Dublin, Ireland
[2]Centre for Synthesis & Chemical Biology, School of Chemistry & Chemical Biology, University College Dublin, Ireland

Abstract:

Background: It has been shown that pulmonary retinol level is decreased during lung morphogenesis in the nitrofen induced PH in congenital diaphragmatic hernia (CDH). Placenta has a major role in the retinol homeostasis in fetal life. Since there is no fetal retinol synthesis, maternal retinol has to cross the placenta. Placenta is the main fetal retinol store where retinol is stored in retinyl-ester formation. Trophoblasts have to produce its own retinol-binding protein (RBP) for retinol transport from placenta to fetus. Recently, we demonstrated that trophoblastic RBP expression is decreased in the nitrofen model of CDH. The aim of this study was to investigate the retinol transfer from mother to the placenta in nitrofen model of CDH.

Methods: Pregnant rats were exposed to either olive oil or nitrofen on day9 of gestation (D9). Fetal placenta harvested on D21 and divided into two groups:control (n=11) and nitrofen with CDH (n=11). Retinoids levels in placenta were measured using HPLC. Immunohistochemistry was performed to evaluate trophoblastic expression of main RSP genes.

Results: Total retinol levels in the placenta were significantly increased in CDH placenta compared to control placenta. The retinyl-ester levels were significantly increased in CDH placenta compared to control placenta. Markedly decreased immunoreactivity of retinoid signaling pathway was observed in trophoblast cells in CDH compared to control placenta.

Conclusions: Increased placental retinol levels show that retinol is transferred from mother to placenta and stored in the placenta in nitrofen model of CDH

during lung morhogenesis. Nitrofen may disturb the mobilization of retinol from placenta to fetal circulation causing PH in CDH.

Keywords: Retinol, Placenta, Nitrofen, Congenital diaphragmatic hernia

Introduction:

Despite prenatal diagnosis and improved postnatal treatment strategies, the mortality rate of infants born with congenital diaphragmatic hernia (CDH) remains high [1, 2]. The high mortality is mainly attributed to pulmonary hypoplasia (PH) and associated persistent pulmonary hypertension [3, 4]. Much of the current understanding of pathogenesis of pulmonary hypoplasia in CDH originates from experimental studies. Maternal exposure of nitrofen (2,4-dichlorophenyl-*p*-nitrophenyl ether) in rodents during specific time in gestation results in a high rate of CDH and associated pulmonary hypoplasia to their fetuses, which is strikingly similar to the condition seen in the human [5, 6]. However, the exact molecular mechanism by which nitrofen induces hypoplastic lung in this model still remains unclear.

It is well understood that retinoids, vitamin A and its derivates are essential for the morphogenesis of most developing organs and tissues, including lungs [7]. Placenta has a major role in the retinol homeostasis in fetal life [8]. Since there is no fetal retinol synthesis, the fetus relies on circulating maternal retinol that reaches the embryo through the maternal-fetal barrier in the placenta [9]. Furthermore, placenta serves as a site of retinol stores where retinol is stored in retinyl-ester formation until the embryonic liver becomes functional [9, 10]. The placenta has also been proposed to buffer retinoid delivery, by releasing retinol to the fetus when maternal intake is deficient and by storing it to protect the embryo from a potential toxic excess of maternal retinoids [10]. Moreover, maternal RBP do not pass the placenta [11]. Therefore, to enter the fetal circulation, maternal retinol bound to maternal RBP must be released at the maternal-fetal interface. Fetal RBP, produced by the trophoblast, then form a complex with retinol to be subsequently released into the fetal circulation and delivered to the target organs [10-13]. Within cells, target cells take up the retinol-RBP complex, and retinol is bind to cellular binding protein (CRBP) [14]. The CRBP-retinol complex can either be the substrate in the metabolic pathway

which leads to the production of retinoic acid (RA) by retinol dehydrogenase (RALDH) or esterified to retinyl-ester by lecithin:retinol acyltransferase (LRAT) for storage [15, 16]. RA exerts its biological effects through biding to nuclear receptors, the retinoic acid receptors (RARs) and retinoid X receptors (RXRs) [17, 18]. The LRAT activity has been shown to be strongly regulated by the retinol status [19] and RA signaling is tightly regulated by negative feedback mechanism: elevated RA suppresses the production of CRBP which down-regulate the activation of RARs and RXRs [14]. It has been shown that trophoblastic RXR isoforms are important in the normal development of placenta. Moreover, RA through RXR and RAR control many of the placental trophoblastic endocrine production, which is essential to establish and sustain pregnancy and embryonic development in mammals [20, 21].

In recent years retinoid signaling pathway (RSP) disruption has been implicated in the pathogenesis of pulmonary hypoplasia and congenital diaphragmatic hernia (CDH) in the nitrofen model of CDH [15, 22] and in human newborns with CDH [23]. Recent work from our laboratory has shown that pulmonary total retinol levels are significantly decreased and RSP are significantly up-regulated in nitrofen-induced hypoplastic lungs during late lung morphogenesis, supporting the hypothesis that a disturbed retinol status is involved in the pathogenesis of CDH [15]. In human newborns with CDH, both retinol and its bounding protein in the serum, retinol-binding protein (RBP) has been reported to be decreased, whereas maternal levels were comparable between mothers of CDH patients and mothers of healthy children in a case control study [23]. The above findings suggested that maternal-fetal retinol transport by placenta may be disrupted causing PH in CDH. Recently, we demonstrated that nitrofen disturb the mobilization of retinol from placenta to fetal circulation since trophoblastic RBP expression is decreased in the nitrofen model of CDH [24]. However, the retinol transfer from mother to the placenta and trophoblastic RSP activation has not been investigated during lung morphogenesis in nitrofen model of CDH. We hypothesized that retinol is transferred from mother to placenta and stored in the placenta in nitrofen model of CDH during lung morhogenesis. Thus, we designed this study to investigate placental retinol and retinyl-ester levels and RSP activation in the nitrofen CDH model.

Materials and methods:

Animals and drugs

Adult Sprague–Dawley rats were mated, and the females were checked daily for plugging. The presence of spermatozoids in the vaginal smear was considered as a proof of pregnancy; the day of observation determined gestational day 0. Pregnant female rats were then randomly divided into two groups. At 9 days of gestation (term, 22 days), animals in the experimental group received intragastrically 100 mg of nitrofen (WAKO Chemicals, Osaka, Japan) dissolved in 1 ml of olive oil under short anesthesia, whereas those in control group received only vehicle. Fetuses were harvested by cesarian section on day 21 (D21) of gestation and divided into two groups: control (n=11) and nitrofen with CDH (n=11). The Department of Health and Children approved the protocol of these animal experiments (REC:668b) under the Cruelty to Animals Act, 1876; as amended by European Communities Regulations 2002 and 2005, all animals were treated according to the current guidelines of animal care.

Tissue collection

After sedation with isoflurane, term fetuses were harvested free from the dams. Placentas were dissected from each fetus. Blood was taken from dams by intracardiac puncture for serum total retinol determination. Samples for high-performance liquid chromatography (HPLC) were snap frozen in liquid nitrogen and then stored at −80 °C. Samples for immunohistochemistry were fixed in 4 % formalin and embedded in paraffin.

Immunohistochemistry

The paraffin-embedded placentas were sectioned at a thickness of 5 μm, and the sections were deparaffinized with xylene and then rehydrated through ethanol and distilled water. Tissue sections were immersed in target retrieval solution (DAKO Ltd, Cambridgeshire, UK) heated for 10 min at 121 °C followed by incubation in 0.03 % H_2O_2 for 30 min to block endogenous peroxidase activity. Sections were incubated overnight at 4 °C with a 1:100 dilution of mouse monoclonal primary antibody against CRBP1 (ab24090; Abcam, Cambridge, UK), 1:100 dilution of rabbit polyclonal primary antibody against

LRAT (ab137304; Abcam, Cambridge, UK), 1:50 dilution of goat polyclonal primary antibody against RALDH1a3 (sc26713; Santa Cruz Biotechnology, USA), 1:50 dilution of goat polyclonal primary antibody against RARa (ab28767; Abcam, Cambridge, UK) and 1:100 dilution of rabbit polyclonal primary antibody raised against RXRa (sc553; Santa Cruz Biotechnology, USA). Sections were then incubated with horseradish peroxidase-labeled anti-mouse, anti-rabbit or anti-goat secondary antibodies and then processed using a DAKO EnVision kit® (DAKO Ltd, Cambridgeshire, UK), developed with a diaminobenzidine–H_2O_2 substrate complex, and counterstained with hematoxylin.

High-performance liquid chromatography analysis

Preparation of samples for measurement of total retinol (including retinol, retinyl-ester, retinoid acid and other metabolite of Vitamin A) concentration was performed by modification of a previously described protocol [15, 25]. Total retinol concentrations of placenta were analysed by high-performance liquid chromatography provided with SPD-10A Shimadzu UV-Vis detector on 3.9x150 mm, 5 mm reverse phase Resolve C18 column (Waters, Milford). The elution phase was acetonitrile/methanol/DMSO (90:10:1) and flow rate was 1.0 mL/min. Chromatograms were extracted at a wave lens of 325 nm. The concentration of each sample was extrapolated from calibration curve obtained with pure retinol samples (Sigma-Aldrich, Steinheim, Germany) of a concentration from 0.1 to 10 *μ*g/mL.

Preparation of samples for simultaneous determination of retinol and retinyl-ester was performed by modification of a previously described protocol [26]. Retinol and retinyl-ester concentrations of placenta were analysed by high-performance liquid chromatography provided with SPD-10A Shimadzu UV-Vis detector on 3.9x150 mm, 5 mm reverse phase Resolve C18 column (Waters, Milford). The elution phase was acetonitrile/methanol/DMSO (90:10:1) and flow rate was 1.0 mL/min. Chromatograms were extracted at a wave lens of 325 nm. The concentration of each sample was extrapolated from calibration curve obtained with pure retinol samples (Sigma-Aldrich, Steinheim, Germany) of a concentration from 0.1 to 10 *μ*g/mL.

Statistical analysis

All numerical data are presented as mean ± standard error. Differences between two groups at D21 were tested using an unpaired *t* test or *U* test, depending on the distribution of data. Statistical significance was accepted at *P* values <0.05.

Results:

Immunohistochemical staining of retinoid signalling pathway in trophoblasts

Immunohistochemistry showed markedly increased LRAT immunoreactivity in CDH placenta compared to controls (Figure1). Markedly decreased immunoreactivity of CRBP1, RALDH1a3, RARa and RXRa were observed in trophoblast cells in CDH compared to control placenta (Figure1).

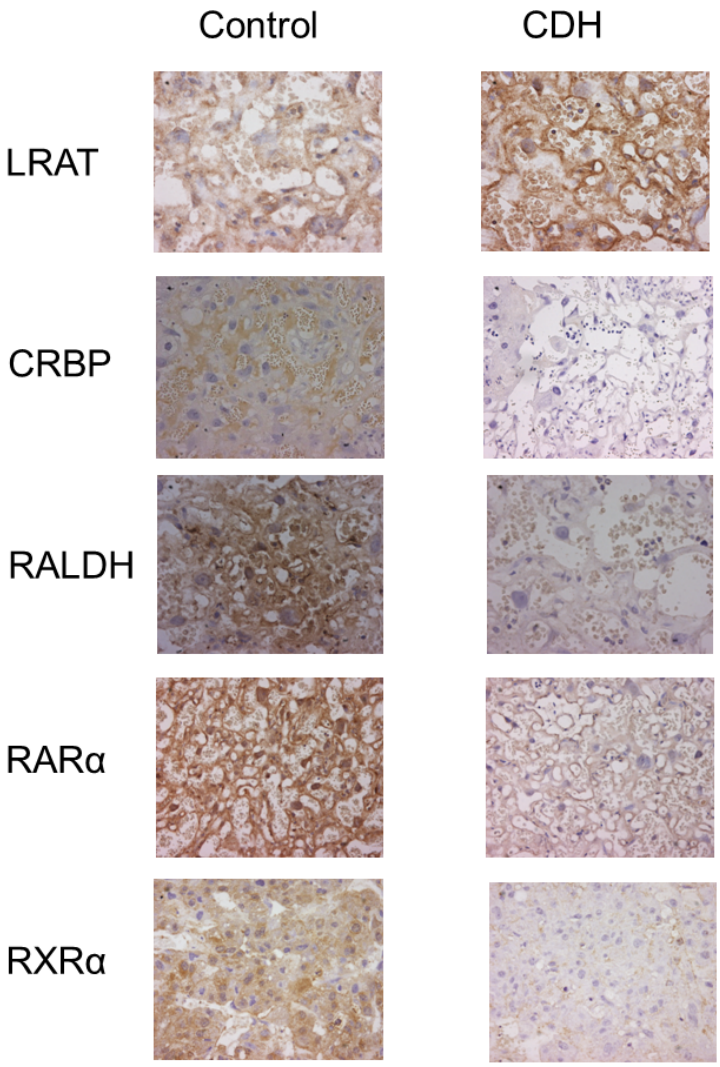

Figure 1 immunohistochemical staining of retinoid signaling pathway in trophoblasts in control and nitrofen induced CDH (40x magnification)

Total retinol levels

There were no significant differences in total serum retinol levels between nitrofen-exposed mothers (n = 4, 0.2056 ± 0.02 *μM/*g) and control mothers (n = 4, 0.1967 ± 0.08 *μM/*g). Total retinol levels in the placenta were significantly increased in CDH placenta (0.2437± 0.015 *μM/*g) compared to control placenta (0.1013 ± 0.02 *μM/*g, $p<0.05$) (Table 1).

	Control (n=11)	CDH (n=11)
Total retinol level (*μM/*g)	0.1013 ± 0.02	0.2437± 0.015
Retinol (*μM/*g)	0.011± 0.02	0.017 ± 0.003
Retinyl-ester (*μM/*g)	0.081 ± 0.03	0.186 ± 0.03 *

*:p<0.05

Table 1 placenta total and simultaneously detected retinol and retinyl-ester level

Simultaneously detected retinol and retinyl-ester level in placenta

There were no significant differences in retinol levels between control (0.011± 0.02 *μM/*g) and CDH placenta (0.017 ± 0.003 *μM/*g) (Table1). The retinyl-ester levels were significantly increased in CDH placenta (0.186 ± 0.03 *μM/*g) compared to control placenta (0.081 ± 0.03 *μM/*g, p<0.05) (Table1).

Discussion:

It is well understood that retinoids, especially retinol, play a key role during fetal lung morphogenesis [7, 12]. Placenta has a major role in fetal development and in the retinol homeostasis in fetal life [8]. In mammals, the exchange of gas and nutrients between mother and fetus occur within the placenta. In the mature placenta, this exchange takes place at the level of the microvillus and basal membranes separate the maternal blood from the fetal circulation. In rats, this barrier is composed of a bilayer of syncytiotrophoblasts adjacent to the fetal endothelium and a layer of trophoblast cells that lines the maternal blood sinusoids [27, 28]. Because there is no *de novo* synthesis of retinol, the developing mammalian embryo requires retinol from the maternal circulation for normal organ development [29]. Retinol normally passes the placenta via the trophoblast. Placenta serves as a site of retinol stores where retinol is stored in retinyl-ester formation until the embryonic liver becomes functional [9, 10]. The placenta has also been proposed to buffer retinoid delivery, by releasing retinol to the fetus when maternal intake is deficient and by storing it to protect the embryo from a potential toxic excess of maternal retinoids [10]. Retinol is bound

in a complex of the transport proteins retinol binding protein (RBP) and transthyretin (TTR). Quadro *et al.* [11] investigated the fetal retinoid delivery in mice and they found that maternal RBP does not cross the placenta. Hence, they concluded that RBP of embryonic origin plays a key role in distributing retinol to the developing tissues [29]. It has been reported that the liver is the main source of RBP in adults, whereas fetal RBP levels are mainly dependent on trophoblastic RBP synthesis [29].

After target organs take up the retinol-RBP complex, the retinol binds to CRBP [14]. The CRBP can prevent intracellular retinol from non-specific oxidation or elimination and acts as a carrier protein to present the retinol to respective RALDH for oxidation or to LRAT for esterification [14]. LRAT is the key enzyme in the generation of retinol stores and has been proposed to play a crucial role in maintaining retinoid homeostasis by diverting retinol away from its oxidative activation to RA in adult mammalian tissues [9]. This action of LRAT has been proposed to be important especially under condition of excessive retinoid intake [9]. Kim et al showed that placental LRAT play a crucial role in maintaining a tight regulation of retinoid levels during embryonic development and that this regulation is achieved by striking a balance between retinyl-ester synthesis and RA degradation [30].

The transcriptional regulatory activities of retinoids are known to result from the action of RA [19]. These actions of RA mediated through ligand-dependent transcription factors, retinoid acid receptors, and retinoid X receptors [23]. Wendling et al demonstrated that activation of RXRs is critical to proper placental development [31]. In humans, RAs have been suggested to affect steroidogenesis by placental trophoblast cells via the RAR and/or RXR signaling [32]. A number of studies have shown that RAs regulate the production of human chorionic gonadotropin, placental lactogen and leptin [10, 20, 33]. However the essential of the activation of trophoblastic RA signaling pathway through placental endocrine function in normal pregnancy and embryonic development has been shown, it has not been investigated in CDH.

Several authors have shown that the RA signaling pathway is disrupted in both humans and animal models of CDH and decreased pulmonary retinol levels have been associated with the development of PH in CDH [6, 15, 23]. Beurskens *et al.* [23] have found decreased RBP and retinol levels in human

newborns with CDH compared to controls whereas mothers of both have comparable levels of RBP and retinol. These authors concluded that the maternal-fetal transport may be disrupted, leading to CDH and PH. The importance of the retinoid signaling pathway during fetal development and especially in lung morphogenesis is further supported by a study showing that RA administration attenuates the development of PH in the nitrofen-induced CDH model [34]. The nitrofen CDH model is one of the most widely used animal models to study the pathogenesis of PH in CDH [35-39]. However, the exact molecular mechanism underlying nitrofen-induced PH in CDH still remains unclear. It has recently been reported that nitrofen does not directly interfere with retinoic acid signaling but induce a dose-dependent apoptosis [40]. Clugston et al demonstrated that the level of nitrofen estimated to reach the embryo would be too low to induce apoptosis directly [41]. Recently we proposed that nitrofen disrupts the mobilization of retinol from placenta to fetal circulation through trophoblastic apoptosis, resulting in reduced pulmonary RBP and TTR protein levels and subsequently pulmonary hypoplasia in the nitrofen CDH model [24].

In the present study we investigated the maternal-placental retinol transfer in CDH during lung development. We showed that total retinol levels as well retinyl-ester levels were significantly increased in CDH placenta compared to controls. These suggest that nitrofen does not disturb the retinol transfer from mother to placenta. The increased placental retinyl-ester level and increased trophoblastic LRAT expression suggest that retinol is stored in placenta in the nitrofen treated animals. This may be as a result to nitrofen impairing retinol mobilization from placenta to fetal circulation. The increased retinol storage in the placenta may have dual action, protecting the embryo from potential toxic excess of maternal retinoids and at the same time the high level of total retinol down regulates trophoblastic RA signaling pathway by negative feedback mechanism which is essential for the placental normal endocrine function and normal placental and embryonic development. Nitrofen induced changes in the placenta may play a key role in the pathogenesis of PH in CDH.

References

1. Colvin J, Bower C, Dickinson JE, et al: Outcomes of congenital diaphragmatic hernia: a population-based study in Western Australia. *Pediatrics* 2005, 116(3):e356-363.
2. Stege G, Fenton A, Jaffray B: Nihilism in the 1990s: the true mortality of congenital diaphragmatic hernia. *Pediatrics* 2003, 112(3 Pt 1):532-535.
3. Gosche JR, Islam S, Boulanger SC: Congenital diaphragmatic hernia: searching for answers. *Am J Surg* 2005, 190(2):324-332.
4. Robinson PD, Fitzgerald DA: Congenital diaphragmatic hernia. *Paediatr Respir Rev* 2007, 8(4):323-334; quiz 334-325.
5. Montedonico S, Nakazawa N, Puri P: Congenital diaphragmatic hernia and retinoids: searching for an etiology. *Pediatr Surg Int* 2008, 24(7):755-761.
6. Noble BR, Babiuk RP, Clugston RD, et al: Mechanisms of action of the congenital diaphragmatic hernia-inducing teratogen nitrofen. *Am J Physiol Lung Cell Mol Physiol* 2007, 293(4):L1079-1087.
7. Clagett-Dame M, DeLuca HF: The role of vitamin A in mammalian reproduction and embryonic development. *Annu Rev Nutr* 2002, 22:347-381.
8. Wassef L, Quadro L: Uptake of dietary retinoids at the maternal-fetal barrier: in vivo evidence for the role of lipoprotein lipase and alternative pathways. *The Journal of biological chemistry* 2011, 286(37):32198-32207.
9. Spiegler E, Kim YK, Wassef L, et al: Maternal-fetal transfer and metabolism of vitamin A and its precursor beta-carotene in the developing tissues. *Biochimica et biophysica acta* 2012, 1821(1):88-98.
10. Sapin V, Chaib S, Blanchon L, et al: Esterification of vitamin A by the human placenta involves villous mesenchymal fibroblasts. *Pediatr Res* 2000, 48(4):565-572.
11. Quadro L, Hamberger L, Gottesman ME, et al: Transplacental delivery of retinoid: the role of retinol-binding protein and lipoprotein retinyl ester. *Am J Physiol Endocrinol Metab* 2004, 286(5):E844-851.
12. Morriss-Kay GM, Ward SJ: Retinoids and mammalian development. *Int Rev Cytol* 1999, 188:73-131.
13. Sapin V, Ward SJ, Bronner S, et al: Differential expression of transcripts encoding retinoid binding proteins and retinoic acid receptors during placentation of the mouse. *Dev Dyn* 1997, 208(2):199-210.
14. Kam RK, Deng Y, Chen Y, et al: Retinoic acid synthesis and functions in early embryonic development. *Cell & bioscience* 2012, 2(1):11.
15. Nakazawa N, Montedonico S, Takayasu H, et al: Disturbance of retinol transportation causes nitrofen-induced hypoplastic lung. *J Pediatr Surg* 2007, 42(2):345-349.
16. Paik J, Vogel S, Quadro L, et al: Vitamin A: overlapping delivery pathways to tissues from the circulation. *The Journal of nutrition* 2004, 134(1):276S-280S.
17. Kato Y, Braunstein GD: Retinoic acid stimulates placental hormone secretion by choriocarcinoma cell lines in vitro. *Endocrinology* 1991, 128(1):401-407.
18. Nakazawa N, Takayasu H, Montedonico S, et al: Altered regulation of retinoic acid synthesis in nitrofen-induced hypoplastic lung. *Pediatr Surg Int* 2007, 23(5):391-396.
19. O'Byrne SM, Wongsiriroj N, Libien J, et al: Retinoid absorption and storage is impaired in mice lacking lecithin:retinol acyltransferase (LRAT). *The Journal of biological chemistry* 2005, 280(42):35647-35657.
20. Csapo AI, Pulkkinen MO, Kaihola HL: The effect of luteectomy-induced progesterone-withdrawal on the oxytocin and prostaglandin response of the first trimester pregnant human uterus. *Prostaglandins* 1973, 4(3):421-429.
21. Itoh K, Hiromori Y, Kato N, et al: Placental steroidogenesis in rats is independent of signaling pathways induced by retinoic acids. *General and comparative endocrinology* 2009, 163(3):285-291.

22. Gallot D, Marceau G, Coste K, et al: Congenital diaphragmatic hernia: a retinoid-signaling pathway disruption during lung development? *Birth Defects Res A Clin Mol Teratol* 2005, 73(8):523-531.
23. Beurskens LW, Tibboel D, Lindemans J, et al: Retinol status of newborn infants is associated with congenital diaphragmatic hernia. *Pediatrics*, 126(4):712-720.
24. Kutasy B, Gosemann JH, Doi T, et al: Nitrofen interferes with trophoblastic expression of retinol-binding protein and transthyretin during lung morphogenesis in the nitrofen-induced congenital diaphragmatic hernia model. *Pediatr Surg Int* 2012, 28(2):143-148.
25. Hosotani K, Kitagawa M: Improved simultaneous determination method of beta-carotene and retinol with saponification in human serum and rat liver. *Journal of chromatography B, Analytical technologies in the biomedical and life sciences* 2003, 791(1-2):305-313.
26. Moulas AN ZI, Taitzoglou IA, Tsantarliotou MP, et al: Simultaneous determination of retinoic acid, retinol, and retinyl palmitate in ram plasma by liquid chromatography. *J Liq Chromatogr* 2003, 26:559–572.
27. Watson ED, Cross JC: Development of structures and transport functions in the mouse placenta. *Physiology (Bethesda)* 2005, 20:180-193.
28. Ain R, Canham LN, Soares MJ: Gestation stage-dependent intrauterine trophoblast cell invasion in the rat and mouse: novel endocrine phenotype and regulation. *Developmental biology* 2003, 260(1):176-190.
29. Quadro L, Hamberger L, Gottesman ME, et al: Pathways of vitamin A delivery to the embryo: insights from a new tunable model of embryonic vitamin A deficiency. *Endocrinology* 2005, 146(10):4479-4490.
30. Kim YK, Wassef L, Hamberger L, et al: Retinyl ester formation by lecithin: retinol acyltransferase is a key regulator of retinoid homeostasis in mouse embryogenesis. *The Journal of biological chemistry* 2008, 283(9):5611-5621.
31. Wendling O, Chambon P, Mark M: Retinoid X receptors are essential for early mouse development and placentogenesis. *Proceedings of the National Academy of Sciences of the United States of America* 1999, 96(2):547-551.
32. Nakanishi T, Hiromori Y, Yokoyama H, et al: Organotin compounds enhance 17beta-hydroxysteroid dehydrogenase type I activity in human choriocarcinoma JAr cells: potential promotion of 17beta-estradiol biosynthesis in human placenta. *Biochemical pharmacology* 2006, 71(9):1349-1357.
33. Nakanishi T, Nishikawa J, Hiromori Y, et al: Trialkyltin compounds bind retinoid X receptor to alter human placental endocrine functions. *Mol Endocrinol* 2005, 19(10):2502-2516.
34. Montedonico S, Nakazawa N, Puri P: Retinoic acid rescues lung hypoplasia in nitrofen-induced hypoplastic foetal rat lung explants. *Pediatr Surg Int* 2006, 22(1):2-8.
35. Guilbert TW, Gebb SA, Shannon JM: Lung hypoplasia in the nitrofen model of congenital diaphragmatic hernia occurs early in development. *Am J Physiol Lung Cell Mol Physiol* 2000, 279(6):L1159-1171.
36. Jay PY, Bielinska M, Erlich JM, et al: Impaired mesenchymal cell function in Gata4 mutant mice leads to diaphragmatic hernias and primary lung defects. *Dev Biol* 2007, 301(2):602-614.
37. Doi T, Hajduk P, Puri P: Upregulation of Slit-2 and Slit-3 gene expressions in the nitrofen-induced hypoplastic lung. *J Pediatr Surg* 2009, 44(11):2092-2095.
38. Doi T, Puri P: Up-regulation of Wnt5a gene expression in the nitrofen-induced hypoplastic lung. *J Pediatr Surg* 2009, 44(12):2302-2306.
39. Ruttenstock E, Doi T, Dingemann J, et al: Prenatal administration of retinoic acid upregulates insulin-like growth factor receptors in the nitrofen-induced hypoplastic lung. *Birth Defects Res B Dev Reprod Toxicol*, 92(2):148-151.
40. Kling DE, Cavicchio AJ, Sollinger CA, et al: Nitrofen induces apoptosis independently of retinaldehyde dehydrogenase (RALDH) inhibition. *Birth Defects Res B Dev Reprod Toxicol*, 89(3):223-232.

41. Clugston RD, Zhang W, Greer JJ: Early development of the primordial mammalian diaphragm and cellular mechanisms of nitrofen-induced congenital diaphragmatic hernia. *Birth Defects Res A Clin Mol Teratol*, 88(1):15-24.

Acknowledgements

Acknowledgements

First of all I would like to thank Dr. Francesca Paradisi for the opportunity she gave me with this PhD project and for introducing me to the world of research; I would also like to thank her and my second supervisor Dr. Gethin McBean for their help and guidance.

A big thanks go to the post docs Daniele Balducci and Elaine O'Reilly for teaching me how to work in a chemistry lab when I first arrived in UCD and to Therese Montgomery for teaching me so much about biology.

Thanks to Andrea, one of the best 4th year students one could have, for his hard work and contribution towards the macrocycle project and nevertheless for his tiramisù.

Many thanks to the present and past people in the Paradisi's group, especially Daniela and Jenny for being good friends, Anita for being the heir of the ACCA knowledge and for taking good care of our precious amino acid. To Lorenzo, my desk mate for the past few months, who put up with me and made sure I did not forget my first language. Thanks also to Keith and Phil for making me laugh with their jokes and mockeries and thanks to Diya and Gabriele.

Thanks to the administrative and technical staff, especially Jimmy and Yannick for their precious assistance with NMRs.

Thanks to my chemists friends Frauke, Michelle, AJ, Wojtek, Kev, Sharon, Brendan for listening to my complaints about Irish weather, for all the lunches together in the chemistry building and the parties outside (and at times inside) the chemistry building.

A big thanks also to all my volleyball team mates and friends for the great times I spent with them and for keeping me away from the lab.

Last but not least, thanks a million to my family, most of all to my mum and dad for the support and for letting me undertake this fantastic adventure far from home for the past four years.